

BEHAVIOUR OF PRESTRESSED REINFORCED GRANULAR BED OVERLYING SOFT SOIL

Thesis

Submitted in partial fulfillment of the requirements for the award of

DOCTOR OF PHILOSOPHY

by

JAYAMOHAN. J



DEPARTMENT OF CIVIL ENGINEERING

NATIONAL INSTITUTE OF TECHNOLOGY KARNATAKA

SURATHKAL, MANGALORE – 575025

DECEMBER 2013

DECLARATION

I hereby declare that the Research Thesis entitled “**BEHAVIOUR OF PRESTRESSED REINFORCED GRANULAR BED OVERLYING SOFT SOIL**” which is being submitted to the **NATIONAL INSTITUTE OF TECHNOLOGY KARNATAKA, SURATHKAL** in partial fulfillment of the requirements for the award of the degree of **Doctor of Philosophy** in Civil Engineering is a *bonafide report of the research work carried out by me*. The material contained in this Research Thesis has not been submitted to any University or Institution for the award of any degree.

Register Number :CV09 P03, Jayamohan. J

Department of Civil Engineering

Place : NITK, Surathkal

Date :

CERTIFICATE

This is to certify that the Research Thesis entitled “**BEHAVIOUR OF PRESTRESSED REINFORCED GRANULAR BED OVERLYING SOFT SOIL**” submitted by **Jayamohan.J** (Register Number CV09P03) as the record of the research work carried out by him is *accepted as the Research Thesis Submission* in partial fulfillment of the requirements for the award of degree of **Doctor of Philosophy**.

Dr. R. Shivashankar
Research Guide and Professor
Department of Civil Engineering
NITK, Surathkal

Chairman – DRPC

ACKNOWLEDGEMENT

I am grateful to the Almighty God for having given me the divine guidance and patience to complete this research. I would like to express my great indebtedness to my guide **Prof.R.Shivashankar**, Professor, Department of Civil Engineering, NITK, Surathkal for his guidance, valuable suggestions, untiring effort in reviewing this thesis and continuous encouragement throughout the course of my research work.

I sincerely acknowledge the help and support of **Prof. Katta Venkatramana**, Head of Civil Engineering Department for permitting me to use the departmental computing and laboratory facilities and for his continuous support in completing the work.

I would like to express my gratitude to **Prof. Sitaram Nayak**, Member, RPAC, for his help and encouragement provided at various stages of this work. I also wish to thank **Prof. Shrikantha .S. Rao** , Member, RPAC, for his valuable inputs that helped in steering research in right direction. I also express my gratitude to **Prof. M. C. Narasimhan** and **Prof. A.U. Ravishankar** for the help and encouragement given by them. I would like to express my sincere thanks to all the faculty of Department of Civil Engineering for their suggestions, encouragement and co-operation during my research work.

I would like to extend my sincere appreciation to the **Director, NITK**, for extending all departmental facilities for this research.

I express my deep sense of gratitude to the **Director, Lal Bahadur Shastri Centre for Science & Technology, Thiruvananthapuram** for permitting me to do my research work at NITK, Surathkal.

I gratefully acknowledge the support and help rendered by **Ms. Aswathy, Ms. Vigey Mary** and **Ms. Nileena Suresh**, M.Tech students of Geotechnical Engineering. I express my thanks to all my friends and fellow research scholars for their help and support during my research work.

I sincerely thank the laboratory staff **Sri. Chandrasekhar Karanth, Sri. Dinesh Acharya, Sri. Sadananda Kadri, Sri. Narayan Naik** for the help rendered during the experimental stages of the work. I also thank the office staff of Department of Civil Engineering for their help.

Jayamohan. J

ABSTRACT

The use of geosynthetics to improve the bearing capacity and settlement performance of shallow foundations has proven to be a cost-effective foundation system. In marginal ground conditions, geosynthetics enhance the ability to use shallow foundations. This is done by either reinforcing cohesive soil directly or replacing the poor soils with stronger granular fill in combination with geosynthetic reinforcement. In low-lying areas with poor foundation soils, the geosynthetic reinforced granular bed can be placed over the weak soil. The resulting composite ground (reinforced granular bed) will improve the load carrying capacity of the footing and provide better pressure distribution on top of the underlying weak soils, hence reducing the associated settlements.

It is now well established that geosynthetics demonstrate their beneficial effects only after considerable settlements, since the strains occurring during initial settlements are insufficient to mobilize significant tensile load in the geosynthetic. This is not a desirable feature for foundations of certain structures, since their permissible values of settlement are small. Thus there is a need for a technique which will allow the geosynthetic to increase the load bearing capacity of soil without the occurrence of large settlements. One technique yet to be comprehensively studied is the effect of prestressing the geosynthetic layer before implementing them as reinforcement in field applications.

In this thesis, extensive investigations are made to study the effects of prestressing the geosynthetic reinforcement on the behaviour of reinforced granular bed overlying weak soil. The study involved laboratory scale plate load tests to observe the physical behaviour of prestressed geosynthetic-reinforced soil system. Non-linear FE analyses were carried out using the FE program PLAXIS, version 8, and the results were compared with those obtained from model tests.

The parameters studied are effects of magnitude of prestress, direction of prestress, number of layers of prestressed reinforcement, type of geosynthetic reinforcement, size of reinforcement, thickness of granular bed, strength of underlying weak soil, presence of voids in granular bed and weak soil etc.

In this thesis an analytical model is proposed to predict the improvement in bearing capacity due to prestressing the reinforcement in the granular bed. The results of the analytical model are validated by comparing it with those obtained from experimental and finite element studies.

Key words: Geogrid, Geotextile, Reinforced Granular Bed, Prestress, Model Test, Finite Element Analysis, Analytical model

CONTENTS

	Page no:
Title Page	i
Declaration	ii
Certificate	iii
Acknowledgements	iv
Abstract	v
Contents	vii
List of Tables	xii
List of Figures	xiii
Nomenclature	xxiv
1. INTRODUCTION	1
1.1 Background	1
1.2 Objective and Scope of Research	1
1.3 Outline of the thesis	3
2. LITERATURE REVIEW	5
2.1 Introduction	5
2.2 Bearing Capacity of footings on layered soils	5
2.3 Experimental work on Bearing Capacity of Reinforced soil	6
2.4 Analytical Modeling of Reinforced Granular Bed	10
2.5 Prestressed Reinforced Soil	13
2.6 Effect of formation of void / cavity in Reinforced Soil	16
3. EXPERIMENTAL METHODOLOGY	20
3.1 Introduction	20
3.2 Properties of Soil used	20
3.2.1 Granular Bed	20
3.2.2 Weak Soil	21
3.3 Experimental Setup	22
3.4 Preparation of Test Bed	24
3.5 Thickness of Granular Bed	25
3.6 Magnitude of Prestress	25
3.7 Direction of Prestress	26
3.8 Number of Layers of Reinforcement	27
3.9 Size of Reinforcement	28

3.10. Type of Geosynthetic Reinforcement	28
3.11. Strength of Weak Soil	29
3.12 Experimental Programme	30
4. FINITE ELEMENT ANALYSIS	31
4.1 Introduction	31
4.2 Finite element modeling	31
4.3 Comparison between Experimental and FEA Results	36
4.3.1 Effect of Magnitude of Prestress	36
4.3.1.1 PRGB with single layer geogrid of size 5Bx5B overlying weak soil 1 (moist soil)	36
4.3.1.2 PRGB with single layer geogrid of size 5Bx5B overlying weak soil 2 (submerged soil)	39
4.3.1.3 PRGB with single layer geotextile of size 5Bx5B overlying weak soil 1 (moist soil)	41
4.3.1.4 PRGB with single layer geotextile of size 5Bx5B overlying weak soil 2 (submerged soil)	44
4.3.1.5 PRGB with single layer geogrid of size 2Bx2B overlying weak soil 1 (moist soil)	47
4.3.1.6 PRGB with single layer geogrid of size 2Bx2B overlying weak soil 2 (submerged soil)	50
4.3.1.7 PRGB with double layer geogrid of size 5Bx5B overlying weak soil 1 (moist soil)	52
4.3.1.8 PRGB with double layer geogrid of size 5Bx5B overlying weak soil 2 (submerged soil)	55
4.3.2 Effect of Direction of Prestress	58
4.3.2.1 PRGB with single layer geogrid of size 5Bx5B overlying weak soil 1 (moist soil)	58
4.3.2.2 PRGB with single layer geogrid of size 5Bx5B overlying weak soil 2 (submerged soil)	59
4.3.2.3 PRGB with single layer geotextile of size 5Bx5B overlying weak soil 1 (moist soil)	61
4.3.2.4 PRGB with single layer geotextile of size 5Bx5B overlying weak soil 2 (submerged soil)	62

4.3.2.5 PRGB with single layer geogrid of size 2Bx2B overlying weak soil 1 (moist soil)	63
4.3.2.6 PRGB with single layer geogrid of size 2Bx2B overlying weak soil 2 (submerged soil)	65
4.3.2.7 PRGB with double layer geogrid of size 5Bx5B overlying weak soil 1 (moist soil)	66
4.3.2.8 PRGB with double layer geogrid of size 5Bx5B overlying weak soil 2 (submerged soil)	67
4.3.3 Effect of number of layers of prestressed geosynthetic reinforcement	69
4.3.3.1 PRGB overlying weak soil 1 (moist soil)	69
4.3.3.2 PRGB overlying weak soil 2 (submerged soil)	70
4.3.4 Effect of type of geosynthetic reinforcement	71
4.3.4.1 PRGB overlying weak soil 1 (moist soil)	71
4.3.4.2 PRGB overlying weak soil 2 (submerged soil)	72
4.3.5 Effect of size of prestressed geosynthetic reinforcement	72
4.3.5.1 PRGB overlying weak soil 1 (moist soil)	73
4.3.5.2 PRGB overlying weak soil 2 (submerged soil)	73
4.3.6 Effect of thickness of granular bed	74
4.3.6.1 PRGB overlying weak soil 1 (moist soil)	74
4.3.6.2 PRGB overlying weak soil 2 (submerged soil)	77
4.3.7 Effect of strength of underlying weak soil	80
4.3.7.1 PRGB with single layer geogrid of size 5Bx5B	81
4.3.7.2 PRGB with single layer geotextile of size 5B x 5B	82
4.3.7.3 PRGB with single layer geogrid of size 2B x 2B	83
4.3.7.4 PRGB with double layer geogrid of size 5B x 5B	85
4.4 Chapter Summary	87
5. ANALYTICAL MODELING	88
5.1 Introduction	88
5.2 Punching Shear Model of Strip Footing (Shivashankar et al. 1993)	88
5.2.1 Shear Layer Effect	89
5.2.2 Confinement Effect	89
5.2.3 Additional Surcharge Effect	90
5.3 Modeling of Square Footing on Unreinforced or Reinforced Granular Beds (RGB) in present study	91

5.3.1	Modeling of Square Footing on Prestressed Reinforced Granular Beds in Present Study	92
5.3.1.1	Shear Layer Effect	92
5.3.1.2	Confinement Effect	92
5.3.1.3	Additional Surcharge Effect	93
5.4	Comparison between Results of Analytical Model and Experimental Studies	94
5.5	Comparison between Results of Analytical Model and Finite Element Analysis	98
5.6	Chapter Summary	101
6.	PRGB ON VOIDS	103
6.1	Introduction	103
6.2	Granular Beds of Thickness B	104
6.2.1	Void just above the interface between granular bed and weak soil	104
6.2.2	Void at the interface between granular bed and weak soil	107
6.2.3	Void just below the interface between granular bed and weak soil	110
6.2.4	Void at a depth of 0.75B below the interface between granular bed and weak soil	113
6.3	Granular Beds of Thickness 2B	117
6.3.1	Void just above the interface between granular bed and weak soil	117
6.3.2	Void at the interface between granular bed and weak soil	120
6.3.3	Void just below the interface between granular bed and weak soil	124
6.3.4	Void at a depth of 0.75B below the interface between granular bed and weak soil	127
6.4	Reduction Factor	130
6.4.1	Variation of Reduction factor with prestress	130
6.4.2	Variation of Reduction factor with depth of void	132
6.4.3	Variation of Reduction factor with eccentricity of void	136
6.4.3.1	Granular Beds of Thickness B	136
6.4.3.2	Granular Beds of Thickness 2B	138
6.5	Chapter Summary	141
7.	STRESSES AND SETTLEMENTS AT INTERFACE	142
7.1	Introduction	142
7.2	Stress Distribution at Interface	142
7.2.1	Granular Beds overlying (moist) Weak Soil 1	142
7.2.2	Granular Beds overlying (submerged) Weak Soil 2	144

7.3 Distribution of Settlement at Interface	145
7.3.1 Granular Beds overlying (moist) Weak Soil 1	145
7.3.2 Granular Beds overlying (submerged) Weak Soil 2	147
7.4 Chapter Summary	148
8. SUMMARY, CONCLUSIONS AND FUTURE SCOPE	149
8.1 Summary	149
8.2 Conclusions	149
8.2.1 Effect of Magnitude of Prestress	150
8.2.2 Effect of Direction of Prestress	150
8.2.3 Effect of Number of layers of reinforcement	150
8.2.4 Effect of Size of reinforcement	151
8.2.5 Effect of type of geosynthetic reinforcement	151
8.2.6 Effect of thickness of Granular Bed	151
8.2.7 Effect of strength of underlying weak soil	151
8.2.8 Analytical modeling	152
8.2.9 Effect of development of voids in granular bed and weak soil	152
8.2.10 Stresses and Settlements at the Interface	152
8.3 Future Scope	153
REFERENCES	154
PUBLICATIONS	159
BRIEF RESUME	161

LIST OF TABLES

Table no:	Title of the table	Page no:
3.1	Properties of sand used for granular bed	20
3.2	Properties of Weak soil used for the investigation	21
3.3	Properties of geogrid used for the investigation	28
3.4	Properties of geotextile used for the investigation	29
3.5	Experimental Programme	30

LIST OF FIGURES

Figure no:	Title of the figure	Page no:
1.1	Footing supported on Reinforced Granular Bed	2
2.1	Proposed failure mode for reinforced crushed lime stone (Meyerhof and Hanna, 1978)	8
2.2	Proposed foundation model (Deb et al. 2006)	12
2.3	Modeling using FLAC (Deb et al. 2007)	13
2.4	Experimental setup for prestressing the geotextile (Lovisa et al. 2010)	14
2.5	Modeling prestressed geotextile reinforced sand in PLAXIS (Lovisa et al. 2010)	14
2.6	Concept of Prestressed reinforced soil by compaction (PRSC)(Lackner et al. 2013)	15
2.7	Concept of Permanently prestressed reinforced soil (PRSP))(Lackner et al. 2013)	16
2.8	Concept of Temporarily prestressed reinforced soil (PRST))(Lackner et al. 2013)	16
2.9	Descretized model of footing above void (Baus and Wang, 1983)	17
2.10	Typical Finite Element Mesh (Kiyosumi et al. 2007)	18
3.1	Particle size distribution of sand used in granular bed	21
3.2	Particle size distribution of Weak soil used for the investigation	22
3.3	Test Setup	23
3.4	View of Test Setup	23
3.5	Arrangement for measuring load and deformation	24
3.6	Compaction of sand using Plate Vibrator	24
3.7	Details of Granular Bed	25
3.8	Prestressing force applied through three pulleys	26
3.9	Application of Prestress to reinforcement	26
3.10	Uniaxial Prestressing	26
3.11	Biaxial Prestressing	27
3.12	Test setup for double layer reinforcement	27
3.13	Arrangement of double layer reinforcement	28

3.14	Peizometers for monitoring the level of water table	29
4.1	Geometric model of PRGB	31
4.2	Descrretized model of PRGB	32
4.3	Deformed shape of PRGB after loading	33
4.4	Stress distribution in soil after loading	34
4.5	Stress distribution at the interface between granular bed and weak soil after loading	34
4.6	Typical Load-deformation curve	35
4.7	Stress distribution at the interface between reinforcement and granular bed	35
4.8	Stress vs normalized settlement curves for PRGB of thickness B with uniaxially prestressed single layer geogrid of size 5B x 5B overlying (moist) weak soil 1	36
4.9	Stress vs normalized settlement curves for PRGB of thickness B with biaxially prestressed single layer geogrid of size 5B x 5B overlying (moist) weak soil 1	37
4.10	Stress vs normalized settlement curves for PRGB of thickness 2B with uniaxially prestressed single layer geogrid of size 5B x 5B overlying (moist) weak soil 1	38
4.11	Stress vs normalized settlement curves for PRGB of thickness 2B with biaxially prestressed single layer geogrid of size 5B x 5B overlying (moist) weak soil 1	38
4.12	Stress vs normalized settlement curves for PRGB of thickness B with uniaxially prestressed single layer geogrid of size 5B x 5B overlying (submerged) weak soil 2	39
4.13	Stress vs normalized settlement curves for PRGB of thickness B with biaxially prestressed single layer geogrid of size 5B x 5B overlying (submerged) weak soil 2	40
4.14	Stress vs normalized settlement curves for PRGB of thickness 2B with uniaxially prestressed single layer geogrid of size 5B x 5B overlying (submerged) weak soil 2	40
4.15	Stress vs normalized settlement curves for PRGB of thickness 2B with biaxially prestressed single layer geogrid of size 5B x 5B overlying (submerged) weak soil 2	41
4.16	Stress vs normalized settlement curves for PRGB of thickness B with uniaxially prestressed single layer geotextile of size 5B x 5B overlying (moist) weak soil 1	42
4.17	Stress vs normalized settlement curves for PRGB of thickness B with biaxially prestressed single layer geotextile of size 5B x 5B overlying (moist) weak soil 1	42
4.18	Stress vs normalized settlement curves for PRGB of thickness 2B with uniaxially prestressed single layer geotextile of size 5B x 5B overlying (moist)	43

	weak soil 1	
4.19	Stress vs normalized settlement curves for PRGB of thickness 2B with biaxially prestressed single layer geotextile of size 5B x 5B overlying (moist) weak soil 1	43
4.20	Stress vs normalized settlement curves for PRGB of thickness B with uniaxially prestressed single layer geotextile of size 5B x 5B overlying (submerged) weak soil 2	44
4.21	Stress vs normalized settlement curves for PRGB of thickness B with biaxially prestressed single layer geotextile of size 5B x 5B overlying (submerged) weak soil 2	45
4.22	Stress vs normalized settlement curves for PRGB of thickness 2B with uniaxially prestressed single layer geotextile of size 5B x 5B overlying (submerged) weak soil 2	46
4.23	Stress vs normalized settlement curves for PRGB of thickness 2B with biaxially prestressed single layer geotextile of size 5B x 5B overlying (submerged) weak soil 2	46
4.24	Stress vs normalized settlement curves for PRGB of thickness B with uniaxially prestressed single layer geogrid of size 2B x 2B overlying (moist) weak soil 1	47
4.25	Stress vs normalized settlement curves for PRGB of thickness B with biaxially prestressed single layer geogrid of size 2B x 2B overlying (moist) weak soil 1	48
4.26	Stress vs normalized settlement curves for PRGB of thickness 2B with uniaxially prestressed single layer geogrid of size 2B x 2B overlying (moist) weak soil 1	48
4.27	Stress vs normalized settlement curves for PRGB of thickness 2B with biaxially prestressed single layer geogrid of size 2B x 2B overlying (moist) weak soil 1	49
4.28	Stress vs normalized settlement curves for PRGB of thickness B with uniaxially prestressed single layer geogrid of size 2B x 2B overlying (submerged) weak soil 2	50
4.29	Stress vs normalized settlement curves for PRGB of thickness B with biaxially prestressed single layer geogrid of size 2B x 2B overlying (submerged) weak soil 2	51
4.30	Stress vs normalized settlement curves for PRGB of thickness 2B with uniaxially prestressed single layer geogrid of size 2B x 2B overlying (submerged) weak soil 2	51
4.31	Stress vs normalized settlement curves for PRGB of thickness 2B with biaxially prestressed single layer geogrid of size 2B x 2B overlying (submerged) weak	52

	soil 2	
4.32	Stress vs normalized settlement curves for PRGB of thickness B with uniaxially prestressed double layer geogrid of size 5B x 5B overlying (moist) weak soil 1	53
4.33	Stress vs normalized settlement curves for PRGB of thickness B with biaxially prestressed double layer geogrid of size 5B x 5B overlying (moist) weak soil 1	53
4.34	Stress vs normalized settlement curves for PRGB of thickness 2B with uniaxially prestressed double layer geogrid of size 5B x 5B overlying (moist) weak soil 1	54
4.35	Stress vs normalized settlement curves for PRGB of thickness 2B with biaxially prestressed double layer geogrid of size 5B x 5B overlying (moist) weak soil 1	54
4.36	Stress vs normalized settlement curves for PRGB of thickness B with uniaxially prestressed double layer geogrid of size 5B x 5B overlying (submerged) weak soil 2	55
4.37	Stress vs normalized settlement curves for PRGB of thickness B with biaxially prestressed double layer geogrid of size 5B x 5B overlying (submerged) weak soil 2	56
4.38	Stress vs normalized settlement curves for PRGB of thickness 2B with uniaxially prestressed double layer geogrid of size 5B x 5B overlying (submerged) weak soil 2	57
4.39	Stress vs normalized settlement curves for PRGB of thickness 2B with biaxially prestressed double layer geogrid of size 5B x 5B overlying (submerged) weak soil 2	57
4.40	Stress vs normalized settlement curves for PRGB of thickness B with uniaxially and biaxially prestressed single layer geogrid of size 5B x 5B overlying (moist) weak soil 1	58
4.41	Stress vs normalized settlement curves for PRGB of thickness 2B with uniaxially and biaxially prestressed single layer geogrid of size 5B x 5B overlying (moist) weak soil 1	59
4.42	Stress vs normalized settlement curves for PRGB of thickness B with uniaxially and biaxially prestressed single layer geogrid of size 5B x 5B overlying (submerged) weak soil 2	59
4.43	Stress vs normalized settlement curves for PRGB of thickness 2B with uniaxially and biaxially prestressed single layer geogrid of size 5B x 5B overlying (submerged) weak soil 2	60
4.44	Stress vs normalized settlement curves for PRGB of thickness B with uniaxially and biaxially prestressed single layer geotextile of size 5B x 5B overlying	61

	(moist) weak soil 1	
4.45	Stress vs normalized settlement curves for PRGB of thickness 2B with uniaxially and biaxially prestressed single layer geotextile of size 5B x 5B overlying (moist) weak soil 1	61
4.46	Stress vs normalized settlement curves for PRGB of thickness B with uniaxially and biaxially prestressed single layer geotextile of size 5B x 5B overlying (submerged) weak soil 2	62
4.47	Stress vs normalized settlement curves for PRGB of thickness 2B with uniaxially and biaxially prestressed single layer geotextile of size 5B x 5B overlying (submerged) weak soil 2	63
4.48	Stress vs normalized settlement curves for PRGB of thickness B with uniaxially and biaxially prestressed single layer geogrid of size 2B x 2B overlying (moist) weak soil 1	64
4.49	Stress vs normalized settlement curves for PRGB of thickness 2B with uniaxially and biaxially prestressed single layer geogrid of size 2B x 2B overlying (moist) weak soil 1	64
4.50	Stress vs normalized settlement curves for PRGB of thickness B with uniaxially and biaxially prestressed single layer geogrid of size 2B x 2B overlying (submerged) weak soil 2	65
4.51	Stress vs normalized settlement curves for PRGB of thickness 2B with uniaxially and biaxially prestressed single layer geogrid of size 2B x 2B overlying (submerged) weak soil 2	66
4.52	Stress vs normalized settlement curves for PRGB of thickness B with uniaxially and biaxially prestressed double layer geogrid of size 5B x 5B overlying (moist) weak soil 1	66
4.53	Stress vs normalized settlement curves for PRGB of thickness 2B with uniaxially and biaxially prestressed double layer geogrid of size 5B x 5B overlying (moist) weak soil 1	67
4.54	Stress vs normalized settlement curves for PRGB of thickness B with uniaxially and biaxially prestressed double layer geogrid of size 5B x 5B overlying (submerged) weak soil 2	68
4.55	Stress vs normalized settlement curves for PRGB of thickness 2B with uniaxially and biaxially prestressed double layer geogrid of size 5B x 5B overlying (submerged) weak soil 2	68
4.56	BCR vs prestress curves for PRGB with single and double layer geogrid of size 5B x 5B overlying (moist) weak soil 1	69

4.57	BCR vs prestress curves for PRGB with single and double layer geogrid of size 5B x 5B overlying (submerged) weak soil 2	70
4.58	BCR vs prestress curves for PRGB with single layer geogrid and geotextile reinforcement of size 5B x 5B overlying (moist) weak soil 1	71
4.59	BCR vs prestress curves for PRGB with single layer geogrid and geotextile reinforcement of size 5B x 5B overlying (submerged) weak soil 2	72
4.60	BCR vs prestress curves for PRGB with single layer geogrid reinforcement of size 5B x 5B and 2B x 2B overlying (moist) weak soil 1	73
4.61	BCR vs prestress curves for PRGB with single layer geogrid reinforcement of size 5B x 5B and 2B x 2B overlying (submerged) weak soil 2	74
4.62	BCR vs thickness of GB curves for PRGB with single layer geogrid reinforcement of size 5B x 5B overlying (moist) weak soil 1	75
4.63	BCR vs thickness of GB curves for PRGB with single layer geotextile reinforcement of size 5B x 5B overlying (moist) weak soil 1	75
4.64	BCR vs thickness of GB curves for PRGB with single layer geogrid reinforcement of size 2B x 2B overlying (moist) weak soil 1	76
4.65	BCR vs thickness of GB curves for PRGB with double layer geogrid reinforcement of size 5B x 5B overlying (moist) weak soil 1	77
4.66	BCR vs thickness of GB curves for PRGB with single layer geogrid reinforcement of size 5B x 5B overlying (submerged) weak soil 2	77
4.67	BCR vs thickness of GB curves for PRGB with single layer geotextile reinforcement of size 5B x 5B overlying (submerged) weak soil 2	78
4.68	BCR vs thickness of GB curves for PRGB with single layer geogrid reinforcement of size 2B x 2B overlying (submerged) weak soil 2	79
4.69	BCR vs thickness of GB curves for PRGB with double layer geogrid reinforcement of size 5B x 5B overlying (submerged) weak soil 2	80
4.70	Stress vs normalized settlement curves for PRGB of thickness B with single layer geogrid of size 5B x 5B overlying (moist) weak soil 1 and (submerged) weak soil 2	81
4.71	Stress vs normalized settlement curves for PRGB of thickness 2B with single layer geogrid of size 5B x 5B overlying (moist) weak soil 1 and (submerged) weak soil 2	82
4.72	Stress vs normalized settlement curves for PRGB of thickness B with single layer geotextile of size 5B x 5B overlying (moist) weak soil 1 and (submerged) weak soil 2	82
4.73	Stress vs normalized settlement curves for PRGB of thickness 2B with single	83

	layer geotextile of size 5B x 5B overlying (moist) weak soil 1 and (submerged) weak soil 2	
4.74	Stress vs normalized settlement curves for PRGB of thickness B with single layer geogrid of size 2B x 2B overlying (moist) weak soil 1 and (submerged) weak soil 2	84
4.75	Stress vs normalized settlement curves for PRGB of thickness 2B with single layer geogrid of size 2B x 2B overlying (moist) weak soil 1 and (submerged) weak soil 2	84
4.76	Stress vs normalized settlement curves for PRGB of thickness B with double layer geogrid of size 5B x 5B overlying (moist) weak soil 1 and (submerged) weak soil 2	85
4.77	Stress vs normalized settlement curves for PRGB of thickness 2B with double layer geogrid of size 5B x 5B overlying (moist) weak soil 1 and (submerged) weak soil 2	86
5.1	Shear Layer Effect (Shivashankar et al. 1993)	89
5.2	Confinement Effect (Shivashankar et al. 1993)	90
5.3	Additional Surcharge Effect (Shivashankar et al. 1993)	91
5.4	Proposed Additional Surcharge Effect for Prestressed RGB (Square footing)	93
5.5	Comparison between observed and predicted values of BCR for GB, RGB and PRGB with single layer geogrid reinforcement of size 5B x 5B	94
5.6	Comparison between observed and predicted values of BCR for GB, RGB and PRGB with single layer geotextile reinforcement of size 5B x 5B	95
5.7	Comparison between observed and predicted values of BCR for GB, RGB and PRGB with single layer geogrid reinforcement of size 2B x 2B	96
5.8	Comparison between observed and predicted values of BCR for GB, RGB and PRGB with double layer geogrid reinforcement of size 5B x 5B	97
5.9	Comparison between predicted values of BCR using numerical model and FE analysis for GB, RGB and PRGB with single layer geogrid reinforcement of size 5B x 5B	98
5.10	Comparison between predicted values of BCR using numerical model and FE analysis for GB, RGB and PRGB with single layer geotextile reinforcement of size 5B x 5B	99
5.11	Comparison between predicted values of BCR using numerical model and FE analysis for GB, RGB and PRGB with single layer geogrid reinforcement of size 2B x 2B	100
5.12	Comparison between predicted values of BCR using numerical model and FE	101

	analysis for GB, RGB and PRGB with double layer geogrid reinforcement of size $5B \times 5B$	
6.1	Void just above the interface between GB and weak soil, $x = 0, y = 0.7B$	104
6.2	Geometric model for PRGB of thickness B having void with $x = 0, y = 0.7B$	104
6.3	Stress vs normalized settlement curves for GB, RGB and PRGB of thickness B with void having $x = 0, y = 0.7B$	105
6.4	Void just above the interface between GB and weak soil, $x = 0.2B, y = 0.7B$	105
6.5	Geometric model for PRGB of thickness B having void with $x = 0.2B, y = 0.7B$	106
6.6	Stress vs normalized settlement curves for GB, RGB and PRGB of thickness B with void having $x = 0.2B, y = 0.7B$	106
6.7	Void at the interface between GB and weak soil, $x = 0, y = B$	107
6.8	Geometric model for PRGB of thickness B having void with $x = 0, y = B$	107
6.9	Stress vs normalized settlement curves for GB, RGB and PRGB of thickness B with void having $x = 0, y = B$	108
6.10	Void at the interface between GB and weak soil, $x = 0.2B, y = B$	108
6.11	Geometric model for PRGB of thickness B having void with $x = 0.2B, y = B$	109
6.12	Stress vs normalized settlement curves for GB, RGB and PRGB of thickness B with void having $x = 0.2B, y = B$	110
6.13	Void just below the interface between GB and weak soil, $x = 0, y = 1.3B$	110
6.14	Geometric model for PRGB of thickness B having void with $x = 0, y = 1.3B$	111
6.15	Stress vs normalized settlement curves for GB, RGB and PRGB of thickness B with void having $x = 0, y = 1.3B$	111
6.16	Void just below the interface between GB and weak soil, $x = 0.2B, y = 1.3B$	112
6.17	Geometric model for PRGB of thickness B having void with $x = 0.2B, y = 1.3B$	112
6.18	Stress vs normalized settlement curves for GB, RGB and PRGB of thickness B with void having $x = 0.2B, y = 1.3B$	113
6.19	Void at a depth of $0.75B$ below the interface between GB and weak soil, $x = 0, y = 1.75B$	114
6.20	Geometric model for PRGB of thickness B having void with $x = 0, y = 1.75B$	114
6.21	Stress vs normalized settlement curves for GB, RGB and PRGB of thickness B with void having $x = 0, y = 1.75B$	115
6.22	Void at a depth of $0.75B$ below the interface between GB and weak soil, $x = 0.2B, y = 1.75B$	115
6.23	Geometric model for PRGB of thickness B having void with $x = 0.2B, y = 1.75B$	116
6.24	Stress vs normalized settlement curves for GB, RGB and PRGB of thickness B	116

	with void having $x=0.2B$, $y = 1.75 B$	
6.25	Void just above the interface between GB and weak soil, $x = 0$, $y = 1.7B$	117
6.26	Geometric model for PRGB of thickness $2B$ having void with $x = 0$, $y = 1.7B$	118
6.27	Stress vs normalized settlement curves for GB, RGB and PRGB of thickness $2B$ with void having $x=0$, $y = 1.7 B$	118
6.28	Void just above the interface between GB and weak soil, $x = 0.2B$, $y = 1.7B$	119
6.29	Geometric model for PRGB of thickness $2B$ having void with $x = 0.2B$, $y =$ $1.7B$	119
6.30	Stress vs normalized settlement curves for GB, RGB and PRGB of thickness $2B$ with void having $x=0.2B$, $y = 1.7 B$	120
6.31	Void at the interface between GB and weak soil, $x = 0$, $y = 2B$	121
6.32	Geometric model for PRGB of thickness $2B$ having void with $x = 0$, $y = 2B$	121
6.33	Stress vs normalized settlement curves for GB, RGB and PRGB of thickness $2B$ with void having $x=0$, $y = 2 B$	122
6.34	Void at the interface between GB and weak soil, $x = 0.2B$, $y = 2B$	122
6.35	Geometric model for PRGB of thickness $2B$ having void with $x = 0.2B$, $y = 2B$	123
6.36	Stress vs normalized settlement curves for GB, RGB and PRGB of thickness $2B$ with void having $x=0.2B$, $y = 2 B$	123
6.37	Void just below the interface between GB and weak soil, $x = 0$, $y = 2.3B$	124
6.38	Geometric model for PRGB of thickness $2B$ having void with $x = 0$, $y = 2.3B$	124
6.39	Stress vs normalized settlement curves for GB, RGB and PRGB of thickness $2B$ with void having $x=0$, $y = 2.3 B$	125
6.40	Void just below the interface between GB and weak soil, $x = 0.2B$, $y = 2.3B$	125
6.41	Geometric model for PRGB of thickness $2B$ having void with $x = 0.2B$, $y =$ $2.3B$	126
6.42	Stress vs normalized settlement curves for GB, RGB and PRGB of thickness $2B$ with void having $x=0.2B$, $y = 2.3 B$	126
6.43	Void at a depth of $0.75B$ below the interface between GB and weak soil, $x = 0$, y $= 2.75B$	127
6.44	Geometric model for PRGB of thickness $2B$ having void with $x = 0$, $y = 2.75B$	127
6.45	Stress vs normalized settlement curves for GB, RGB and PRGB of thickness $2B$ with void having $x=0$, $y = 2.75 B$	128
6.46	Void at a depth of $0.75B$ below the interface between GB and weak soil, x $= 0.2B$, $y = 2.75B$	129
6.47	Geometric model for PRGB of thickness $2B$ having void with $x = 0.2B$, $y =$ $2.75B$	129
6.48	Stress vs normalized settlement curves for GB, RGB and PRGB of thickness $2B$	130

	with void having $x=0.2B$, $y=2.75 B$	
6.49	Reduction factor vs prestress curves for GB, RGB and PRGB of thickness B with various positions of void	131
6.50	Reduction factor vs prestress curves for GB, RGB and PRGB of thickness $2B$ with various positions of void	131
6.51	Reduction factor vs depth of void curves for GB, RGB and PRGB of thickness B with $x = 0$	132
6.52	Relationship between Reduction factor and depth of void for GB, RGB and PRGB of thickness B with $x = 0$	132
6.53	Reduction factor vs depth of void curves for GB, RGB and PRGB of thickness B with $x = 0.2B$	133
6.54	Relationship between Reduction factor and depth of void for GB, RGB and PRGB of thickness B with $x = 0.2B$	133
6.55	Reduction factor vs depth of void curves for GB, RGB and PRGB of thickness $2B$ with $x = 0$	134
6.56	Relationship between Reduction factor and depth of void for GB, RGB and PRGB of thickness $2B$ with $x = 0$	134
6.57	Reduction factor vs depth of void curves for GB, RGB and PRGB of thickness $2B$ with $x = 0.2B$	135
6.58	Relationship between Reduction factor and depth of void for GB, RGB and PRGB of thickness $2B$ with $x = 0.2B$	135
6.59	Reduction factor vs eccentricity of void curves for GB, RGB and PRGB of thickness B with $y=0.7B$	136
6.60	Reduction factor vs eccentricity of void curves for GB, RGB and PRGB of thickness B with $y=B$	137
6.61	Reduction factor vs eccentricity of void curves for GB, RGB and PRGB of thickness B with $y=1.3B$	137
6.62	Reduction factor vs eccentricity of void curves for GB, RGB and PRGB of thickness B with $y=1.75B$	138
6.63	Reduction factor vs eccentricity of void curves for GB, RGB and PRGB of thickness $2B$ with $y=1.7B$	139
6.64	Reduction factor vs eccentricity of void curves for GB, RGB and PRGB of thickness $2B$ with $y=2B$	140
6.65	Reduction factor vs eccentricity of void curves for GB, RGB and PRGB of thickness $2B$ with $y=2.3B$	140
6.66	Reduction factor vs eccentricity of void curves for GB, RGB and PRGB of thickness $2B$ with $y=2.75B$	141
7.1	Vertical stress at interface vs distance from centre of footing curves for GB, RGB and PRGB of thickness B overlying (moist) weak soil 1	142
7.2	Vertical stress at interface vs distance from centre of footing curves for GB,	143

	RGB and PRGB of thickness 2B overlying (moist) weak soil 1	
7.3	Vertical stress at interface vs distance from centre of footing curves for GB, RGB and PRGB of thickness B overlying (submerged) weak soil 2	144
7.4	Vertical stress at interface vs distance from centre of footing curves for GB, RGB and PRGB of thickness 2B overlying (submerged) weak soil 2	145
7.5	Settlement at interface vs distance from centre of footing curves for GB, RGB and PRGB of thickness B overlying (moist) weak soil 1	146
7.6	Settlement at interface vs distance from centre of footing curves for GB, RGB and PRGB of thickness 2B overlying (moist) weak soil 1	146
7.7	Settlement at interface vs distance from centre of footing curves for GB, RGB and PRGB of thickness B overlying (submerged) weak soil 2	147
7.8	Settlement at interface vs distance from centre of footing curves for GB, RGB and PRGB of thickness 2B overlying (submerged) weak soil 2	148

NOMENCLATURE

GB	Granular Bed
RGB	Reinforced Granular Bed
PRGB	Prestressed Reinforced Granular Bed
BCR	Bearing Capacity Ratio
B	Width of the square footing
ΔBCR_{SL}	Improvement in bearing capacity ratio due to Shear layer effect
ΔBCR_{CE}	Improvement in bearing capacity ratio due to Confinement effect
ΔBCR_{SE}	Improvement in bearing capacity ratio due to Additional Surcharge effect
N_q	Bearing Capacity Factor
Q	Bearing capacity of underlying weak soil
τ_1	Total vertical force in the punching shear failure (vertical) plane due to Shear Layer Effect
τ_2	Total vertical force in the punching shear failure plane (vertical) due to Confinement effect of reinforcement
P_p	Passive force developed on the sides of failure surface per unit length
P'_p	passive force developed on each of four sides of the square column of granular soil beneath the square footing
Φ_s	Angle of shearing resistance
T_R	Tensile stress mobilized in the reinforcement
T'_R	Tensile stress mobilized in reinforcement beyond each of the four sides of square column of granular soil beneath the square footing
L	Length of reinforcement beyond the failure surface
σ_v	Vertical stress at the level of reinforcement
δ	angle of friction between reinforcement and soil
q_0	Intensity of surcharge stress at the edge of the vertical failure plane (on weak soil), due to shear layer and confinement effects
q'	Bearing capacity with void at 5 mm settlement
q	Bearing capacity without void at 5 mm settlement
x	Eccentricity of void
y	Depth of void from the base of footing
R	Reduction factor
F	Reduced Bearing Capacity Factor

CHAPTER 1

INTRODUCTION

1.1 BACKGROUND

The decreasing availability of proper construction sites has led to the increased use of marginal ones, where the bearing capacity of the underlying deposits is very low. The conventional method is to provide deep and costly foundation on such weak deposits. The necessity to develop cost effective solutions has made ground improvement a major research area. The use of geosynthetics to improve the bearing capacity and settlement performance of shallow foundations has proven to be a cost-effective foundation system. In marginal ground conditions, geosynthetics enhance the ability to use shallow foundations in lieu of the more expensive deep foundations. This is done by either reinforcing cohesive soil directly or replacing the poor soils with stronger granular fill in combination with geosynthetics reinforcement. In low-lying areas with poor foundation soils, the geosynthetic reinforced granular bed can be placed over the weak soil. The resulting composite ground (reinforced granular bed) will improve the load carrying capacity of the footing and provide better pressure distribution on top of the underlying weak soils, hence reducing the associated settlements. During the past 30 years, the use of reinforced soils to support shallow foundations has received considerable attention. A number of studies have expanded the knowledge on the failure mechanisms and the potential benefits of soil reinforcement on the bearing capacity and settlement of shallow foundations (eg. Binquet and Lee (1975a,b), Guido et al. 1986, Shivashankar et al. (1993)). Several experimental and analytical studies were conducted to evaluate the bearing capacity of footings on reinforced soil (eg. Shivashankar et al. (1993); Shivashankar and Reddy (1998); Lee et al. (1999); Madhavalatha and Somwanshi (2009a,b); Alamshahi and Hataf (2009); Vinod et al. (2009) etc).

1.2 OBJECTIVE AND SCOPE OF RESEARCH

The bearing capacity and settlement response of weak soils can be improved by laying a compacted granular bed over it. The bearing capacity can be further improved by reinforcing the granular bed with single or multi- layers of geosynthetics (Fig.1.1). The geosynthetics used in

granular beds contribute to the ultimate bearing capacity by mobilizing tensile forces in the reinforcement.

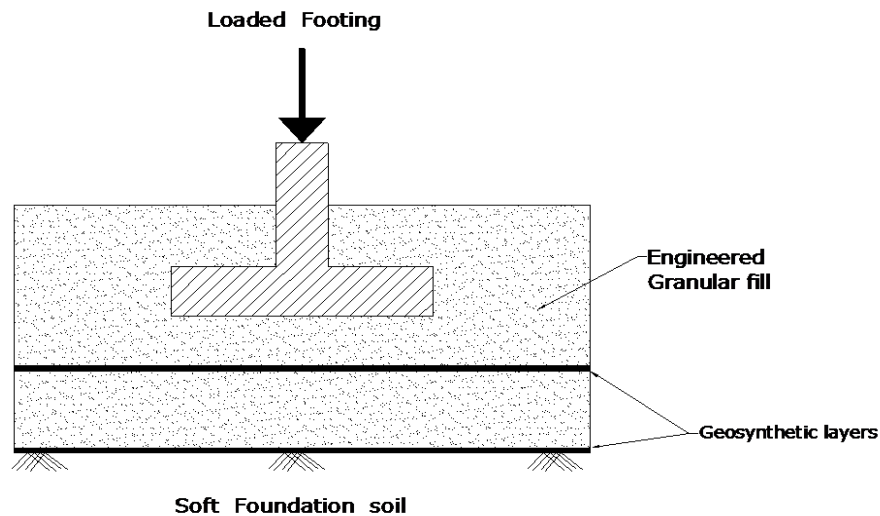


Fig.1.1 Footing supported on Reinforced Granular Bed

Geosynthetics are extensible reinforcements and require some strain for mobilizing the required tensile stress. The strain in reinforcement occurring due to initial settlement is not sufficient to mobilize the required tensile stress in it. Hence geosynthetics demonstrate their beneficial effects only after considerably large settlements, which is not a desirable feature sometimes for shallow foundations. Thus there is a need for a technique which will allow the geosynthetic to increase the load bearing capacity of soil without the occurrence of large settlements.

Prestressing the reinforcement is a promising technique to increase the load bearing capacity of a geosynthetic reinforced soil without the occurrence of large settlements. Lovisa et al. (2010) conducted laboratory model studies and finite element analyses on a circular footing resting on sand reinforced with geotextile to study the effect of prestressing the reinforcement. It was found that the addition of prestress to reinforcement resulted in significant improvement in the load bearing capacity and reduction in settlement of foundation.

A possible method of improving bearing capacity of footings is to provide a geosynthetic reinforced granular bed over the weak soil. Also rather than a circular footing; square or rectangular footings are commonly used. Hence in this investigation an attempt is made to evaluate the effects of prestressing the reinforcement in further improving the bearing capacity of square footings supported on geosynthetic reinforced granular beds overlying weak soil.

The specific objectives of the research are to study the following

1. Effect of magnitude of prestress in the geosynthetic reinforcement
2. Effect of direction of prestress in the geosynthetic reinforcement
3. Effect of number of layers of prestressed geosynthetic reinforcement
4. Effect of type of geosynthetic reinforcement
5. Effect of size of prestressed geosynthetic reinforcement
6. Effect of thickness of granular bed
7. Effect of strength of underlying weak soil
8. Effect of formation of voids in the granular bed and weak soil
9. Interaction between granular bed and weak soil
10. To propose an analytical model for predicting the improvement in bearing capacity of reinforced granular beds overlying weak soil due to prestressing the reinforcement.

The physical behaviour of the prestressed geosynthetic reinforced granular bed is observed by conducting laboratory scale plate load tests. Non-linear finite element analyses are carried out using the FE program PLAXIS, version 8 to validate the results obtained from experimental and analytical studies.

1.3 OUTLINE OF THE THESIS

The thesis is divided into eight chapters. The following is a brief summary of the contents of each chapter

In **Chapter 1**, an introduction to the subject of prestressed reinforced granular bed is given and the objectives and scope of research is elaborated. A broad outline of the following chapters is also given. A review of relevant literature is given in **Chapter 2**. It provides a survey of research about experimental studies, analytical modeling and finite element analyses on reinforced soil. **Chapter 3** describes the materials and test setup used in this study, experimental methodology and the testing program. The finite element analyses done for various cases of granular bed, reinforced granular bed and prestressed reinforced granular bed are explained in **Chapter 4**. The comparison of results obtained from experimental study and finite element analysis are also detailed in this chapter. In **Chapter 5**, the development of an analytical model for predicting the improvement in bearing capacity due to prestressing the reinforcement is explained. The comparison between bearing capacity ratios predicted by the proposed analytical model and

those obtained from experimental and finite element studies are presented in this chapter. The results of finite element analysis on prestressed reinforced granular beds (PRGB) with voids at various locations are detailed in **Chapter 6**. An analysis of the settlements and stresses at the interface between weak soil and granular bed, obtained from FE analysis, are presented in **Chapter 7**. Finally, **Chapter 8** summarizes and concludes this research work and provides some suggestions for future research.

CHAPTER 2

LITERATURE REVIEW

2.1 INTRODUCTION

The geosynthetic-reinforced foundation soils are being used to support footings of many structures including ware houses, oil drilling platforms, bridge abutments, platforms of heavy industrial equipments etc. In usual construction practice, one or more layers of geosynthetic (geotextile, geogrid, geocell or geocomposites) are placed inside a controlled granular fill beneath the footings. Such reinforced foundation soils provide improved load bearing capacity and reduced settlements by distributing the imposed loads over a wider area of weak subsoil. In the conventional construction technique, without any use of reinforcement, a thick granular layer is needed which may be costly or may not be possible, especially in sites of limited availability of good quality granular materials. In general the improved performance of a geosynthetic-reinforced foundation soil can be attributed to an increase in shear strength of the foundation soil from the inclusion of the geosynthetic layers. The soil-geosynthetic system forms a composite material that prevents development of the soil failure wedge beneath shallow spread footings (Shukla and Yin, 2006).

2.2 BEARING CAPACITY OF FOOTINGS ON LAYERED SOILS

The earliest studies conducted on footings supported on stronger soil underlain by weaker soil were by **Terzaghi & Peck (1948)**. They proposed that the total footing load can be assumed to be uniformly distributed over the base of a truncated pyramid whose sides slope from the edges of the footing to the upper surface of underlying weak soil is at an angle of 60° with the horizontal. A punching shear failure mechanism was proposed by **Meyerhof (1974)** for the case of dense sand overlying soft clay. The ultimate bearing capacity of footings resting on dense sand underlain by soft clay was determined from punching shear coefficients. For footings resting on loose sand underlain by stiff clay, he proposed modified bearing capacity coefficients or an empirical interaction relationship.

Madhav and Sharma (1991) proposed that for a footing resting on stiff upper layer overlying soft clay, the stiffer layer distributes the applied stress on to the underlying soft soil over a much larger width. The loading on soft clay is considered to be uniform over a width B , and then to

decrease either linearly or exponentially with distance. **Madhav and Datye (1993)** estimated the bearing capacity of footing on a soil in an undrained condition but with surcharge varying with distance and extending to only a finite distance beyond the footing. Three types of variation of surcharge stress, viz., uniform, linear and exponential decay were considered. They proposed equations for increase in bearing capacity for all the three cases.

2.3 EXPERIMENTAL WORK ON BEARING CAPACITY OF REINFORCED SOIL

Madhavilatha and Somwanshi (2009a) conducted laboratory model tests and numerical simulations of reinforced sand supporting a square footing. The parameters varied in the study are type of geosynthetic, depth of reinforced zone, number of reinforcement layers and width of reinforcement. The laboratory tests were simulated using the software FLAC 3D. They concluded that the effective depth of reinforced zone below a square footing is equal to twice the width of the footing and the most optimum spacing of reinforcement is equal to 0.4 times the width of footing. The improvement in bearing capacity depends upon the layout, configuration and the tensile strength of reinforcement. The most optimum width of reinforcement was found to be equal to four times the width of footing.

Vinod et al. (2009), conducted laboratory scale plate load tests to study the behaviour of loose sand reinforced with braided coir rope. They concluded that the optimum depth of single layer braided coir rope reinforcement is equal to 0.4 times the width of footing. They conducted a regression analysis and developed an empirical relationship to determine the strength improvement. They found out that the strength of loose sand can be increased by up to six times and settlement reduced by up to 90% by reinforcing with braided coir rope.

Sadoglu et al. (2009) conducted a series of laboratory model tests on eccentrically loaded strip footings supported on reinforced dense sands. The experimental results were compared with commonly used approaches such as Meyerhof's effective width concept and the customary analysis. They concluded that the addition of geotextile reinforcement increased the ultimate load bearing capacity of strip footing under eccentric loads. The decrease in ultimate bearing capacity due to eccentricity of load in the unreinforced case was in good agreement with Meyerhof's theory and that of reinforced case was generally in good agreement with the customary analysis. They also reported that the vertical displacement at failure decreases with increasing eccentricity for both reinforced and unreinforced case.

Madhavilatha and Somwanshi (2009b) conducted laboratory scale experimental and numerical studies to determine the effect of reinforcement form on the improvement in bearing capacity of a square footing resting on reinforced sand. They used two types of reinforcement, viz. geonet and biaxial geogrid. The geonet was used in planar form and in geocell form. The biaxial geogrid was used in planar, geocell and randomly distributed mesh forms. Numerical studies were carried out using the software FLAC 3D. They concluded that the improvement in bearing capacity is significantly affected by the form of reinforcement. They have reported that reinforcement in the form of randomly distributed mesh is inferior to both planar and geocell forms. The best form of reinforcement is geocell, if there is no rupture of the material. From the numerical results they concluded that geocell transfers the stress from footing to deeper soil layers and hence the stresses and strains underneath the footing are reduced. It also prevents the surface heave near the footings.

Alamshahi and Hataf (2009) studied the effect of providing grid anchors to geogrid in a reinforced sand slope. They conducted a series of laboratory scale model tests on a strip footing resting on a reinforced sand slope. They also conducted finite element analysis on a prototype slope using the FE software PLAXIS. The parameters studied are type of geogrid, number of layers of reinforcement, vertical spacing of reinforcement and location of the topmost reinforcement layer. They found that the addition of grid anchors to geogrid enhances the pullout strength of the reinforcement and results in a better improvement of bearing capacity.

Chen et al. (2009), conducted laboratory model tests on spread footings supported on reinforced crushed lime stone. They studied the effects of parameters like number of layers of reinforcement, type of reinforcement and tensile modulus of reinforcement etc. They proposed that a punching shear failure occurs partially in the reinforced zone and is followed by a general shear failure.

To estimate the ultimate bearing capacity of reinforced crushed lime stone, they improvised the solution for footings on two layer soil system by **Meyerhof and Hanna(1978)**, by adding an additional term Δq_T , to include the effect of tensile force in the reinforcement.

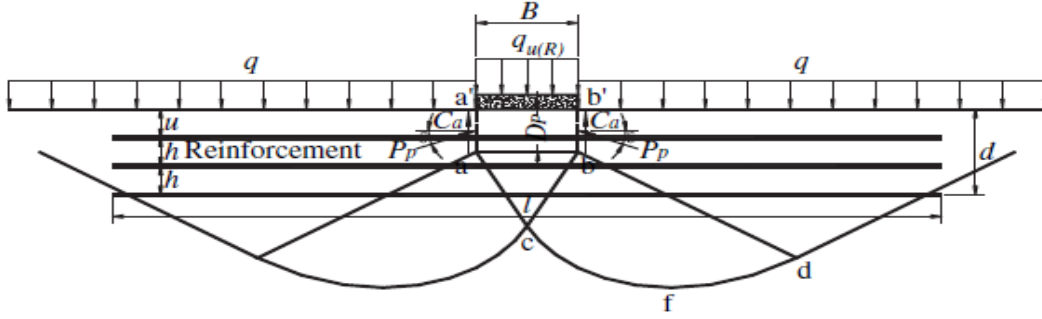


Fig.2.1 Proposed failure mode for reinforced crushed lime stone (Meyerhof and Hanna, 1978)

The equation proposed for the ultimate bearing capacity of strip footing on reinforced crushed lime stone (Fig.2.1) was

$$q_{u(R)} = q_{u(g)} + \frac{2c_a D_p}{B} + \gamma D_p^2 \left(1 + \frac{2D_f}{D_p} \right) \frac{K_s \tan \phi}{B} - \gamma D_p + \Delta q_T$$

For horizontal confinement effect of reinforcement,

$$\Delta q_T = 2 \sum_{i=1}^{N_p} \frac{T_i}{B} \tan \delta + \sum_{i=N_p+1}^N \frac{4T_i [u + (i-1)h - D_p]}{B^2}$$

For reinforcement tension along the faces of the soil wedge,

$$\Delta q_T = 2 \sum_{i=1}^{N_p} \frac{T_i}{B} + \sum_{i=N_p+1}^N \frac{2T_i \sin((\pi/4) + (\phi/2))}{B}$$

Where

$q_{u(R)}$ = ultimate bearing capacity of reinforced soil

$q_{u(g)}$ = ultimate bearing capacity of unreinforced soil located in the general shear failure zone

γ = Unit weight of soil

D_f = embedment depth of the footing

K_s = punching shear coefficient

T_i = tensile force in the i^{th} layer of reinforcement

N = number of reinforcement layers

N_p = number of reinforcement layers located in the punching shear failure zone

They also conducted finite element analysis of square footings of various sizes on crushed lime stone to study the scale effect. They concluded that the bearing capacity of crushed lime stone can be increased considerably by the addition of reinforcement. By increasing the number of reinforcement layers, the

bearing capacity ratio increases and the settlement reduction factor decreases. They observed that geogrids with higher tensile modulus performed better than those with lower tensile modulus. They also observed that crushed lime stone reinforced with steel mesh performed better than that with geogrids.

Tafreshi and Dawson (2010a) conducted laboratory model tests on strip footings supported on sand beds reinforced with geocell and planar forms of reinforcement. They studied the effects of various parameters like number of reinforcement layers, width of reinforcement and depth of geocell below the footing. They concluded that for the same quantity of geotextile material geocell gives more improvement than equivalent planar reinforcement. They also concluded that even though an increase in the number of reinforcement layers, reinforcement width, height of geocell etc may increase the load bearing capacity, the efficiency of the reinforcement decreases.

Mohamed (2010) carried out laboratory model tests to investigate the efficiency of reinforcement layers in improving the bearing capacity of soils having localized soft pockets. At predetermined locations within the sand bed a relatively softer material was embedded to form soft pockets. The parameters studied were the effect of depth of reinforcement, length of reinforcement, number of layers of reinforcement, width of soft pocket and depth of soft pocket. They observed that the ultimate bearing capacity reduced by up to 70% due to the influence of soft pocket. The ultimate bearing capacity was also influenced by the location of the soft pocket.

Tafreshi and Dawson (2010 b) conducted experimental studies on model strip footings supported on sand reinforced with planar and 3D geotextile, under static and repeated loading. They recorded the footing settlement due to initial static load and up to 20,000 subsequent load repetitions. They concluded that for given amplitude of repeated load, the increase in the layers of planar reinforcement and the height of 3D reinforcement decreases the settlement; however the efficiency of reinforcement decreases. They reported that the 3D geotextile offers more resistance to plastic deformation than planar geotextile.

Choudhary et al. (2010) conducted laboratory scale bearing capacity tests on strip footing resting on a reinforced flyash slope. The effect of parameters like location and depth of embedment of single reinforcement layer, number of layers of reinforcement, location of footing relative to the crest of the slope, width of footing, slope angle etc. They concluded that the edge distance has an important effect on the bearing capacity of footings on unreinforced as well as reinforced slopes. They reported that the bearing capacity of footing decreases with increase in

slope angle and the location of single layer reinforcement deeper than 2.5 times the width of footing does not appreciably increase the bearing capacity.

2.4 ANALYTICAL MODELING OF REINFORCED GRANULAR BED

Binquet and Lee (1975a, b) were the first to study the problem of bearing capacity of reinforced foundation beds analytically and experimentally. They conducted studies on model strip footings supported on sand reinforced with aluminium foil. They developed an analytical method for estimating the increase in bearing capacity and validated it with their experimental results. They found out that the, by the inclusion of reinforcement in soil, ultimate bearing capacities of footings can be improved by a factor of about 2 to 4 times that of an unreinforced soil. They observed that the improvement in bearing capacity increased with the number of layers up to 8 layers, beyond which further improvement was negligible.

Huang and Tatsuoka (1990) conducted a series of plane strain model tests on strip footing resting on reinforced sand, to develop a method for the prediction of bearing capacity. They observed that even with reinforcement layers having length equal to the width of the footing, the bearing capacity increased remarkably. The portion of reinforcement outside the footing width contributed to the increase in bearing capacity only in a secondary way.

Shivashankar et al. (1993) studied the improvement in bearing capacity of footings resting on granular bed overlying soft clay, assuming a punching shear failure mechanism in the foundation soil. The improvement is attributed to three effects such as (a) shear layer effect, (b) confinement effect and (c) additional surcharge effect. The improvement in bearing capacity, defined in terms of bearing capacity ratio (BCR), as the ratio of improved bearing capacity to the original bearing capacity is given as

$$BCR = 1 + \Delta BCR_{SL} + \Delta BCR_{CE} + \Delta BCR_{SE}$$

Where ΔBCR_{SL} , ΔBCR_{CE} , ΔBCR_{SE} = Improvement in bearing capacity ratio due to Shear layer, Confinement and Additional Surcharge effects respectively

Ghosh and Madhav (1994a) developed a simple mathematical model to account for the membrane effect of a reinforcement layer on the load-settlement response of a reinforced granular fill-soft soil foundation system. Parametric studies, carried out on a uniformly loaded strip footing, showed that the reduction in settlement of footing due to the membrane action of

reinforcement is more than due to the effect of granular fill. **Ghosh and Madhav** (1994b) further developed a model for analysis of a reinforced foundation bed by incorporating the confinement effect of a single layer of reinforcement.

Yamamoto and Otani (2002) conducted a rigid-plastic finite element analysis considering the effect of geometrical nonlinearity to investigate the increase in bearing capacity and progress in deformation localization due to the settlement of a loaded plate. Both the reinforced soil and soft ground were modeled using the Von-Mises failure criterion.

Madhav and Umashankar (2003) presented an approach for the analysis of sheet reinforcement subjected to transverse force. They assumed the reinforcement as inextensible and a Winkler type model for the response of ground. Under the action of transverse force or displacement, the soil beneath the reinforcement mobilizes additional normal stresses as the reinforcement deforms transversely. Considering linear subgrade response and inextensible reinforcement, the resistance to transverse force is estimated. They established that the pullout resistance of reinforcement, subjected to transverse pull, in dense granular fills is larger than the pure axial pullout capacity.

Michalowski and Shi (2003) conducted laboratory scale load tests on strip footings resting on sand reinforced with geotextile to investigate the kinematics of collapse. They digitally recorded sequential images of the deformation field under the model footing. They arrived at an incremental displacement field under the model footing using a correlation based motion detection technique. They observed that horizontal motion of sand above the reinforcement was prevented due to the presence of the reinforcement. Relative sliding between reinforcement and sand occurs only at the bottom side interface. Hence the rate at which work is dissipated is different at the two interfaces of the reinforcement.

Deb et al. (2006) (Fig 2.2) presented a model for the analysis of reinforced granular foundation beds with many geosynthetic layers. The reinforcement has been modeled as stretched rough elastic membranes and the granular bed as Pasternak shear layer. The soft soil has been modeled as a series of nonlinear springs. They have assumed plane strain conditions for the reinforced foundation soil system and for loading. Parametric studies have been carried out to investigate the overall behaviour of multilayer geosynthetic reinforced soil. Solutions were formulated using finite difference method and the results are presented in nondimensional form. The behaviour of extensible reinforcement are compared with that of inextensible reinforcements.

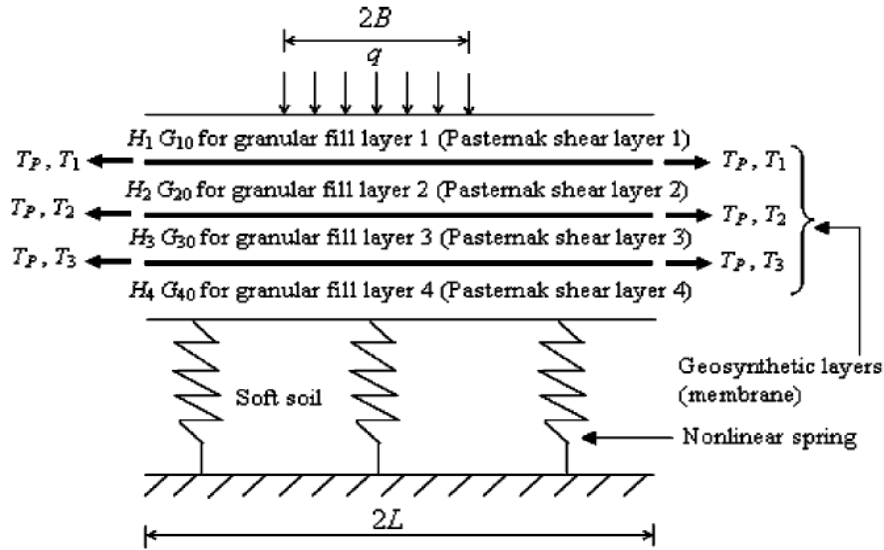


Fig.2.2 Proposed foundation model (Deb et al., 2006)

They observed that the reduction in settlement is more with inextensible reinforcement than with extensible reinforcement. The mobilized tension is more in inextensible reinforcements than in extensible reinforcements. With an increase in the number of layers of reinforcement, the nonlinear behaviour of soil decreases. As the ultimate bearing capacity of soft soil increases, the mobilized tension in the geosynthetic layer decreases.

Deb et al. (2007) carried out a numerical study to investigate the behaviour of multi layer reinforced granular bed overlying soft soil using Fast Lagrangian Analysis of Continua (FLAC) software (Fig. 2.3). They considered the reinforcement, soft soil and granular bed as linearly elastic materials. They modeled the reinforcements as cable elements fully bonded with the granular fill, thereby neglecting any slip. The results are compared with those obtained from finite element analyses and lumped parameter modeling.

They observed that the results from FLAC were in close agreement with those obtained from finite element analyses and lumped parameter modeling. As the number of layers of reinforcement increases the maximum settlement reduces at a decreasing rate. The lateral stresses increased with an increase in the number of layers of reinforcement. This is due to the confinement effect of reinforcement. The increase in the number of layers of reinforcement caused a reduction in the shear stresses in the reinforced zone.

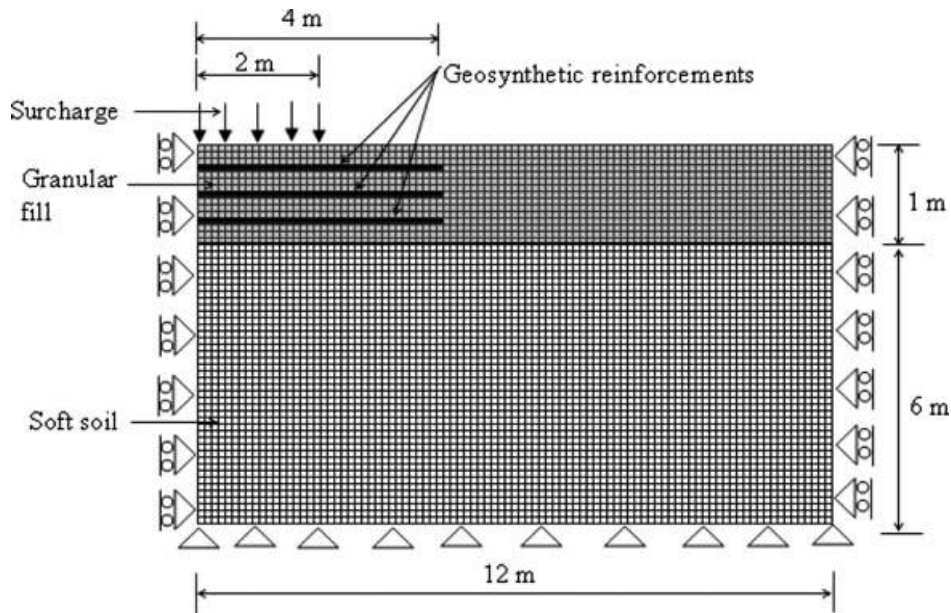


Fig.2.3 Modeling using FLAC (Deb et al., 2007)

Sharma et al. (2009) developed analytical solutions and proposed failure mechanisms for reinforced soil foundations for sand and silty clay, based on earlier studies and based on the results of their large scale and small scale model tests. They proposed new bearing capacity formulae which consider the contribution of reinforcement tension in the improvement of bearing capacity of reinforced soil foundations. The proposed formula was validated using the results of the large scale and small scale model tests conducted by them.

2.5 PRESTRESSED REINFORCED SOIL

Roh and Tatsuoka (2001) conducted a series of plane strain compression tests on reinforced saturated soft clay to investigate the effects of preloading and prestressing on its stress-strain properties. They observed that the application of drained preloading to a load level higher than the drained strength of unreinforced clay will considerably improve the peak strength of reinforced clay under undrained conditions. The initial stiffness at small strains of the preloaded clay increases with the increase in prestress if the prestress level and preload level are not too close to each other. They concluded that high water content clay backfill can be made stronger and stiffer by the inclusion of tensile reinforcement together with an appropriate preloading and prestressing procedure.

Lovisa et al. (2010) conducted laboratory model studies (Fig.2.4) on a circular footing resting on sand reinforced with geotextile. The improvement in bearing capacity due to prestressing the reinforcement was studied. It was found that the addition of prestress resulted in significant improvement in the load bearing capacity and reduction in settlement of foundation. The prestress applied was equal to 2% of the tensile strength of reinforcement. They observed that the load carrying capacity at 5 mm settlement with prestressed reinforcement is approximately double that of reinforced sand without prestress.



Fig.2.4 Experimental setup for prestressing the geotextile (Lovisa et al., 2010)

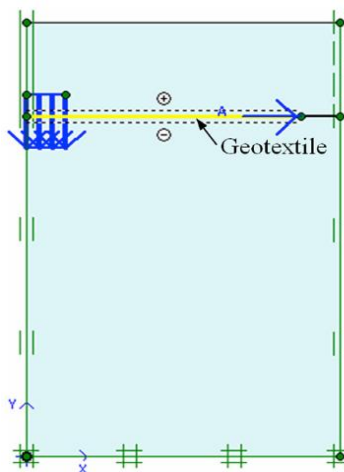


Fig.2.5 Modeling prestressed geotextile reinforced sand in PLAXIS (Lovisa et al., 2010)

They also carried out finite element analysis using the FE software PLAXIS (Fig.2.5). The analysis was carried out using an axisymmetric model. The geotextile was modeled using a 5

noded tension element. The settlement of the rigid footing was simulated using non zero prescribed displacements. The results obtained from finite element analysis were generally in good agreement with the experimental results.

Lackner et al. (2013) presented the results of laboratory scale model tests conducted on prestressed reinforced soil. They conducted about 60 path controlled static load displacement tests and 80 cyclic load displacement tests to determine the load-displacement behaviour of prestressed reinforced soil structures. They also conducted a detailed meoscopic analysis using particle image velocimetry method. They proposed three possible modes of prestressing, viz. Prestressed reinforced soil by compaction (PRS_C), Permanently prestressed reinforced soil (PRS_P) and Temporarily prestressed reinforced soil (PRS_T).

If the reinforcement gets prestressed due to the spreading forces caused by the compaction of the overlying granular layer, it is called Prestressed reinforced soil by compaction (PRS_C) (Fig.2.6).

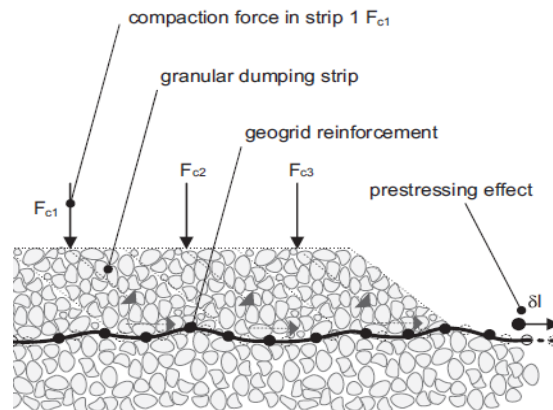


Fig.2.6 Concept of Prestressed reinforced soil by compaction (PRS_C)(Lackner et al. 2013)

In Permanently prestressed reinforced soil (PRS_P) (Fig2.7), the reinforcement is tensioned before the laying granular soil above it and the prestress is maintained permanently.

In Temporarily prestressed reinforced soil (PRS_T) (Fig2.8), the reinforcement is tensioned before laying the granular fill over it. After laying and compacting the granular fill over the reinforcement, the prestress is released. This will cause the reinforcement to contract and additional compressive forces will act on the granular particles.

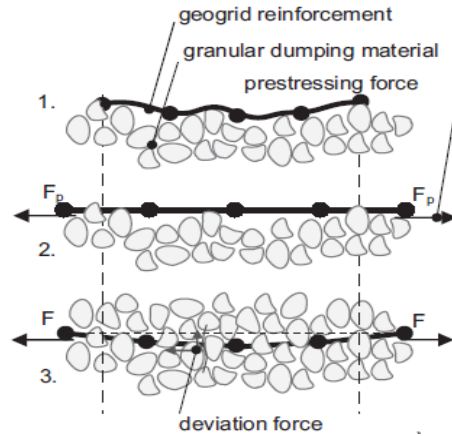


Fig.2.7 Concept of Permanently prestressed reinforced soil (PRS_p) (Lackner et al. 2013)

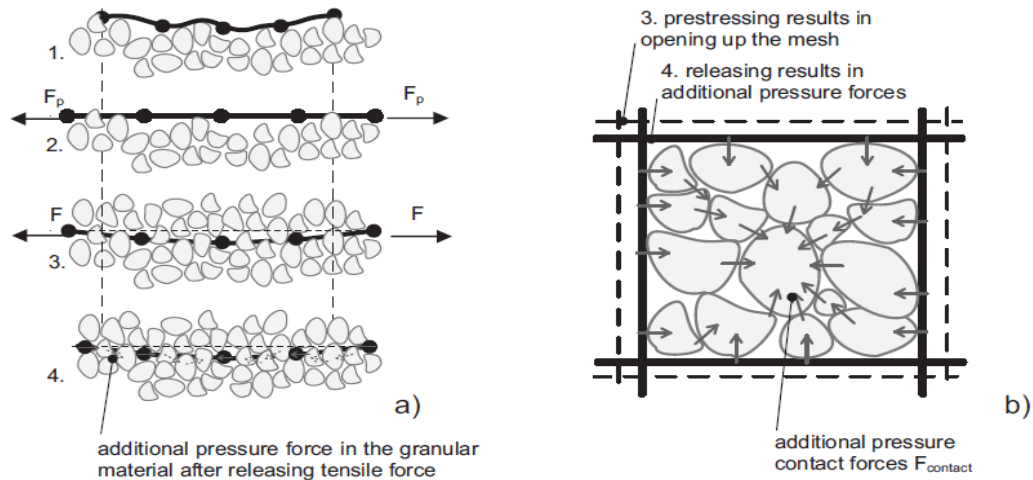


Fig.2.8 Concept of Temporarily prestressed reinforced soil (PRS_T) (Lackner et al. 2013)

They concluded that prestressing the reinforcement improves the load-displacement behaviour of reinforced soil structures. They observed that in static tests the highest increase in bearing capacity was attained by temporarily prestressed reinforced soil (PRS_T). Results of PIV analyses indicated that an additional bedding support was activated due to prestressing of reinforcement. The settlement under cyclic loading was reduced by 80% due to prestressing the reinforcement.

2.6 EFFECT OF FORMATION OF VOID / CAVITY IN REINFORCED SOIL

Baus and Wang (1983) investigated experimentally and analytically the behaviour of a strip footing located above a continuous void in silty clay soil. Laboratory scale model tests were

conducted in a test tank of dimensions 1.7m length x 1.4 m width x 1.2 m height. Sides of the tank were made with plexiglass so that deformation of soil was visible. They also conducted finite element analysis (Fig.2.9) to investigate the behaviour of continuous footing situated above a continuous void which is either circular or rectangular in cross section. In the finite element analysis they considered soil as an elastic perfectly plastic material.

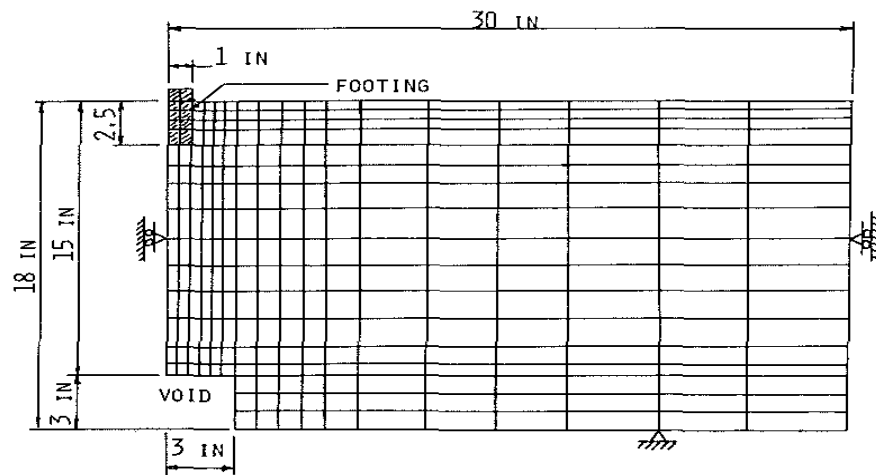


Fig.2.9 Descretized model of footing above void (Baus and Wang, 1983)

They concluded that there exists a critical depth below which the void has only a negligible effect on the behaviour of foundation. When the void is located above the critical depth, the bearing capacity of footing depends upon factors like depth of foundation, size of void, location of void etc.

Wang and Badie (1985) investigated the effect of an underground void on the stability of shallow foundation using a three dimensional finite element computer program. The parameters varied were shape of the footing, shape of the void, orientation of void axis with respect to strip footing axis and location of void. They developed relationships between bearing capacity and void locations for different footing shapes, void shapes and void orientations. They concluded that the underground void will influence the footing only if it is located above a critical depth. The critical depth depends upon various factors like shape of the void, shape of the footing, type of soil, size of void, orientation of void etc.

Wang and Hseigh (1987) conducted numerical analysis using upper bound theorem of limit analysis to determine the collapse footing pressure of strip footings centered above continuous circular voids. In the analysis the footing was assumed as a rigid body and soil as a rigid-plastic

material. They developed equations relating collapse footing pressure, soil properties and the size and location of void.

Azam et al. (1991) conducted finite element studies to investigate the behaviour of strip footings on homogeneous soil and stratified soil with and without void. They concluded that for a soil layer underlain by bed rock the footing performance will be influenced by the presence of bedrock only if the depth of bed rock is within six times the width of footing. If a void is present in the soil its influence on the behaviour of footing depends upon void location, depth to bed rock, thickness of soil layer, strength ratio etc.

Kiyosumi et al. (2007) conducted a two dimensional plane strain finite element analysis (Fig.2.10) to investigate the effect of multiple voids on the yielding pressure of strip footing. They also developed a practical calculation formula to estimate the yielding pressure of strip footing over multiple voids.

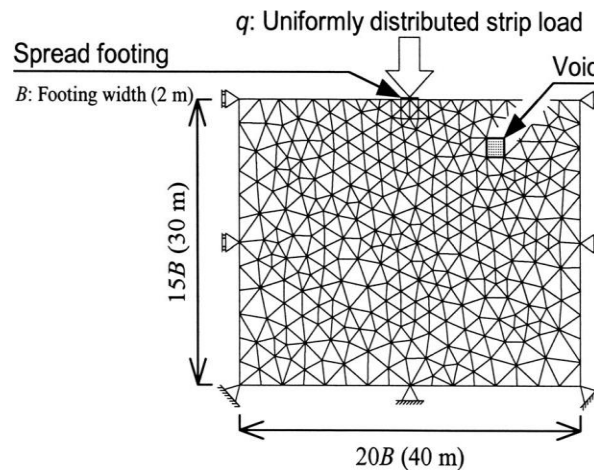


Fig.2.10 Typical Finite Element Mesh (Kiyosumi et al. 2007)

They concluded that if only a single void is present the influence of void on the behaviour of footing depends upon the parameters indicating the location of void. The failure zone extends from the edge of the footing to the nearest corners of the void. If multiple voids are present there is a strong tendency for the failure zone to develop to the nearest void.

Briancon and Villard (2008) proposed a new analytical design method for geosynthetic reinforced platforms spanning localized sink holes by considering the stretching of the reinforcement in the anchorage areas and the increase in stress on the edges of cavity. The analytical method was validated by the results of full scale experimental results and finite element calculations. They also developed a design chart for a particular case. Results of

parametric studies conducted indicated that for the design of geosynthetic reinforced platforms over voids, an accurate knowledge about the void diameter is required. Hence they concluded that geotechnical studies which can provide relevant information about the existing voids and about the evolutionary mechanisms of collapse are of great importance.

Sireesh et al. (2009) conducted a series of laboratory scale model tests to investigate the benefits of providing a geocell mattress over a clay subgrade with a void. The parameters studied in the investigation are width and height of geocell mattress, thickness of unreinforced sand above clay layer, relative density of sand fill in the geocell and influence of an additional layer of planar geogrid at the base of geocell mattress. They concluded that geocell mattress can considerably improve the bearing capacity and reduce the settlement of clay layer with void. They observed that the geocell mattress must spread beyond the void by a distance at least equal to the diameter of the void in order to get the beneficial effects. An increase in the height of the geocell mattress further improved its performance. They also observed that the bearing capacity increases with the increase in the density of fill soil in the geocell.

Kiyosumi et al. (2011) conducted a series of laboratory scale model tests under plane strain condition on stiff soil with continuous square voids. The aim of the investigation was to determine the behaviour of shallow foundations resting on calcareous sediment rocks which are susceptible to the formation of voids due to water dissolution. They concluded that there were three types of failure for a single void

1. Bearing failure without void failure
2. Bearing failure with void failure
3. Void failure without bearing failure

They also observed that there were three types of propagation of slip lines.

1. Slip lines developing downwards from both edges of the footing
2. Slip lines developing downward from the edges of footing as well as upwards from the upper corner of voids
3. Slip lines developing only upwards from the upper corners of voids.

They also observed that if two voids of serial configuration are at shallow depth, the lower void has no influence on the behaviour of footing.

CHAPTER 3

EXPERIMENTAL METHODOLOGY

3.1 INTRODUCTION

In order to observe physically the behaviour of prestressed reinforced granular beds overlying weak soil, extensive experimental investigations are carried out. A series of laboratory scale model tests are carried out on square footings resting on unreinforced granular bed (GB), reinforced granular bed (RGB) and prestressed reinforced granular bed (PRGB). The details of experimental set up, test methodology, materials used and parameters studied are explained in the following sections.

3.2 PROPERTIES OF SOIL USED

3.2.1 Granular Bed

The material used for granular bed is sand. Its properties are given in Table 3.1 and particle size distribution shown in Fig. 3.1. The sand was used in the dry condition in all the tests.

Table 3.1 Properties of sand used for granular bed

Property	Value
Specific Gravity	2.61
Average dry unit weight during model test (KN/m ³)	16.60
Void ratio during model test	0.54
Effective Grain size D ₁₀ (mm)	0.50
D ₆₀ (mm)	1.30
D ₃₀ (mm)	0.80
Coefficient of Uniformity C _u	2.60
Coefficient of Curvature C _c	1.00
Friction angle Φ°	31.0
Cohesion (kPa)	0
Relative Density	0.86

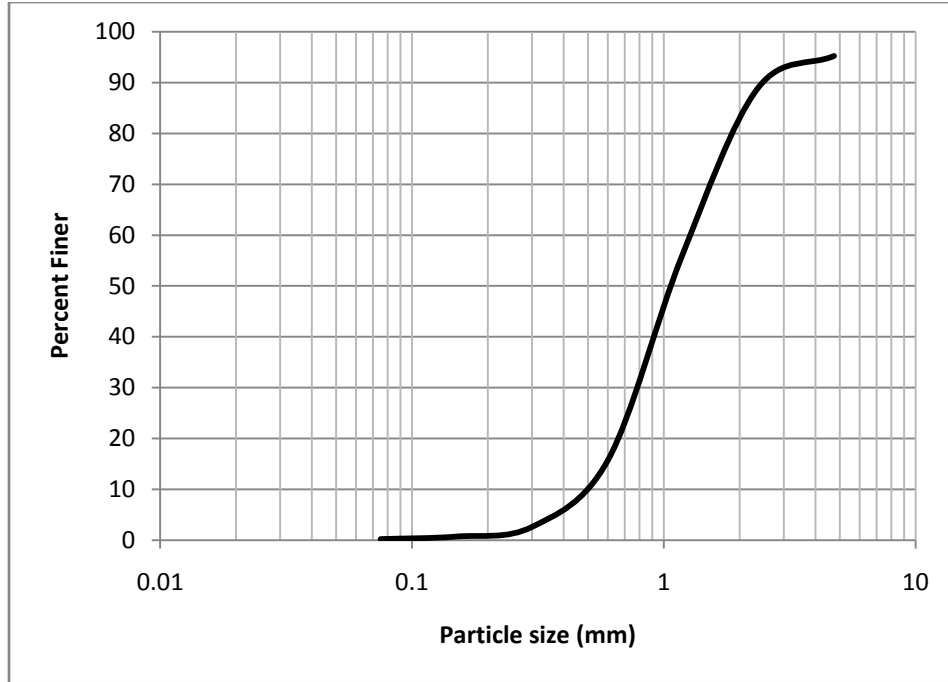


Fig. 3.1. Particle size distribution of sand used in granular bed

3.2.2 Weak soil

Locally available soil termed as Shedi soil is used as weak soil. The Shedi soil is used in two conditions namely moist condition (termed as moist soil or weak soil 1) and also used in submerged condition (termed as submerged soil or weak soil 2).

Table 3.2 Properties of Weak soil used for the investigation

Property	Value
Specific Gravity	2.32
Average dry unit weight during model test (KN/m ³)	16.00
Void ratio during model test	0.42
Effective Grain size D ₁₀ (mm)	0.11
Liquid Limit (%)	37.4
Plastic Limit (%)	32.9
Shrinkage Limit (%)	25.7
Shear parameters of Moist (Weak soil 1)	
Friction angle Φ°	12
Cohesion (kPa)	10
Moisture Content (%)	10
Shear parameters of Submerged (Weak soil 2)	
Friction angle Φ°	6
Cohesion (kPa)	5.5
Moisture Content (%)	31.5

Shedi soils are dispersive soils and are predominantly found in the western coast of peninsular India, which receives heavy rainfall during monsoon. Their strength reduces drastically under saturation condition. Many foundation and slope stability problems are reported wherever this soil is encountered (Bhat et al (2008), Shivashankar and Setty(2000)). Its properties are given in Table 3.2 and particle size distribution shown in Fig. 3.2.

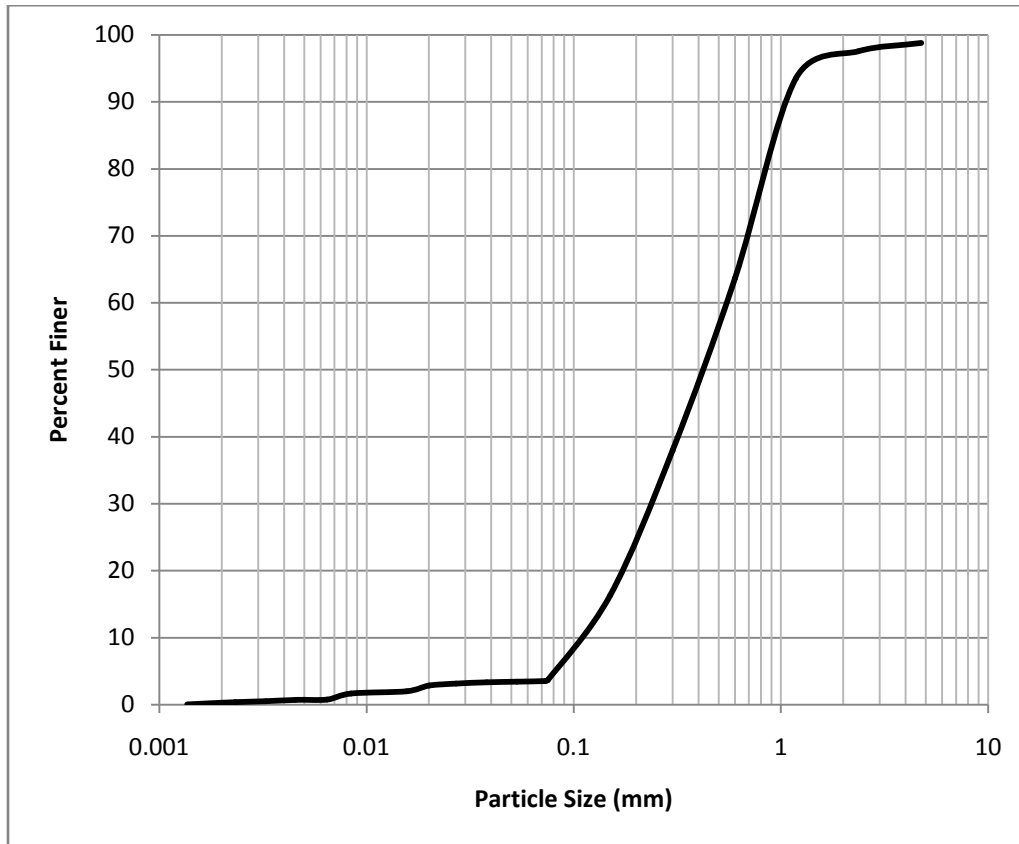


Fig.3.2. Particle size distribution of Weak soil used for the investigation

3.3 EXPERIMENTAL SETUP

The load tests are conducted in a combined test bed and loading frame assembly. The test beds are prepared in a ferrocement tank which is designed keeping in mind the size of the model footing to be tested and the zone of influence. The dimensions of the tank are 750 mm length x 750 mm width x 750 mm depth. The model footing is a rigid mild steel plate of 100 mm x 100 mm size and 20 mm thickness.

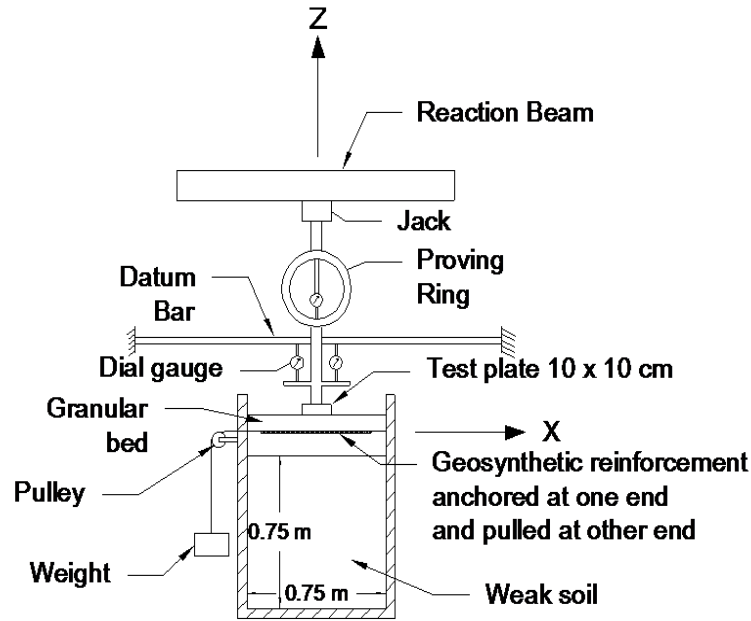


Fig.3.3. Test Setup

The footing was loaded by a hand operated Jack of 10 kN capacity supported against a reaction frame. The load is measured using a proving ring and deformation using two dial gauges placed diametrically opposite to each other. The load is applied in increments of 0.15 kN to the model footing. Each load increment is maintained constant till the footing settlement stabilizes. The details of the test setup are shown in Fig. 3.3 and photograph in Fig. 3.4. The arrangement for measuring loads and deformations are shown in Fig. 3.5.



Fig.3.4. View of Test Setup



Fig.3.5. Arrangement for measuring load and deformation

3.4 PREPARATION OF TEST BED

At first the weak soil is filled in the ferrocement tank to the required level with compaction done in layers, to achieve the pre-determined density. Then sand is filled up to the bottom level of reinforcement and compacted. The reinforcement is then placed with its centre exactly beneath the jack, and the prestress is applied. Then sand above the reinforcement is placed and compacted to the pre-determined density.

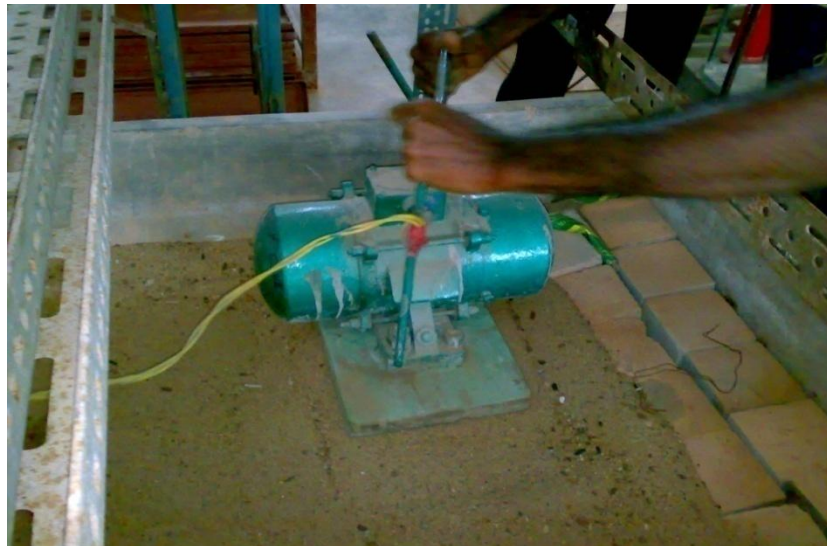


Fig. 3.6. Compaction of sand using Plate Vibrator

The densities to which the soils were compacted are indicated in Tables 3.1 and 3.2. The compactive effort required to achieve the required density of both the soils is determined by trial

and error. Preparation of underlying soil in all the tests involved compaction of soil using a rammer. In the preparation of granular bed, the sand was compacted using a small plate vibrator as shown in Fig.3.6.

3.5 THICKNESS OF GRANULAR BED

Tests are carried out for two thicknesses of granular bed equal to B and $2B$, where B is the width of the model footing (Fig.3.7).

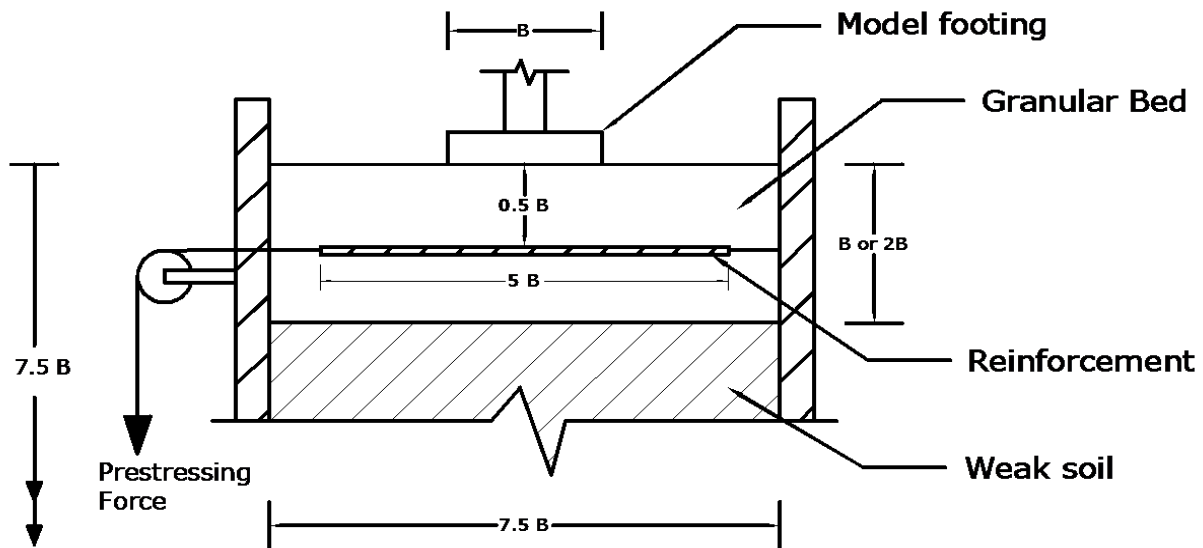


Fig.3.7. Details of Granular Bed

In all the tests, the reinforcement was kept at a depth of $0.5 B$ from the base of the footing. When the thickness of granular bed is B , reinforcement is at the middle of granular bed and when the thickness of granular bed is $2B$, reinforcement is at the top quarter point.

3.6 MAGNITUDE OF PRESTRESS

In order to investigate the effect of magnitude of prestress in the behaviour of prestressed reinforced granular bed, tests are carried out with three different magnitudes. Prestress applied are equal to 1%, 2% and 3% of the tensile strength of the reinforcement. The prestressing force is distributed over three pulleys as shown in Fig. 3.8.



Fig.3.8. Prestressing force applied through three pulleys

Prestress is applied to the reinforcement through light steel cables attached to thin mild steel flats bolted to the edges of the reinforcement. This arrangement is shown in Fig. 3.9.



Fig.3.9. Application of Prestress to reinforcement

3.7 DIRECTION OF PRESTRESS

To determine the relationship between the direction of prestress and improvement in bearing capacity, tests are carried out with two directions of prestress, viz. uniaxial and biaxial. In uniaxial prestressing the prestress is applied only in the X-direction as shown in Fig. 3.10.

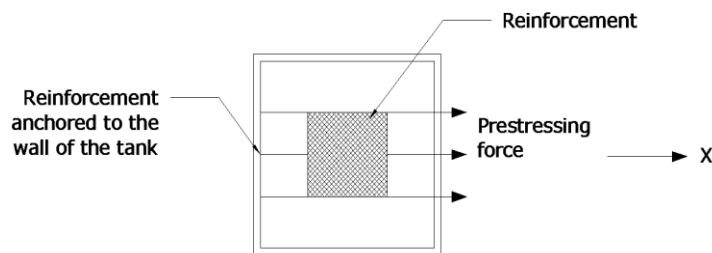


Fig.3.10. Uniaxial Prestressing

In biaxial prestressing, the prestress is applied in both X and Y directions as shown in Fig 3.11.

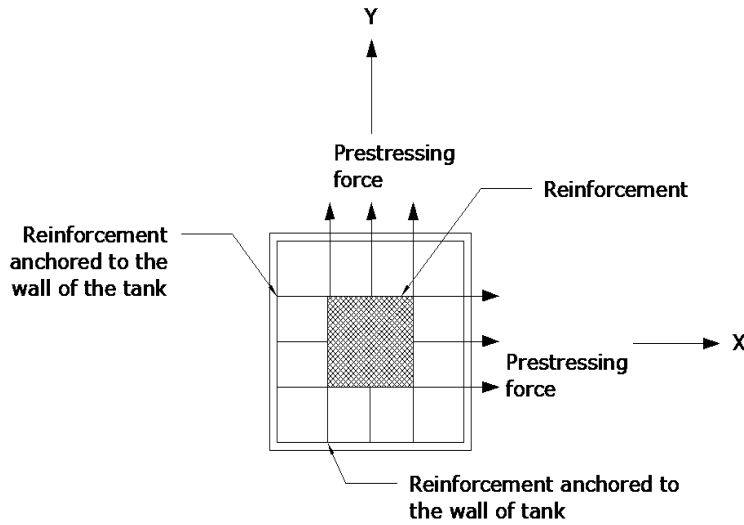


Fig.3.11. Biaxial Prestressing

3.8 NUMBER OF LAYERS OF REINFORCEMENT

To assess the improvement in bearing capacity due to an increase in the number of layers of prestressed reinforcement, tests are carried out with single and double layers of prestressed reinforcement. The test setup for double layer reinforcement is shown in Fig. 3.12

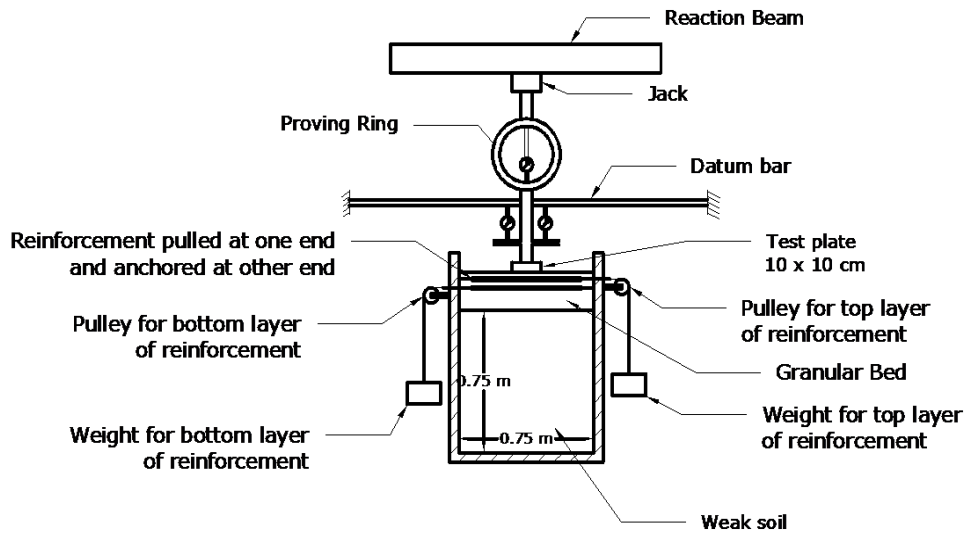


Fig.3.12. Test setup for double layer reinforcement

In the literature, it is reported that optimum depth of placement of the first layer of reinforcement is $0.2B$ to $0.5B$ (B is the width of footing) (Sharma et al. 2009). The depth of reinforcement from the base of footing is adopted as $0.5B$ for all the tests with single layer reinforcement. In case of

double layer reinforcement, the depth of top layer is $0.25B$ from the base of footing and that of bottom layer is $0.5B$ from the base of footing. The arrangement of reinforcement for double layer is shown in Fig.3.13.

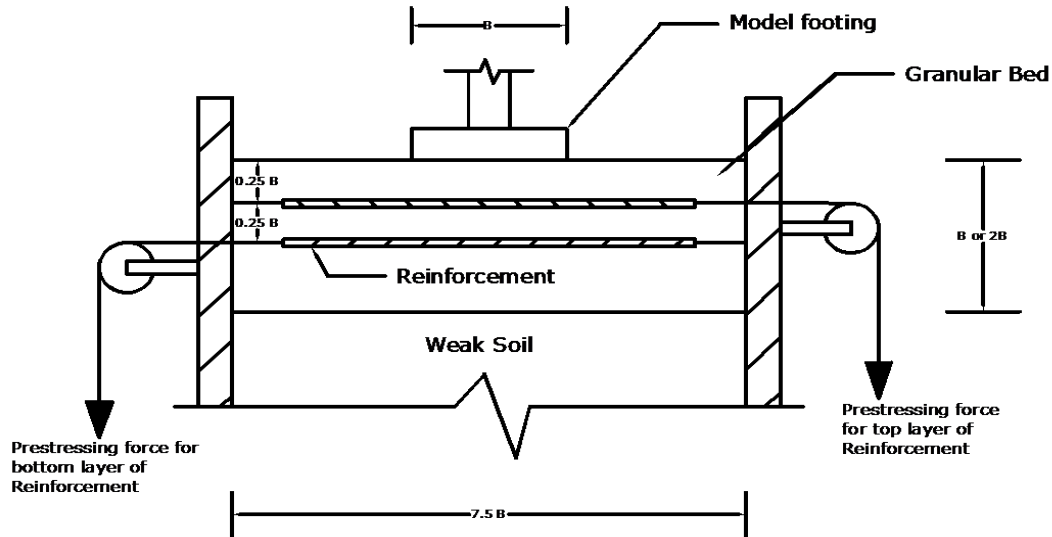


Fig.3.13. Arrangement of double layer reinforcement

3.9 SIZE OF REINFORCEMENT

Previous studies have shown that for footings supported on reinforced soil, the optimum size of reinforcement is equal to 5 to 7 times the width of square footing (Lee et al. 1999). In order to investigate the effect of size of prestressed reinforcement in improving the bearing capacity, tests are carried out with two sizes of reinforcement. The sizes of reinforcement used for the tests are $5B$ and $2B$, where B is the size of square footing.

3.10 TYPE OF GEOSYNTHETIC REINFORCEMENT

Table 3.3 Properties of geogrid used for the investigation

Property	Value
Mass per unit area (gm/m^2)	730.00
Aperture Size (mm)	8 x 6
Thickness (mm)	3.30
Tensile Strength (KN/m)	7.68
Extension at maximum load (%)	20.20
Interfacial friction angle with sand($^\circ$)	30.50
Colour	Black
Polymer	HD-Polyethelene

The improvement in bearing capacity attained will depend upon the properties of geosynthetic reinforcement used. In order to investigate the effect of the type of geosynthetic on the performance of prestressed reinforcement, tests are carried out with two types of geosynthetics, viz. geogrid and geotextile. The properties of geogrid used are given in Table 3.3 and that of geotextile in Table 3.4.

Table 3.4 Properties of geotextile used for the investigation

Property	Value
Mass per unit area (gm/m ²)	206.00
Thickness (mm)	0.58
Breaking Strength – Warp (5 x 20 cm) (Kg)	257.7
Breaking Strength – Weft (5 x 20 cm) (Kg)	181.90
Extension at Break (%) - Warp	36.90
Extension at Break (%) - Weft	30.20
Interfacial friction angle with sand(°)	24
Style (Quality no:)	P.D. 381
Material	Polypropylene

3.11 STRENGTH OF WEAK SOIL

The weak soil used was a locally available soil called as Shedi soil. This soil is a dispersive soil whose strength reduces drastically on saturation. In order to investigate the effect of strength of weak soil on the improvement in bearing capacity of footing, tests are carried out with Shedi soil in two conditions, namely moist condition (termed as moist soil or weak soil 1) and also in submerged condition (termed as submerged soil or weak soil 2). The properties of Shedi soil in both the conditions are given in Table 3.2. In the submerged condition, the level of water table is maintained at the surface of weak soil. The level of water table is monitored by installing peizometers (Fig.3.14)



Fig 3.14. Peizometers for monitoring the level of water table

3.12 EXPERIMENTAL PROGRAMME

The experimental programme is given in Table 3.5. Under series A, tests are conducted on weak soil 1 (moist soil) and on weak soil 1 overlain with unreinforced granular bed of thickness B or 2B. Under series B, tests are conducted on weak soil 1 overlain with reinforced granular bed of thickness B or 2B with single and double layer reinforcement. The size of reinforcement is 5B or 2B. The reinforcements used are geogrid and geotextile. Under series C, tests are conducted on weak soil 1 overlain with prestressed reinforced granular bed with single and double layer reinforcement. The prestress applied is uniaxial and biaxial. The parameters varied are magnitude of prestress, type of reinforcement and thickness of granular bed. Series D, E and F are similar to series A, B and C respectively, except that the underlying soft soil is kept submerged (termed as weak soil 2).

Table 3.5. Experimental Programme

Series	Type	Number of layers of reinforcement	Size of Reinforcement	Reinforcement type	Thickness of granular bed	Direction of Prestress	Magnitude of Prestress
A	Weak soil 1 (Moist soil)	--	--	--	--	--	--
	Unreinforced GB on weak soil 1	--	--	--	B & 2B	--	--
B	Reinforced GB on weak soil 1	1 & 2	5B & 2B	Geogrid & Geotextile	B & 2B	--	--
C	Prestressed RGB on weak soil 1	1 & 2	5B & 2B	Geogrid & Geotextile	B & 2B	Uniaxial & Biaxial	1%,2%&3%
D	Weak soil 2 (Submerged soil)	--	--	--	--	--	--
	Unreinforced GB on weak soil 2	--	--	--	B & 2B	--	--
E	Reinforced GB on weak soil 2	1 & 2	5B & 2B	Geogrid & Geotextile	B & 2B	--	--
F	Prestressed RGB on weak soil 2	1 & 2	5B & 2B	Geogrid & Geotextile	B & 2B	Uniaxial & Biaxial	1%,2%&3%

CHAPTER 4

FINITE ELEMENT ANALYSIS

4.1 INTRODUCTION

In the present study the experimental results are validated by carrying out finite element analysis using the FE software PLAXIS version 8. It is a special purpose two dimensional finite element computer program used to perform deformation and stability analyses for various types of geotechnical applications and its enhanced output facilities provide a detailed presentation of computational results.

4.2 FINITE ELEMENT MODELLING

For simulating the behaviour of soil, different constitutive models are available in PLAXIS. In the present study Mohr-Coulomb model is used to simulate soil behaviour. This non linear model is based on the basic soil parameters that can be obtained from direct shear tests; internal friction angle and cohesion intercept. The geometric model for prestressed reinforced granular bed (PRGB) with double layer reinforcement is shown in Fig. 4.1.

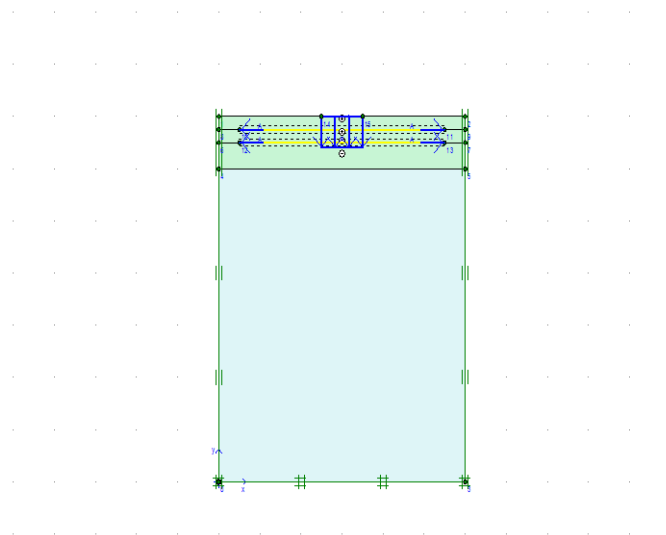


Fig.4.1 Geometric model of PRGB

In PLAXIS, two models are available for the simulation of soil-footing reinforcement system; plane strain model and the axisymmetric model. In the present study, an axisymmetric model is used to carry out the finite element analysis. Since the stresses in soil are of main interest, the footing is assumed as rigid. Hence instead of modeling the footing, the indentation or the settlement caused by the footing is modeled using non zero prescribed displacements. The initial geostatic stress states for the analyses are set according to the unit weight of the soil.

PLAXIS provides an automated mesh generation system, in which the model is discretized into standard elements. The soil is modeled using 15 noded triangular elements. A medium mesh size is adopted for weak soil and fine mesh size is adopted for PRGB in the analysis. The outer boundaries of the mesh are of same dimensions as the tank used for model tests. The boundary conditions are so chosen that the displacement of the bottom boundary is restricted in all directions, while at the vertical sides; displacement is restricted only in the horizontal direction. Fig 4.2 shows a typical discretized model.

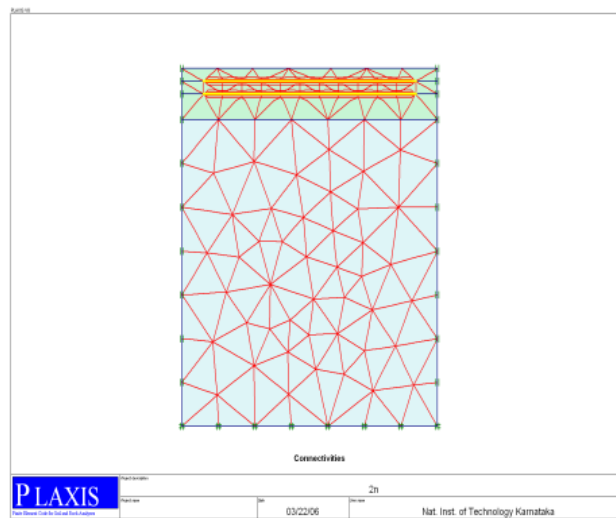


Fig.4.2 Discretized model of PRGB

The reinforcement is modeled using the 5-noded tension element available in PLAXIS. The material property required for reinforcement is elastic axial stiffness EA . The value of EA for geogrid is taken as 7.68 kN/m and for geotextile as 40 kN/m. To simulate the interaction between the reinforcement and surrounding soil, an interface element is provided on both upper and lower surface of reinforcement. The interaction between soil and reinforcement is simulated by choosing an appropriate value for strength reduction factor R_{inter} at the interface. The aperture

size of geogrid is sufficiently large enough to allow soil to soil contact through the apertures and hence the angle of friction between reinforcement and soil is taken equal to the angle of internal friction of sand Φ . Hence the value of R_{inter} , for geogrid, is taken as one. In the case of geotextile, the value of R_{inter} is taken as 0.80. The prestress is modeled as a horizontal tensile load to the reinforcement.

The modulus of elasticity E is different for each simulation due to the variation in strength of soil induced by reinforcement and prestress. The modulus of subgrade reaction is found out for each trial from the experimental data and then the modulus of elasticity is computed using the following relationship (Selvadurai 1979).

$$E = k_s \cdot H(1+\nu) (1-2\nu)$$

E is the modulus of elasticity (kPa), k_s is modulus of subgrade reaction for soil (KN/m³), H is thickness (m) and ν is Poisson's ratio. The value of H is determined by conducting a number of simulations and comparing the results with the experimental values. The value of Poisson's ratio is assumed to be 0.25 for all the cases.

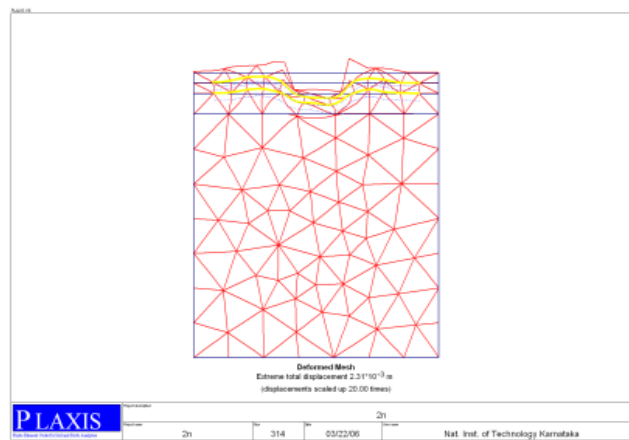


Fig.4.3 Deformed shape of PRGB after loading

Analyses of the FE models were carried out in the output module of the program. In the analysis, the total load level is determined globally by means of the total load multipliers. If the soil does not fail due to a collapse mechanism, the applied load will incrementally increase until the prescribed displacement is reached. Figure 4.3 shows the typical deformed shape of PRGB after loading.

To simulate exactly the testing procedure in the laboratory, staged construction procedure is adopted in the calculation phase. In the first stage, weak soil up to its top level is simulated. In the second stage, sand up to the bottom level of reinforcement is simulated. In the third stage the reinforcement with prestress is simulated and in the fourth stage sand above the reinforcement is simulated. In the final stage the footing with prescribed displacement is simulated. Such a staged construction procedure is necessary because the reinforcement should be prestressed before filling soil above it, otherwise the friction between soil and reinforcement will prevent the elongation of reinforcement due to prestressing. Typical stress distribution in soil after loading is shown in Fig 4.4 and the stress distribution at the interface between granular bed and weak soil is shown in Fig 4.5.

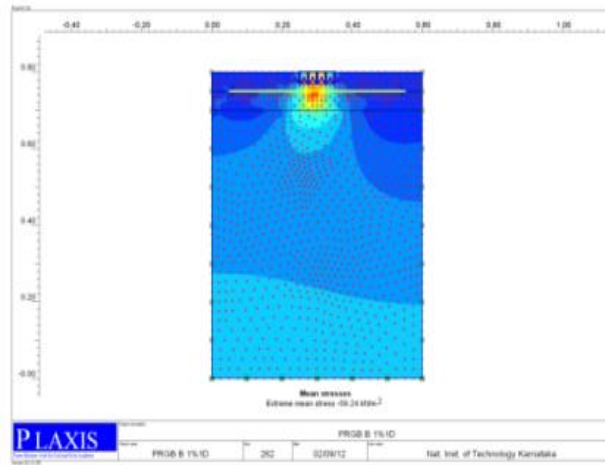


Fig.4.4 Stress distribution in soil after loading

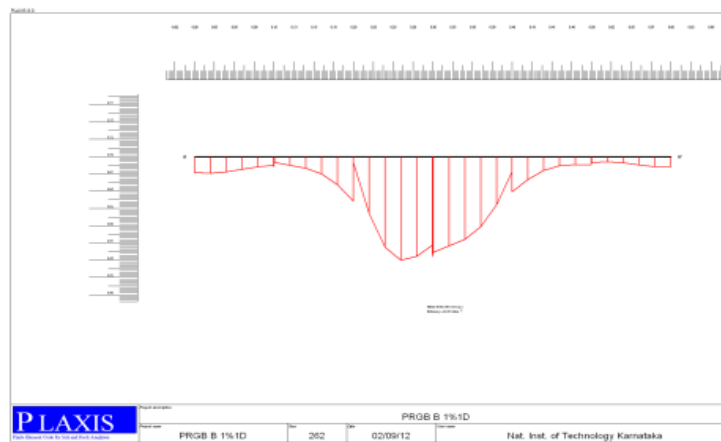


Fig.4.5 Stress distribution at the interface between granular bed and weak soil after loading

A typical load-deformation curve given by PLAXIS is shown in Fig. 4.6 and the stress distribution at the interface between reinforcement and surrounding sand is shown in Fig 4.7.

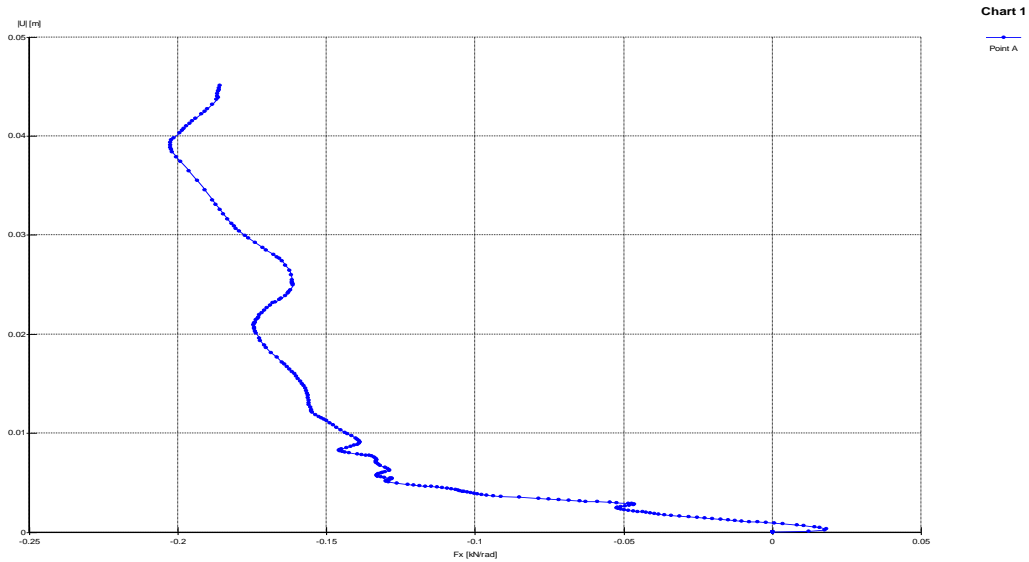


Fig.4.6 Typical Load-deformation curve

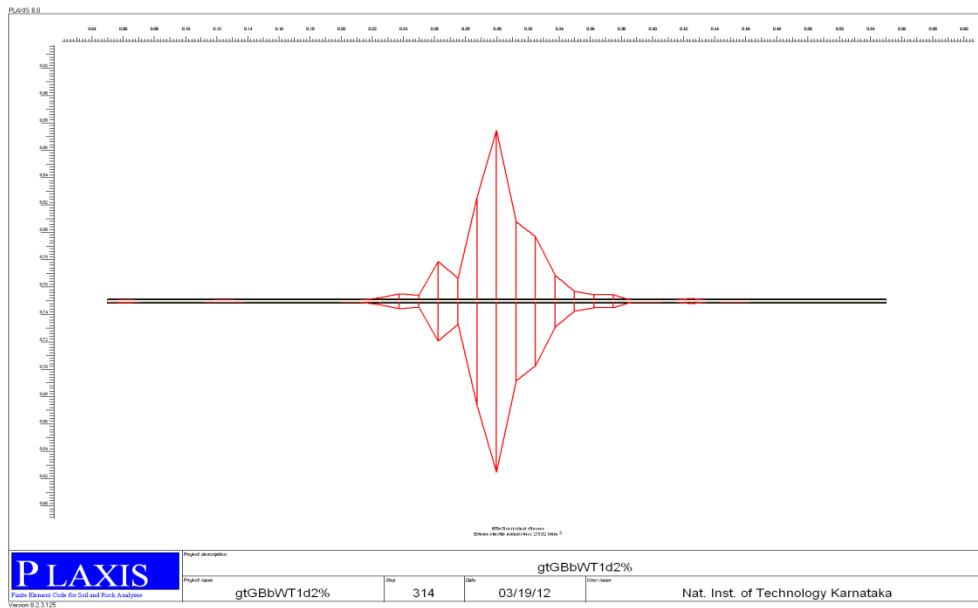


Fig.4.7 Stress distribution at the interface between reinforcement and granular bed

4.3 COMPARISON BETWEEN EXPERIMENTAL AND FEA RESULTS

A comparison between the results obtained from experimental studies and those obtained from finite element analyses are given in the following sections.

4.3.1 Effect of Magnitude of prestress

One among the parameters studied in this investigation is the effect of magnitude of prestress. Lovisa et al (2010) studied the effects of prestressing at a constant prestress of 2% of the tensile strength of geosynthetic. In this study it is attempted to determine the optimum value of prestress for various cases. The magnitudes of prestress applied are equal to 1%, 2% and 3% of the tensile strength of the reinforcement. The footing pressure vs normalized settlement curves for various cases obtained from experimental studies as well as finite element analyses are presented below.

4.3.1.1 PRGB with single layer geogrid of size 5B x 5B overlying weak soil 1 (moist soil)

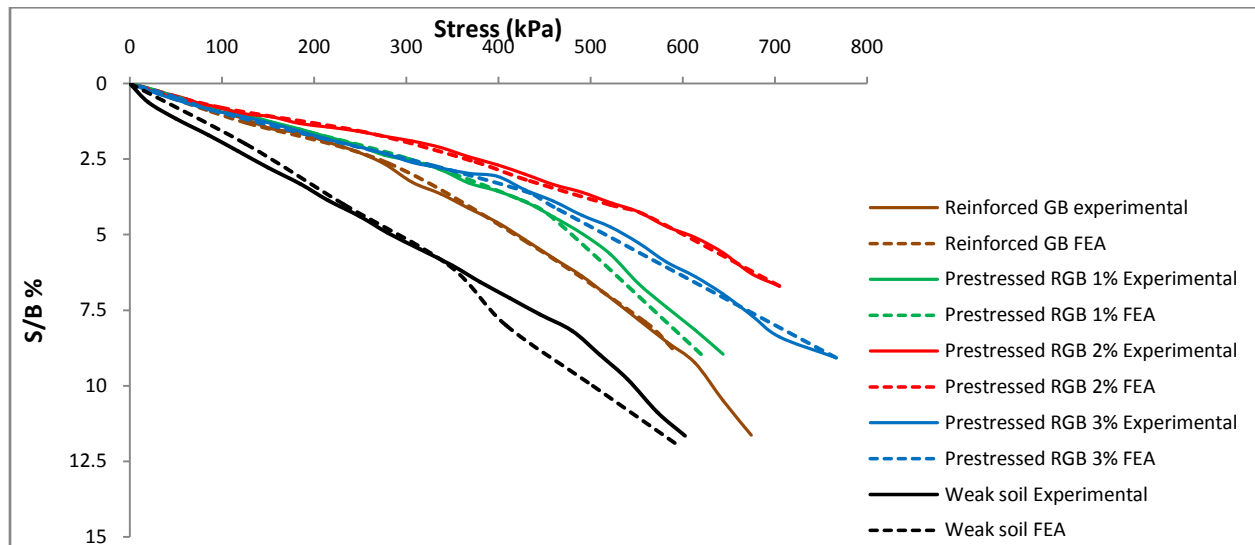


Fig 4.8 Stress vs normalized settlement curves for PRGB of thickness B with uniaxially prestressed single layer geogrid of size 5B x 5B overlying (moist) weak soil 1.

Figure 4.8 represents the variation of bearing pressure with footing settlement of a uniaxially prestressed RGB of thickness B with single layer geogrid reinforcement of size 5B x 5B overlying (moist) weak soil 1. It can be seen from the figure that prestressing the reinforcement caused a considerable improvement in the settlement behaviour. The maximum improvement is attained when the prestress is equal to 2% of the tensile strength of reinforcement. A further increase in prestress decreases the improvement. The results obtained from Finite element analyses are in reasonably good agreement with the experimental results.

The results of experimental studies and finite element analyses of a biaxially prestressed RGB of thickness B with single layer geogrid reinforcement of size $5B \times 5B$ overlying (moist) weak soil-1 is given in Fig 4.9. It is seen from the results that the maximum improvement in settlement behaviour is attained when the biaxial prestress is equal to 1% of the tensile strength of the reinforcement.

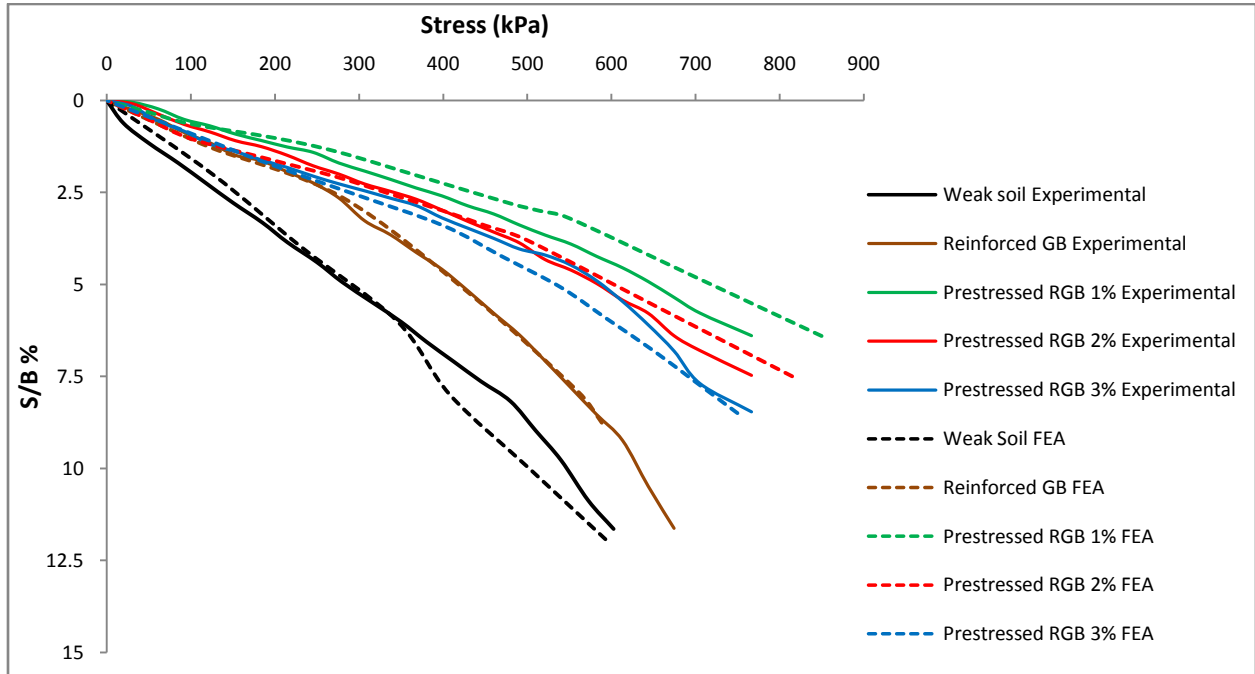


Fig 4.9 Stress vs normalized settlement curves for PRGB of thickness B with biaxially prestressed single layer geogrid of size $5B \times 5B$ overlying (moist) weak soil 1.

The settlement behaviour of uniaxially prestressed PRGB of thickness $2B$ with single layer geogrid reinforcement of size $5B \times 5B$ overlying (moist) weak soil 1 is presented in Fig 4.10. It is observed that the maximum improvement is when the magnitude of prestress is equal to 3% of the tensile strength of reinforcement.

Figure 4.11 shows the variation of bearing pressure with footing settlement of a biaxially prestressed RGB of thickness $2B$ with single layer geogrid reinforcement of size $5B \times 5B$ overlying (moist) weak soil 1. It can be seen from the figure that maximum improvement is attained when the prestress is equal to 3% of the tensile strength of reinforcement. This is similar to the behaviour of uniaxially prestressed RGB of thickness $2B$.

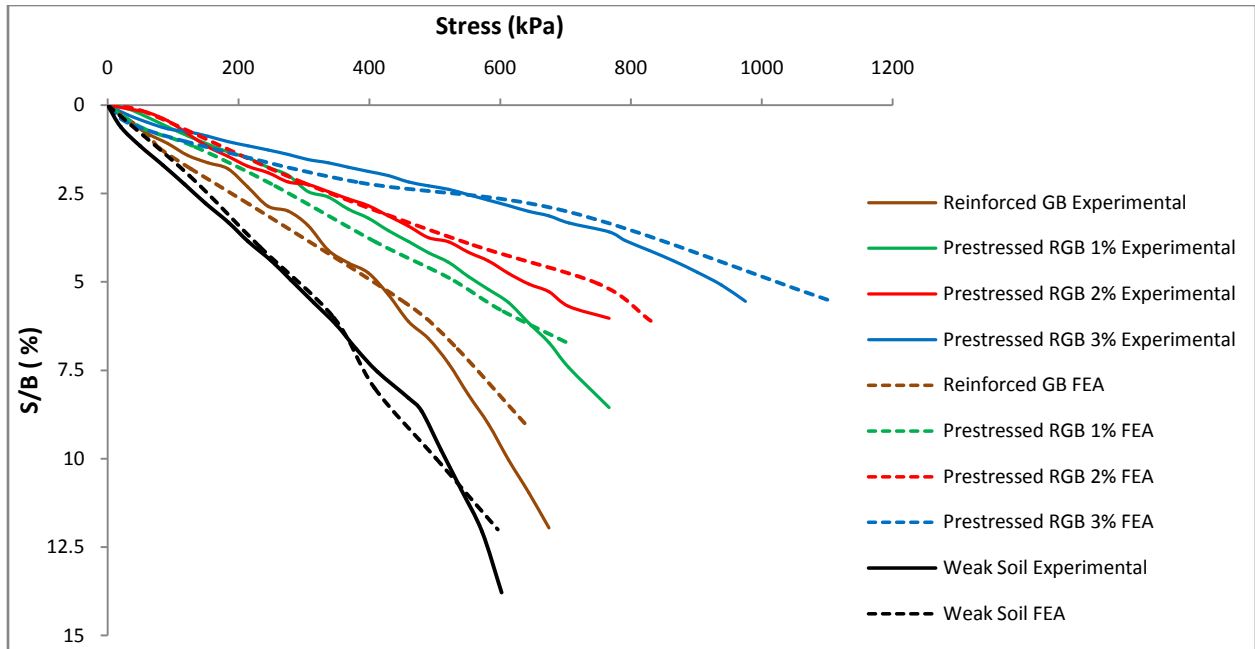


Fig 4.10 Stress vs normalized settlement curves for PRGB of thickness 2B with uniaxially prestressed single layer geogrid of size 5B x 5B overlying (moist) weak soil 1.

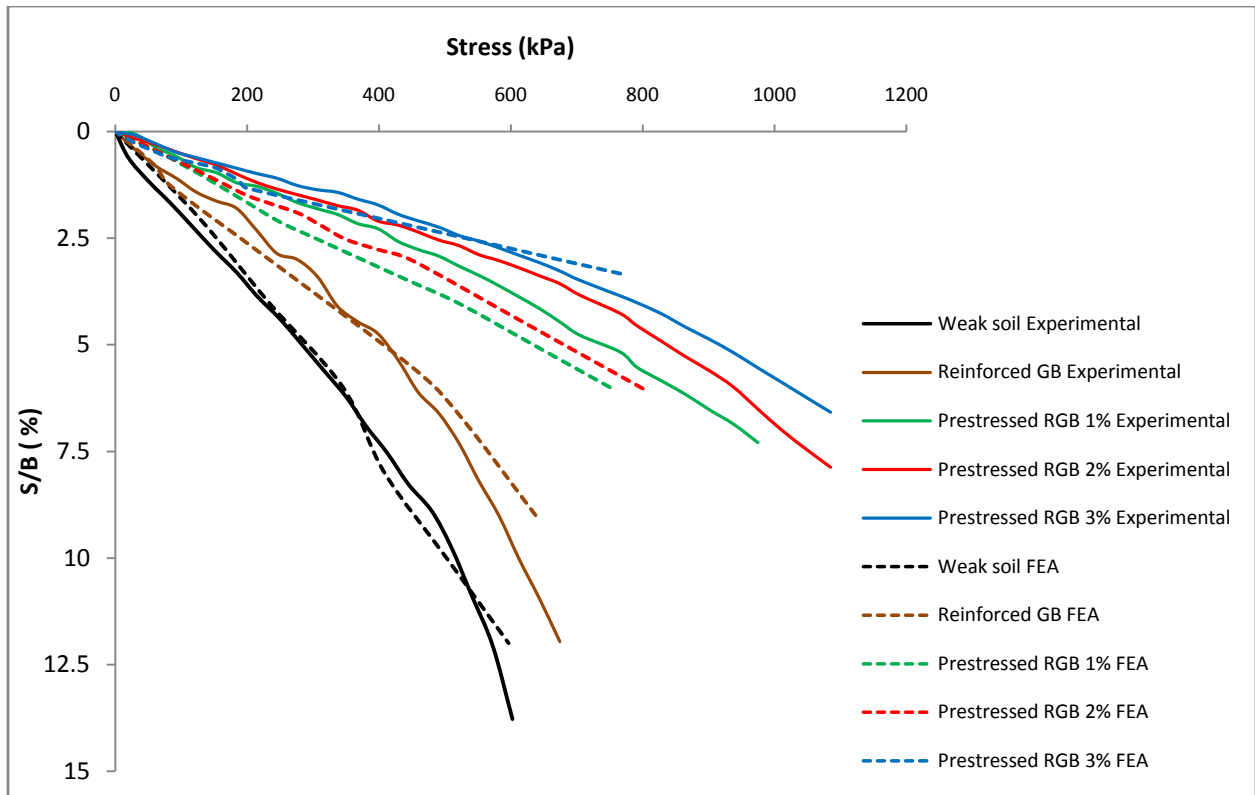


Fig 4.11 Stress vs normalized settlement curves for PRGB of thickness 2B with biaxially prestressed single layer geogrid of size 5B x 5B overlying (moist) weak soil 1.

4.3.1.2 PRGB with single layer geogrid of size 5B x 5B overlying weak soil 2 (submerged soil)

The settlement behaviour of uniaxially prestressed PRGB of thickness B with single layer geogrid reinforcement of size 5B x 5B overlying (submerged) weak soil 2 is presented in Fig 4.12. The submergence of weak soil caused a large reduction in its strength. However due to prestressing the bearing capacity improved and maximum improvement occurred when the prestress is equal to 2% of the tensile strength of the reinforcement. Further increase in prestress decreases the improvement. This is same as in the case of weak soil 1.

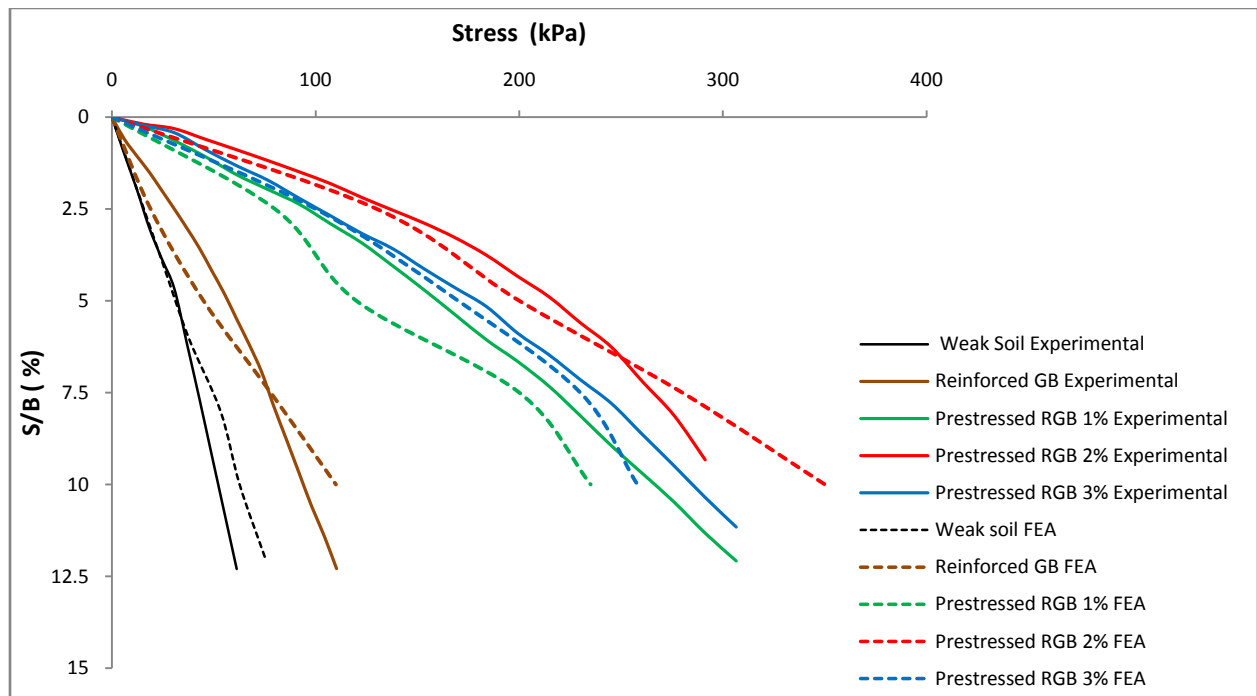


Fig 4.12 Stress vs normalized settlement curves for PRGB of thickness B with uniaxially prestressed single layer geogrid of size 5B x 5B overlying (submerged) weak soil 2.

In case of granular bed of thickness B with biaxial prestressing overlying submerged weak soil, from Fig. 4.13, it is observed that the maximum improvement in settlement behaviour occurs when the magnitude of prestress is equal to 2% of the tensile strength of reinforcement. This is unlike in case of weak soil 1, which peaked at 1% itself.

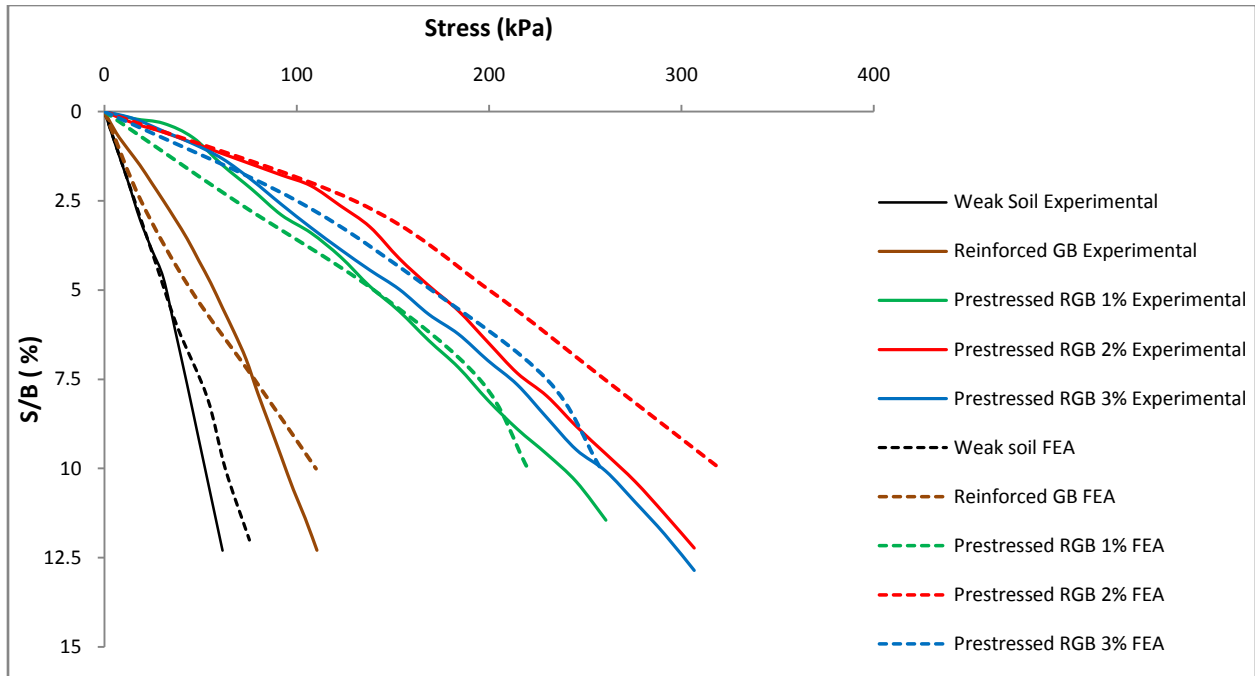


Fig 4.13 Stress vs normalized settlement curves for PRGB of thickness B with biaxially prestressed single layer geogrid of size 5B x 5B overlying (submerged) weak soil 2.

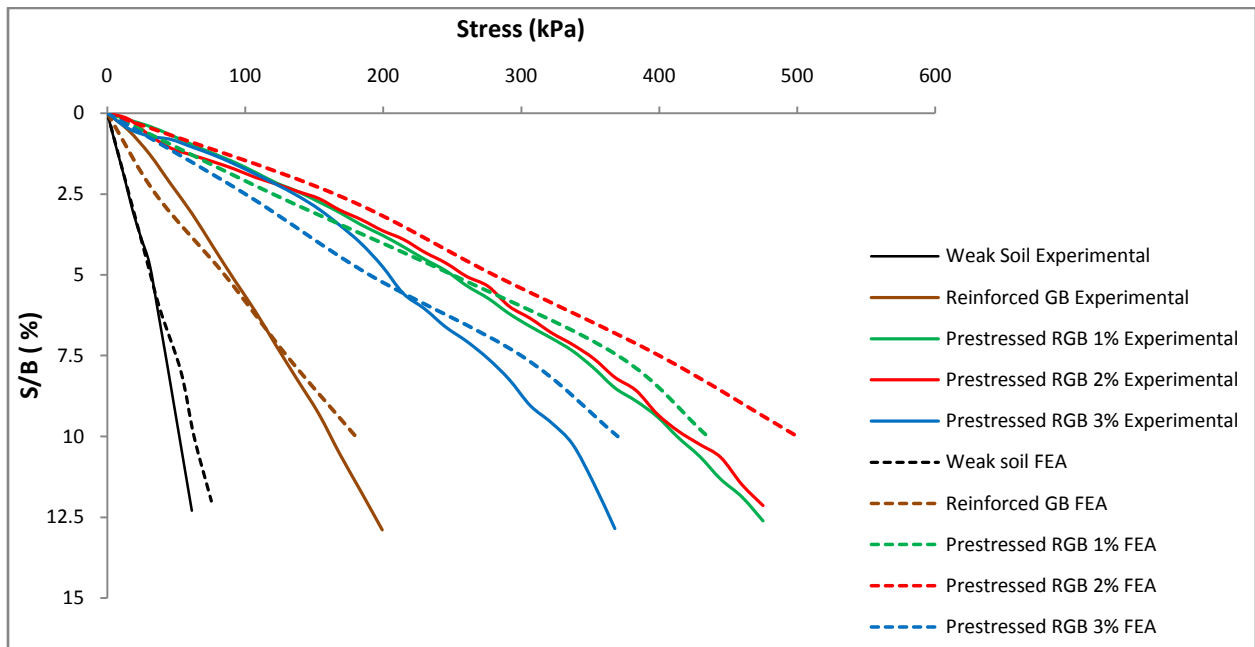


Fig 4.14 Stress vs normalized settlement curves for PRGB of thickness 2B with uniaxially prestressed single layer geogrid of size 5B x 5B overlying (submerged) weak soil 2.

With increased thickness of granular bed to 2B and with uniaxial prestressing overlying (submerged) weak soil 2, it is observed (Fig.4.14) that the maximum improvement is observed when the magnitude of prestress is again equal to 2% of the tensile strength of reinforcement.

Further increase in prestress caused a reduction in the improvement in bearing capacity. This is unlike in case of weak soil 1, which gave maximum improvement at 3% prestress. It is also observed from experimental studies that the improvement in bearing capacity when the prestress was increased from 1% to 2% is only marginal.

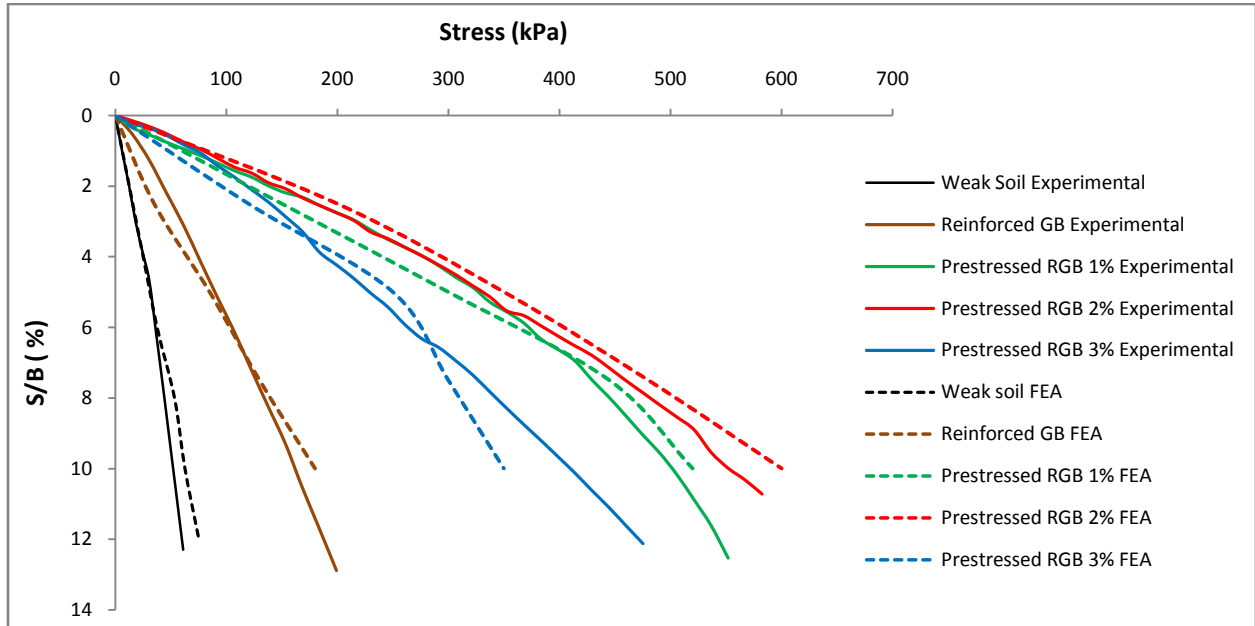


Fig 4.15 Stress vs normalized settlement curves for PRGB of thickness 2B with biaxially prestressed single layer geogrid of size 5B x 5B overlying (submerged) weak soil 2.

From the results obtained from a granular bed of thickness 2B with biaxial prestressing overlying (submerged) weak soil 2, it is observed that the improvement in settlement behaviour with 3% prestress is less than that with 1% and 2% (Fig.4.15). The improvement in settlement behaviour with a prestress of 1% and 2% is almost same up to a pressure of 370 KPa. At stresses more than 370 KPa, the improvement in settlement behaviour is more with prestress of 2%.

4.3.1.3 PRGB with single layer geotextile of size 5B x 5B overlying weak soil 1 (moist soil)

Figure 4.16 shows the variation of bearing pressure with footing settlement of a uniaxially prestressed RGB of thickness B with single layer geotextile reinforcement of size 5B x 5B overlying (moist) weak soil 1. It can be seen from the figure that maximum improvement is attained when the prestress is equal to 2% of the tensile strength of reinforcement. A further

increase in prestress decreases the improvement. The behaviour is similar to that with a single layer geogrid.

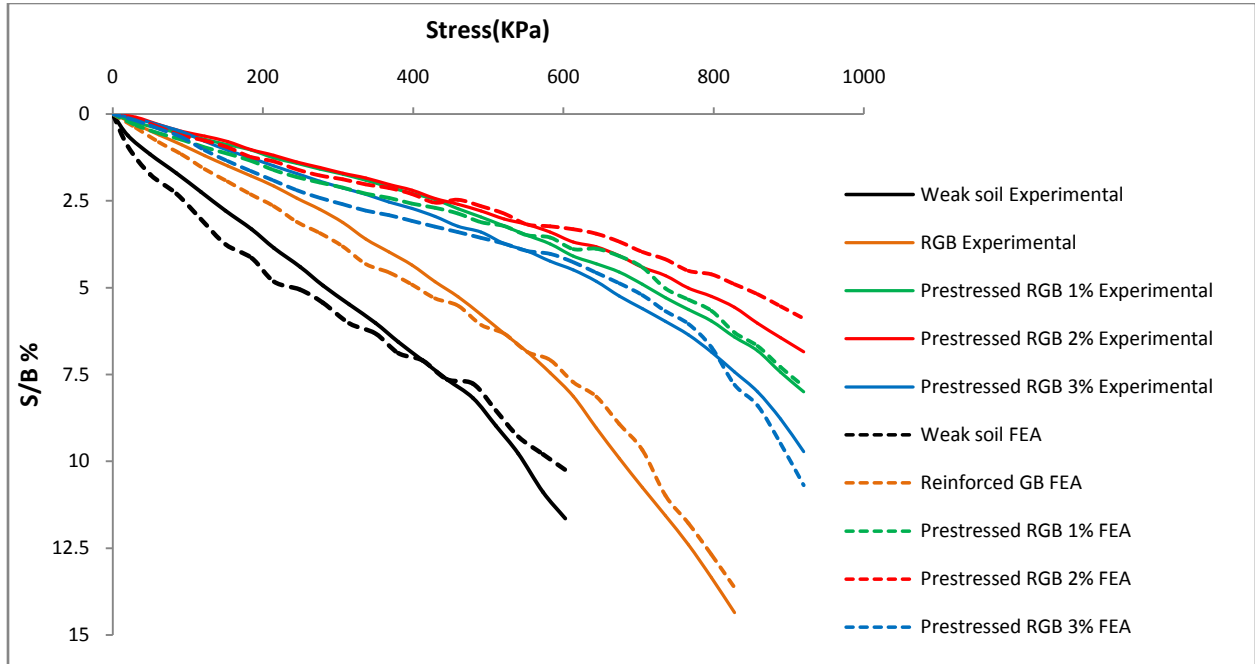


Fig 4.16 Stress vs normalized settlement curves for PRGB of thickness B with uniaxially prestressed single layer geotextile of size 5B x 5B overlying (moist) weak soil 1.

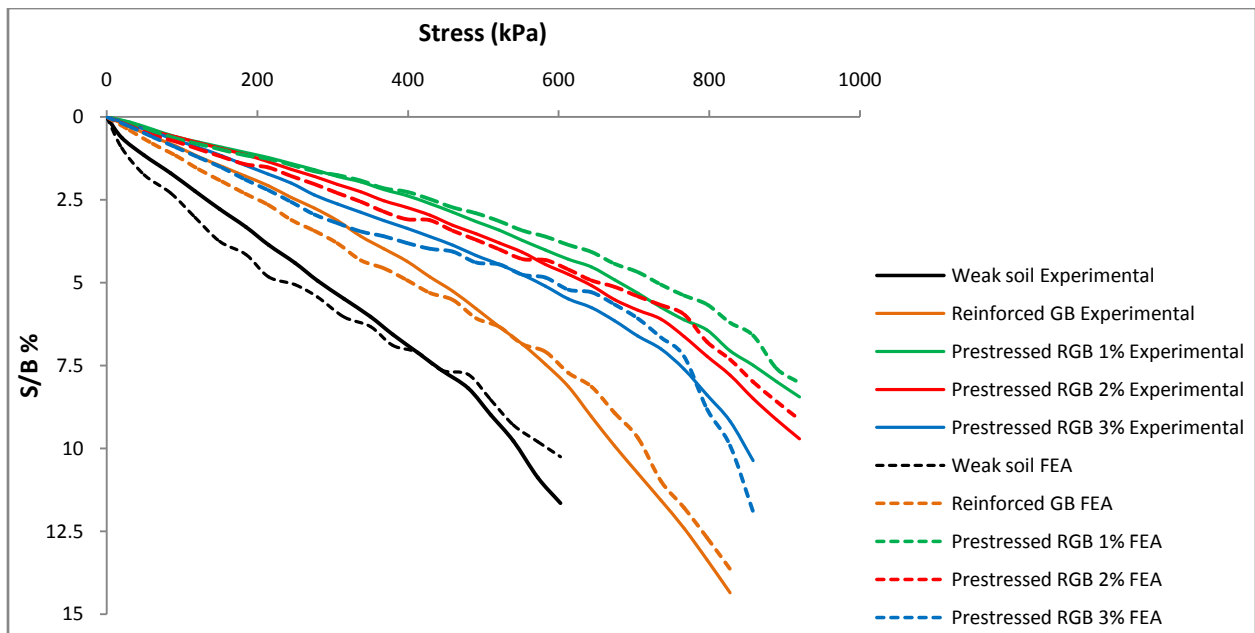


Fig 4.17 Stress vs normalized settlement curves for PRGB of thickness B with biaxially prestressed single layer geotextile of size 5B x 5B overlying (moist) weak soil 1.

The results of experimental studies and finite element analyses of a biaxially prestressed RGB of thickness B with single layer geotextile reinforcement of size $5B \times 5B$ overlying (moist) weak soil-1 is given in Fig 4.17. It is observed that maximum improvement in bearing capacity is attained when the biaxial prestress is equal to 1% of the tensile strength of reinforcement.

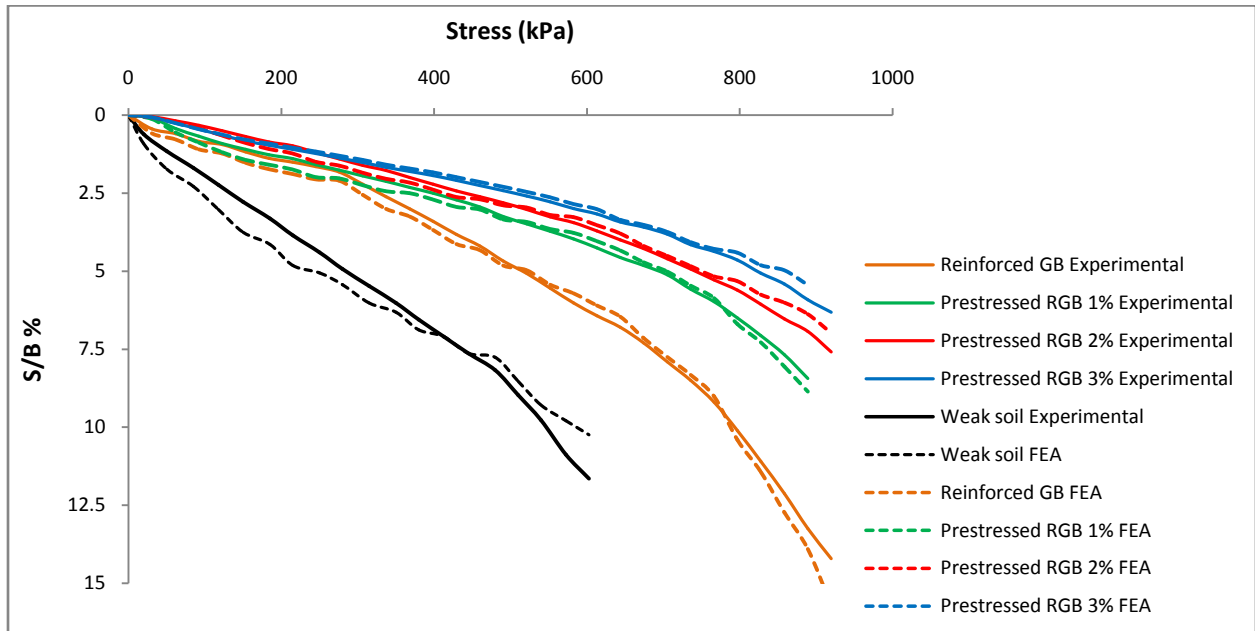


Fig 4.18 Stress vs normalized settlement curves for PRGB of thickness $2B$ with uniaxially prestressed single layer geotextile of size $5B \times 5B$ overlying (moist) weak soil 1.

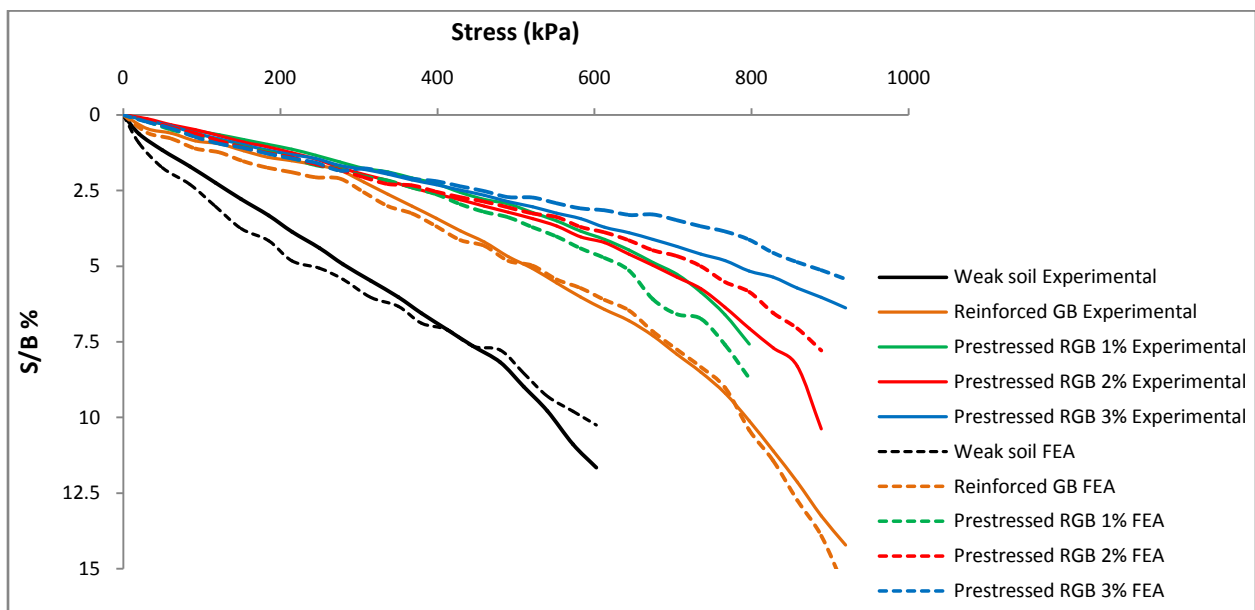


Fig 4.19 Stress vs normalized settlement curves for PRGB of thickness $2B$ with biaxially prestressed single layer geotextile of size $5B \times 5B$ overlying (moist) weak soil 1.

With increased thickness of granular bed to 2B and with uniaxially prestressed single layer geotextile overlying (moist) weak soil 1, it is observed (Fig.4.18) that the maximum improvement is attained when the magnitude of prestress is equal to 3% of the tensile strength of reinforcement. The behaviour is similar to that with geogrid reinforcement.

Figure 4.19 shows the variation of bearing pressure with footing settlement of a biaxially prestressed RGB of thickness 2B with single layer geotextile reinforcement of size 5B x 5B overlying (moist) weak soil 1. It can be seen from the figure that maximum improvement is attained when the prestress is equal to 3% of the tensile strength of reinforcement. This also is similar to that with geogrid reinforcement.

4.3.1.4 PRGB with single layer geotextile of size 5B x 5B overlying weak soil 2 (submerged soil)

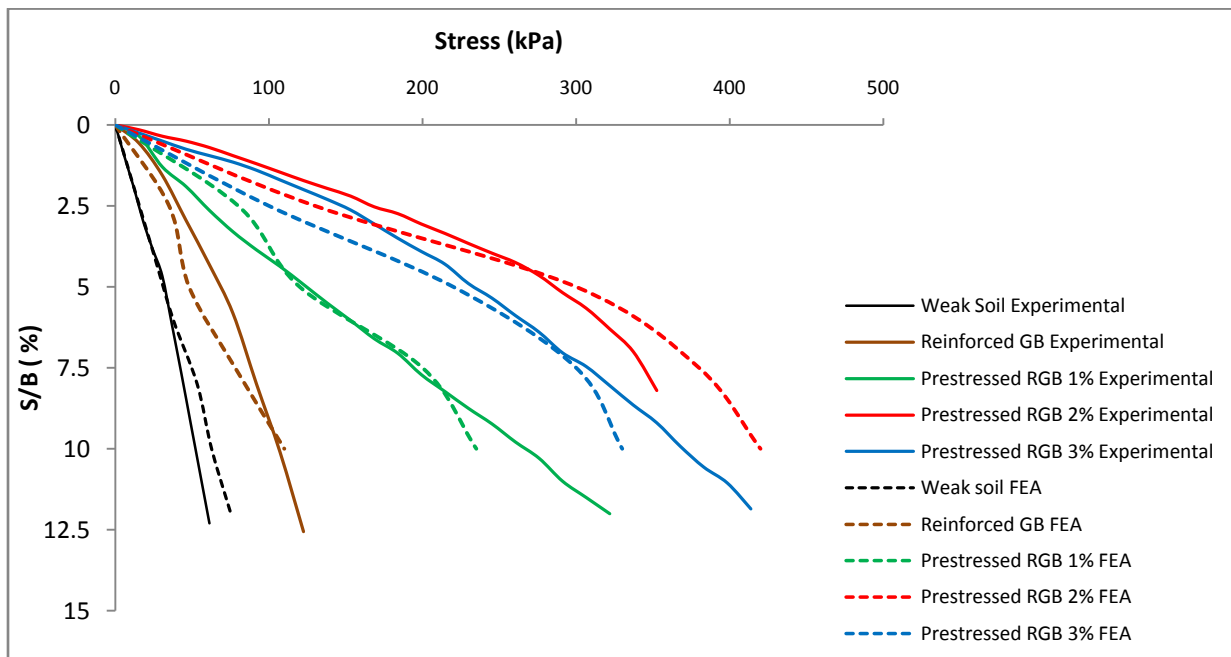


Fig 4.20 Stress vs normalized settlement curves for PRGB of thickness B with uniaxially prestressed single layer geotextile of size 5B x 5B overlying (submerged) weak soil 2.

The settlement behaviour of uniaxially prestressed PRGB of thickness B with single layer geotextile reinforcement of size 5B x 5B overlying (submerged) weak soil 2 is presented in Fig 4.20. It is observed that a large reduction in bearing capacity occurs due to the submergence of Shedi soil. However due to prestressing the bearing capacity improved and maximum

improvement occurred when the prestress is equal to 2% of the tensile strength of the reinforcement. Further increase in prestress decreases the improvement.

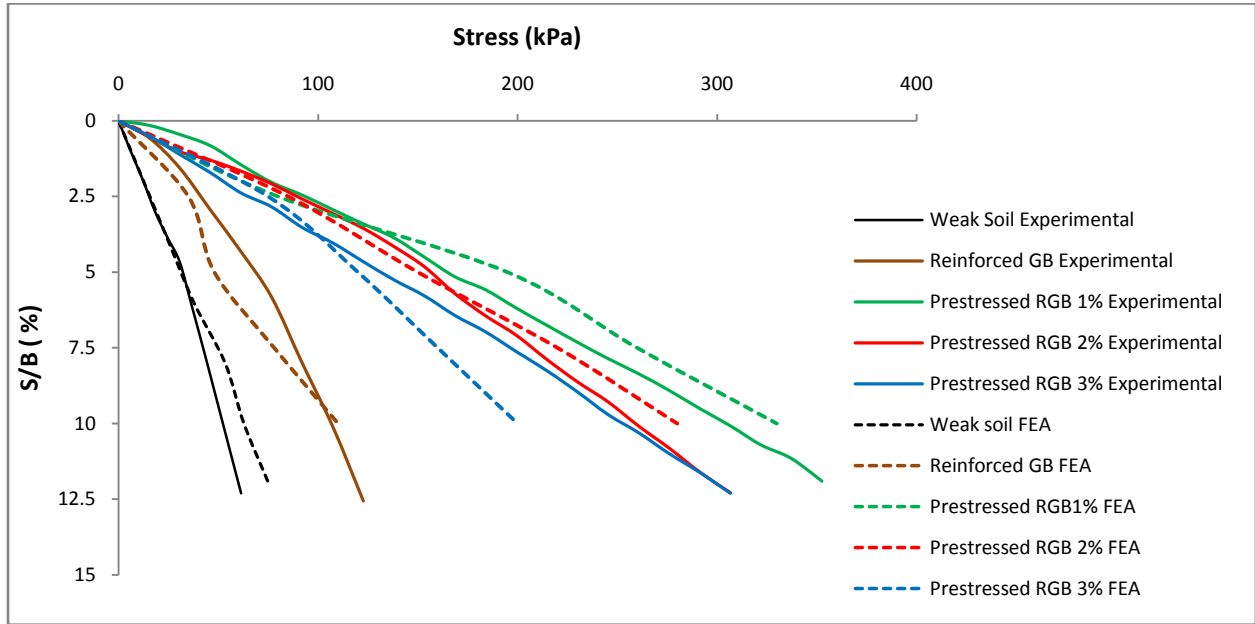


Fig 4.21 Stress vs normalized settlement curves for PRGB of thickness B with biaxially prestressed single layer geotextile of size 5B x 5B overlying (submerged) weak soil 2.

The results of studies on a biaxially prestressed RGB of thickness B with single layer geotextile reinforcement of size 5B x 5B overlying (submerged) weak soil 2 is given in Fig 4.21. It is observed that maximum improvement in bearing capacity is attained when the biaxial prestress is equal to 1% of the tensile strength of reinforcement. The behaviour is similar to that of PRGB overlying weak soil 1.

When the thickness of PRGB is increased to 2B with uniaxially prestressed single layer geotextile reinforcement overlying (submerged) weak soil 2, the maximum improvement in bearing capacity is observed when the prestress is equal to 3% of the tensile strength of reinforcement. The results are shown in Fig 4.22.

Figure 4.23 shows the variation of bearing pressure with footing settlement of a biaxially prestressed RGB of thickness 2B with single layer geotextile reinforcement of size 5B x 5B overlying (submerged) weak soil 2. It can be seen from the figure that maximum improvement is attained when the prestress is equal to 3% of the tensile strength of reinforcement. This is similar to the behaviour with uniaxial prestress.

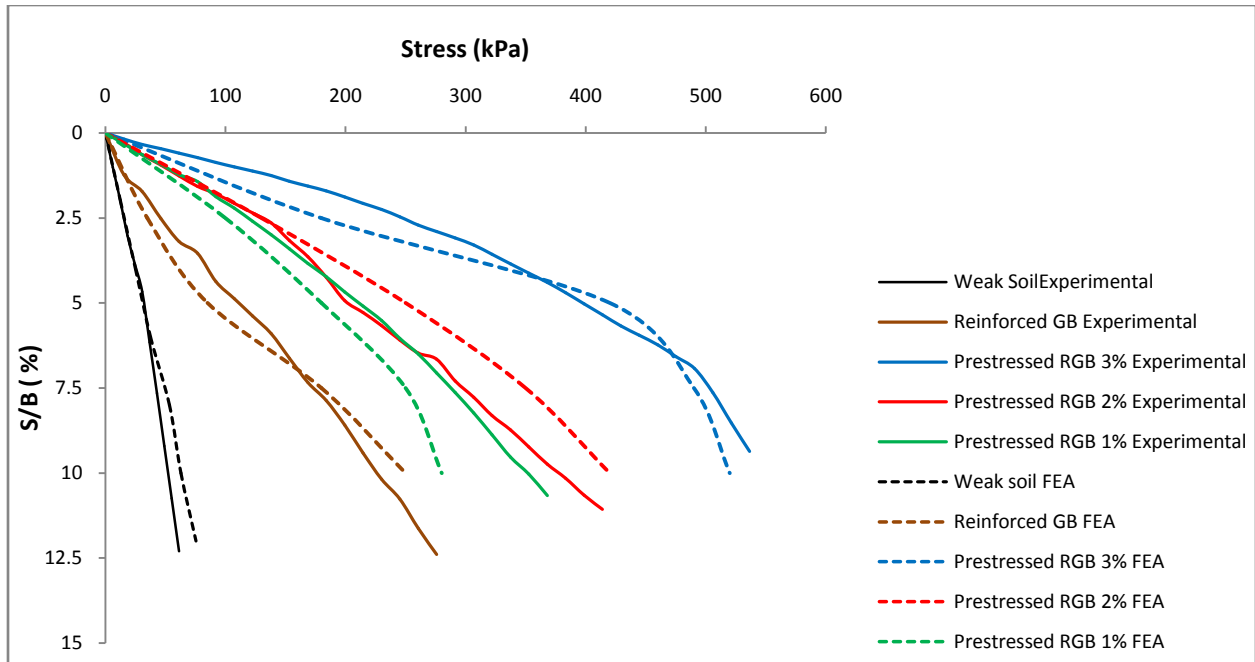


Fig 4.22 Stress vs normalized settlement curves for PRGB of thickness 2B with uniaxially prestressed single layer geotextile of size 5B x 5B overlying (submerged) weak soil 2.

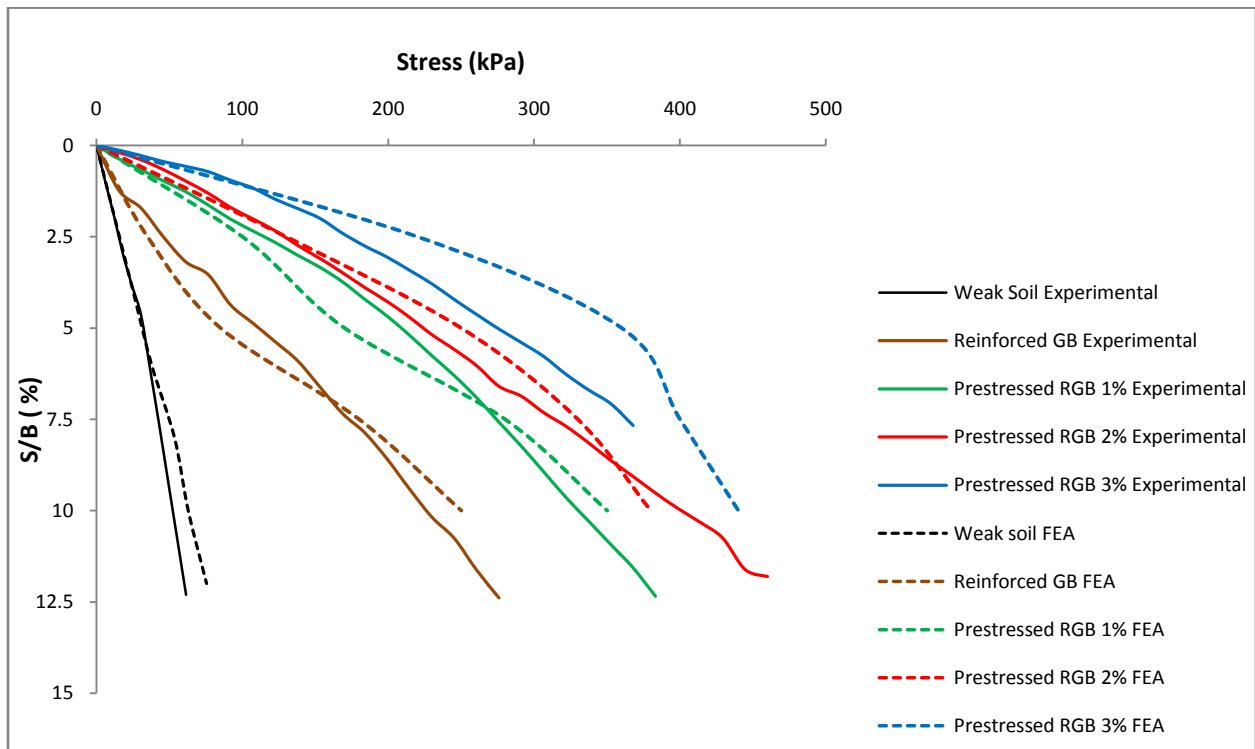


Fig 4.23 Stress vs normalized settlement curves for PRGB of thickness 2B with biaxially prestressed single layer geotextile of size 5B x 5B overlying (submerged) weak soil 2.

4.3.1.5 PRGB with single layer geogrid of size 2B x 2B overlying weak soil 1 (moist soil)

Figure 4.24 represents the variation of bearing pressure with footing settlement of a uniaxially prestressed RGB of thickness B with single layer geogrid reinforcement of size 2B x 2B overlying (moist) weak soil 1. It can be seen from the figure that prestressing the reinforcement caused a considerable improvement in the settlement behaviour even though the size of the reinforcement is small. The maximum improvement is attained when the prestress is equal to 2% of the tensile strength of reinforcement. A further increase in prestress decreases the improvement. The behaviour is similar to that with bigger reinforcement (size 5B x 5B).

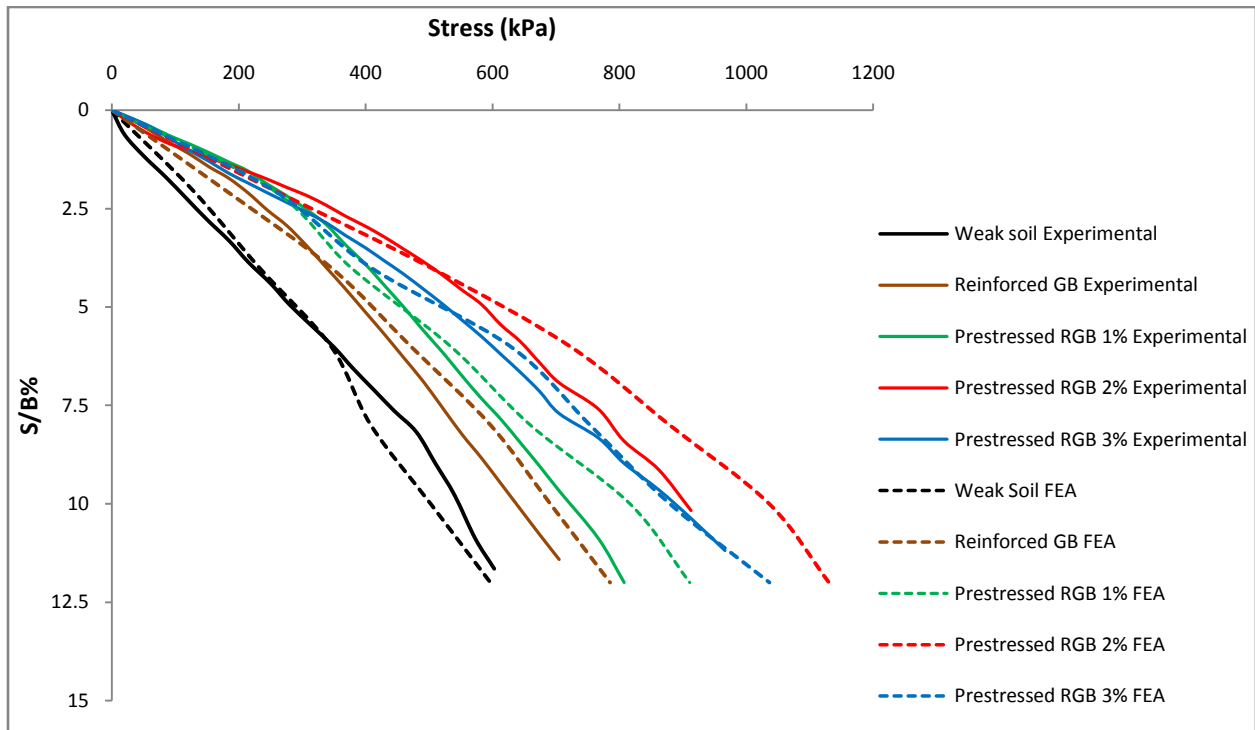


Fig 4.24 Stress vs normalized settlement curves for PRGB of thickness B with uniaxially prestressed single layer geogrid of size 2B x 2B overlying (moist) weak soil 1.

The variation of bearing pressure with footing settlement of a biaxially prestressed RGB of thickness B with single layer geogrid reinforcement of size 2B x 2B overlying (moist) weak soil 1 is shown in Fig 4.25. It can be seen from the figure that maximum improvement occurs when the biaxial prestress is equal to 2% of the tensile strength of reinforcement. This is unlike in the case of bigger reinforcement (5B x 5B), which peaked at 1% itself.

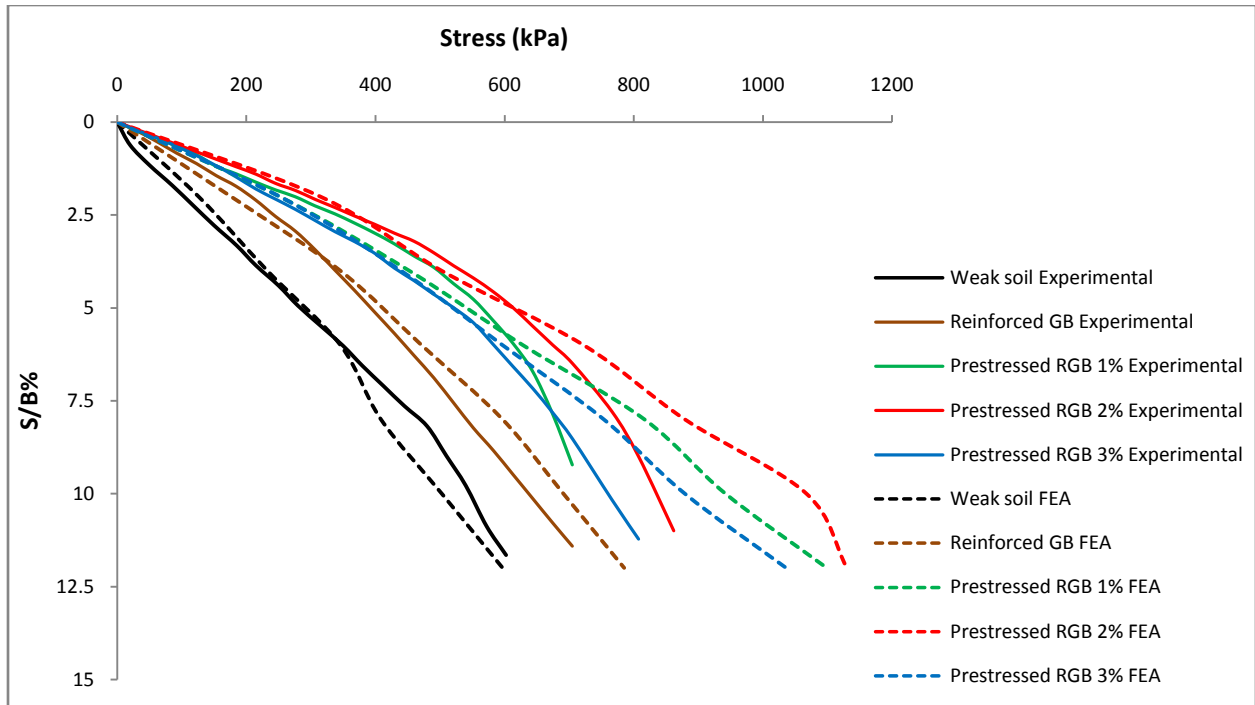


Fig 4.25 Stress vs normalized settlement curves for PRGB of thickness B with biaxially prestressed single layer geogrid of size 2B x 2B overlying (moist) weak soil 1.

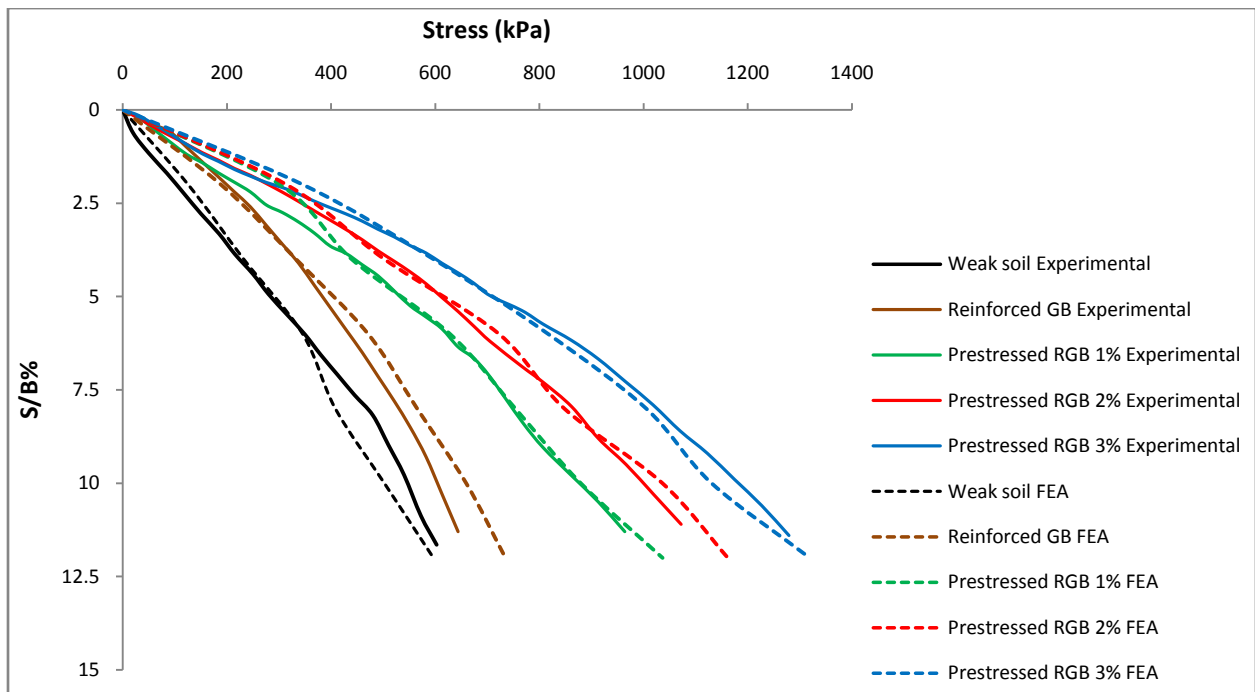


Fig 4.26 Stress vs normalized settlement curves for PRGB of thickness 2B with uniaxially prestressed single layer geogrid of size 2B x 2B overlying (moist) weak soil 1.

Figure 4.26 shows the variation of vertical stress with normalized settlement of a uniaxially prestressed RGB of thickness 2B with single layer geogrid reinforcement of size 2B x 2B overlying (moist) weak soil 1. The maximum improvement is attained when the uniaxial prestress is equal to 3% of the tensile strength of reinforcement. The behaviour is similar to that with bigger reinforcement (size 5B x 5B).

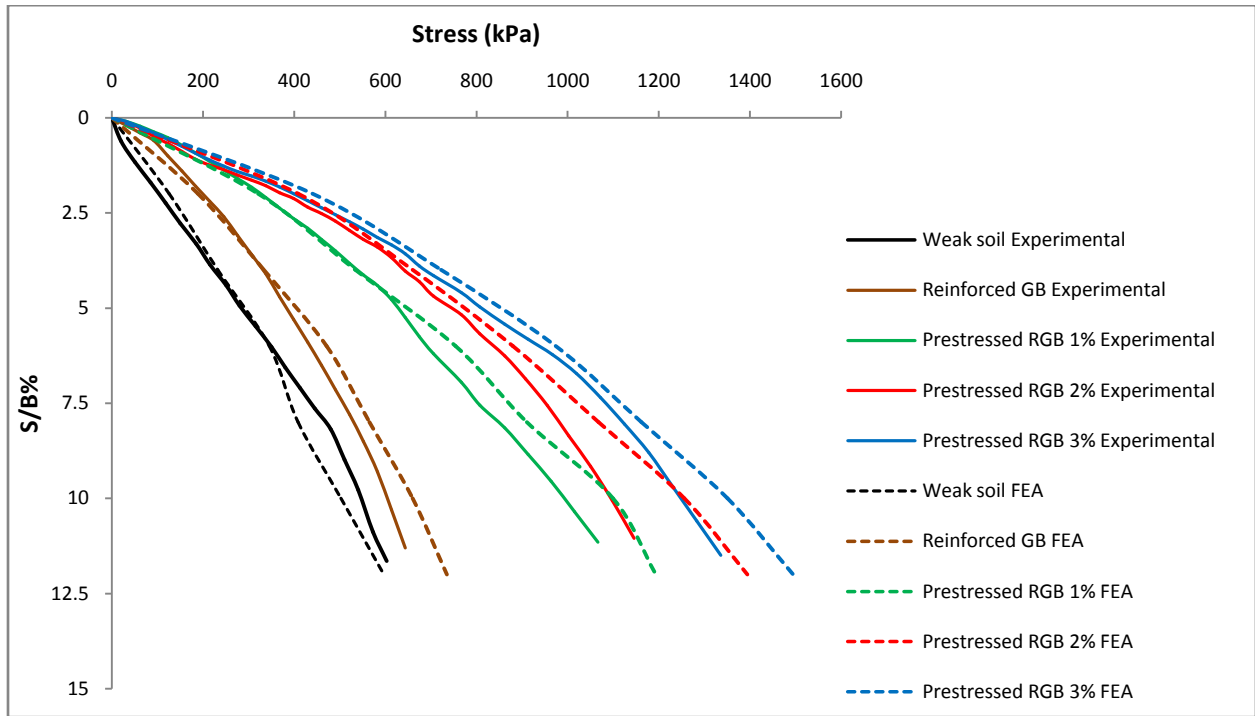


Fig 4.27 Stress vs normalized settlement curves for PRGB of thickness 2B with biaxially prestressed single layer geogrid of size 2B x 2B overlying (moist) weak soil 1.

The results of experimental studies and finite element analyses of a biaxially prestressed RGB of thickness 2B with single layer geogrid reinforcement of size 2B x 2B overlying (moist) weak soil 1 is given in Fig 4.27. It is observed that maximum improvement in bearing capacity is attained when the biaxial prestress is equal to 3% of the tensile strength of reinforcement. This behaviour also is similar to that with bigger reinforcement (size 5B x 5B).

4.3.1.6 PRGB with single layer geogrid of size 2B x 2B overlying weak soil 2 (submerged soil)

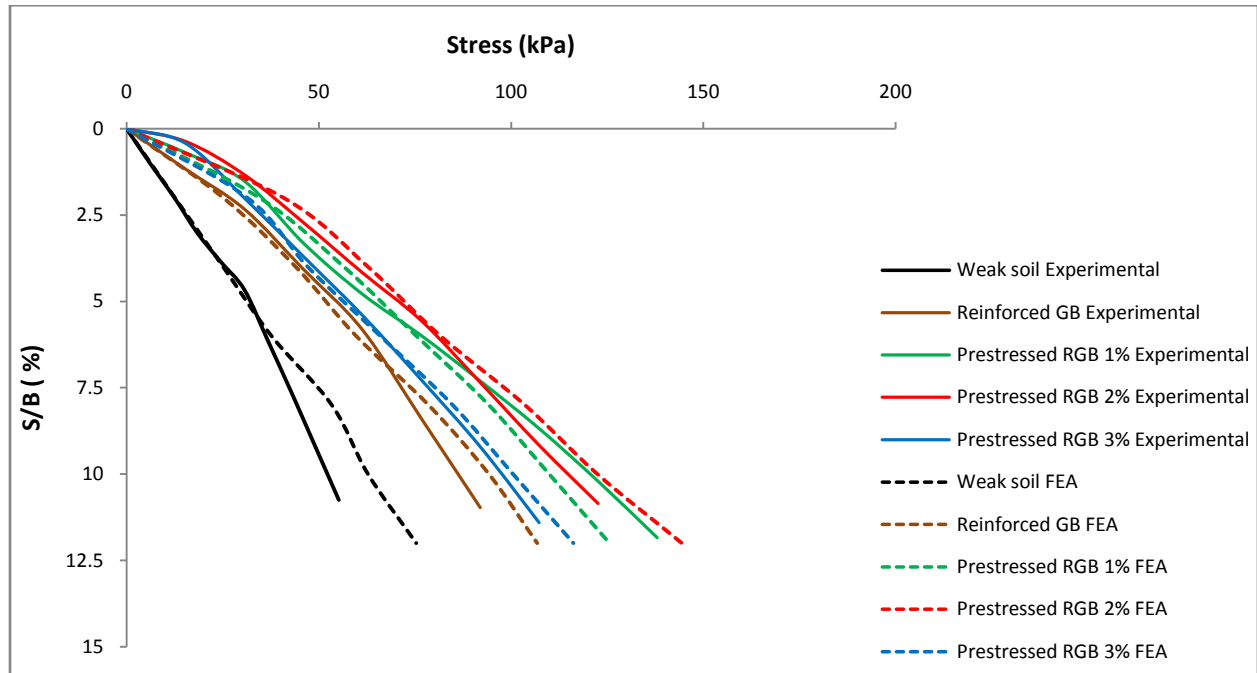


Fig 4.28 Stress vs normalized settlement curves for PRGB of thickness B with uniaxially prestressed single layer geogrid of size 2B x 2B overlying (submerged) weak soil 2.

The settlement behaviour of uniaxially prestressed PRGB of thickness B with single layer geogrid reinforcement of size 2B x 2B overlying (submerged) weak soil 2 is presented in Fig 4.28. The submergence of weak soil caused a large reduction in its strength. However due to prestressing the bearing capacity improved and maximum improvement occurred when the uniaxial prestress is equal to 2% of the tensile strength of the reinforcement. Further increase in prestress decreases the improvement. This is same as in the case of weak soil 1.

Figure 4.29 shows the variation of vertical stress with normalized settlement of a biaxially prestressed RGB of thickness B with single layer geogrid reinforcement of size 2B x 2B overlying (submerged) weak soil 2. The maximum improvement is attained when the biaxial prestress is equal to 2% of the tensile strength of reinforcement. The behaviour is similar to that with bigger reinforcement (size 5B x 5B).

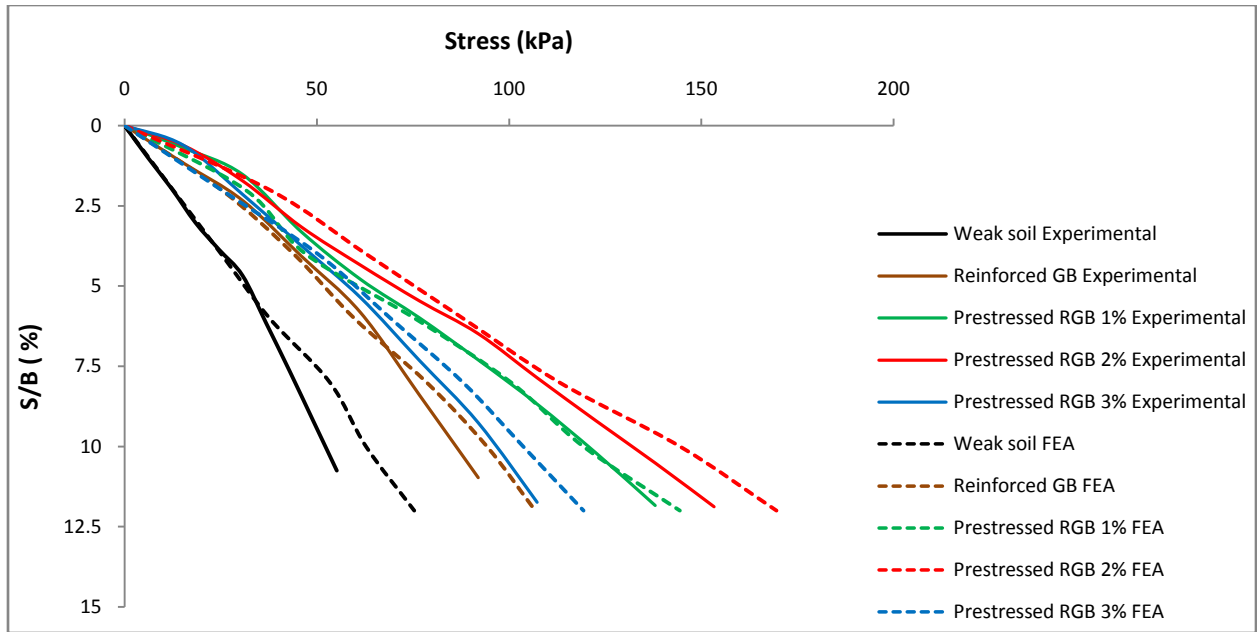


Fig 4.29 Stress vs normalized settlement curves for PRGB of thickness B with biaxially prestressed single layer geogrid of size $2B \times 2B$ overlying (submerged) weak soil 2.

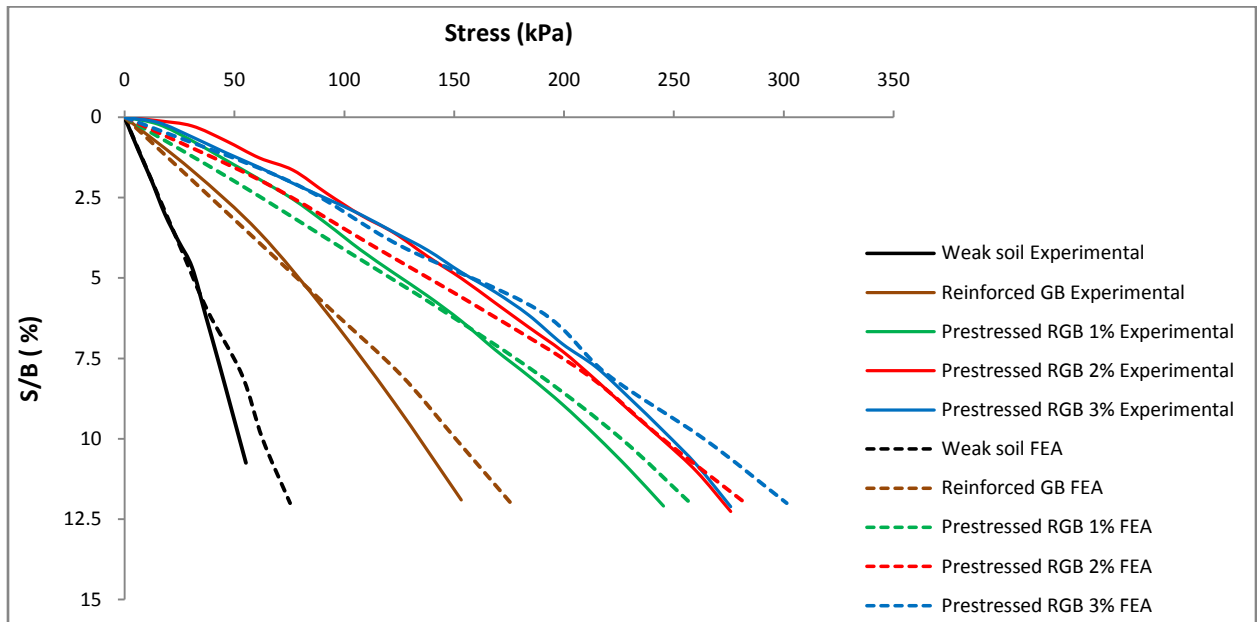


Fig 4.30 Stress vs normalized settlement curves for PRGB of thickness $2B$ with uniaxially prestressed single layer geogrid of size $2B \times 2B$ overlying (submerged) weak soil 2.

With increased thickness of granular bed to $2B$ and with uniaxially prestressed single layer geogrid reinforcement of size $2B \times 2B$ overlying (submerged) weak soil 2, it is observed (Fig.4.30) that the maximum improvement is attained when the magnitude of prestress is equal to

3% of the tensile strength of reinforcement. However, as per the results of experimental studies, the improvement attained when the prestress is increased from 2% to 3% is only marginal.

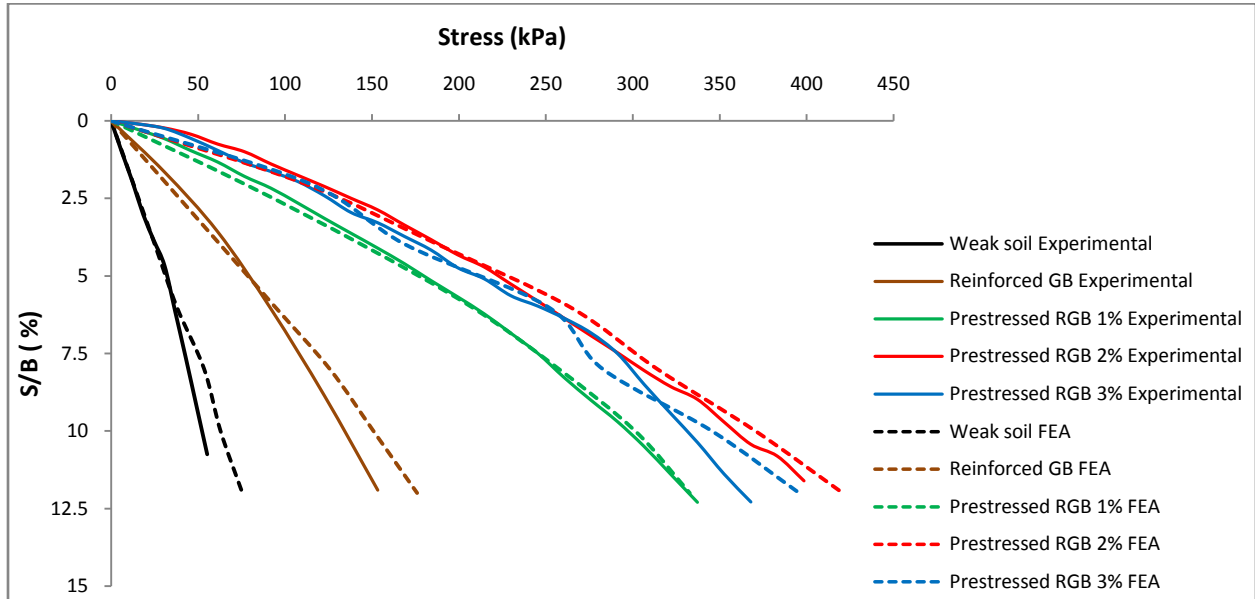


Fig 4.31 Stress vs normalized settlement curves for PRGB of thickness 2B with biaxially prestressed single layer geogrid of size 2B x 2B overlying (submerged) weak soil 2.

The settlement behaviour of biaxially prestressed PRGB of thickness 2B with single layer geogrid reinforcement of size 2B x 2B overlying (submerged) weak soil 2 is presented in Fig 4.31. The maximum improvement occurred when the biaxial prestress is equal to 2% of the tensile strength of the reinforcement. Further increase in prestress decreases the improvement. This is unlike the behaviour with uniaxial prestress which peaked at 3% prestress.

4.3.1.7 PRGB with double layer geogrid of size 5B x 5B overlying weak soil 1 (moist soil)

The results of experimental studies and finite element analyses of a uniaxially prestressed RGB of thickness B with double layer geogrid reinforcement of size 5B x 5B overlying (moist) weak soil 1 is given in Fig 4.32. It is observed that maximum improvement in bearing capacity is attained when the uniaxial prestress is equal to 2% of the tensile strength of reinforcement. An increase of prestress from 2% to 3% caused a marginal decrease in bearing capacity.

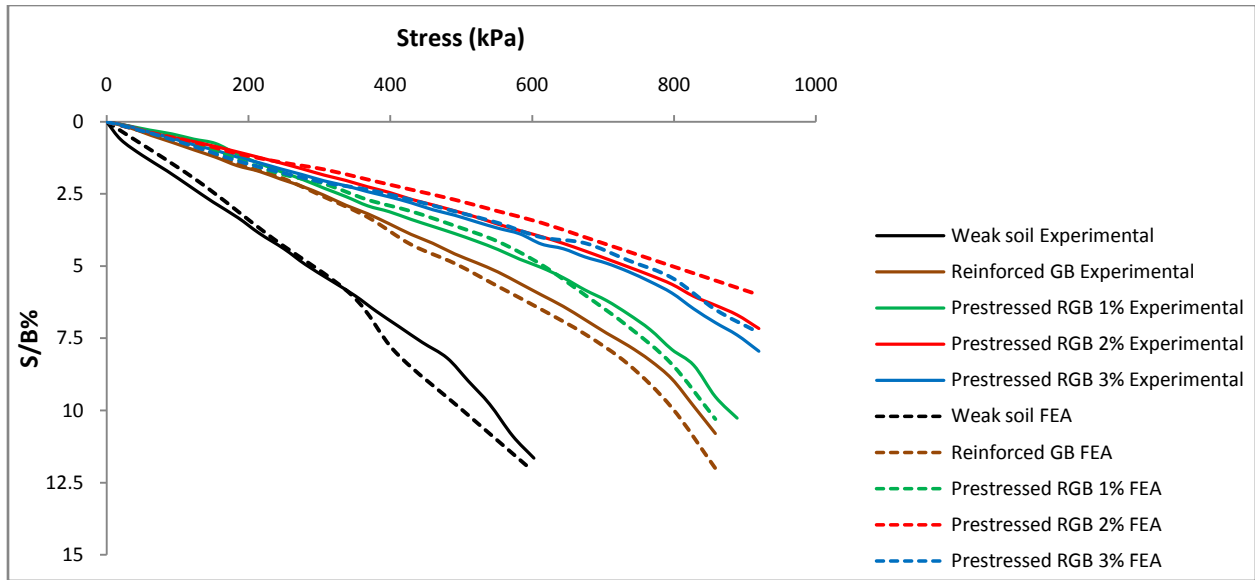


Fig 4.32 Stress vs normalized settlement curves for PRGB of thickness B with uniaxially prestressed double layer geogrid of size 5B x 5B overlying (moist) weak soil 1.

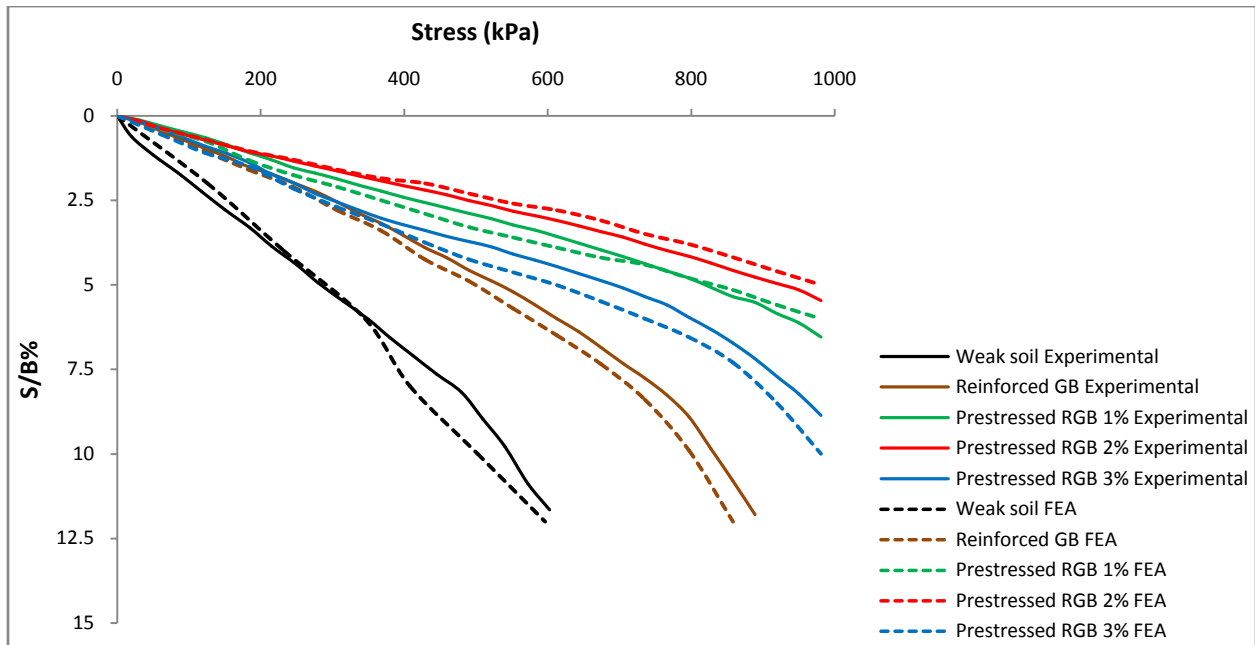


Fig 4.33 Stress vs normalized settlement curves for PRGB of thickness B with biaxially prestressed double layer geogrid of size 5B x 5B overlying (moist) weak soil 1.

Figure 4.33 shows the variation of vertical stress with normalized settlement of a biaxially prestressed RGB of thickness B with double layer geogrid reinforcement of size 5B x 5B overlying (moist) weak soil 1. The maximum improvement is attained when the biaxial prestress

is equal to 2% of the tensile strength of reinforcement. This is unlike the behaviour with single layer reinforcement which peaked at 1% prestress.

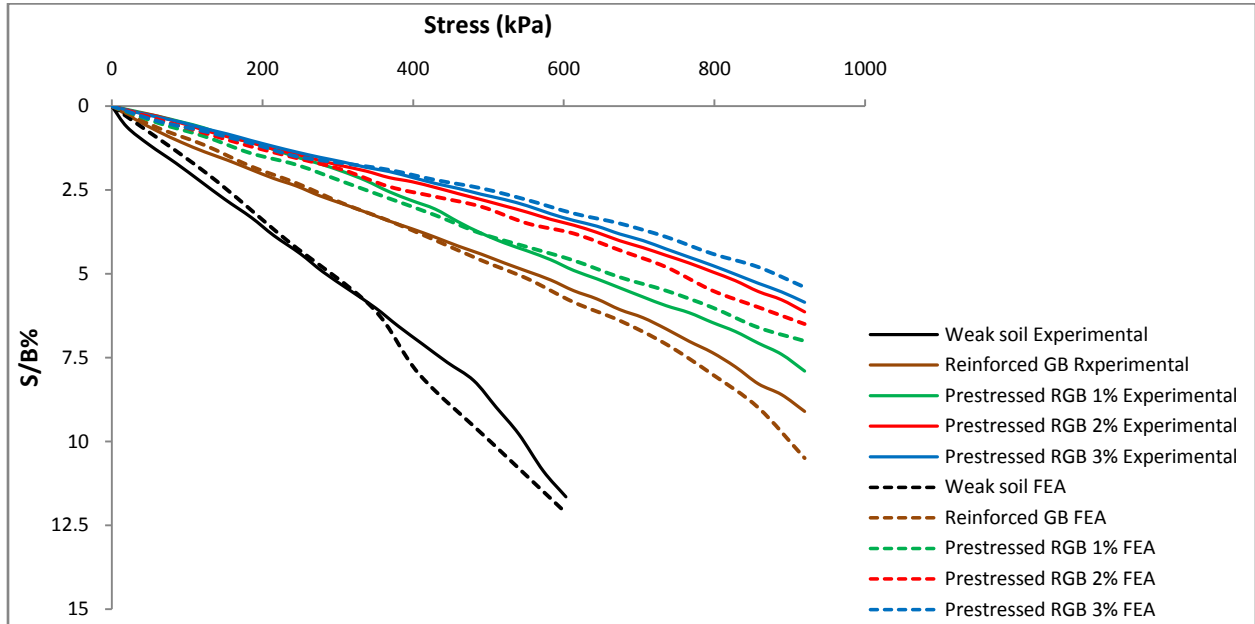


Fig 4.34 Stress vs normalized settlement curves for PRGB of thickness 2B with uniaxially prestressed double layer geogrid of size 5B x 5B overlying (moist) weak soil 1.

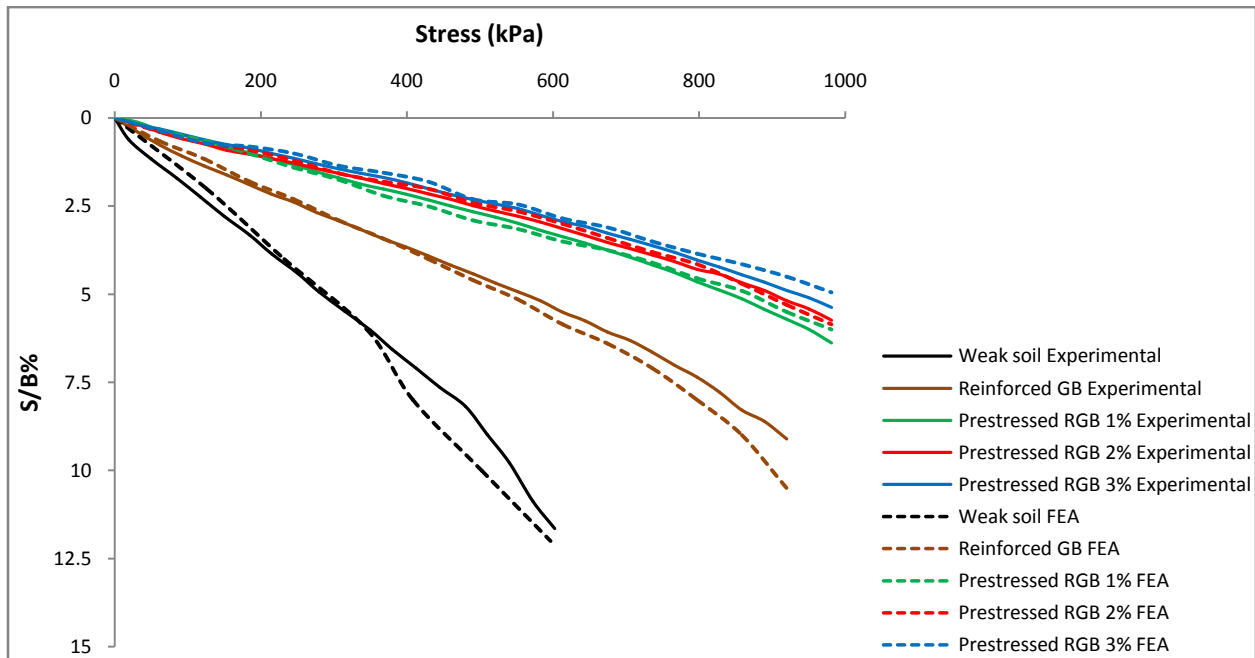


Fig 4.35 Stress vs normalized settlement curves for PRGB of thickness 2B with biaxially prestressed double layer geogrid of size 5B x 5B overlying (moist) weak soil 1.

With increased thickness of granular bed to 2B and with uniaxially prestressed double layer geogrid reinforcement of size 5B x 5B overlying (moist) weak soil 1, it is observed (Fig.4.34) that the maximum improvement is attained when the magnitude of prestress is equal to 3% of the tensile strength of reinforcement. The behaviour is similar to that with single layer reinforcement.

The settlement behaviour of biaxially prestressed PRGB of thickness 2B with double layer geogrid reinforcement of size 5B x 5B overlying (moist) weak soil 1 is presented in Fig 4.35. The maximum improvement occurred when the biaxial prestress is equal to 3% of the tensile strength of the reinforcement. The behaviour is similar to that with single layer reinforcement.

4.3.1.8 PRGB with double layer geogrid of size 5B x 5B overlying weak soil 2 (submerged soil)

The results of experimental studies and finite element analyses of a uniaxially prestressed RGB of thickness B with double layer geogrid reinforcement of size 5B x 5B overlying (submerged) weak soil 2 is given in Fig 4.36. It is observed that maximum improvement in bearing capacity is attained when the uniaxial prestress is equal to 2% of the tensile strength of reinforcement. The behaviour is similar to that with single layer reinforcement.

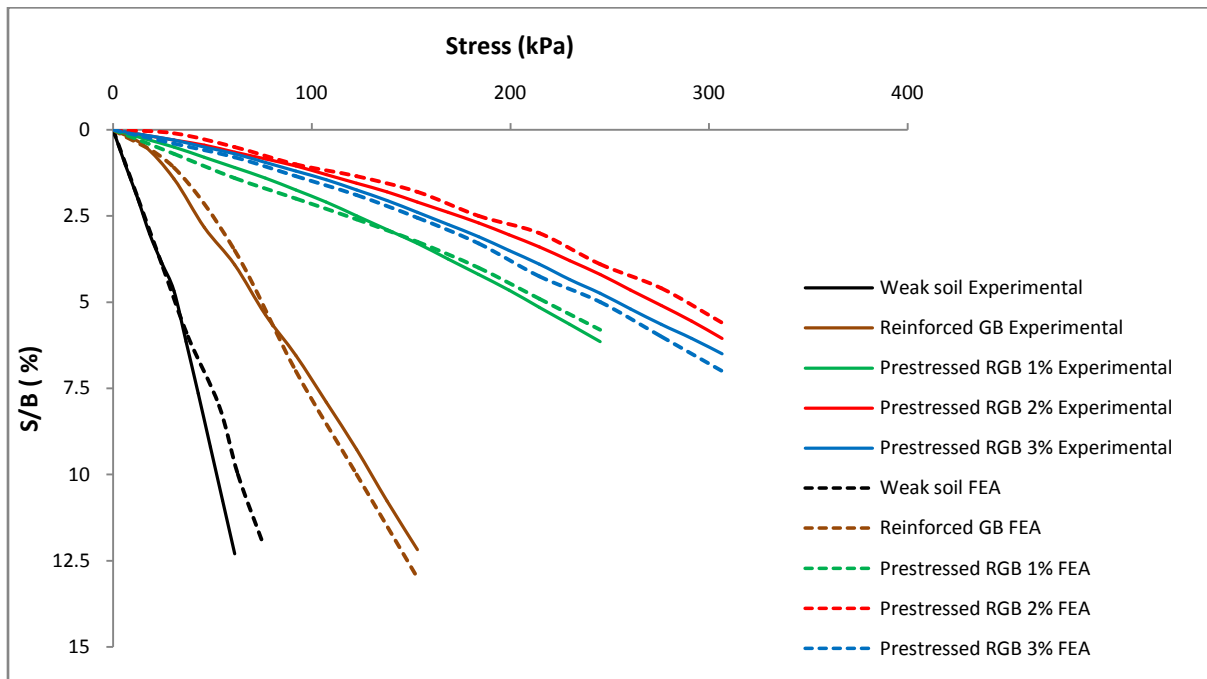


Fig 4.36 Stress vs normalized settlement curves for PRGB of thickness B with uniaxially prestressed double layer geogrid of size 5B x 5B overlying (submerged) weak soil 2.

The settlement behaviour of biaxially prestressed PRGB of thickness B with double layer geogrid reinforcement of size $5B \times 5B$ overlying (submerged) weak soil 2 is presented in Fig 4.37. The maximum improvement occurred when the biaxial prestress is equal to 2% of the tensile strength of the reinforcement. The behaviour is similar to that with single layer reinforcement.

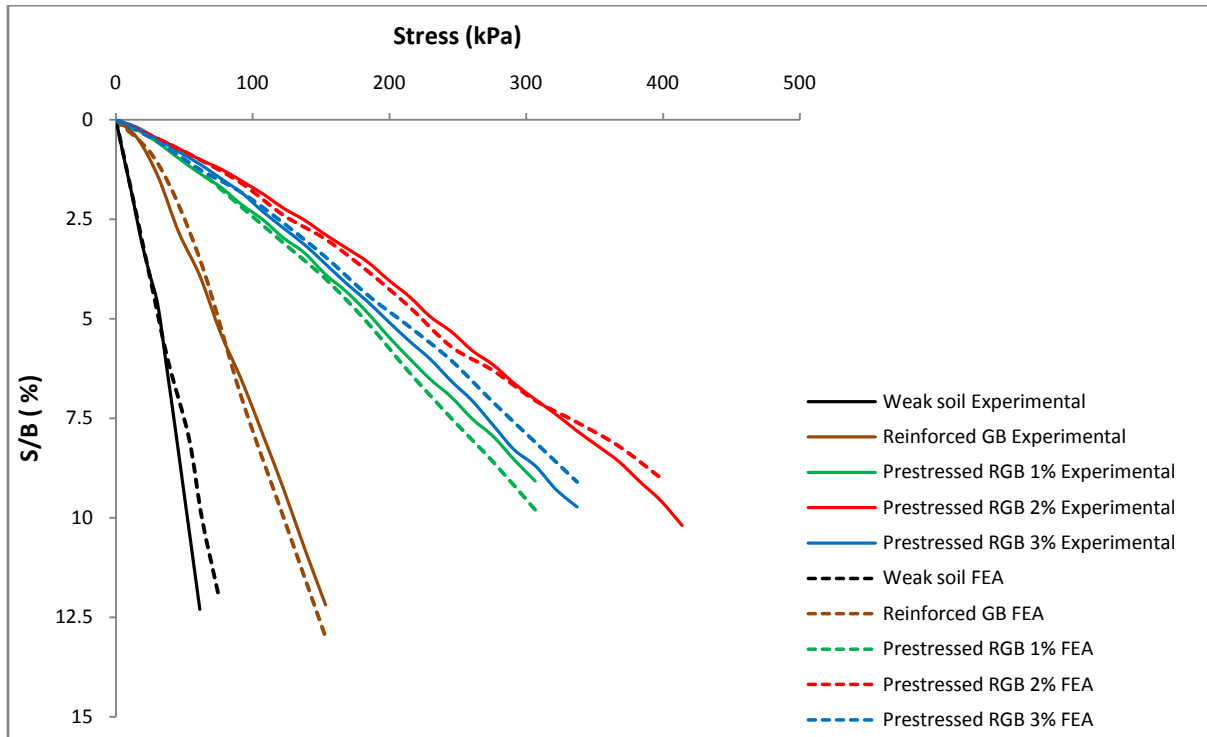


Fig 4.37 Stress vs normalized settlement curves for PRGB of thickness B with biaxially prestressed double layer geogrid of size $5B \times 5B$ overlying (submerged) weak soil 2.

With increased thickness of granular bed to $2B$ and with uniaxially prestressed double layer geogrid reinforcement of size $5B \times 5B$ overlying (submerged) weak soil 2, it is observed (Fig.4.38) that the maximum improvement is attained when the magnitude of prestress is equal to 2% of the tensile strength of reinforcement. This behaviour is similar to that with single layer reinforcement. From the result of experimental studies it is observed that when prestress is increased from 1% to 2% the improvement in bearing capacity is only marginal.

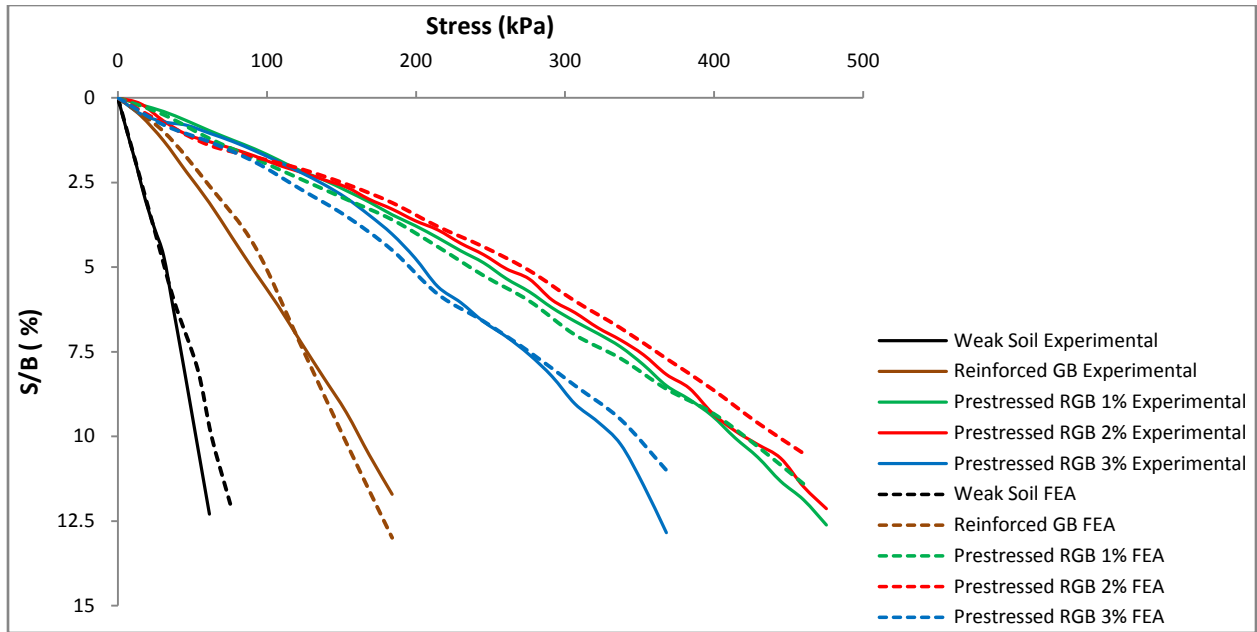


Fig 4.38 Stress vs normalized settlement curves for PRGB of thickness 2B with uniaxially prestressed double layer geogrid of size 5B x 5B overlying (submerged) weak soil 2.

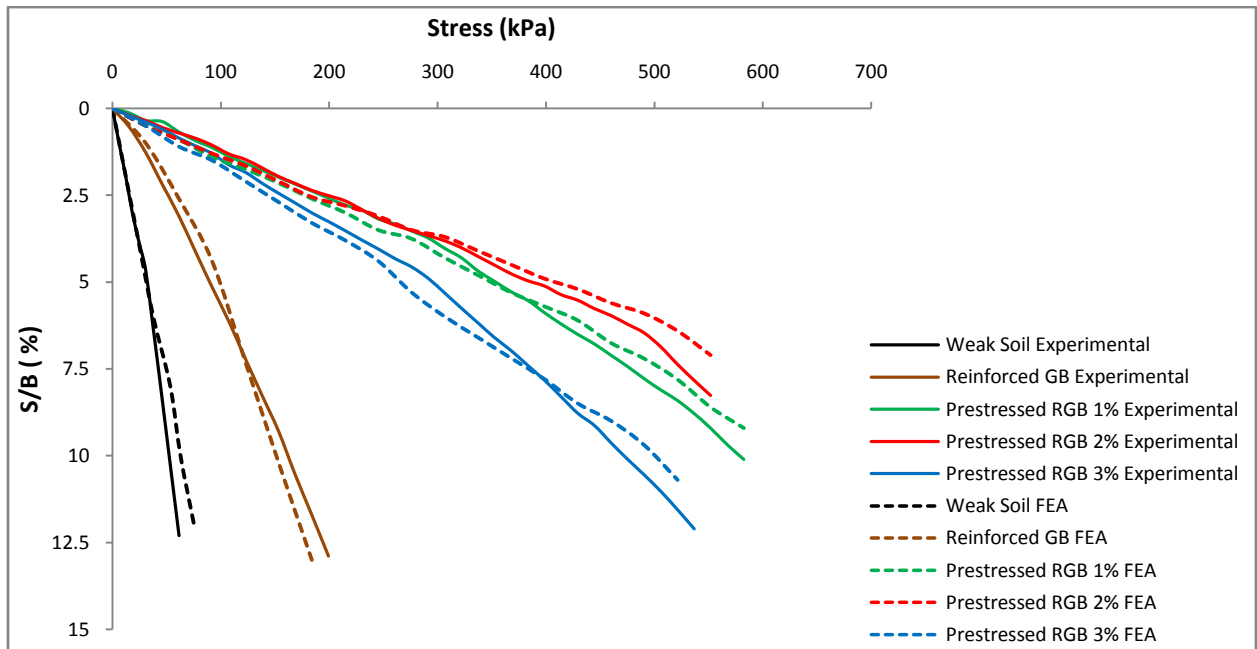


Fig 4.39 Stress vs normalized settlement curves for PRGB of thickness 2B with biaxially prestressed double layer geogrid of size 5B x 5B overlying (submerged) weak soil 2.

The results of experimental studies and finite element analyses of a biaxially prestressed RGB of thickness 2B with double layer geogrid reinforcement of size 5B x 5B overlying (submerged) weak soil 2 is given in Fig 4.39. It is observed that improvement in settlement behaviour with a

prestress of 1% and 2% is almost same up to a pressure of 300 kPa. At stresses more than 300 kPa, the improvement in settlement behaviour is more with prestress of 2%.

4.3.2 Effect of direction of prestress

In this study, prestress is applied in two directions; uniaxially and biaxially, as detailed in section 3.7. Lovisa et al (2010) studied the effects of prestressing only with biaxial prestressing of reinforcement in granular soil. In this study, with RGB overlying weak soil, it is attempted to determine the optimum direction of application of prestress for various cases. A comparison between uniaxial prestressing and biaxial prestressing for various cases are presented below.

4.3.2.1 PRGB with single layer geogrid of size 5B x 5B overlying weak soil 1 (moist soil)

Figure 4.40 represents the variation of bearing pressure with footing settlement of uniaxially and biaxially prestressed RGB of thickness B with single layer geogrid reinforcement of size 5B x 5B overlying (moist) weak soil 1. It is observed that improvement in settlement behaviour is more with biaxial prestressing.

The results of studies on uniaxially and biaxially prestressed RGB of thickness 2B with single layer geogrid reinforcement of size 5B x 5B overlying (moist) weak soil 1 is given in Fig 4.41. It is observed that improvement in settlement behaviour is more with biaxial prestressing. At 3% prestress the improvement attained with both uniaxial and biaxial prestressing are almost same.

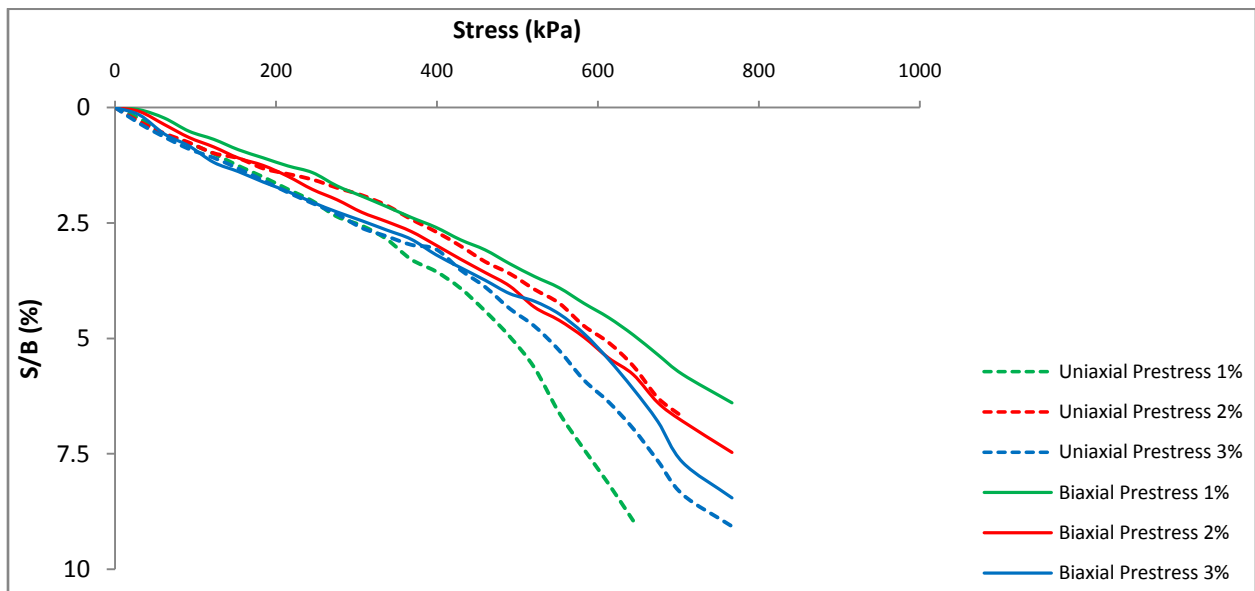


Fig 4.40 Stress vs normalized settlement curves for PRGB of thickness B with uniaxially and biaxially prestressed single layer geogrid of size 5B x 5B overlying (moist) weak soil 1.

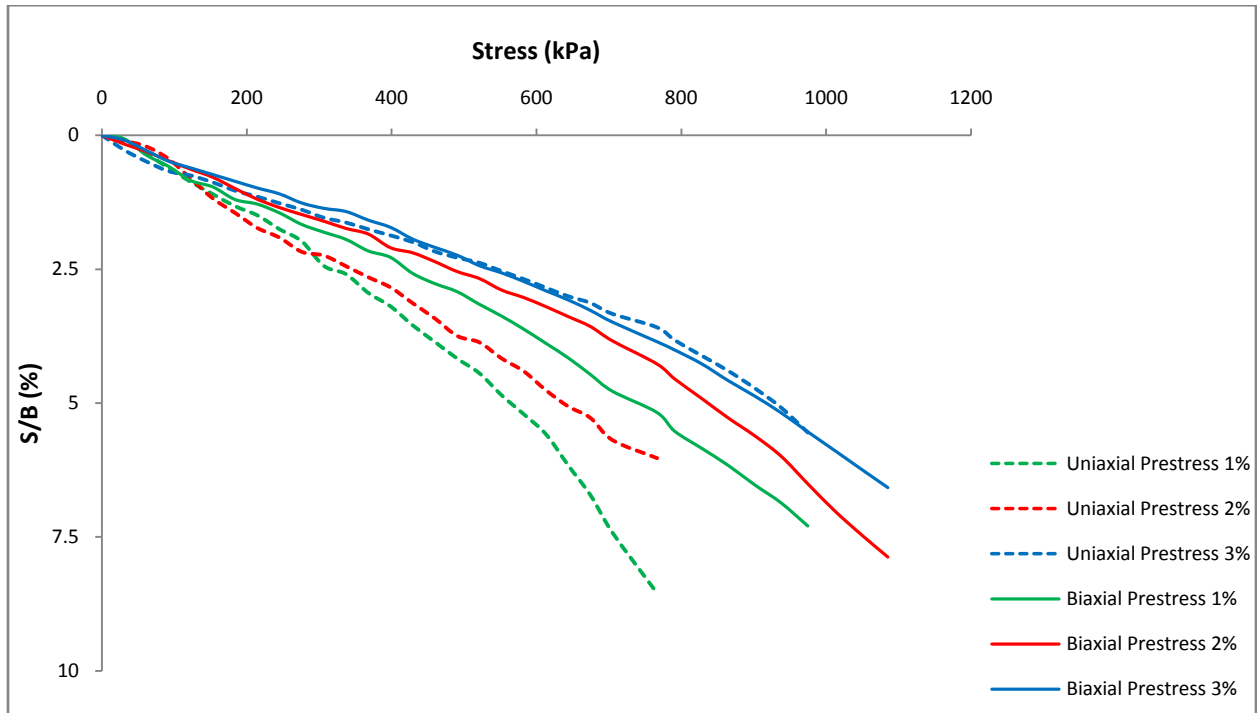


Fig 4.41 Stress vs normalized settlement curves for PRGB of thickness 2B with uniaxially and biaxially prestressed single layer geogrid of size 5B x 5B overlying (moist) weak soil 1.

4.3.2.2 PRGB with single layer geogrid of size 5B x 5B overlying weak soil 2 (submerged soil)

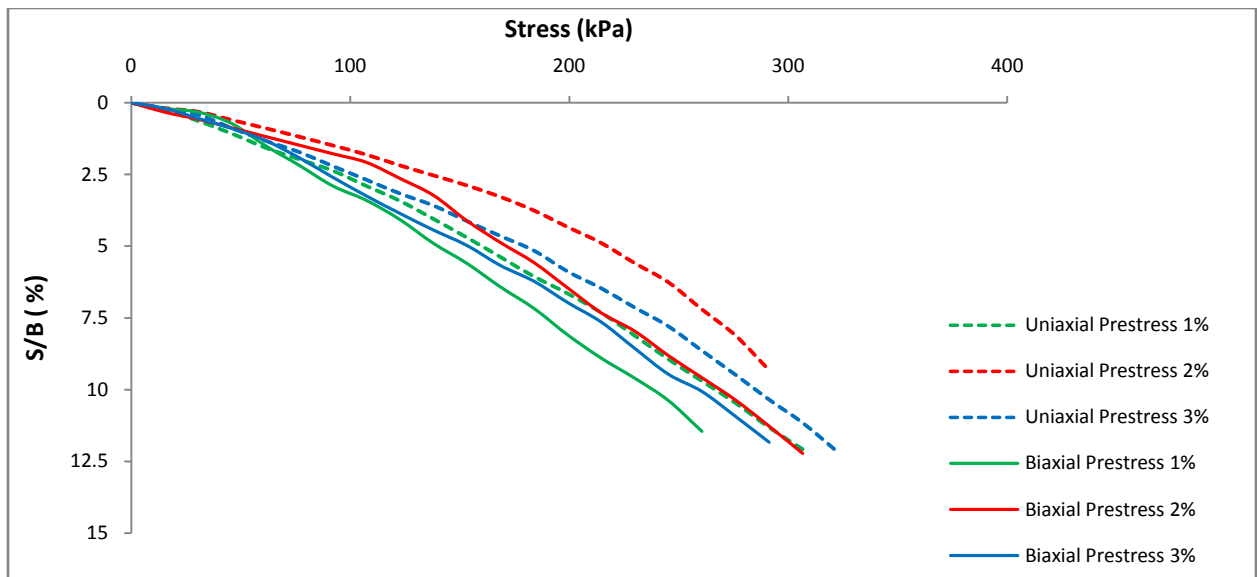


Fig 4.42 Stress vs normalized settlement curves for PRGB of thickness B with uniaxially and biaxially prestressed single layer geogrid of size 5B x 5B overlying (submerged) weak soil 2.

When the underlying weak soil is kept submerged, the improvement in settlement behaviour for PRGB of thickness B with single layer geogrid reinforcement of size $5B \times 5B$ is more with uniaxial prestressing than biaxial prestressing (Fig. 4.42).

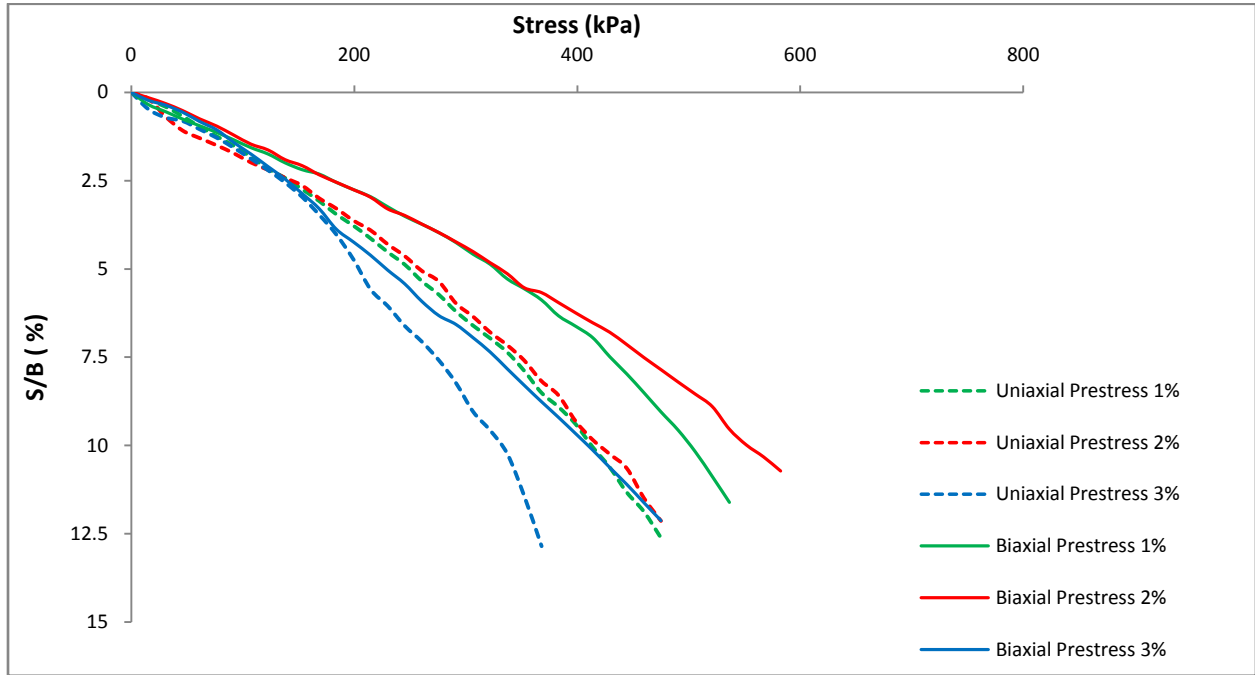


Fig 4.43 Stress vs normalized settlement curves for PRGB of thickness $2B$ with uniaxially and biaxially prestressed single layer geogrid of size $5B \times 5B$ overlying (submerged) weak soil 2.

With increased thickness of PRGB to $2B$ and with single layer geogrid reinforcement of size $5B \times 5B$ overlying (submerged) weak soil 2, the improvement is more with biaxial prestressing than with uniaxial prestressing (Fig 4.43).

During experimental investigation with granular beds overlying (submerged) weak soil 2, it was observed that capillary water rises into the dry sand in granular bed, from the submerged soil below, during the course of experiment. In granular beds of thickness B , the sand surrounding the reinforcement became moist during the experiment. In granular beds of thickness $2B$, the height of reinforcement from the submerged soil surface is more and the capillary moisture at the level of reinforcement is very less compared to that of granular beds of thickness B . The difference in behaviour of granular beds overlying submerged soil could be due to the presence of this capillary moisture in sand.

4.3.2.3 PRGB with single layer geotextile of size 5B x 5B overlying weak soil 1 (moist soil)

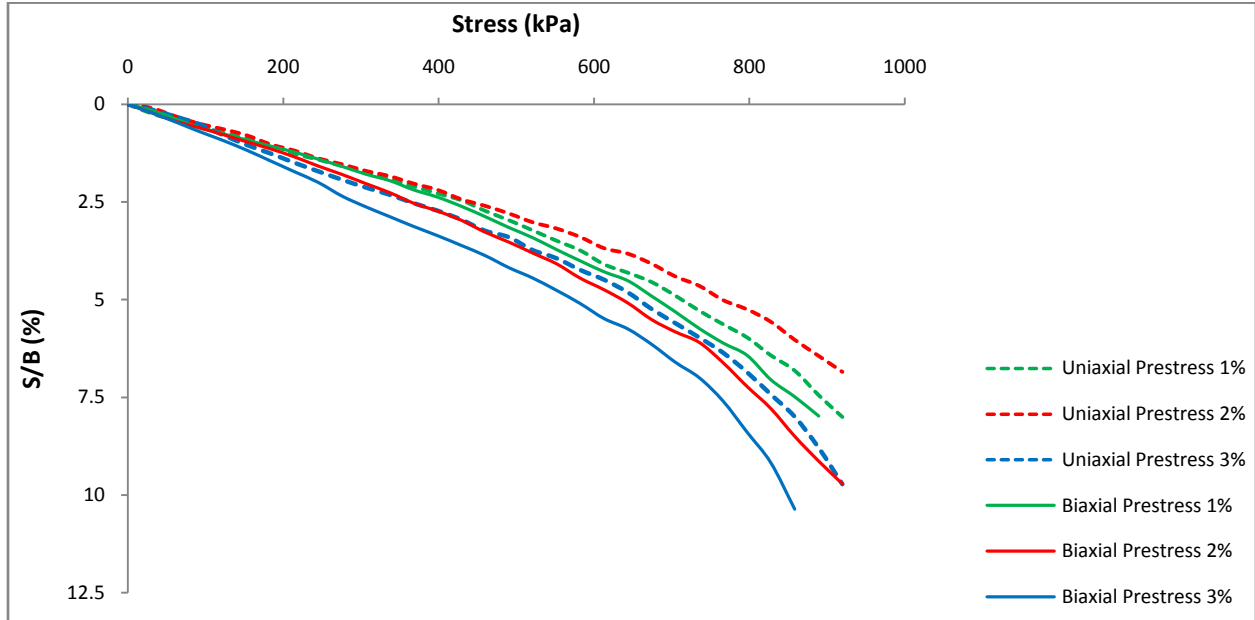


Fig 4.44 Stress vs normalized settlement curves for PRGB of thickness B with uniaxially and biaxially prestressed single layer geotextile of size 5B x 5B overlying (moist) weak soil 1.

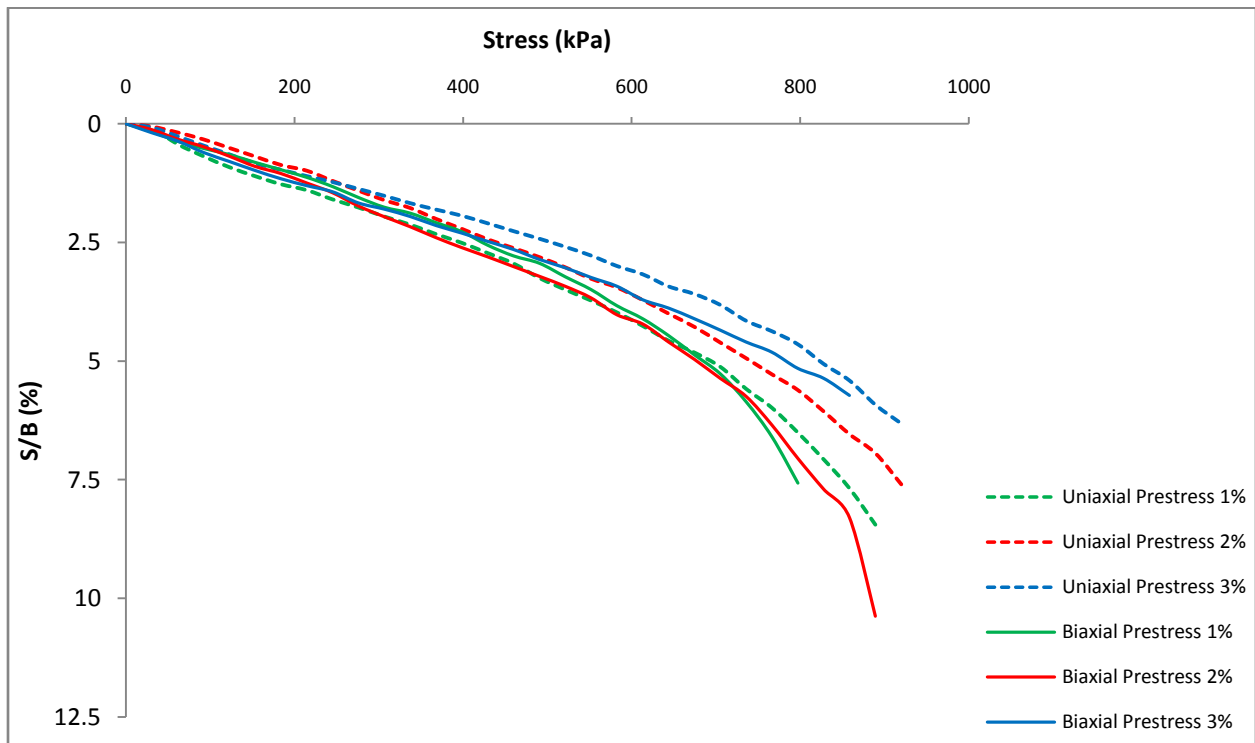


Fig 4.45 Stress vs normalized settlement curves for PRGB of thickness 2B with uniaxially and biaxially prestressed single layer geotextile of size 5B x 5B overlying (moist) weak soil 1.

Figure 4.44 shows the variation of bearing pressure with normalized settlement of uniaxially and biaxially prestressed RGB of thickness B with single layer geotextile reinforcement of size 5B x 5B overlying (moist) weak soil 1. It is observed that improvement in settlement behaviour is more with uniaxial prestressing.

The results of studies on uniaxially and biaxially prestressed RGB of thickness 2B with single layer geotextile reinforcement of size 5B x 5B overlying (moist) weak soil 1 is given in Fig 4.45. It is observed that improvement in settlement behaviour is more with uniaxial prestressing.

4.3.2.4 PRGB with single layer geotextile of size 5B x 5B overlying weak soil 2 (submerged soil)

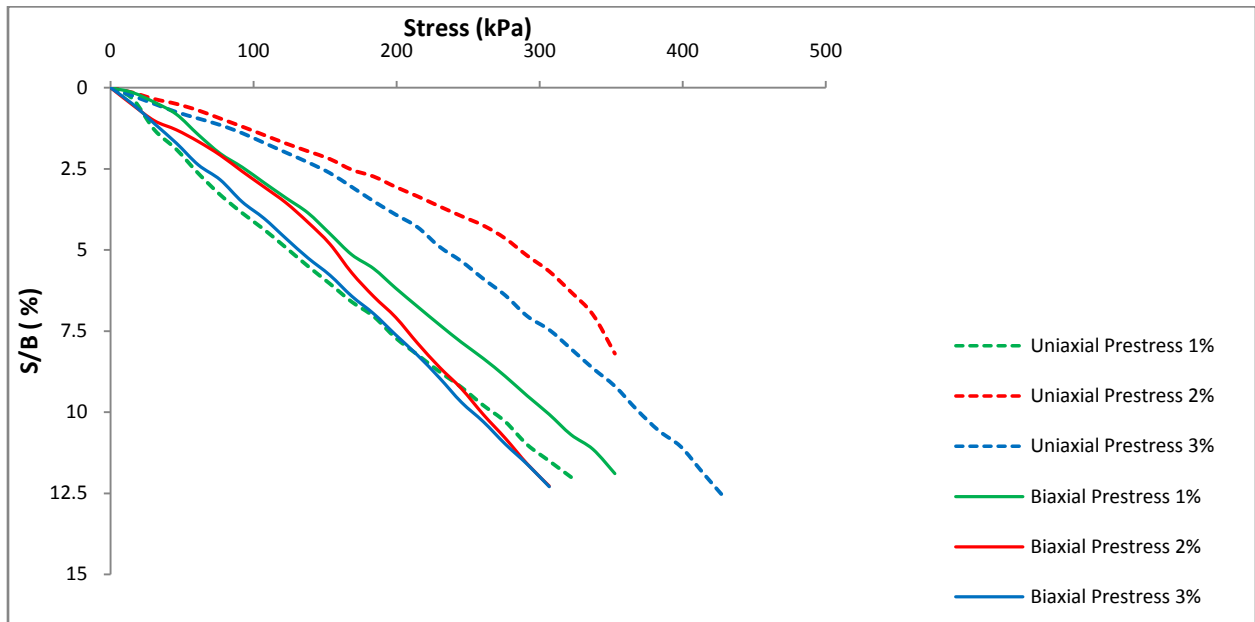


Fig 4.46 Stress vs normalized settlement curves for PRGB of thickness B with uniaxially and biaxially prestressed single layer geotextile of size 5B x 5B overlying (submerged) weak soil 2.

The results of studies on uniaxially and biaxially prestressed RGB of thickness B with single layer geotextile reinforcement of size 5B x 5B overlying (submerged) weak soil 2 is given in Fig 4.46. It is observed that improvement in settlement behaviour is more with uniaxial prestressing at 2% and 3% prestress. However at 1% prestress biaxial prestressing is giving more improvement than uniaxial prestressing.

Figure 4.47 shows the variation of bearing pressure with normalized settlement of uniaxially and biaxially prestressed RGB of thickness 2B with single layer geotextile reinforcement of size 5B x 5B overlying (submerged) weak soil 2. It is observed that at 1% and 2% prestress both uniaxial and biaxial prestressing are giving almost same improvement. At 3% prestress, however, uniaxial prestressing is giving more improvement than biaxial prestressing.

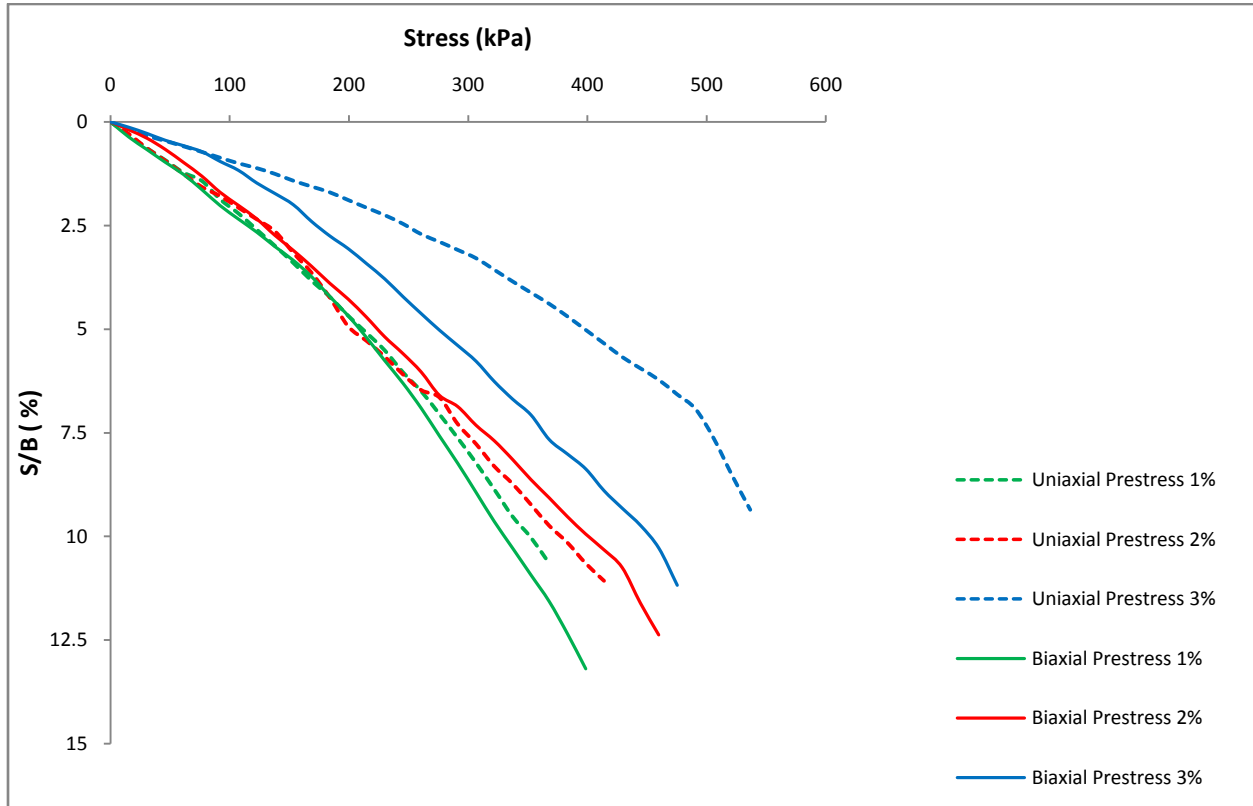


Fig 4.47 Stress vs normalized settlement curves for PRGB of thickness 2B with uniaxially and biaxially prestressed single layer geotextile of size 5B x 5B overlying (submerged) weak soil 2.

4.3.2.5 PRGB with single layer geogrid of size 2B x 2B overlying weak soil 1 (moist soil)

Figure 4.48 represents the variation of bearing pressure with footing settlement of uniaxially and biaxially prestressed RGB of thickness B with single layer geogrid reinforcement of size 2B x 2B overlying (moist) weak soil 1. It is observed that improvement in settlement behaviour is more with biaxial prestressing at 1% and 2% prestress. However at 3% prestress both uniaxial and biaxial prestressing are giving almost the same improvement.

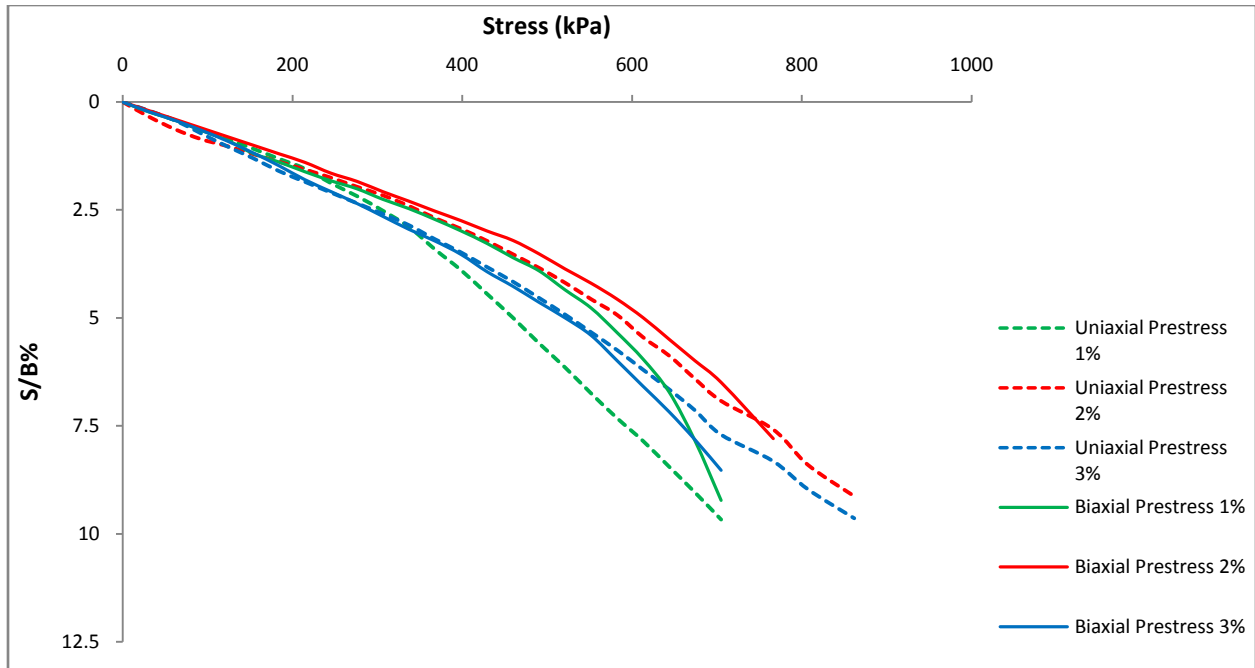


Fig 4.48 Stress vs normalized settlement curves for PRGB of thickness B with uniaxially and biaxially prestressed single layer geogrid of size 2B x 2B overlying (moist) weak soil 1.

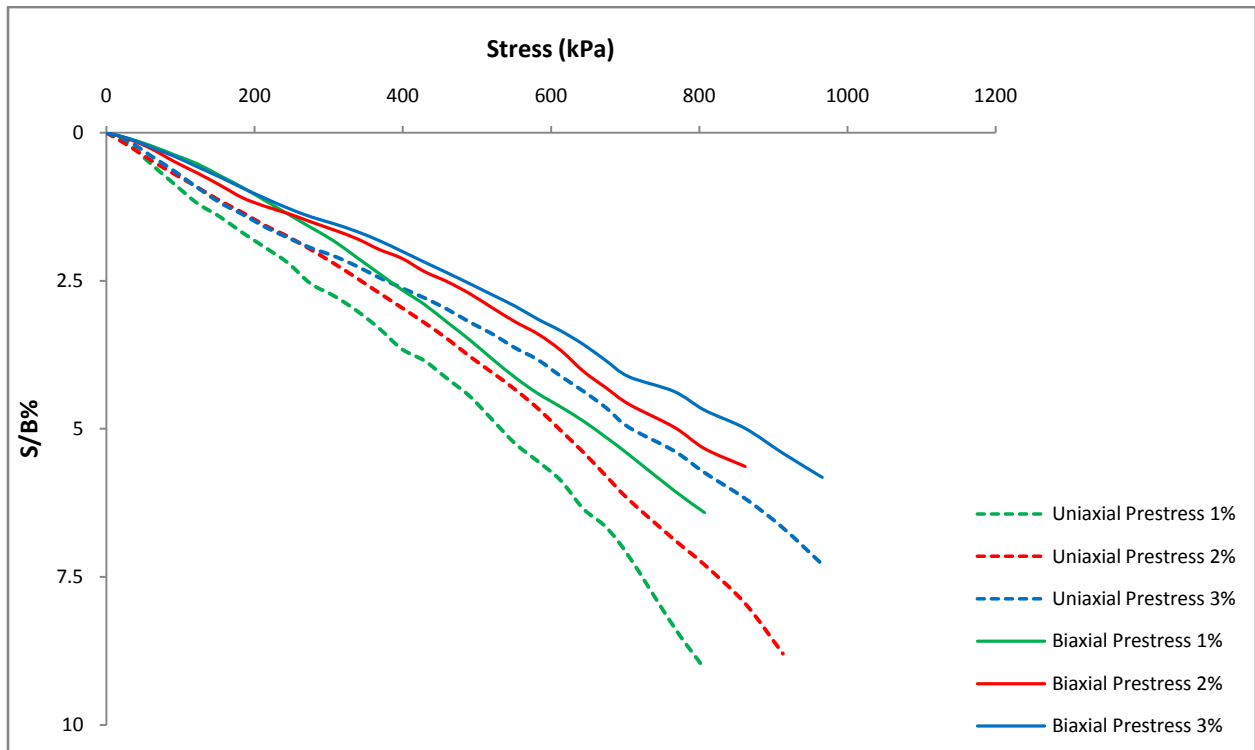


Fig 4.49 Stress vs normalized settlement curves for PRGB of thickness 2B with uniaxially and biaxially prestressed single layer geogrid of size 2B x 2B overlying (moist) weak soil 1.

With the thickness of granular bed increased to 2B and with single layer geogrid reinforcement of size 2B x 2B overlying (moist) weak soil it is observed that improvement in settlement behaviour is more with biaxial prestressing (Fig 4.49).

4.3.2.6 PRGB with single layer geogrid of size 2B x 2B overlying weak soil 2 (submerged soil)

Figure 4.50 shows the variation of bearing pressure with footing settlement of uniaxially and biaxially prestressed RGB of thickness B with single layer geogrid reinforcement of size 2B x 2B overlying (submerged) weak soil 2. It is observed that up to a stress of 75 kPa, the improvement given by both uniaxial and biaxial prestressing are almost same. At higher stresses, for 1% and 2% prestress, biaxial prestressing is giving more improvement, whereas for 3% prestress, uniaxial prestressing is giving more improvement.

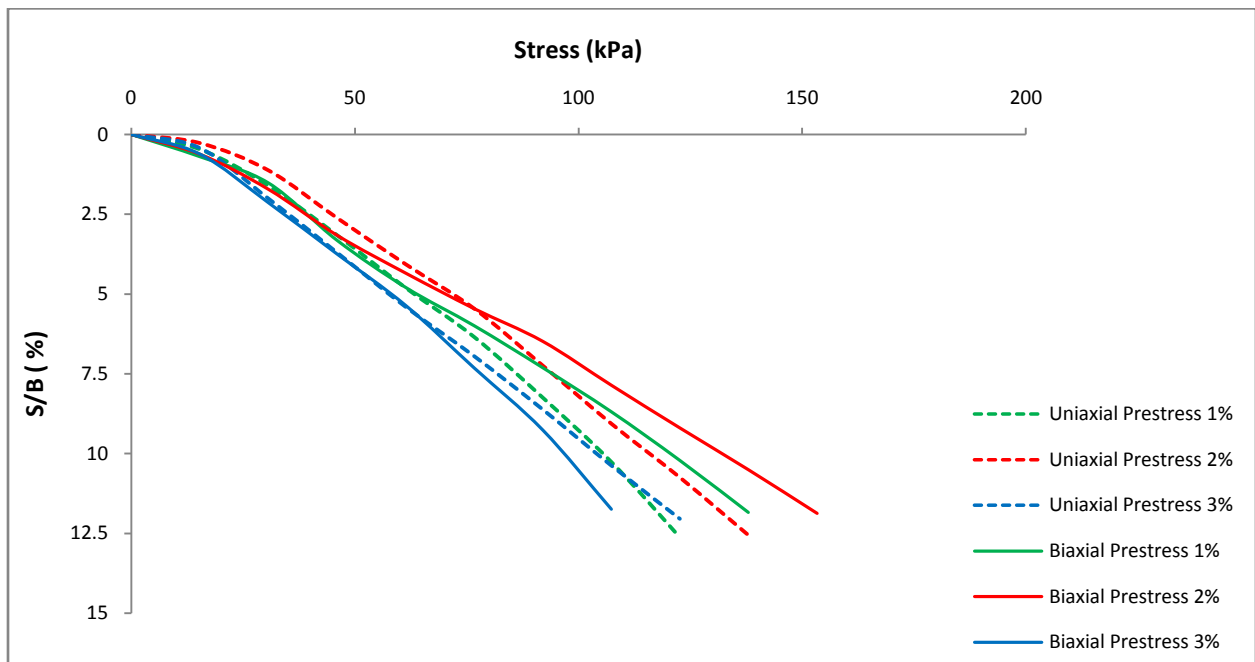


Fig 4.50 Stress vs normalized settlement curves for PRGB of thickness B with uniaxially and biaxially prestressed single layer geogrid of size 2B x 2B overlying (submerged) weak soil 2.

The results of studies on uniaxially and biaxially prestressed RGB of thickness 2B with single layer geogrid reinforcement of size 2B x 2B overlying (submerged) weak soil 2 is given in Fig 4.51. It is observed that improvement in settlement behaviour is more with biaxial prestressing.

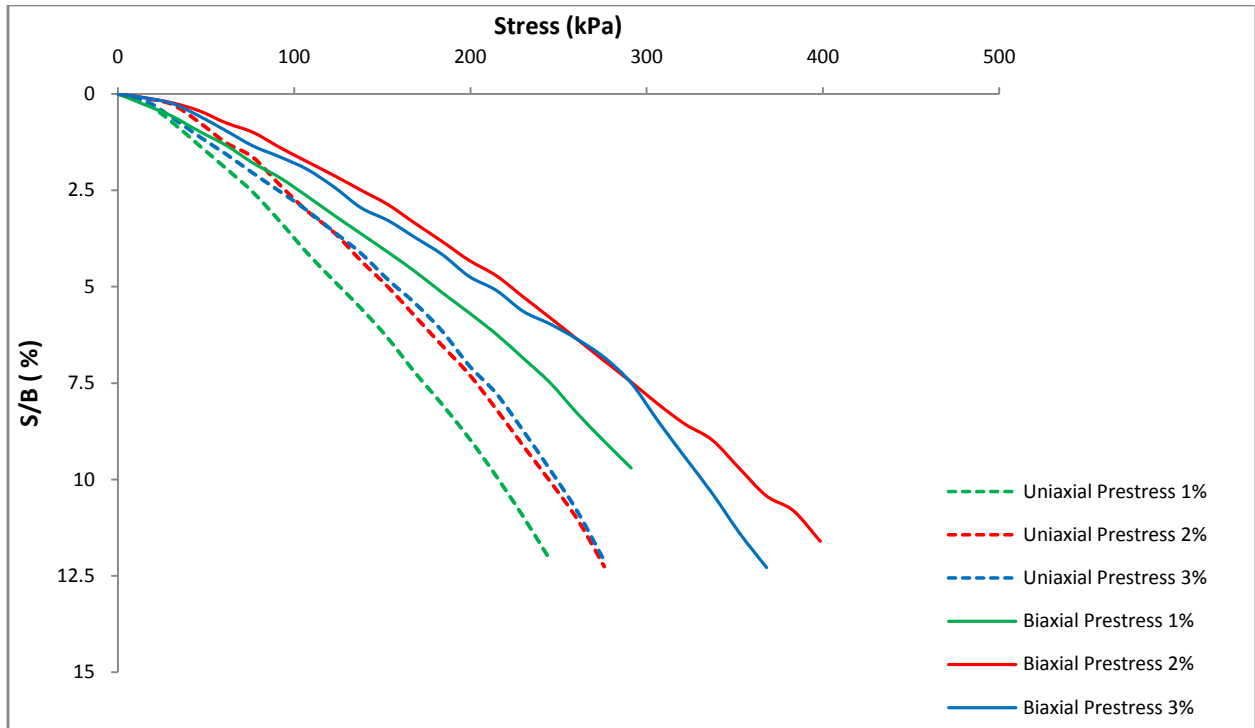


Fig 4.51 Stress vs normalized settlement curves for PRGB of thickness 2B with uniaxially and biaxially prestressed single layer geogrid of size 2B x 2B overlying (submerged) weak soil 2.

4.3.2.7 PRGB with double layer geogrid of size 5B x 5B overlying weak soil 1 (moist soil)

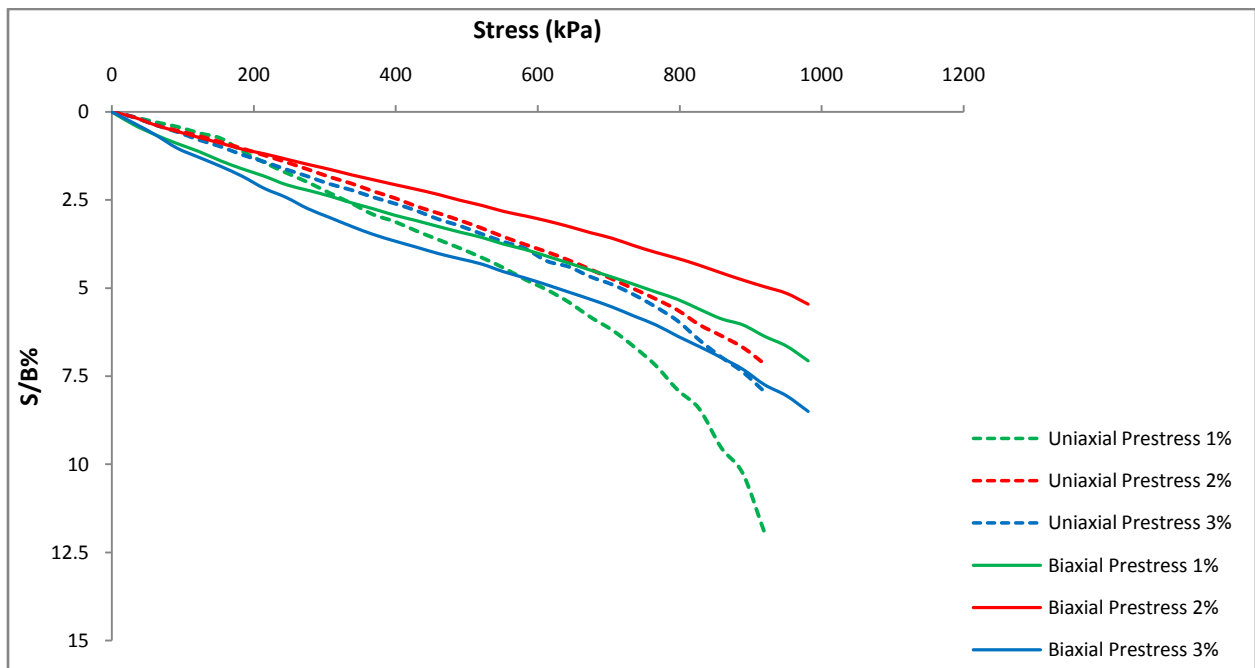


Fig 4.52 Stress vs normalized settlement curves for PRGB of thickness B with uniaxially and biaxially prestressed double layer geogrid of size 5B x 5B overlying (moist) weak soil 1.

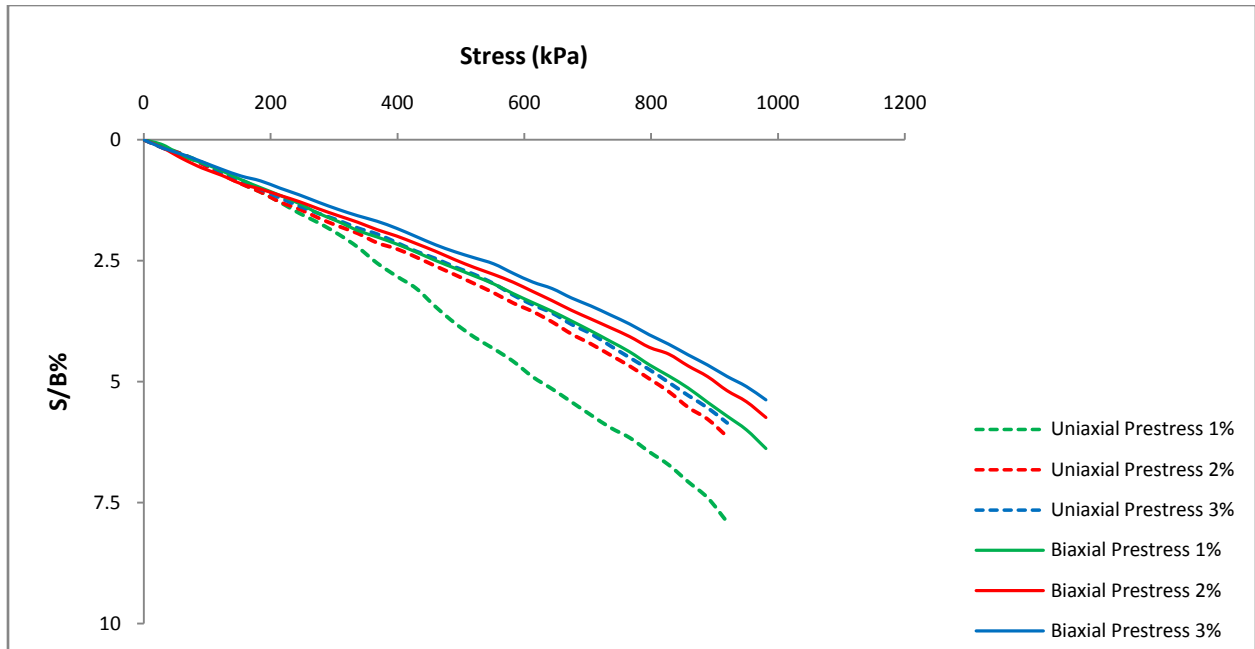


Fig 4.53 Stress vs normalized settlement curves for PRGB of thickness 2B with uniaxially and biaxially prestressed double layer geogrid of size 5B x 5B overlying (moist) weak soil 1.

Figure 4.52 represents the variation of bearing pressure with footing settlement of uniaxially and biaxially prestressed RGB of thickness B with double layer geogrid reinforcement of size 5B x 5B overlying (moist) weak soil 1. It is observed that at 1% and 2% prestress, the improvement in settlement behaviour is more with biaxial prestressing, whereas at 3% prestress, uniaxial prestressing is giving more improvement.

When the thickness of granular bed increased to 2B and with single layer geogrid reinforcement of size 5B x 5B overlying (moist) weak soil it is observed that improvement in settlement behaviour is more with biaxial prestressing at all magnitudes of prestress (Fig 4.53).

4.3.2.8 PRGB with double layer geogrid of size 5B x 5B overlying weak soil 2 (submerged soil)

The results of studies on uniaxially and biaxially prestressed RGB of thickness B with double layer geogrid reinforcement of size 5B x 5B overlying (submerged) weak soil 2 is given in Fig 4.54. It is observed that improvement in settlement behaviour is more with uniaxial prestressing.

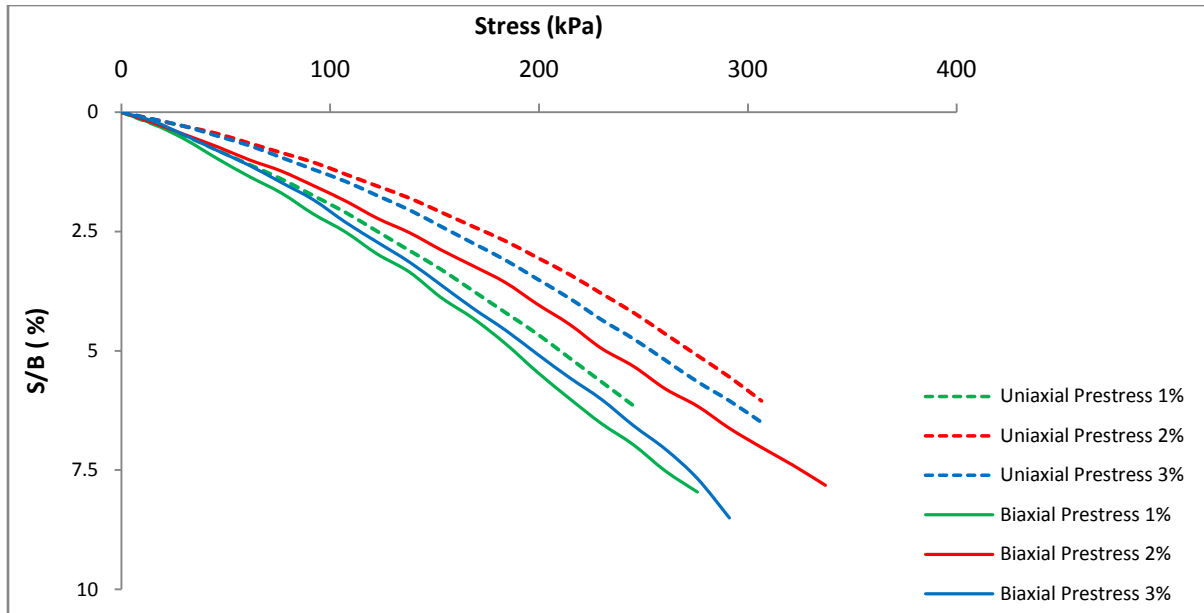


Fig 4.54 Stress vs normalized settlement curves for PRGB of thickness B with uniaxially and biaxially prestressed double layer geogrid of size 5B x 5B overlying (submerged) weak soil 2.

When the thickness of granular bed increased to 2B and with double layer geogrid reinforcement of size 5B x 5B overlying (submerged) weak soil 2 it is observed that improvement in settlement behaviour is more with biaxial prestressing at all magnitudes of prestress (Fig 4.55).

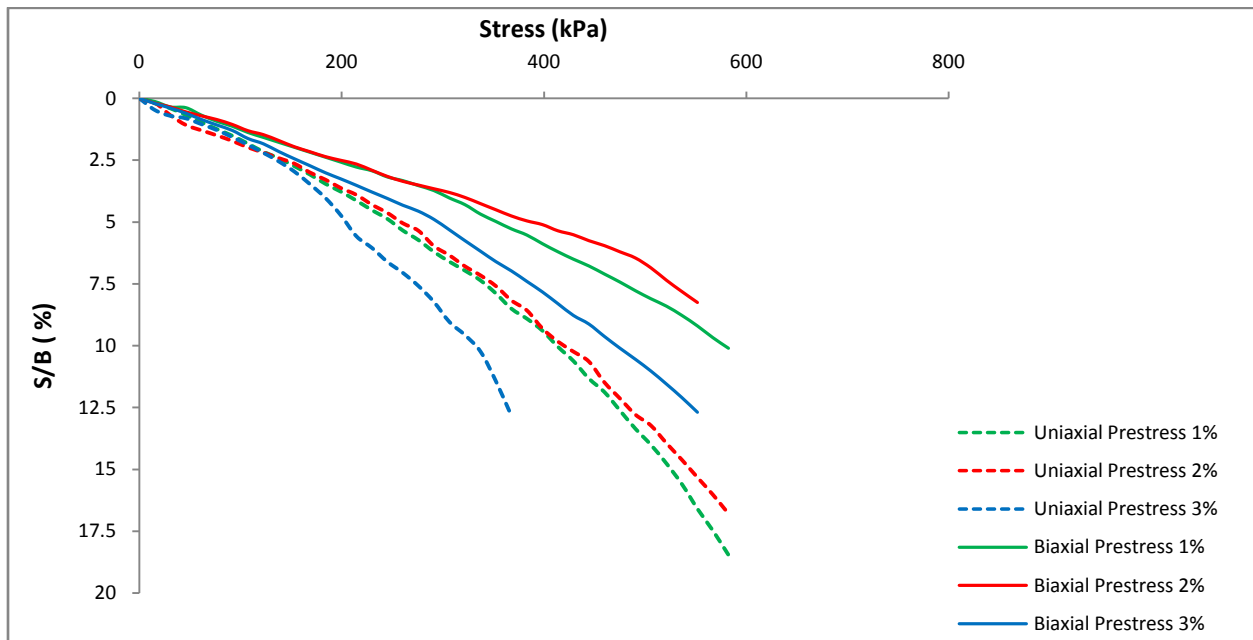


Fig 4.55 Stress vs normalized settlement curves for PRGB of thickness 2B with uniaxially and biaxially prestressed double layer geogrid of size 5B x 5B overlying (submerged) weak soil 2.

4.3.3 Effect of number of layers of prestressed geosynthetic reinforcement

In order to investigate the effect of the number of prestressed geosynthetic reinforcement layers, experimental and finite element studies are carried out with single and double layer geogrid reinforcement of size 5B x 5B. The effect of number of prestressed reinforcement layers is studied by comparing the bearing capacity ratios of various cases. The ratio of bearing capacity of improved soil to that of original soil is termed as bearing capacity ratio (BCR). The BCR values at 5 mm settlement ($S/B = 5\%$) are determined for various cases from the stress vs normalized settlement curves. Comparison between the results obtained with single and double layer geogrid reinforcement for various cases are presented below.

4.3.3.1 PRGB overlying weak soil 1 (moist soil)

Figure 4.56 shows the variation of BCR with prestress for PRGB with single and double layer geogrid reinforcement of size 5B x 5B overlying (moist) weak soil 1. In general double layer reinforcement gave more improvement than single layer reinforcement and biaxial prestressing gave more improvement than uniaxial prestressing.

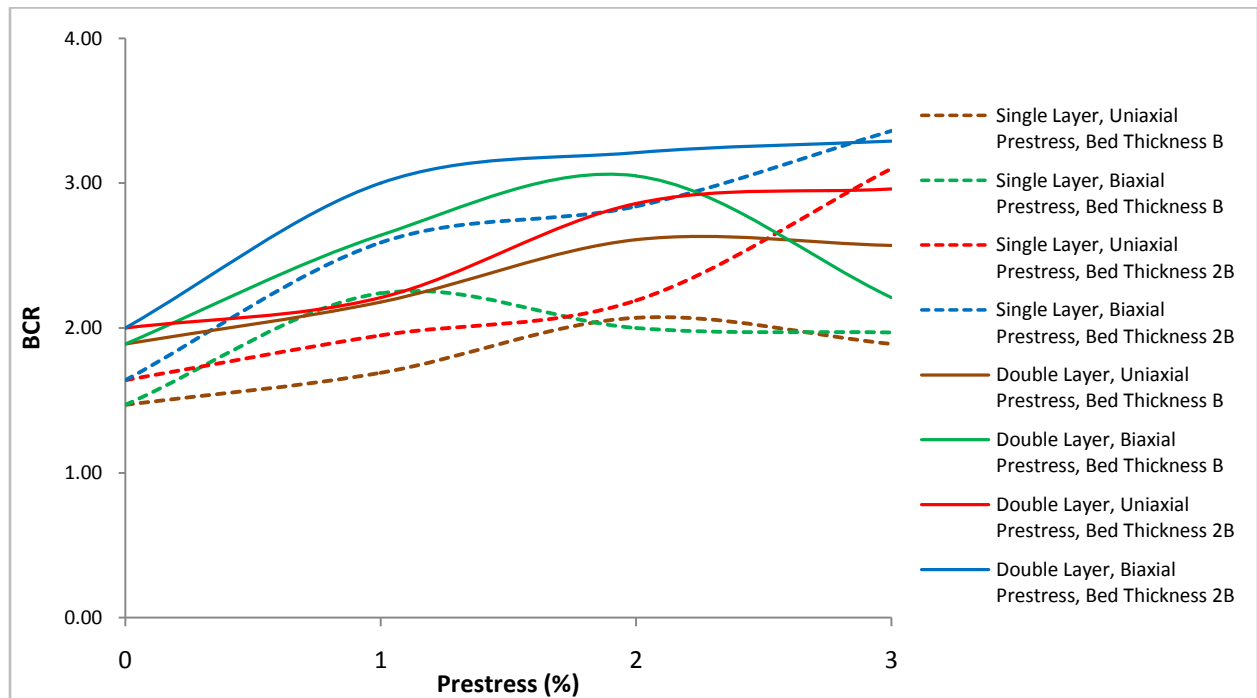


Fig 4.56 BCR vs prestress curves for PRGB with single and double layer geogrid of size 5B x 5B overlying (moist) weak soil 1.

It is observed that at 1% and 2% prestress, granular bed of thickness B with biaxially prestressed double layer reinforcement gives more improvement than granular bed of thickness 2B with uniaxially prestressed double layer reinforcement. It is also observed that granular bed of thickness 2B with biaxially prestressed single layer reinforcement gives more improvement than granular bed of thickness 2B with uniaxially prestressed double layer reinforcement.

4.3.3.2 PRGB overlying weak soil 2 (submerged soil)

The variation of BCR with prestress for PRGB with single and double layer geogrid reinforcement of size 5B x 5B overlying (submerged) weak soil 2 is shown in Fig. 4.57. In general double layer reinforcement gave more improvement than single layer reinforcement. It is observed that PRGB of thickness B with uniaxially prestressed double layer reinforcement is giving more improvement than that of thickness 2B with single layer reinforcement.

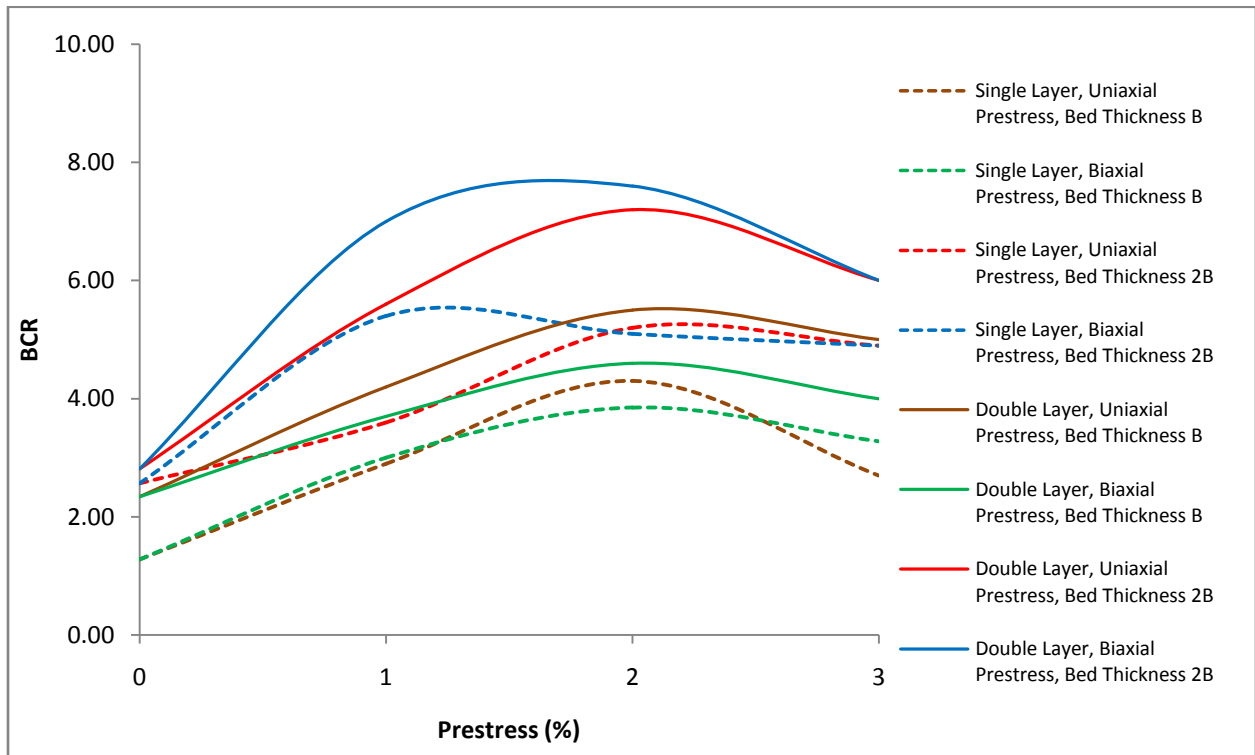


Fig 4.57 BCR vs prestress curves for PRGB with single and double layer geogrid of size 5B x 5B overlying (submerged) weak soil 2.

4.3.4 Effect of type of geosynthetic reinforcement

In order to investigate the effect of type of reinforcement experimental and finite element studies are carried out using geogrid and geotextile as reinforcement. The effect of type of prestressed geosynthetic reinforcement is studied by comparing the bearing capacity ratios of various cases. Comparison between the results obtained with single layer geogrid and geotextile reinforcement for various cases are presented below.

4.3.4.1 PRGB overlying weak soil 1 (moist soil)

Figure 4.58 shows the variation of BCR with prestress for PRGB with single layer geogrid and geotextile reinforcement of size 5B x 5B overlying (moist) weak soil 1. In general PRGB with geotextile reinforcement is giving better improvement than with geogrid reinforcement. The geogrid used for the study is a weak type of geogrid having a tensile strength of only 7.68 KN/m, much lesser than the tensile strength of geotextile. The reason for lesser improvement by geogrid compared to that of geotextile could be attributed to the lower value of tensile strength of the geogrid used.

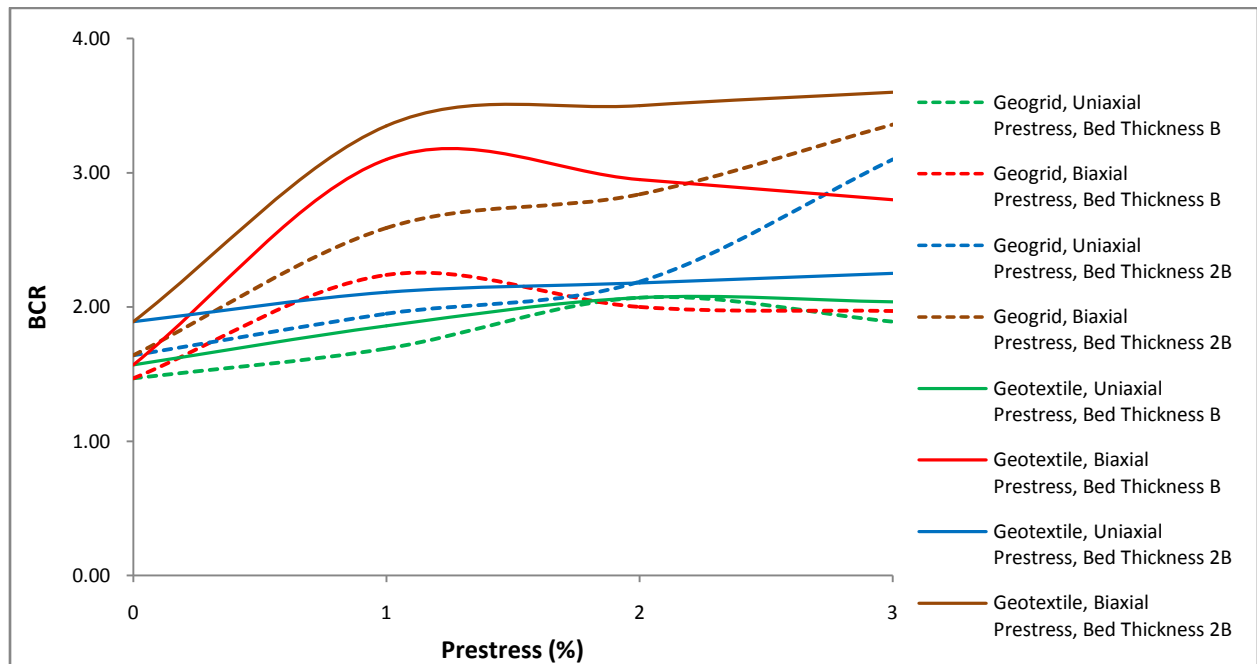


Fig 4.58 BCR vs prestress curves for PRGB with single layer geogrid and geotextile reinforcement of size 5B x 5B overlying (moist) weak soil 1.

4.3.4.2 PRGB overlying weak soil 2 (submerged soil)

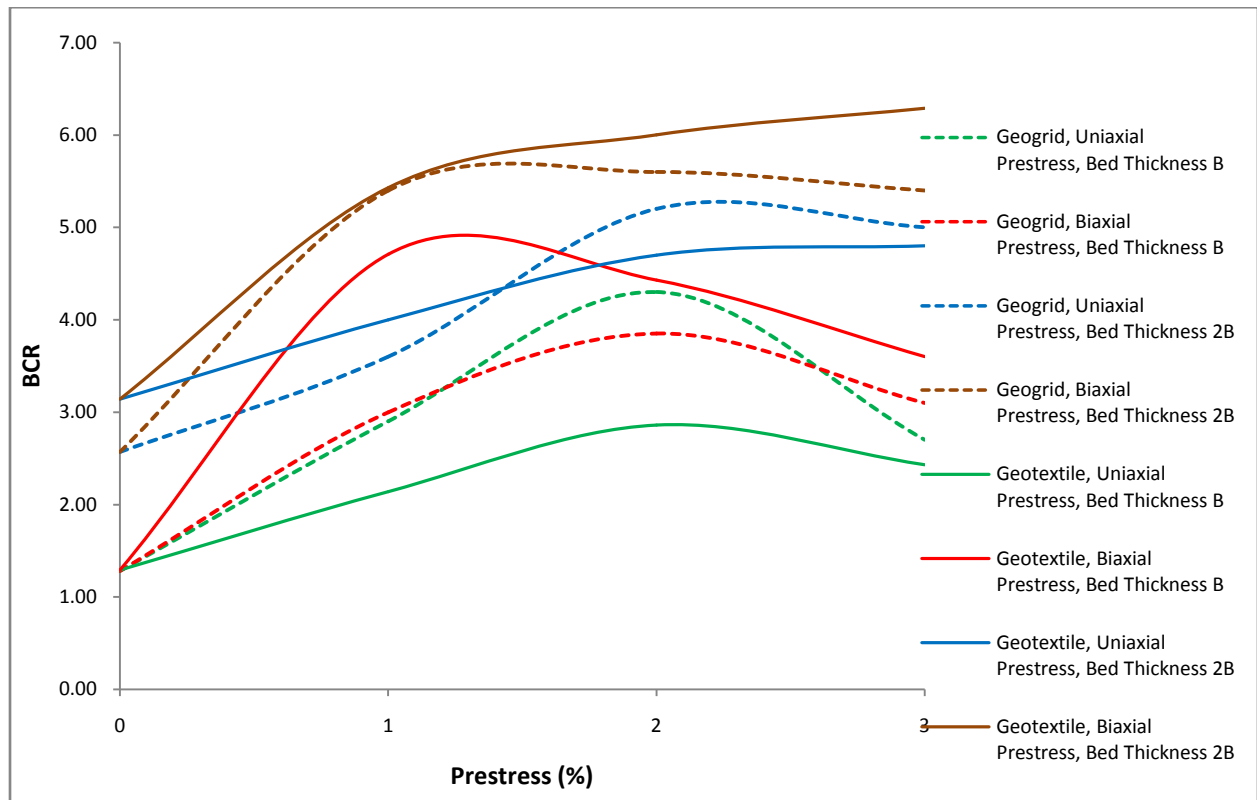


Fig 4.59 BCR vs prestress curves for PRGB with single layer geogrid and geotextile reinforcement of size 5B x 5B overlying (submerged) weak soil 2.

The variation of BCR with prestress for PRGB with single layer geogrid and geotextile reinforcement of size 5B x 5B overlying (submerged) weak soil 2 is shown in Fig. 4.59. It is observed that reinforcing with geogrid gives more improvement when the prestress is uniaxial and geotextile reinforcement gives more improvement when the prestress is biaxial.

4.3.5 Effect of size of prestressed geosynthetic reinforcement

In order to investigate the effect of the size of prestressed geosynthetic reinforcement, experimental and finite element studies are carried out with two sizes of geogrid reinforcement; 5B x 5B and 2B x 2B. Comparison between the results obtained with single layer geogrid of both sizes for various cases are presented below.

4.3.5.1 PRGB overlying weak soil 1 (moist soil)

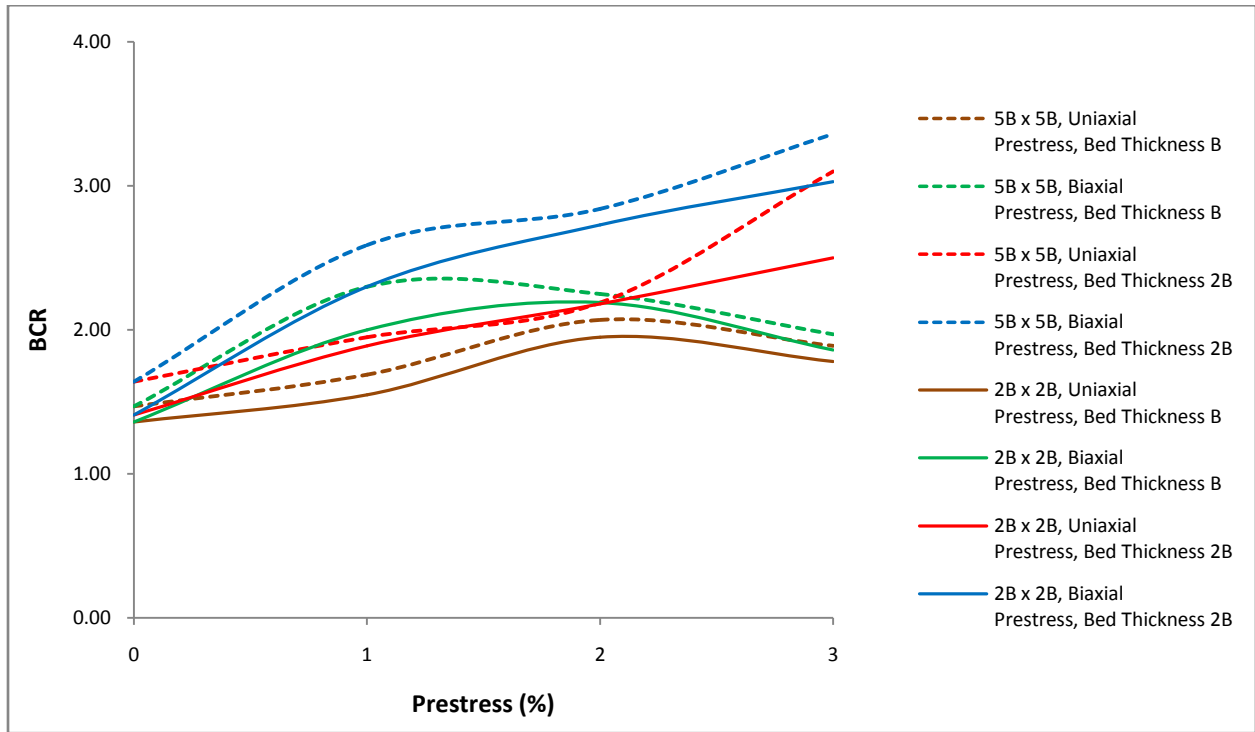


Fig 4.60 BCR vs prestress curves for PRGB with single layer geogrid reinforcement of size 5B x 5B and 2B x 2B overlying (moist) weak soil 1.

Figure 4.60 shows the variation of BCR with prestress for PRGB with single layer geogrid reinforcement of size 5B x 5B and 2B x 2B overlying (moist) weak soil 1. The improvement in bearing capacity attained with bigger reinforcement (size 5B x 5B) is slightly higher than that attained with smaller reinforcement (size 2B x 2B). It is observed that biaxially prestressed RGB of thickness B with reinforcement of size 2B x 2B is giving more improvement than uniaxially prestressed RGB of thickness 2B with reinforcement of size 5B x 5B at 1% and 2% prestress.

4.3.5.2 PRGB overlying weak soil 2 (submerged soil)

The variation of BCR with prestress for PRGB with single layer geogrid reinforcement of size 5B x 5B and 2B x 2B overlying (submerged) weak soil 2 is shown in Fig. 4.61. Similar to weak soil 1, the improvement attained with bigger reinforcement is slightly greater than that with smaller reinforcement. It is observed that PRGB of thickness 2B with reinforcement of size 2B x 2B is giving more improvement than PRGB of thickness B with reinforcement of size 5B x 5B.

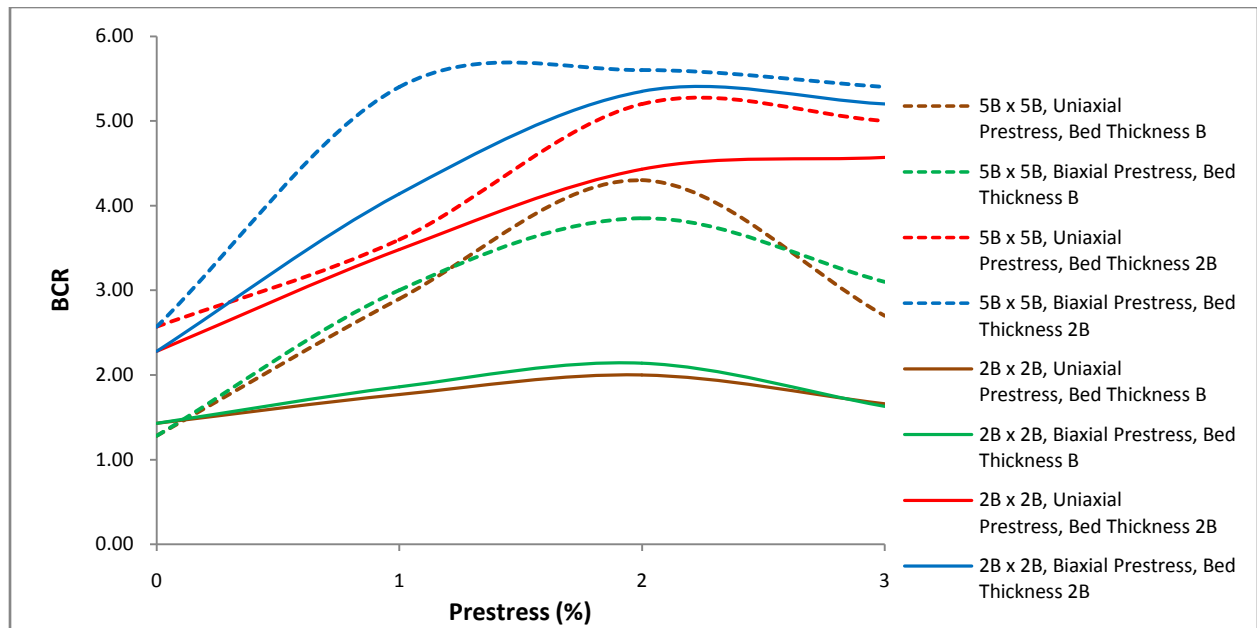


Fig 4.61 BCR vs prestress curves for PRGB with single layer geogrid reinforcement of size 5B x 5B and 2B x 2B overlying (submerged) weak soil 2.

4.3.6 Effect of thickness of granular bed

In order to investigate the effect of the thickness of granular bed, experimental and finite element studies are carried out with two thicknesses of granular bed; B and 2B. Comparison between the results obtained with granular beds of both thicknesses for various cases are presented below.

4.3.6.1 PRGB overlying weak soil 1 (moist soil)

Figure 4.62 shows the variation of BCR with (H/B) for PRGB with single layer geogrid reinforcement of size 5B x 5B overlying (moist) weak soil 1, where H is the thickness of GB and B is the size of footing. It is observed that for all the cases the BCR increases with the thickness of GB. When the thickness of granular bed is B (H/B=1), biaxial prestress of 1% is giving maximum improvement whereas when the thickness of granular bed is 2B, biaxial prestress of 3% is giving maximum improvement.

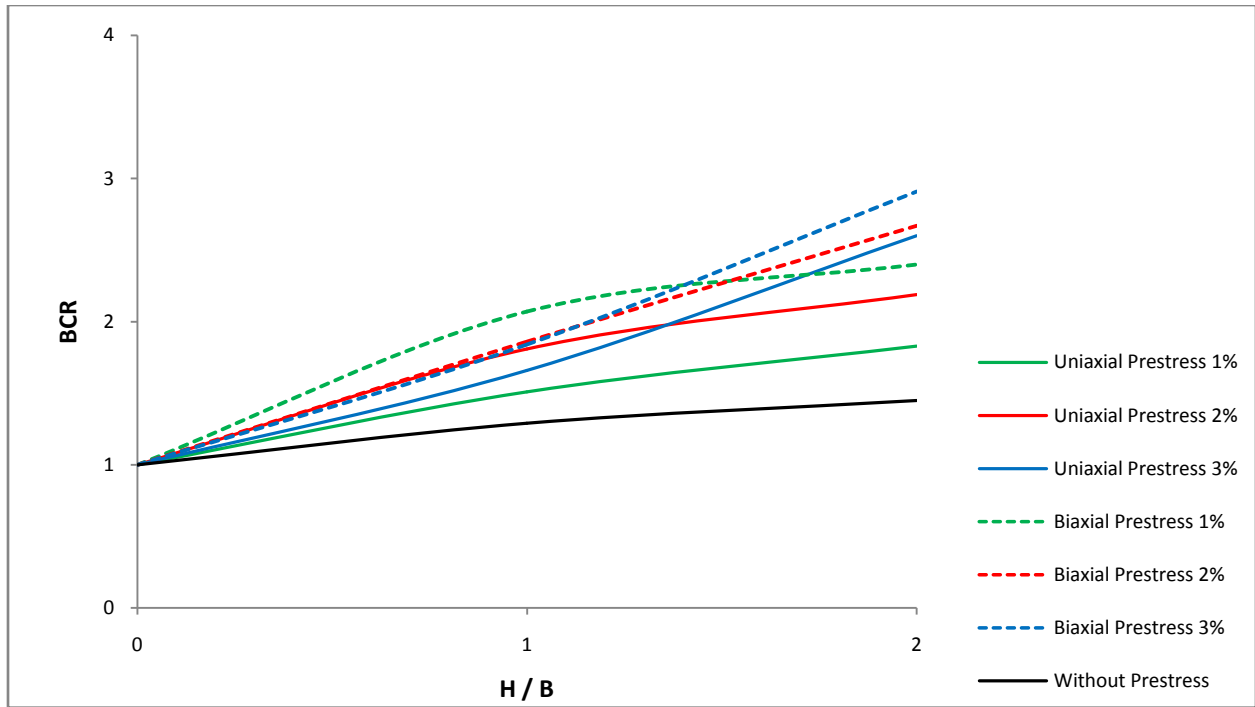


Fig 4.62 BCR vs thickness of GB curves for PRGB with single layer geogrid reinforcement of size 5B x 5B overlying (moist) weak soil 1.

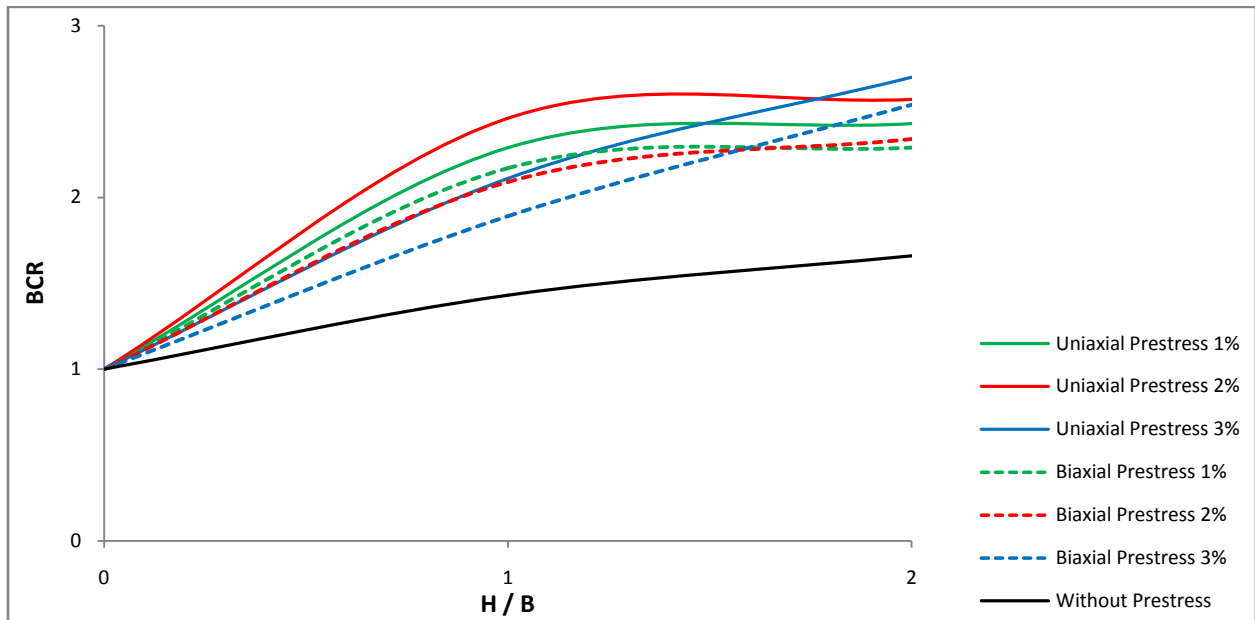


Fig 4.63 BCR vs thickness of GB curves for PRGB with single layer geotextile reinforcement of size 5B x 5B overlying (moist) weak soil 1.

With geotextile reinforcement of size 5B x 5B overlying (moist) weak soil 1 (Fig 4.63) also the BCR increases with the thickness of GB. It is observed that the rate of increase of BCR is less

when the thickness of granular bed is increased from B to 2B for 1% and 2% prestress. When the thickness of granular bed is B, uniaxial prestress of 2% is giving maximum improvement and when the thickness of granular bed is 2B, uniaxial prestress of 3% is giving maximum improvement.

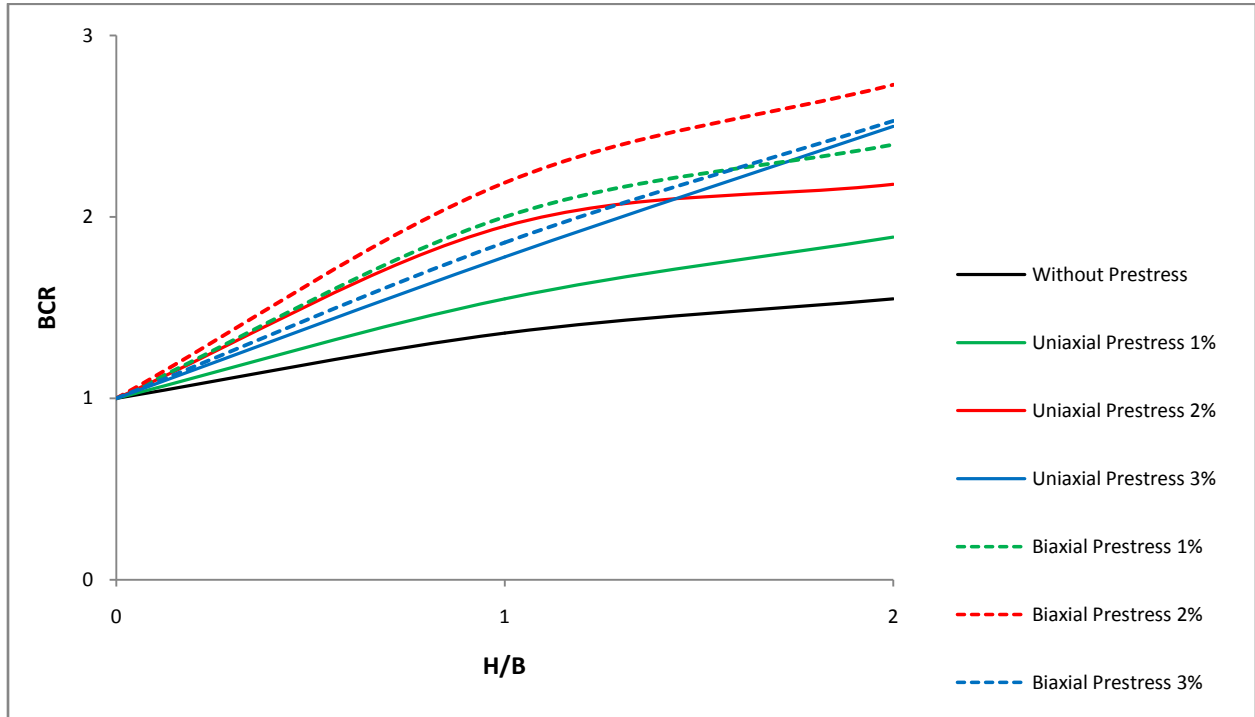


Fig 4.64 BCR vs thickness of GB curves for PRGB with single layer geogrid reinforcement of size 2B x 2B overlying (moist) weak soil 1.

Figure 4.64 shows the variation of BCR with thickness of granular bed for various cases of PRGB with single layer geogrid reinforcement of size 5B x 5B overlying (moist) weak soil 1. It is observed that for all the cases the BCR increases with the thickness of GB. It is also observed that biaxial prestress of 2% gives maximum improvement at both thicknesses of granular bed.

The variation of BCR with thickness of granular bed for various cases of PRGB with double layer geogrid reinforcement of size 5B x 5B overlying (moist) weak soil 1 is shown in Fig 4.65. It is observed that, except for PRGB with biaxial prestress of 3%, the rate of increase of BCR is less when the thickness of granular bed is increased from B to 2B. It is also observed that biaxial prestress of 2% gives maximum improvement at both thicknesses of granular bed.

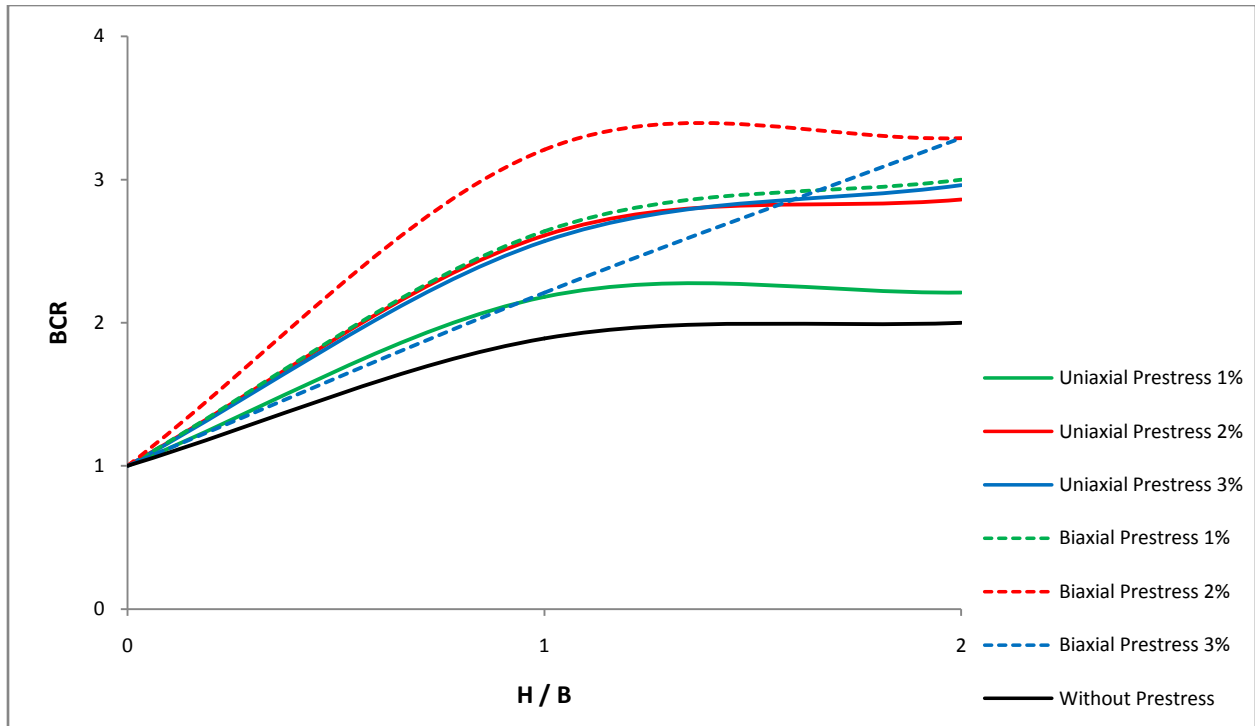


Fig 4.65 BCR vs thickness of GB curves for PRGB with double layer geogrid reinforcement of size 5B x 5B overlying (moist) weak soil 1.

4.3.6.2 PRGB overlying weak soil 2 (submerged soil)

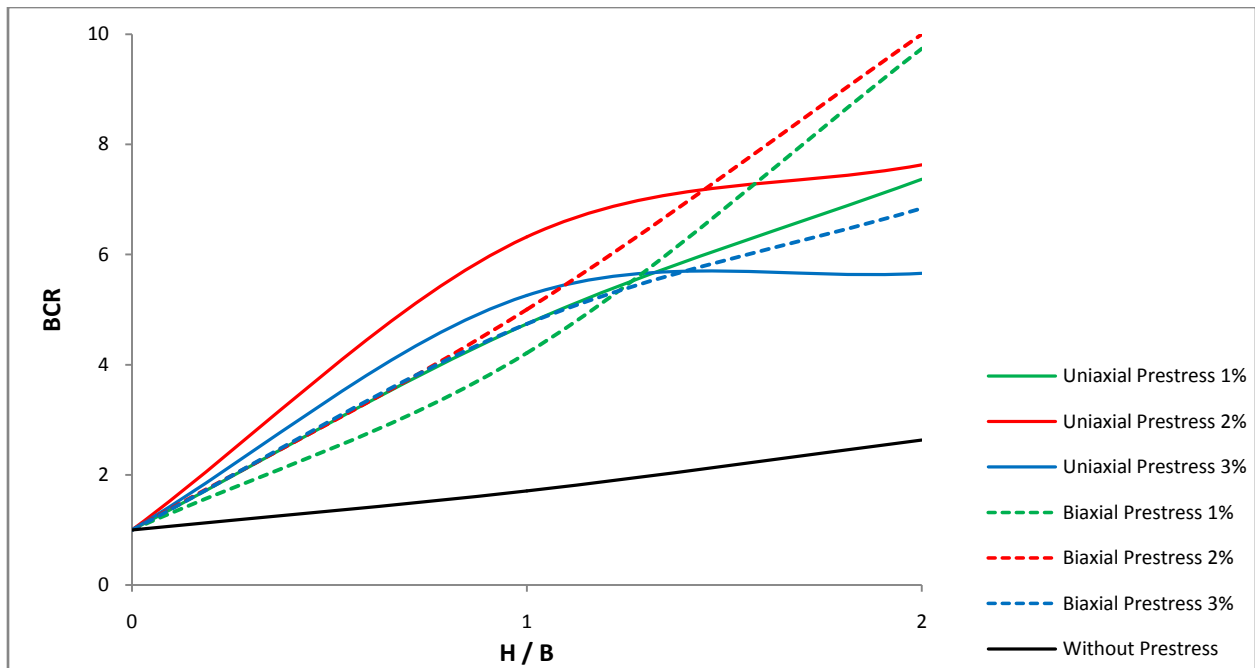


Fig 4.66 BCR vs thickness of GB curves for PRGB with single layer geogrid reinforcement of size 5B x 5B overlying (submerged) weak soil 2.

Figure 4.66 shows the variation of BCR with thickness of granular bed for various cases of PRGB with single layer geogrid reinforcement of size 5B x 5B overlying (submerged) weak soil 2. It is observed that the rate of increase of BCR is less when the thickness of granular bed is increased from B to 2B for uniaxial prestress of 2% and 3%. Uniaxial prestress of 2% gives maximum improvement when the thickness of granular bed is B and biaxial prestress of 2% gives maximum improvement when the thickness of granular bed is 2B.

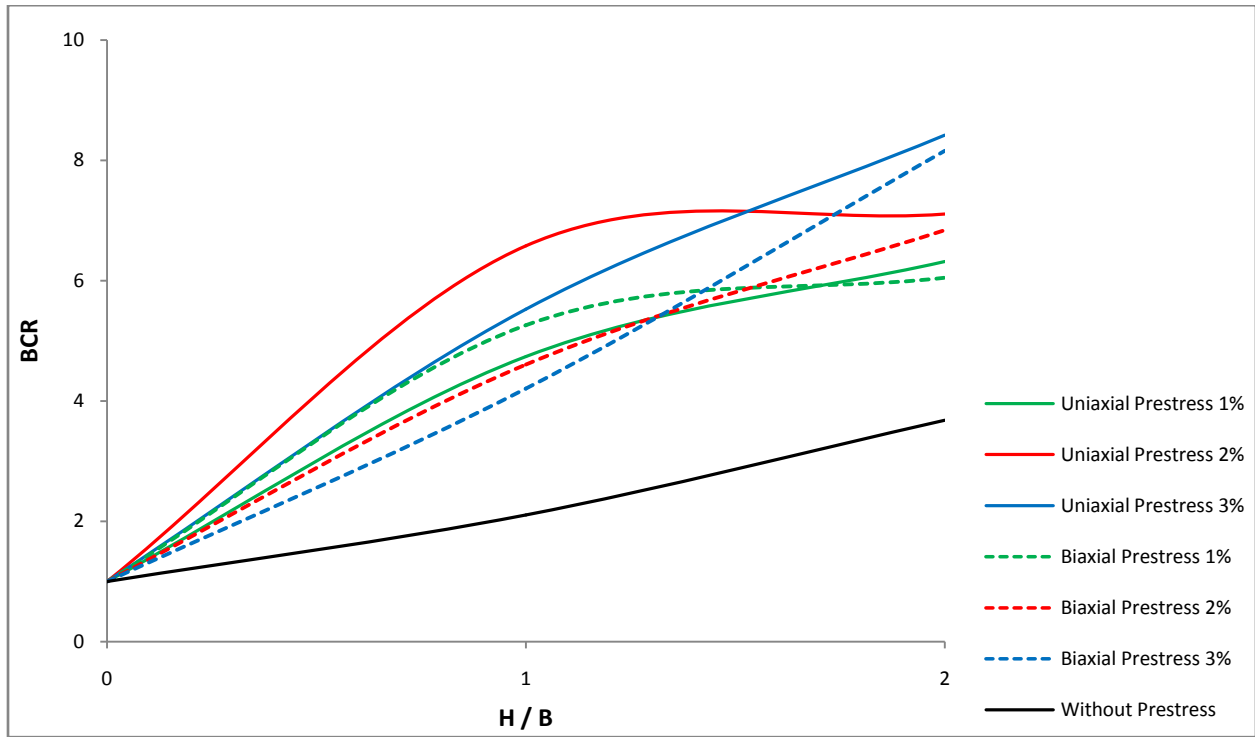


Fig 4.67 BCR vs thickness of GB curves for PRGB with single layer geotextile reinforcement of size 5B x 5B overlying (submerged) weak soil 2.

With geotextile reinforcement of size 5B x 5B overlying (submerged) weak soil 2 (Fig 4.67) also the BCR increases with the thickness of GB. It is observed that the rate of increase of BCR is less when the thickness of granular bed is increased from B to 2B for uniaxial prestress of 1% and 2% and biaxial prestress of 1%. When the thickness of granular bed is B, uniaxial prestress of 2% is giving maximum improvement and when the thickness of granular bed is 2B, uniaxial prestress of 3% is giving maximum improvement.

Figure 4.68 shows the variation of BCR with thickness of granular bed for various cases of PRGB with single layer geogrid reinforcement of size 2B x 2B overlying (submerged) weak soil 2.

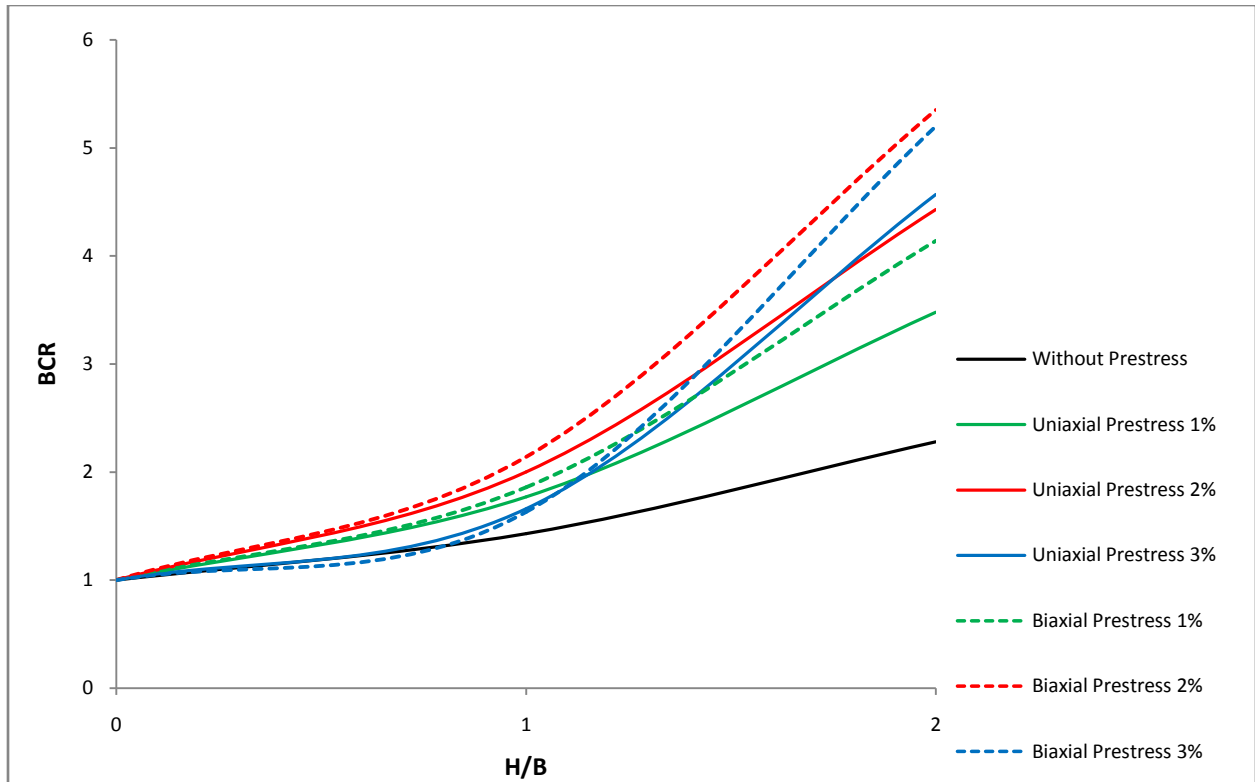


Fig 4.68 BCR vs thickness of GB curves for PRGB with single layer geogrid reinforcement of size 2B x 2B overlying (submerged) weak soil 2.

It is observed that for all the cases the BCR increases with the thickness of granular bed and the rate of increase of BCR when the thickness of granular bed is increased from B to 2B is high. It is also observed that biaxial prestress of 2% gives maximum improvement at both thicknesses of granular bed.

The variation of BCR with thickness of granular bed for various cases of PRGB with double layer geogrid reinforcement of size 5B x 5B overlying (moist) weak soil 1 is shown in Fig 4.65. It is observed that for uniaxial prestress the rate of increase of BCR is less when the thickness of granular bed is increased from B to 2B. It is also observed that uniaxial prestress of 2% gives maximum improvement when the thicknesses of granular bed is B and biaxial prestress gives maximum improvement when the thickness of granular bed is 2B.

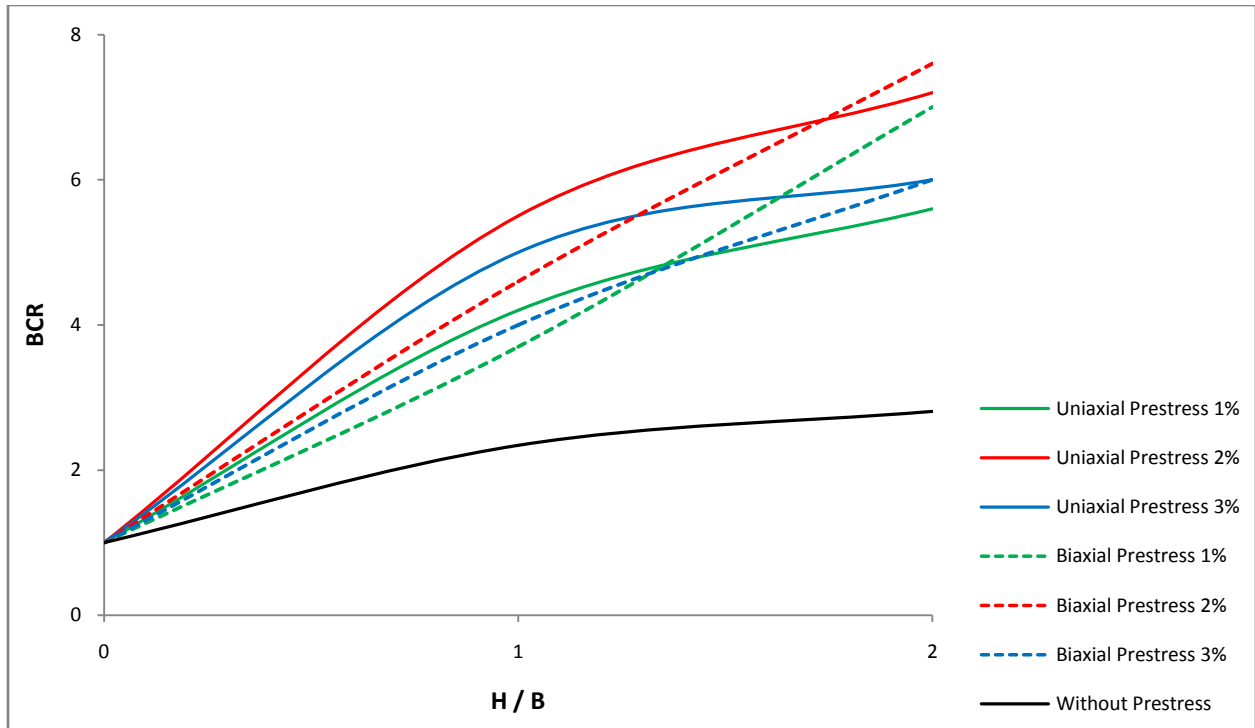


Fig 4.69 BCR vs thickness of GB curves for PRGB with double layer geogrid reinforcement of size 5B x 5B overlying (submerged) weak soil 2.

4.3.7 Effect of strength of underlying weak soil

Locally available soil termed as Shedi soil is used as weak soil. Shedi soils are dispersive soils and are predominantly found in the western coast of peninsular India, which receives heavy rainfall during monsoon. Their strength reduces drastically under saturation condition. Many foundation and slope stability problems are reported wherever this soil is encountered (Bhat et al (2008), Shivashankar and Setty(2000)). Its properties are given in Table 3.2 and particle size distribution shown in Fig. 3.2.

In order to investigate the effect of the strength of underlying weak soil, the Shedi soil is used in two conditions namely moist condition (termed as moist soil or weak soil 1) and also used in submerged condition (termed as submerged soil or weak soil 2). Comparison between the performance of PRGB overlying (moist) weak soil 1 and (submerged) weak soil 2 for various cases are given below.

4.3.7.1 PRGB with single layer geogrid of size 5B x 5B

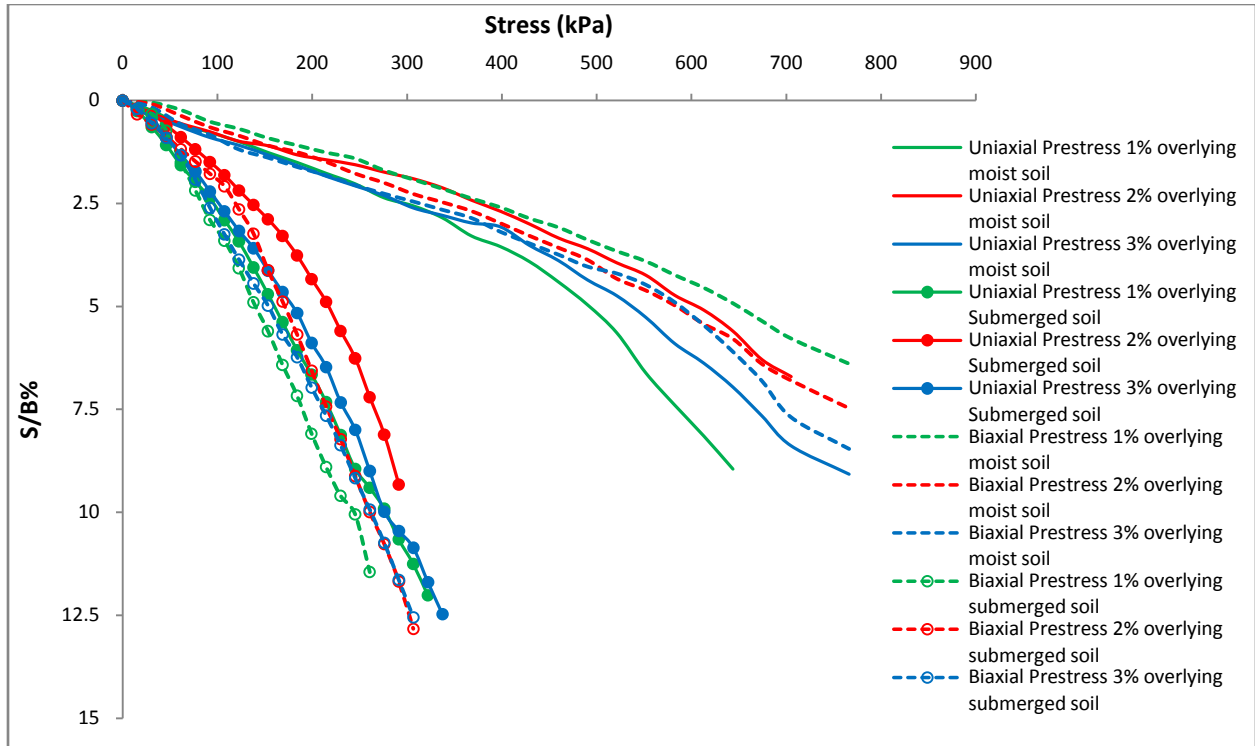


Fig 4.70 Stress vs normalized settlement curves for PRGB of thickness B with single layer geogrid of size 5B x 5B overlying (moist) weak soil 1 and (submerged) weak soil 2.

Figure 4.70 represents the variation of bearing pressure with footing settlement of PRGB of thickness B with single layer geogrid reinforcement of size 5B x 5B overlying (moist) weak soil 1 and (submerged) weak soil 2. It can be seen from the figure that submergence of Shedi soil caused a considerable reduction in bearing capacity. It is observed that biaxial prestressing of 1% gives maximum improvement for moist weak soil and uniaxial prestressing of 2% gives maximum improvement for submerged weak soil.

The results of studies conducted on PRGB of thickness 2B with single layer geogrid reinforcement of size 5B x 5B overlying (moist) weak soil 1 and (submerged) weak soil 2 are presented in Fig 4.71. It is observed that uniaxial prestressing of 3% gives maximum improvement for moist weak soil and biaxial prestressing of 2% gives maximum improvement for submerged weak soil.

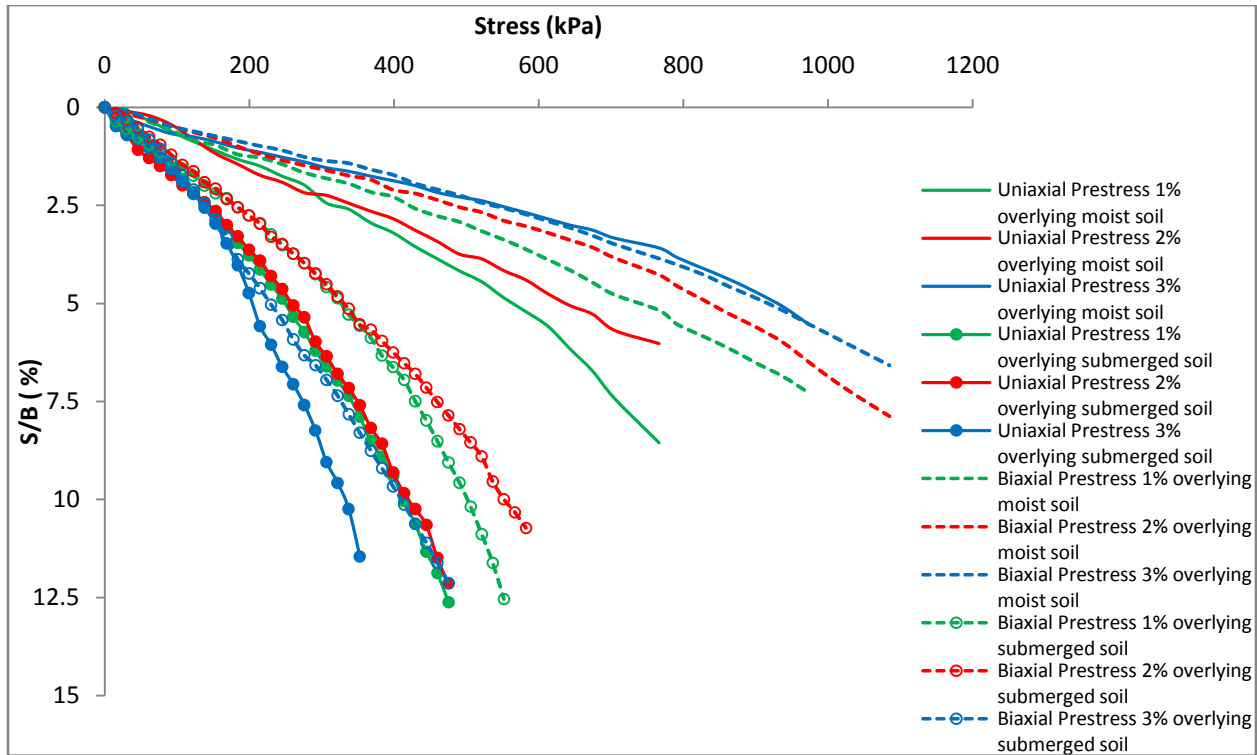


Fig 4.71 Stress vs normalized settlement curves for PRGB of thickness $2B$ with single layer geogrid of size $5B \times 5B$ overlying (moist) weak soil 1 and (submerged) weak soil 2.

4.3.7.2 PRGB with single layer geotextile of size $5B \times 5B$

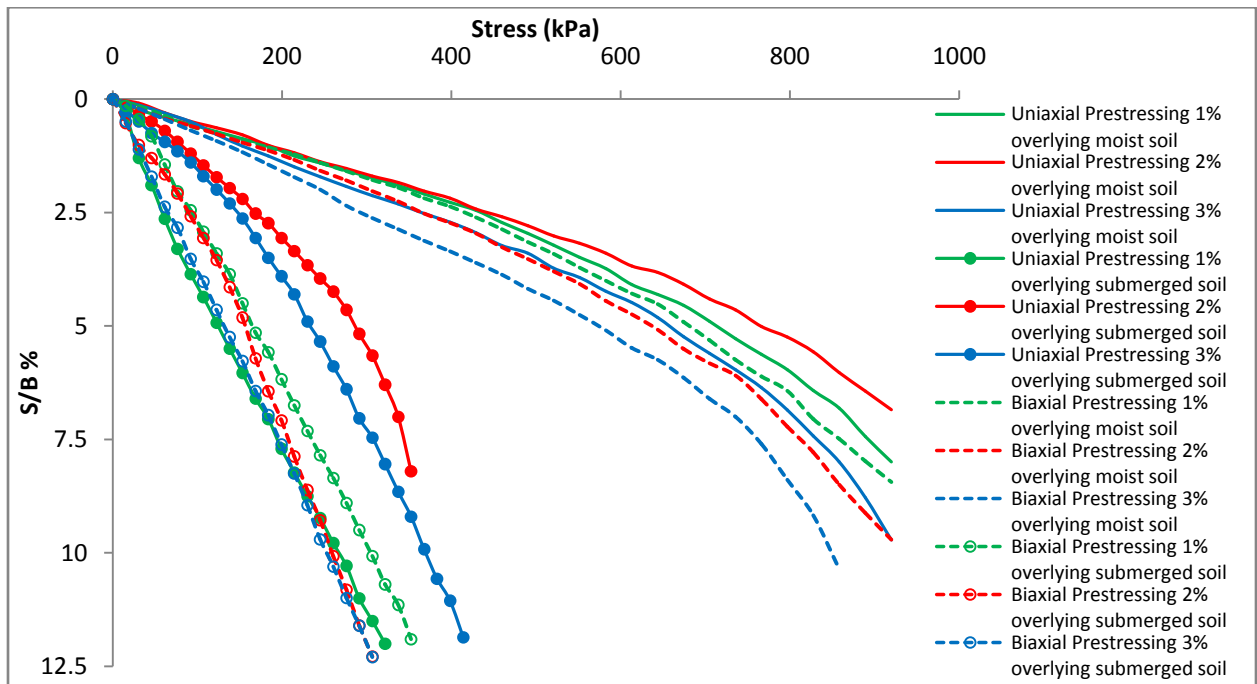


Fig 4.72 Stress vs normalized settlement curves for PRGB of thickness B with single layer geotextile of size $5B \times 5B$ overlying (moist) weak soil 1 and (submerged) weak soil 2.

Figure 4.72 represents the variation of bearing pressure with footing settlement of PRGB of thickness B with single layer geotextile reinforcement of size $5B \times 5B$ overlying (moist) weak soil 1 and (submerged) weak soil 2. It can be seen from the figure that submergence of Shedi soil caused a considerable reduction in bearing capacity. It is observed that uniaxial prestressing of 2% gives maximum improvement for both moist weak soil and submerged weak soil.

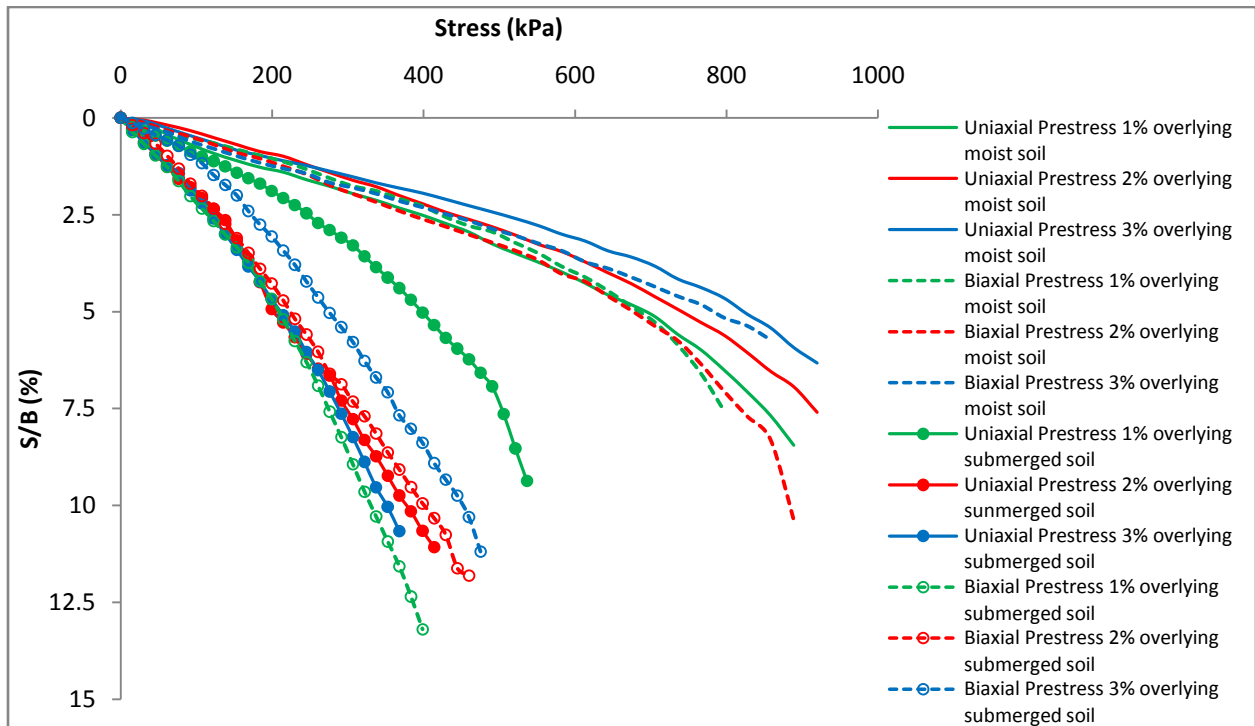


Fig 4.73 Stress vs normalized settlement curves for PRGB of thickness $2B$ with single layer geotextile of size $5B \times 5B$ overlying (moist) weak soil 1 and (submerged) weak soil 2.

The variation of bearing pressure with footing settlement of PRGB of thickness $2B$ with single layer geotextile reinforcement of size $5B \times 5B$ overlying (moist) weak soil 1 and (submerged) weak soil 2 is presented in Fig 4.73. It is observed that uniaxial prestressing of 3% gives maximum improvement for moist weak soil and uniaxial prestressing of 1% gives maximum improvement for submerged weak soil.

4.3.7.3 PRGB with single layer geogrid of size $2B \times 2B$

Figure 4.74 represents the variation of bearing pressure with footing settlement of PRGB of thickness B with single layer geogrid reinforcement of size $2B \times 2B$ overlying (moist) weak soil 1 and (submerged) weak soil 2. It can be seen from the figure that submergence of Shedi soil

caused a large reduction in bearing capacity. It is observed that biaxial prestressing of 2% gives maximum improvement for both moist weak soil and submerged weak soil.

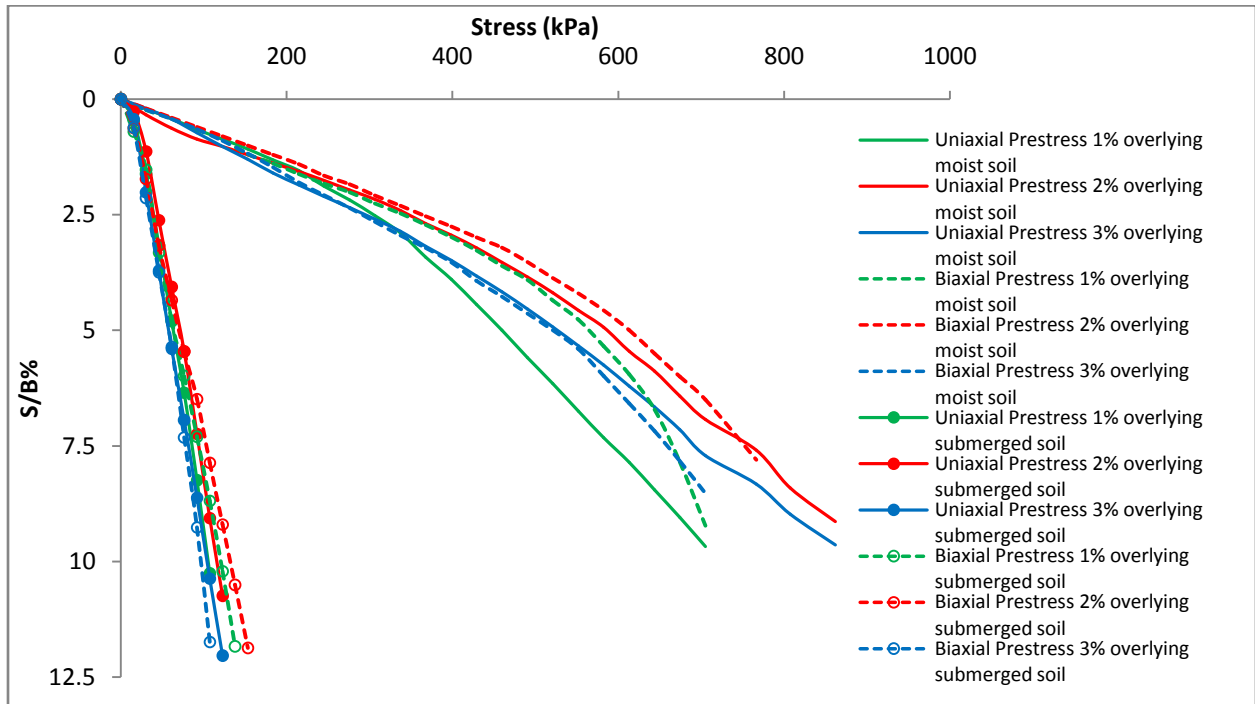


Fig 4.74 Stress vs normalized settlement curves for PRGB of thickness B with single layer geogrid of size 2B x 2B overlying (moist) weak soil 1 and (submerged) weak soil 2.

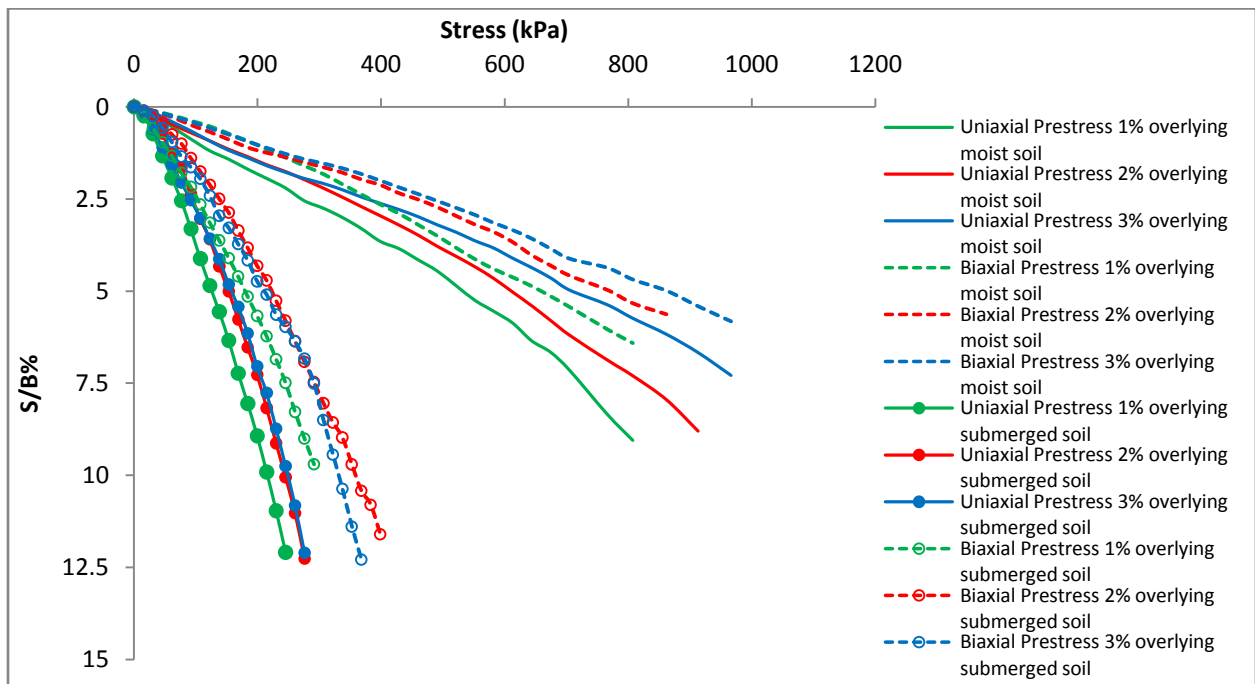


Fig 4.75 Stress vs normalized settlement curves for PRGB of thickness 2B with single layer geogrid of size 2B x 2B overlying (moist) weak soil 1 and (submerged) weak soil 2.

The variation of bearing pressure with footing settlement of PRGB of thickness $2B$ with single layer geogrid reinforcement of size $2B \times 2B$ overlying (moist) weak soil 1 and (submerged) weak soil 2 is presented in Fig 4.75. It is observed that biaxial prestressing of 3% gives maximum improvement for moist weak soil and biaxial prestressing of 2% gives maximum improvement for submerged weak soil.

4.3.7.4 PRGB with double layer geogrid of size $5B \times 5B$

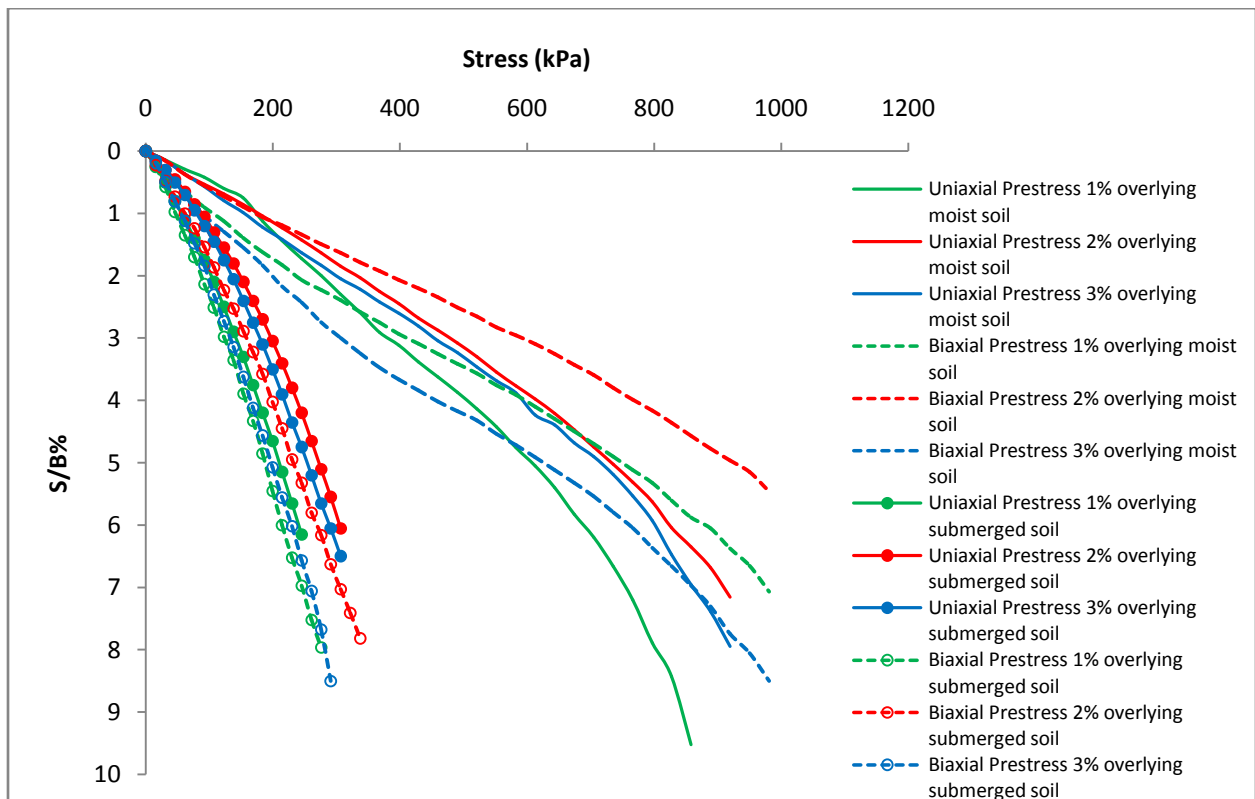


Fig 4.76 Stress vs normalized settlement curves for PRGB of thickness B with double layer geogrid of size $5B \times 5B$ overlying (moist) weak soil 1 and (submerged) weak soil 2.

Figure 4.76 represents the variation of bearing pressure with footing settlement of PRGB of thickness B with double layer geogrid reinforcement of size $5B \times 5B$ overlying (moist) weak soil 1 and (submerged) weak soil 2. It can be seen from the figure that the reduction in bearing capacity due to submergence of Shedi soil is comparatively lesser than that of single layer reinforcement. It is observed that biaxial prestressing of 2% gives maximum improvement for moist weak soil and uniaxial prestressing of 2% gives maximum improvement for submerged weak soil.

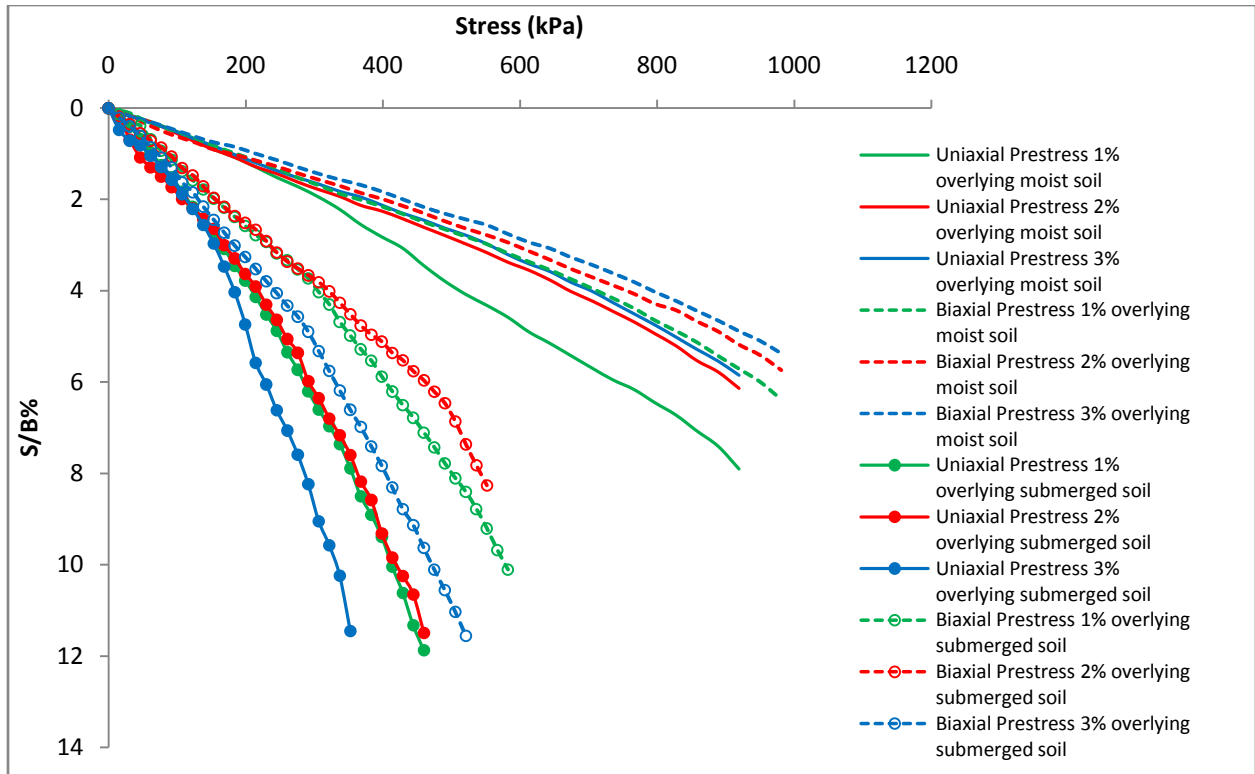


Fig 4.77 Stress vs normalized settlement curves for PRGB of thickness 2B with double layer geogrid of size 5B x 5B overlying (moist) weak soil 1 and (submerged) weak soil 2.

The variation of bearing pressure with footing settlement of PRGB of thickness 2B with double layer geogrid reinforcement of size 5B x 5B overlying (moist) weak soil 1 and (submerged) weak soil 2 is presented in Fig 4.77. It is observed that biaxial prestressing of 3% gives maximum improvement for moist weak soil and biaxial prestressing of 2% gives maximum improvement for submerged weak soil.

During experimental investigation with granular beds overlying (submerged) weak soil 2, it was observed that capillary water rises into the dry sand in granular bed, from the submerged soil below, during the course of experiment. In granular beds of thickness B, the sand surrounding the reinforcement became moist during the experiment. In granular beds of thickness 2B, the height of reinforcement from the submerged soil surface is more and the capillary moisture at the level of reinforcement is very less compared to that of granular beds of thickness B. The difference in behaviour of granular beds overlying submerged soil could be due to the presence of this capillary moisture in sand.

4.4 CHAPTER SUMMARY

1. The results of experimental and finite element studies on PRGB overlying weak soil are presented in this Chapter.
2. There is reasonably good agreement between the results of finite element analyses and experimental studies.
3. From experimental studies as well as finite element analyses, it is observed that after a certain percentage of prestress, the BCR decreases with the increase in prestress. The improvement in bearing capacity depends upon the stress at the interface between reinforcement and granular soil. The tensile stress gets mobilized in the reinforcement due to the applied prestress and due to the friction developed between the reinforcement and surrounding granular soil. Results of finite element analysis indicated that in most of the cases, as the prestress increases, the normal stress at the interface between reinforcement and granular soil decreases. Initially as the prestress is applied, the BCR increases due to an increase in the tensile stress in reinforcement and due to an increase in the interface stress. But as the applied prestress is further increased, the stress transfer between reinforcement and surrounding granular soil reduces resulting in a reduction of BCR.
4. The BCR increases with an increase in the thickness of granular bed.
5. Biaxial prestressing gives better BCR values with geogrid reinforcement whereas uniaxial prestressing gives better results with geotextile reinforcement.
6. Submergence of soft soil causes a large reduction in the Bearing Capacity. The behaviour of PRGB is also influenced by the presence of capillary moisture in the granular bed.

CHAPTER 5

ANALYTICAL MODELLING

5.1 INTRODUCTION

In the present study, an analytical model is proposed to predict the improvement in bearing capacity attained due to prestressing the geosynthetic reinforcement in the RGB. The analytical model is formulated by improvising the Punching shear model proposed by Shivashankar et al (1993) for strip footings supported on unreinforced and reinforced granular beds overlying weak soil.

5.2 PUNCHING SHEAR MODEL OF STRIP FOOTING (SHIVASHANKAR et al. 1993)

Shivashankar et al. (1993) developed a punching shear model for a strip footing on unreinforced or reinforced granular bed overlying weak soil. They proposed a punching shear failure mechanism in which both the footing and the portion of the reinforced granular bed directly beneath the footing are envisaged to act in unison to punch through the soft soil underneath.

The improvement in bearing capacity of a reinforced granular bed is considered to comprise of three components namely Shear layer effect, Confinement effect and Surcharge effect. These effects are represented in Figs 5.1, 5.2 & 5.3 respectively. They proposed the following equations for computing Bearing Capacity Ratio (BCR).

$$BCR = 1 + \Delta BCR_{SL} + \Delta BCR_{CE} + \Delta BCR_{SE} \quad \text{----- (5.1)}$$

Where Bearing Capacity Ratio (BCR) is defined as ratio of bearing capacity of footing on improved ground to bearing capacity of footing on unimproved ground. ΔBCR_{SL} , ΔBCR_{CE} and ΔBCR_{SE} are improvements in bearing capacity ratio due to shear layer effect, confinement effect and additional surcharge effect, respectively.

5.2.1 Shear Layer Effect

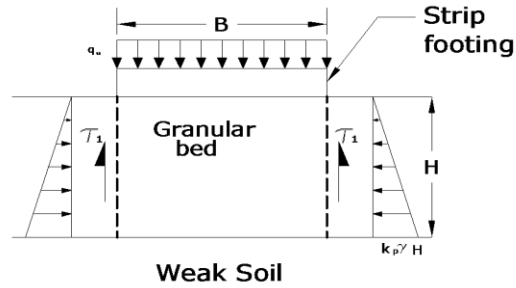


Fig 5.1: Shear Layer Effect (Shivashankar et al. 1993)

In shear layer effect, the shear stress mobilized along the failure surfaces (vertical planes at the edge of the footing) due to the passive pressure developed in granular soil is considered (Fig. 5.1). The equation proposed for strip footings is

$$\Delta BCR_{SL} = 2\tau_1/Q \quad \text{----- (5.2)}$$

$$\tau_1 = P_p \tan\phi_s \quad \text{----- (5.3)}$$

$$\Delta q_{SL} = 2\tau_1/B \quad \text{----- (5.4)}$$

Where

Q = Bearing capacity of underlying weak soil

τ_1 = Total vertical force in the punching shear failure (vertical) plane due to Shear Layer Effect

P_p = Passive force developed on the sides of failure surface per unit length

Φ_s = Angle of shearing resistance.

5.2. 2 Confinement Effect

The tensile stress mobilized in the reinforcement (placed in the granular soil) will provide a confinement effect to the granular soil beneath the footing. The shear stress developed along the failure surfaces (vertical planes at the edge of the footing) due to this confining stress is considered here (Fig. 5.2). The equation proposed for strip footing is

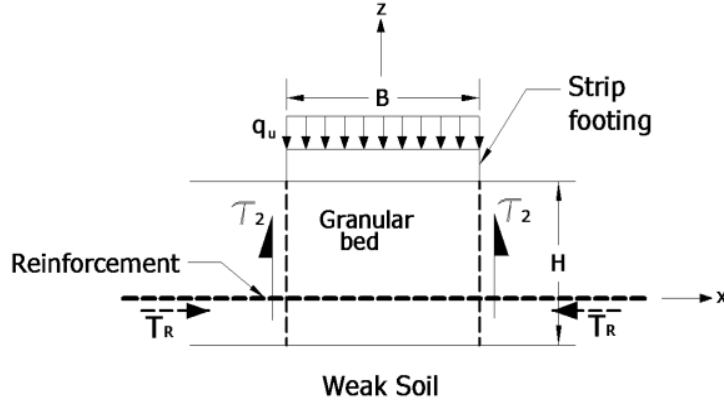


Fig 5.2: Confinement Effect (Shivashankar et al. 1993)

$$\Delta BCR_{CE} = 2\tau_2/Q \quad \text{----- (5.5)}$$

$$\tau_2 = T_R \tan \phi_s \quad \text{----- (5.6)}$$

$$\Delta q_{CE} = 2\tau_2/B \quad \text{----- (5.7)}$$

Where

τ_2 = Total vertical force in the punching shear failure plane (vertical) due to Confinement effect of reinforcement

T_R = Tensile stress mobilized in the reinforcement

$$= 2L\sigma_v \tan \delta$$

L = Length of reinforcement beyond the failure surface

σ_v = Vertical stress at the level of reinforcement

δ = angle of friction between reinforcement and soil

5.2.3 Additional Surcharge Effect

The vertical stresses along the punching shear failure surfaces due to shear layer effect and confinement effect are considered to act as additional surcharge stress on the underlying soft soil. There will be an improvement in bearing capacity due to this additional surcharge stress. The distribution of this surcharge stress is envisaged to be exponential on either side from the edge of the footing as shown in Fig 5.3 for a strip footing. The improvement in bearing capacity due to this surcharge stress is given by the following equation (Eq.5.8)

$$q_o = 0.84(\Delta q_{SL} + \Delta q_{CE}) \quad \text{----- (5.8)}$$

Where

q_o = Intensity of surcharge stress at the edge of the vertical failure plane (on weak soil), due to shear layer and confinement effects

The effect of this additional surcharge, exponentially decreasing from q_o at the edge of the footing to $0.01q_o$, is used in analysis of improvement of bearing capacity i.e. in estimation of ΔBCR_{SE}

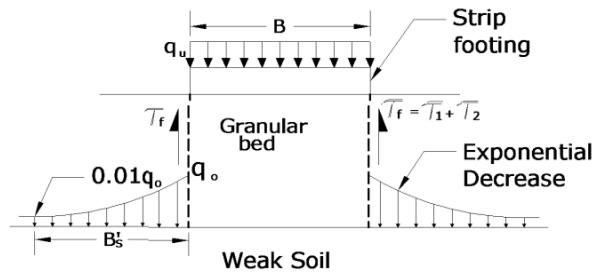


Fig 5.3 Additional Surcharge Effect (Shivashankar et al 1993)

5.3 MODELING OF SQUARE FOOTING ON UNREINFORCED OR REINFORCED GRANULAR BEDS (RGB) IN PRESENT STUDY

In the present study, the model suggested by Shivashankar et al. (1993) for strip footing has been modified and used for validating the results of a square footing on unreinforced or reinforced (without prestressing) granular beds, overlying weak soils. Equations (5.9) and (5.10) are adopted for shear layer effect. Equations (5.11) and (5.12) are adopted for confinement effect, in case of RGB. An exponentially decreasing surcharge as before is envisaged on all four sides, and the effect of this additional surcharge is used in analysis of improvement of bearing capacity i.e. estimation of ΔBCR_{SE} .

5.3.1 Modeling of Square Footing on Prestressed Reinforced Granular Beds in Present Study

The model proposed by Shivashankar et al. (1993) has been modified and improved for the case of square footings on prestressed reinforced granular beds overlying weak soils.

5.3.1.1 Shear Layer Effect

The following equations are used for a square footing of width 'B'

$$\Delta BCR_{SL} = 4\tau_1/Q \quad \text{----- (5.9)}$$

$$\tau_1 = P'_p \tan \phi_s \quad \text{----- (5.10)}$$

where P'_p is the passive force developed on each of four sides of the square column of granular soil beneath the square footing.

5.3.1.2 Confinement Effect

Equations (5.5) and (5.6) for strip footing are modified for square footing as

$$\Delta BCR_{CE} = 4\tau_2/Q \quad \text{----- (5.11)}$$

$$\tau_2 = T'_R \tan \phi_s \quad \text{----- (5.12)}$$

Where T'_R = Tensile stress mobilized in reinforcement beyond each of the four sides of square column of granular soil beneath the square footing

B = Width of the square footing

If the friction in reinforcement (on each side of the square prism) is less than the applied prestress, value of T'_R is taken as equal to the value of applied prestress. If the friction in reinforcement is more than applied prestress, the value of T'_R is taken as equal to value of frictional resistance over the reinforcement.

5.3.1.3 Additional Surcharge Effect

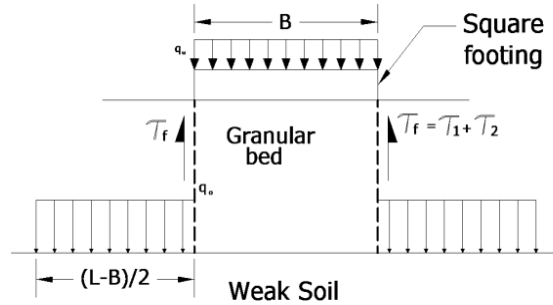


Fig 5.4 Proposed Additional Surcharge Effect for Prestressed RGB (Square footing)

As explained in Sections 5.2.3, the vertical stresses along the punching shear (vertical) failure surface due to shear layer effect and confinement effect is considered to act as additional surcharge stress on the underlying weak soil. This effect will cause a further improvement in bearing capacity (ΔBCR_{SE}). Due to uniform tension in reinforcement due to prestressing, this additional surcharge stress is envisaged to be uniform over the area of reinforcement in the direction of prestressing (Fig.5.4). In uniaxial prestressing, the surcharge is considered to be uniform (q_s) over the area of reinforcement, in the direction of prestress. In the other perpendicular direction, it is considered to decrease exponentially from (q_o) at edge of footing and $0.01 (q_o)$ at the end of the reinforcement. Overall, an average surcharge (average of uniform surcharge in one direction and exponential decrease on the other side) is considered for estimation of ΔBCR_{SE} . In case if biaxial prestressing, the surcharge is considered to be uniform (q_s) over the area of reinforcement, in both X and Y directions. The following equations are used.

$$\Delta q_{SE} = q_s N_q \quad \text{-----(5.13)}$$

where N_q is the bearing capacity factor.

$$\Delta BCR_{SE} = \Delta q_{SE}/Q \quad \text{-----(5.14)}$$

$$q_s = [(\tau_1 + \tau_2).2H]/(L - B) \quad \text{-----(5.15)}$$

5.4 COMPARISON BETWEEN RESULTS OF ANALYTICAL MODEL AND EXPERIMENTAL STUDIES

The values of BCR predicted by the 'improved model' of Shivashankar et al. (1993), proposed in this thesis, are compared with those obtained from experimental studies and are presented below.

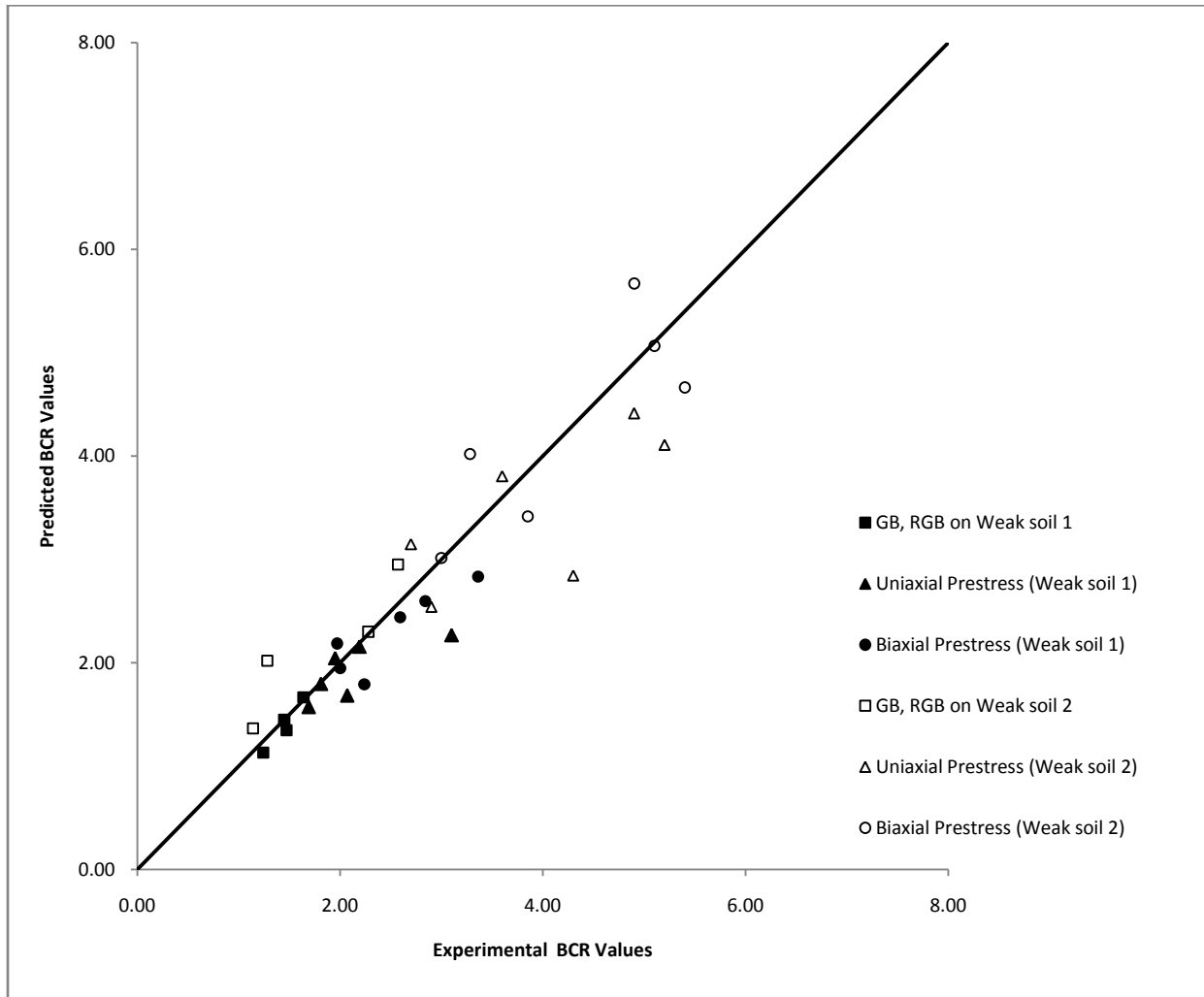


Fig 5.5. Comparison between observed and predicted values of BCR for GB, RGB and PRGB with single layer geogrid reinforcement of size 5B x 5B

Figure 5.5 shows a comparison between the values of BCR predicted by the proposed numerical model and those observed experimentally for PRGB with single layer geogrid of size 5B x 5B overlying (moist) weak soil 1 and (submerged) weak soil 2. It is observed that the proposed analytical model predicts the value of BCR with reasonable accuracy.

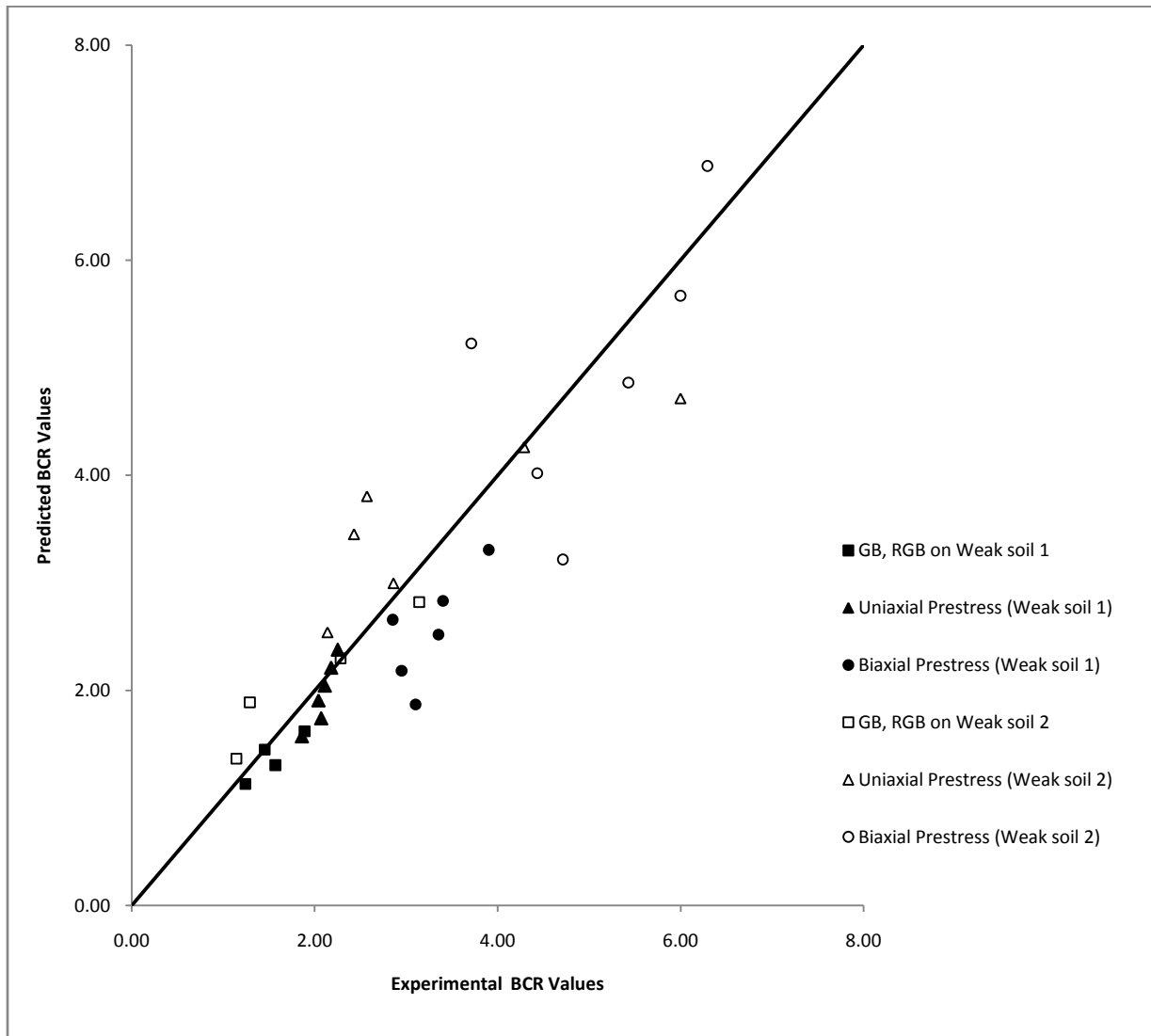


Fig 5.6. Comparison between observed and predicted values of BCR for GB, RGB and PRGB with single layer geotextile reinforcement of size 5B x 5B

The comparison between the values of BCR predicted by the proposed numerical model and those observed experimentally for PRGB with single layer geotextile of size 5B x 5B overlying (moist) weak soil 1 and (submerged) weak soil 2 is presented in Fig 5.6. It is observed that the proposed analytical model predicts the value of BCR with reasonable accuracy.

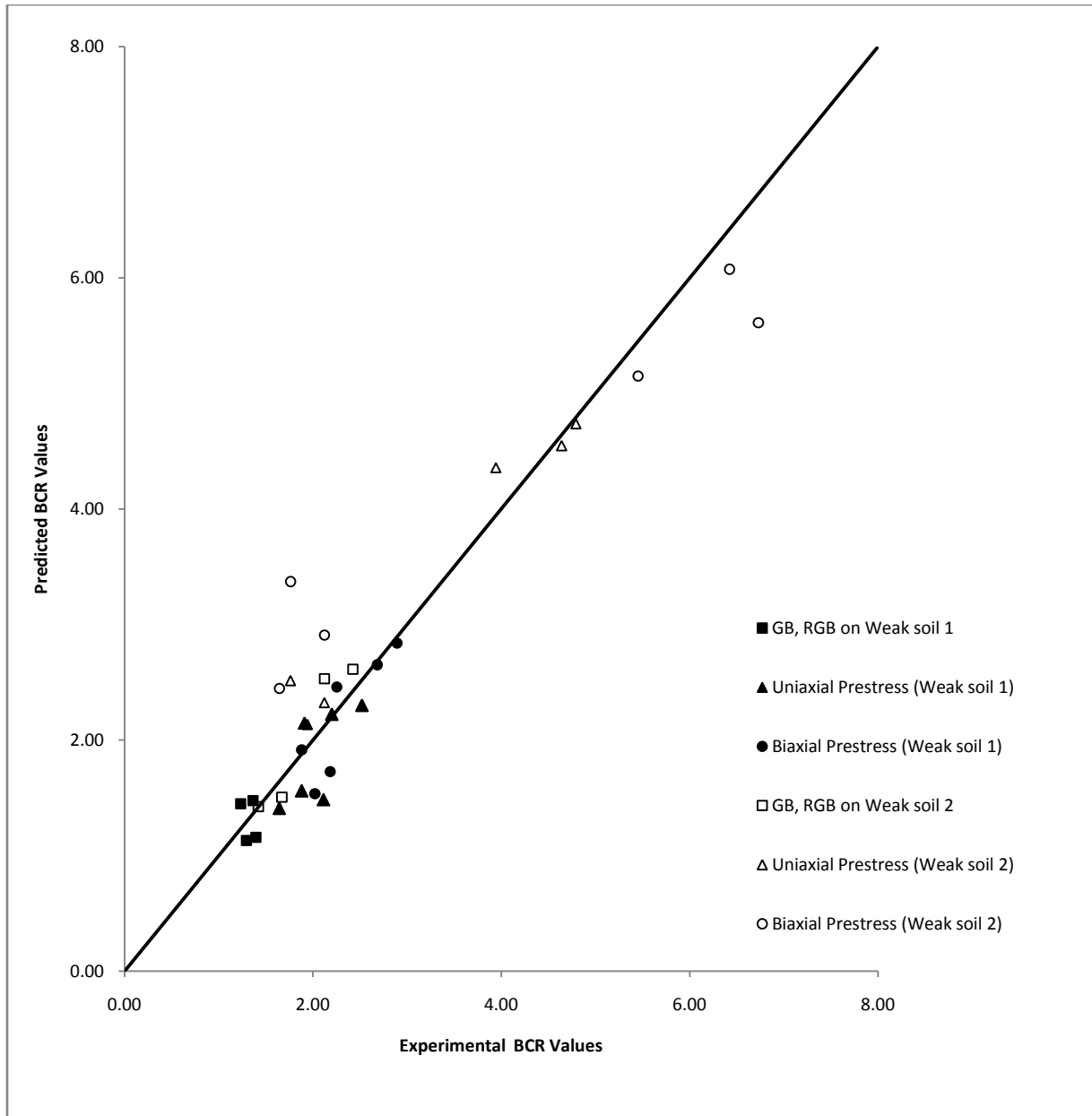


Fig 5.7. Comparison between observed and predicted values of BCR for GB, RGB and PRGB with single layer geogrid reinforcement of size 2B x 2B

Figure 5.7 shows a comparison between the values of BCR predicted by the proposed numerical model and those observed experimentally for PRGB with single layer geogrid of size 2B x 2B overlying (moist) weak soil 1 and (submerged) weak soil 2. It is observed that the proposed analytical model predicts the value of BCR with reasonable accuracy.

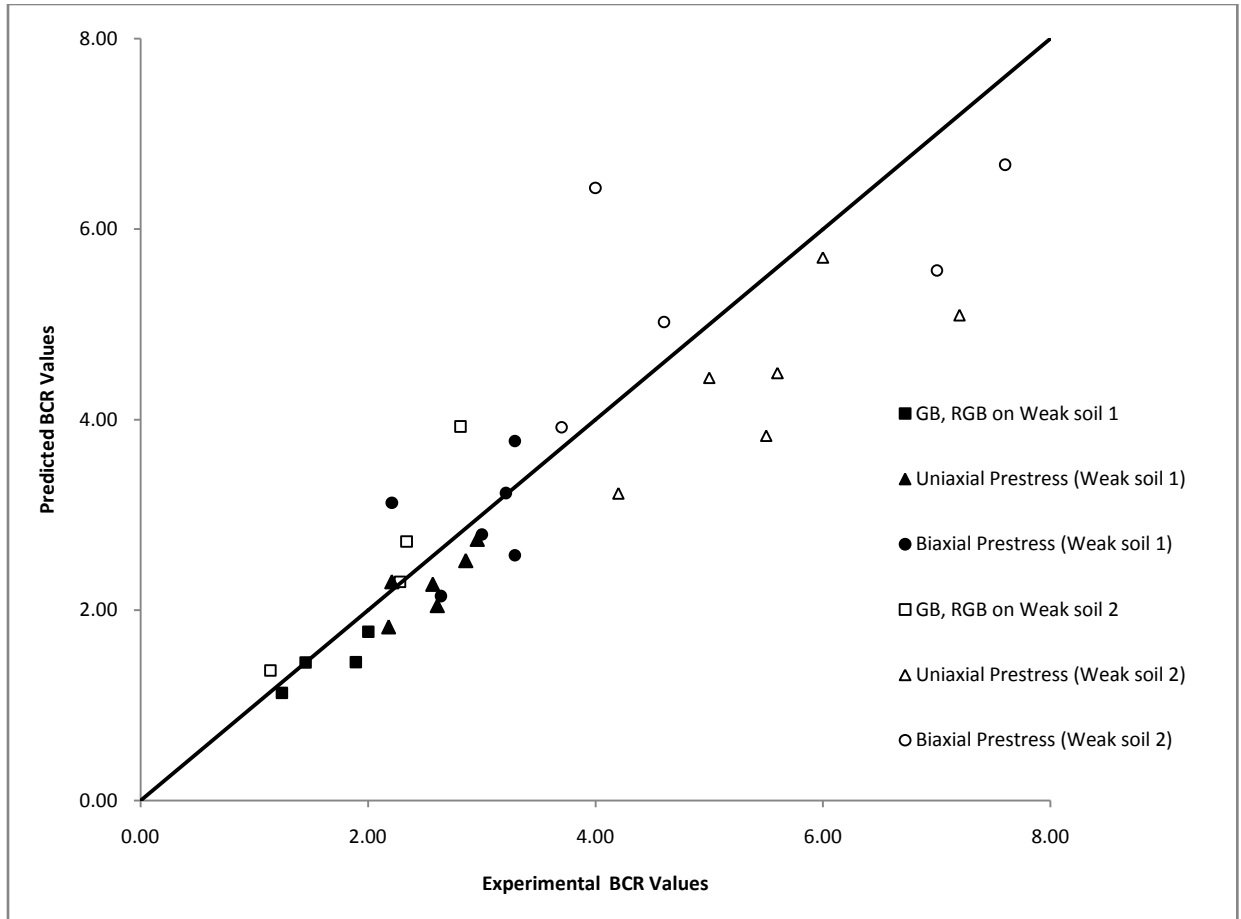


Fig 5.8. Comparison between observed and predicted values of BCR for GB, RGB and PRGB with double layer geogrid reinforcement of size 5B x 5B

Figure 5.8 shows a comparison between the values of BCR predicted by the proposed numerical model and those observed experimentally for PRGB with double layer geogrid of size 5B x 5B overlying (moist) weak soil 1 and (submerged) weak soil 2. It is observed that the proposed analytical model predicts the value of BCR with reasonable accuracy. It is also observed that prediction is better for moist soil than submerged soil. It implies that the punching shear failure mechanism is predominant failure mechanism in case of weak soil 1.

5.5 COMPARISON BETWEEN RESULTS OF ANALYTICAL MODEL AND FINITE ELEMENT ANALYSIS

The values of BCR predicted by the 'improved model' of Shivashankar et al. (1993), proposed in this thesis, are compared with those obtained from finite element analyses and are presented below.

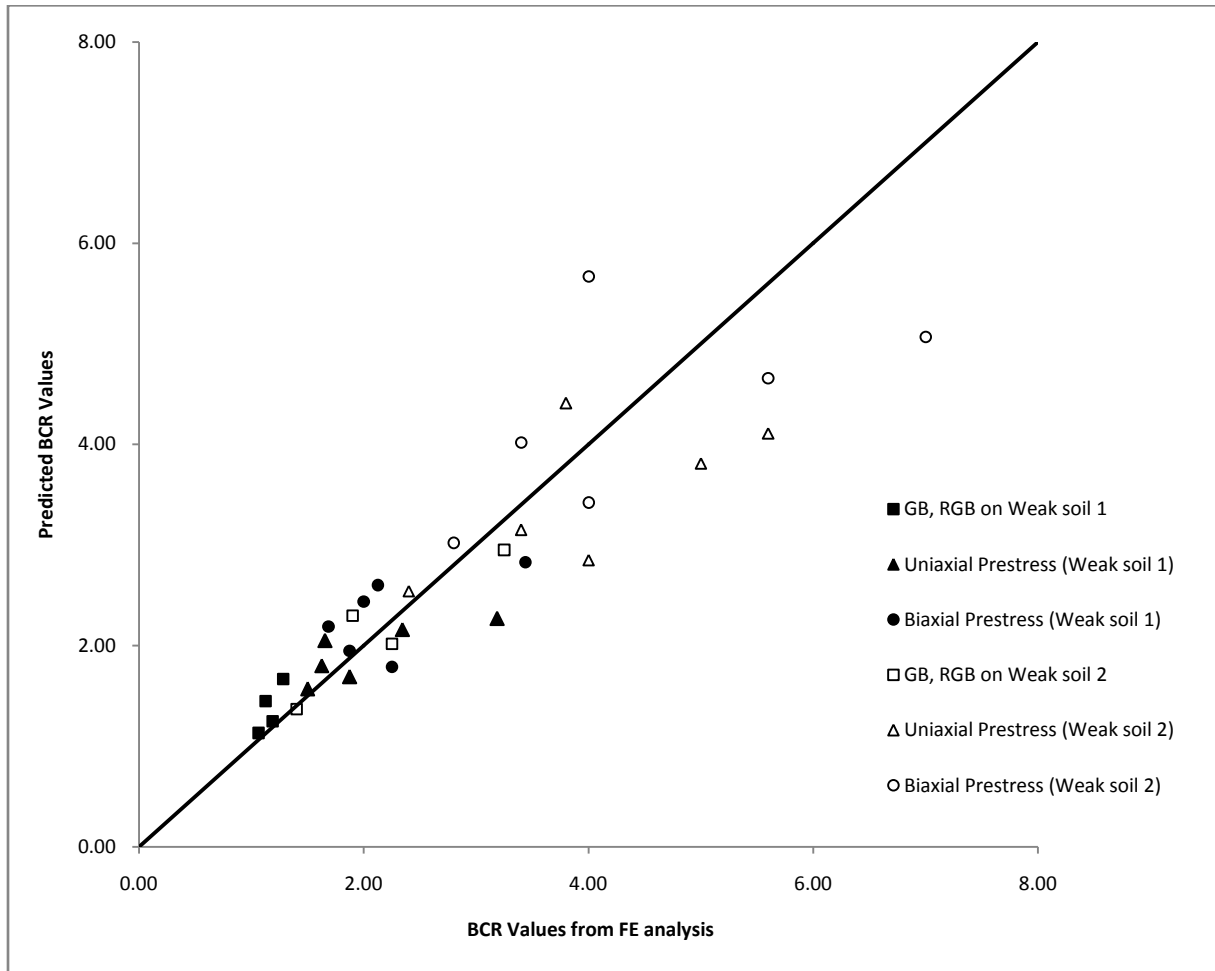


Fig 5.9. Comparison between predicted values of BCR using analytical model and FE analysis for GB, RGB and PRGB with single layer geogrid reinforcement of size 5B x 5B.

Figure 5.9 shows a comparison between the values of BCR predicted by the proposed analytical model and finite element analyses for PRGB with single layer geogrid of size 5B x 5B overlying (moist) weak soil 1 and (submerged) weak soil 2. It is observed that the proposed analytical model predicts the value of BCR with reasonable accuracy. It is also observed that prediction is better for moist soil than submerged soil.

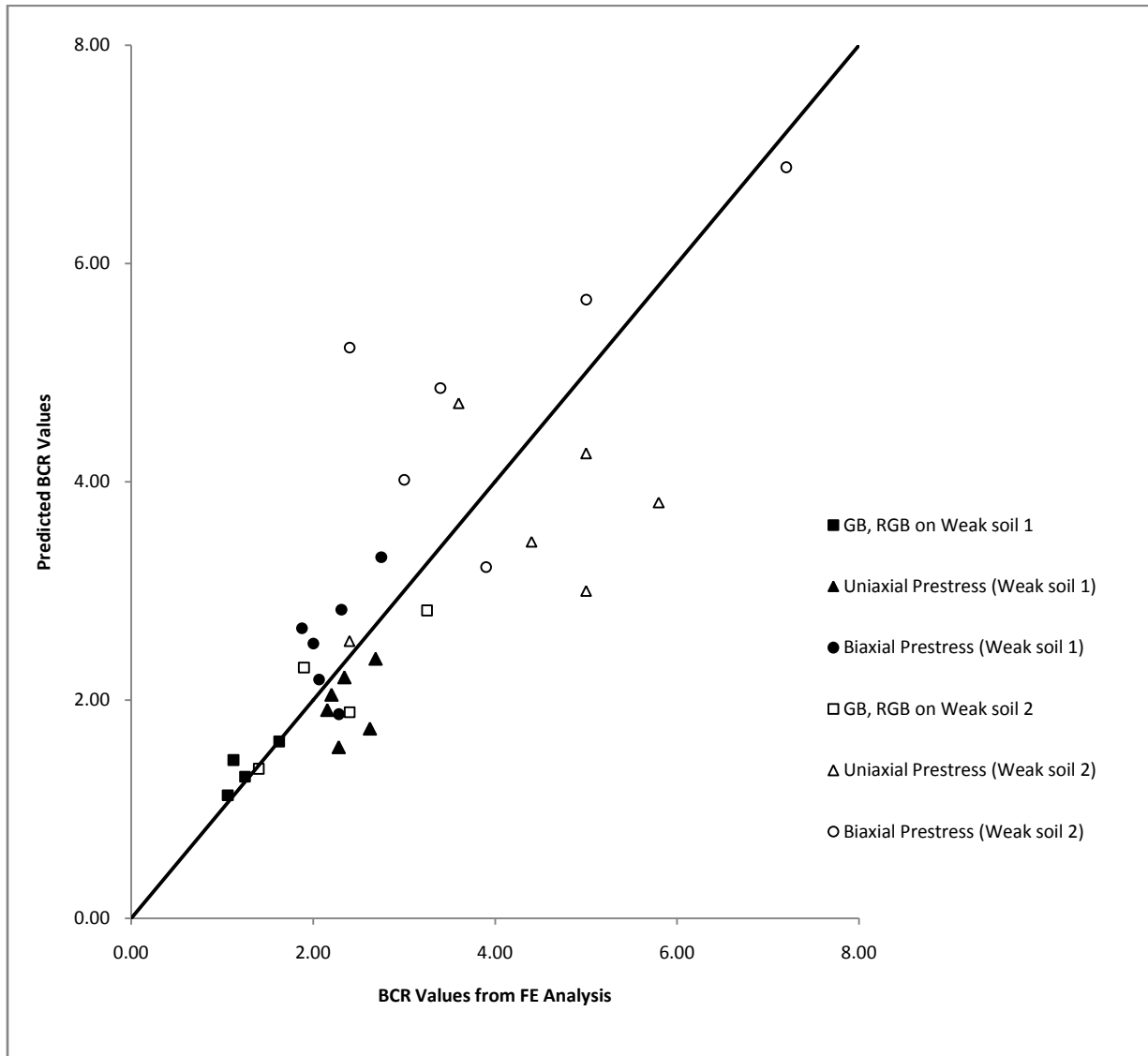


Fig 5.10. Comparison between predicted values of BCR using analytical model and FE analysis for GB, RGB and PRGB with single layer geotextile reinforcement of size 5B x 5B.

The comparison between the values of BCR predicted by the proposed analytical model and finite element analyses for PRGB with single layer geotextile of size 5B x 5B overlying (moist) weak soil 1 and (submerged) weak soil 2 is presented in Fig 5.10. It is observed that the proposed analytical model predicts the value of BCR with reasonable accuracy. It is also observed that prediction is better for moist soil than submerged soil.

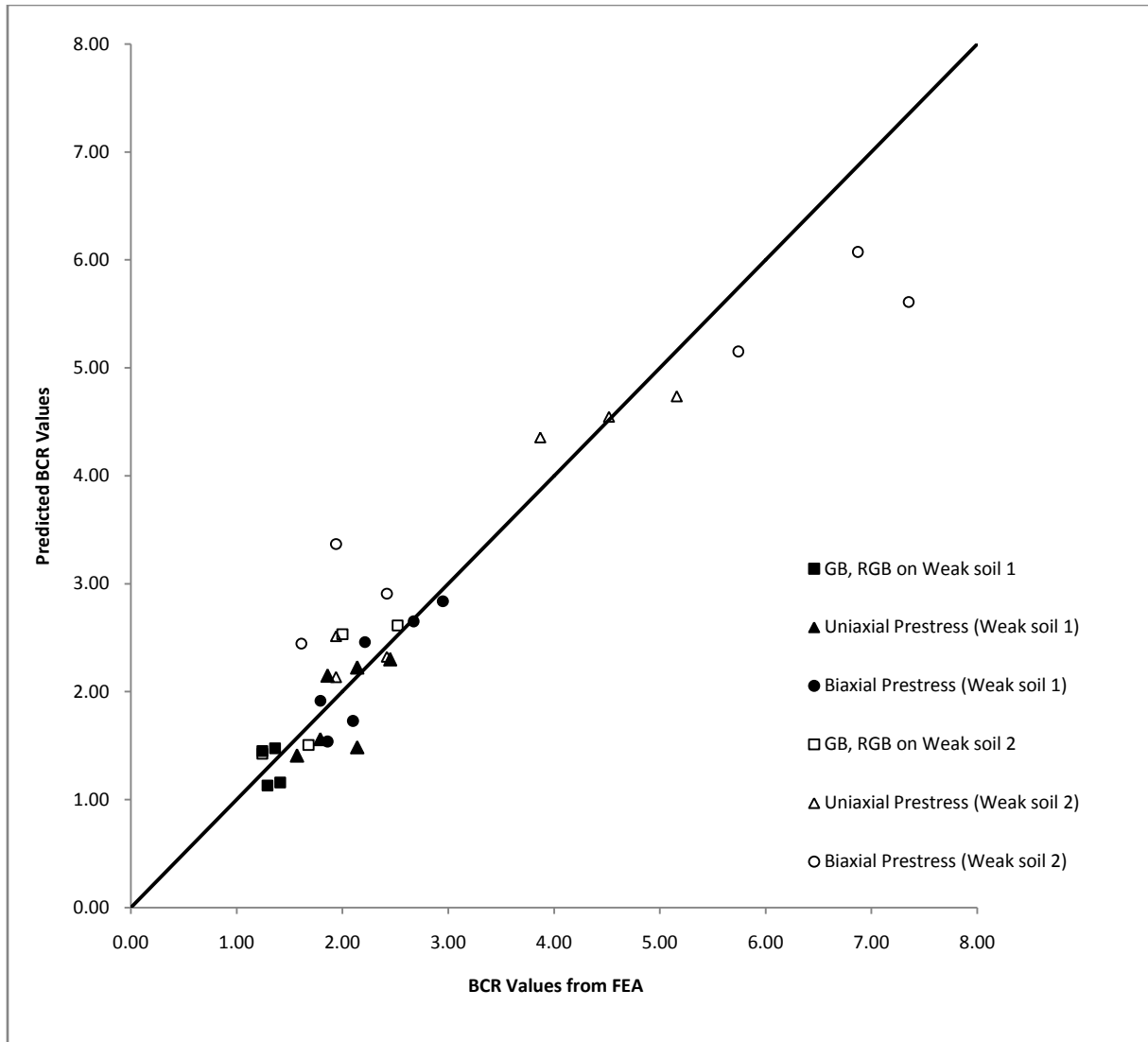


Fig 5.11. Comparison between predicted values of BCR using analytical model and FE analysis for GB, RGB and PRGB with single layer geogrid reinforcement of size 2B x 2B.

Figure 5.11 shows a comparison between the values of BCR predicted by the proposed analytical model and finite element analyses for PRGB with single layer geogrid of size 2B x 2B overlying (moist) weak soil 1 and (submerged) weak soil 2. It is observed that the proposed analytical model predicts the value of BCR with reasonable accuracy.

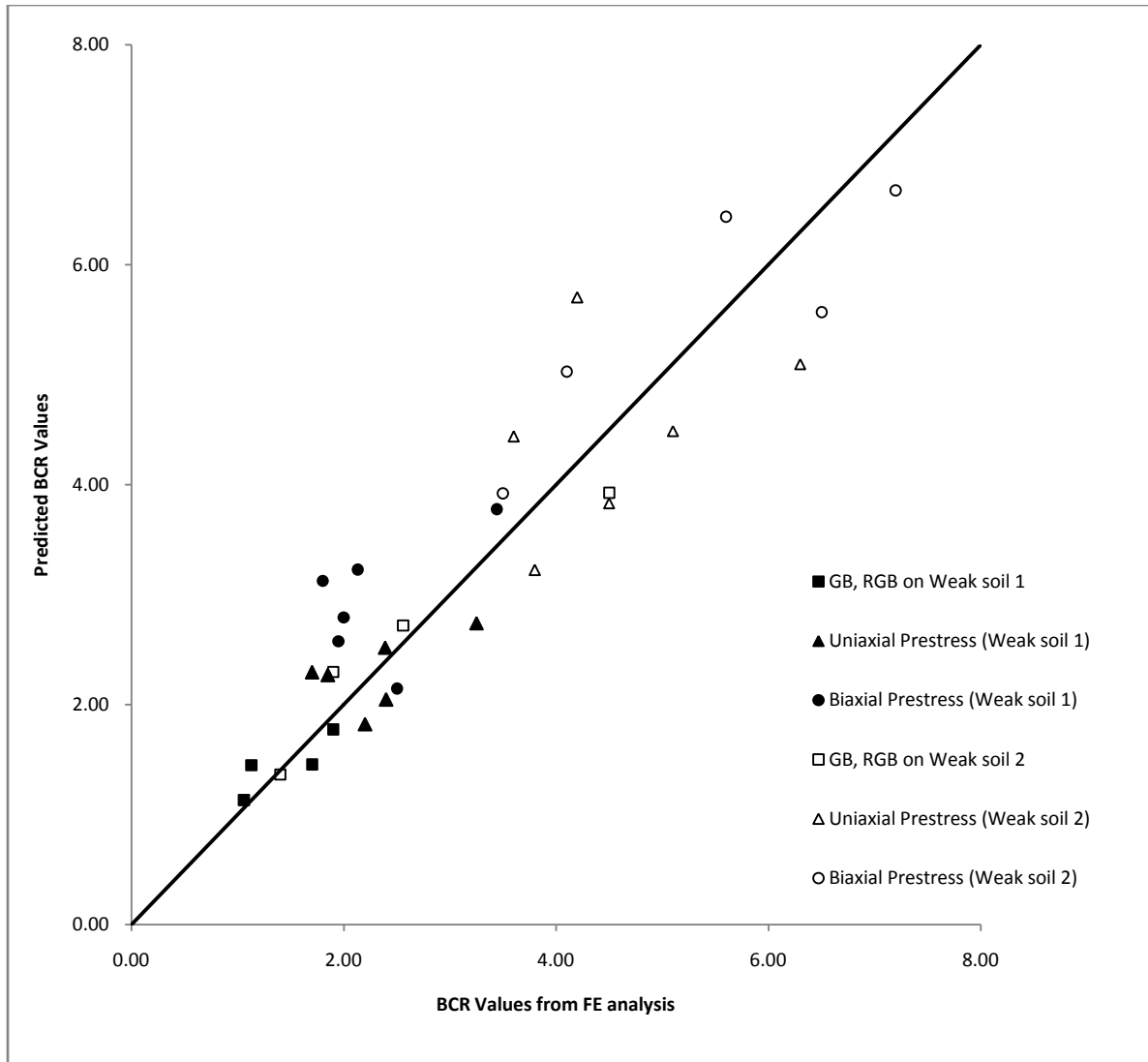


Fig 5.12. Comparison between predicted values of BCR using analytical model and FE analysis for GB, RGB and PRGB with double layer geogrid reinforcement of size 5B x 5B.

Figure 5.12 shows a comparison between the values of BCR predicted by the proposed analytical model and finite element analyses for PRGB with double layer geogrid of size 5B x 5B overlying (moist) weak soil 1 and (submerged) weak soil 2. It is observed that the proposed analytical model predicts the value of BCR with reasonable accuracy.

5.6 CHAPTER SUMMARY

1. The development of an analytical model for the prediction of BCR of PRGB overlying weak soil is presented in this Chapter
2. A punching shear failure mechanism is envisaged in the analytical model.

3. The improvement in bearing capacity of a reinforced granular bed is considered to comprise of three components namely Shear layer effect, Confinement effect and Surcharge effect.
4. The values of BCR predicted by the proposed analytical model are in reasonably good agreement with those obtained from finite element and experimental studies.
5. Prediction is better for moist soil than for submerged soil, which implies that the punching shear failure mechanism is predominant failure mechanism in case of moist soil.

CHAPTER 6

PRGB ON VOIDS

6.1 INTRODUCTION

The presence of underground void can cause serious engineering problem leading to instability of the foundation and severe damage to the super structure. If the void is located at shallow depth, the consequence can be very costly and dangerous. Voids can be caused due to tension cracks in unsaturated cohesive soils; differential settlement of municipal soil waste; settlement of localized lens of compressible soil; settlement of poorly compacted trench backfill; collapse of underground cavities such as natural caves, tunnels, mine workings, pipes and tanks.

When void is found in the foundation soil, the potential remedial measures the designer may consider are to fill the void with competent material through grouting, use piles to bypass the void and transmit the load to a competent layer underneath or to place the foundation at a suitable depth as per stability analysis that the void lies below the critical depth thereby does not influence the performance of the proposed foundation. Among these, the last alternative is relatively easy and less expensive. However, in many cases the available cover soil above the void may be of less thickness than the critical one. In such situations, an additional layer of competent soil could be provided on the ground; over this the foundation should be placed. This fill soil when reinforced adequately would further enhance the performance of the footing.

In this investigation, extensive studies are carried out using the software PLAXIS, to determine the effects of prestressing the reinforcement in improving the bearing capacity of reinforced granular beds overlying weak soil with voids. The parameters varied are magnitude of prestress, thickness of granular bed, depth of void and eccentricity of the void. The diameter of the void is taken as equal to 0.6 times the width of footing for all the cases. The eccentricity of the void is defined by the parameter 'x' and depth of void by the parameter 'y'.

x = Horizontal distance between centre of void and midpoint of square footing

y = Vertical distance of the centre of void from the base of square footing

Analysis is done for four different cases.

1. Void just above the interface between GB and weak soil
2. Void at the interface between GB and weak soil

3. Void just below the interface between GB and weak soil
4. Void at a depth of $0.75B$ below the interface between GB and weak soil.

6.2 GRANULAR BEDS OF THICKNESS B

6.2.1 Void just above the interface between granular bed and weak soil

Figure 6.1 shows a PRGB with a void placed just above the interface between granular bed and weak soil. The void is placed vertically below the centre line of the footing i.e. eccentricity $x = 0$. Figure 6.2 shows the geometric model for the finite element analysis in PLAXIS.

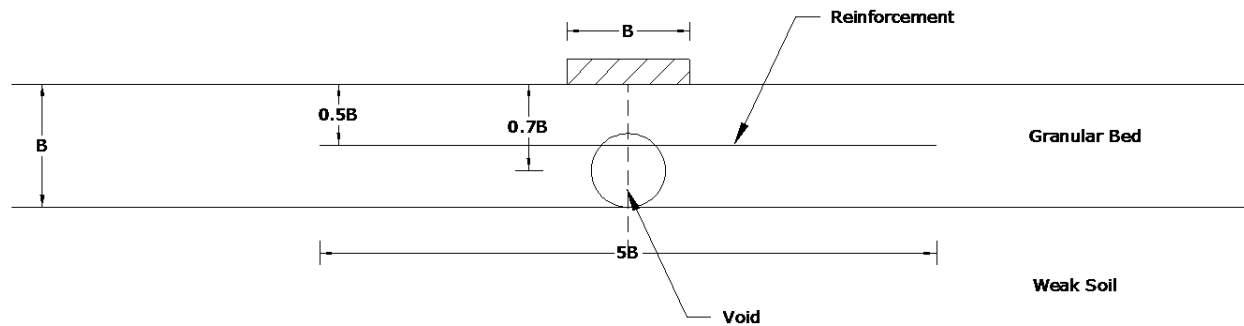


Fig 6.1. Void just above the interface between GB and weak soil, $x = 0$, $y = 0.7B$

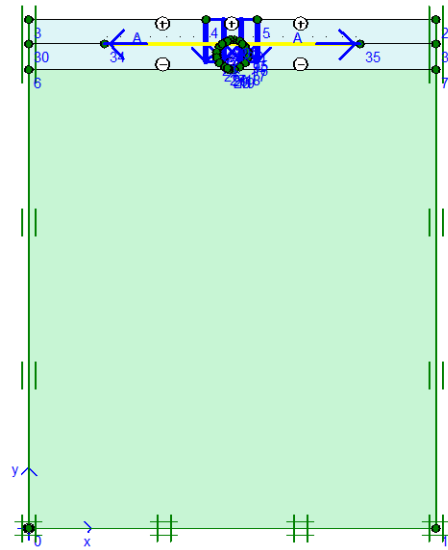


Fig 6.2. Geometric model for PRGB of thickness B having void with $x = 0$, $y = 0.7B$

Vertical stress vs normalized settlement curves of GB, RGB and PRGB for the above case are presented in Fig 6.3. The curve for unreinforced GB without void also is included so that the

reduction in strength due to the presence of void and the improvement due to the addition of reinforcement and prestress could be understood.

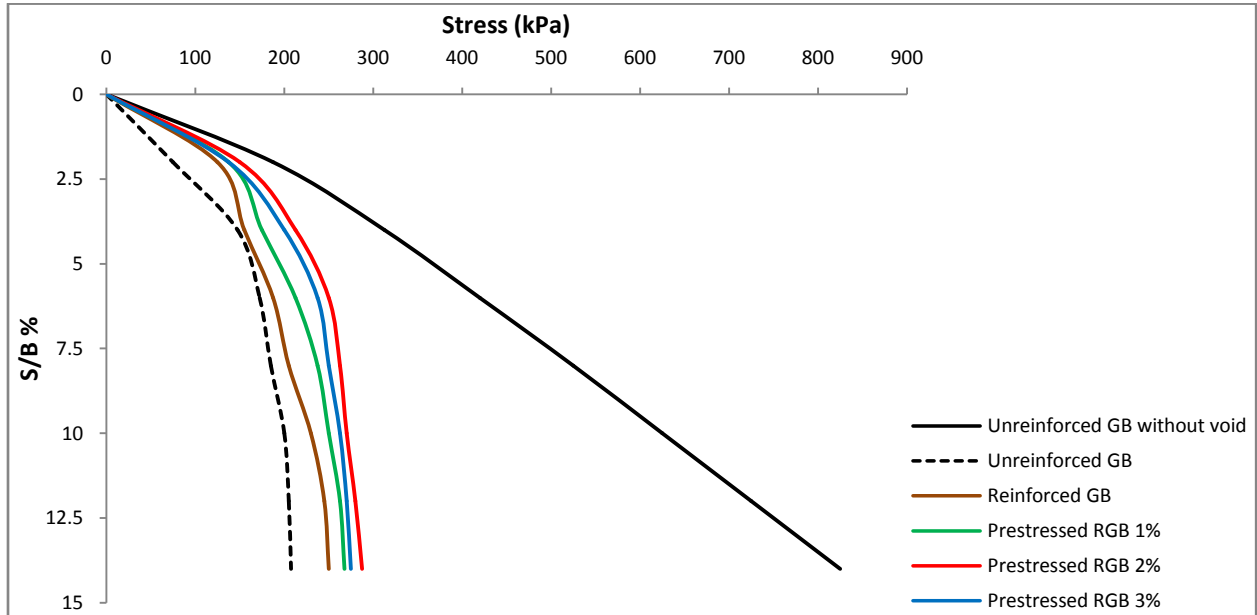


Fig 6.3 Stress vs normalized settlement curves for GB, RGB and PRGB of thickness B with void having $x=0, y = 0.7B$

From Fig 6.3, it can be seen that the presence of void inside the granular bed at a depth of $0.7B$ and zero eccentricity, drastically reduces the bearing capacity. With the addition of reinforcement and prestress the bearing capacity improved and maximum improvement is seen when the prestress is equal to 2% of the tensile strength of the reinforcement.

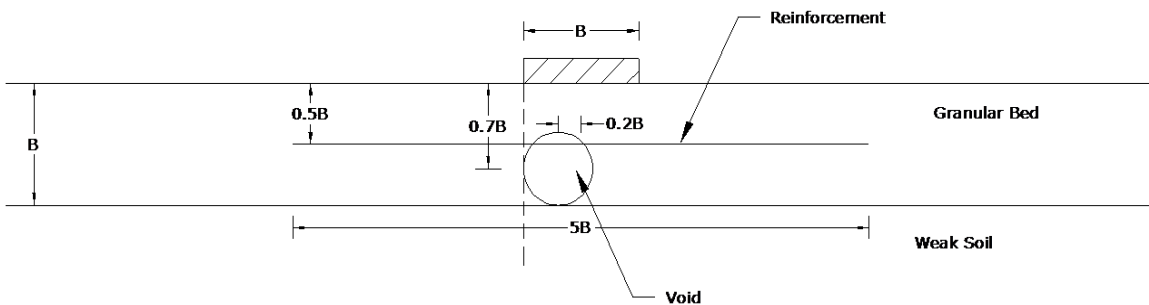


Fig 6.4. Void just above the interface between GB and weak soil, $x = 0.2B, y = 0.7B$

Figure 6.4 shows a PRGB with a void placed just above the interface between granular bed and weak soil and with an eccentricity of $0.2B$. The edge of the void is vertically below the edge of the footing. Figure 6.5 shows its geometric model for finite element analysis.

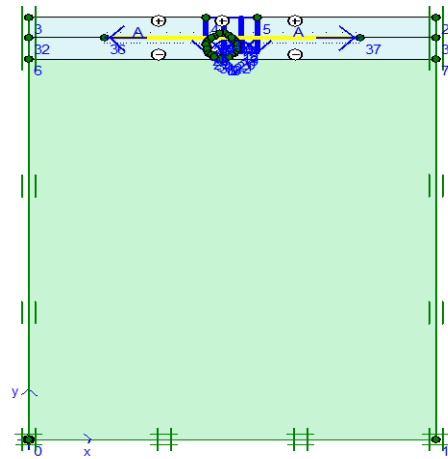


Fig 6.5. Geometric model for PRGB of thickness B having void with $x = 0.2B$, $y = 0.7B$

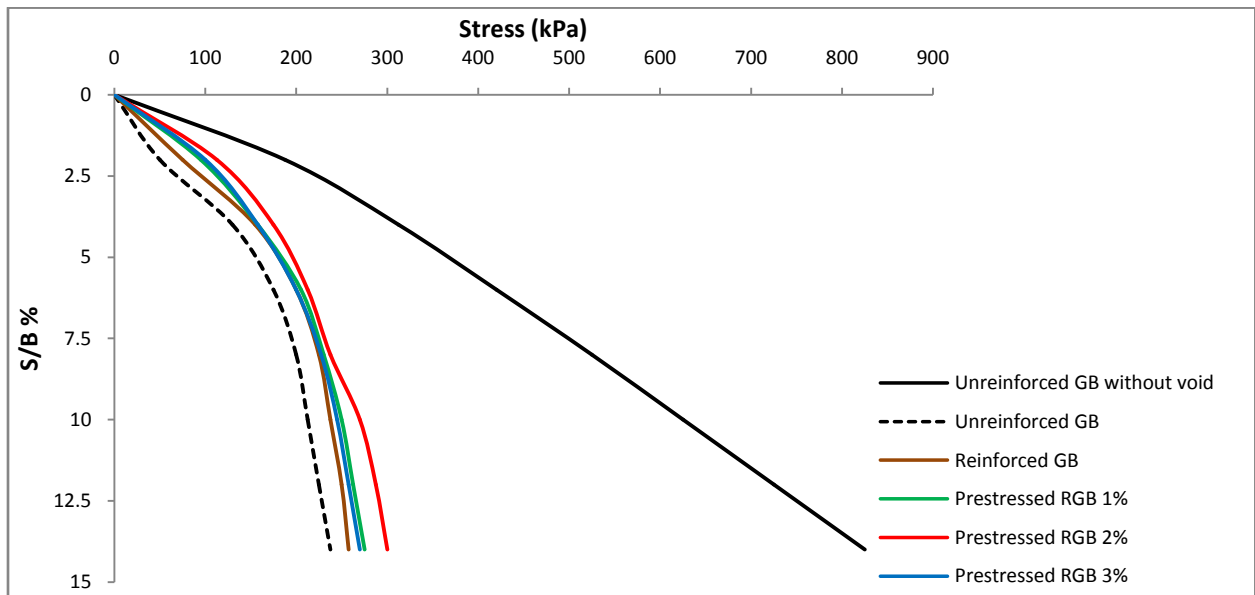


Fig 6.6 Stress vs normalized settlement curves for GB, RGB and PRGB of thickness B with void having $x=0.2B$, $y = 0.7B$

Figure 6.6 shows the variation of vertical stress with normalized settlement for GB, RGB and PRGB with a void placed inside the GB just above the interface with weak soil and at an eccentricity of $0.2B$. Similar to the previous case it can be seen that the presence of void inside the GB drastically reduces the bearing capacity and maximum improvement is seen when the prestress is equal to 2% of the tensile strength of reinforcement.

6.2.2 Void at the interface between granular bed and weak soil

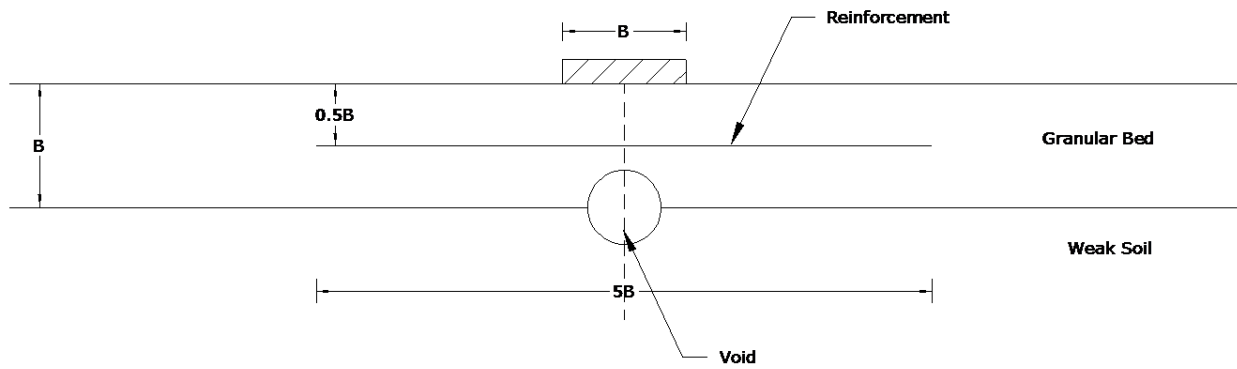


Fig 6.7. Void at the interface between GB and weak soil, $x = 0$, $y = B$

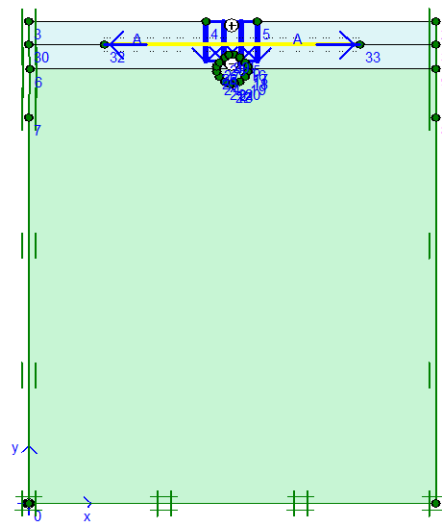


Fig 6.8. Geometric model for PRGB of thickness B having void with $x = 0$, $y = B$

Figure 6.7 shows a PRGB with a void placed at the interface between granular bed and weak soil. The upper half of the void is in the GB and lower half in weak soil. The void is placed vertically below the centre line of the footing ie eccentricity $x = 0$. Figure 6.8 shows the geometric model for the finite element analysis in PLAXIS.

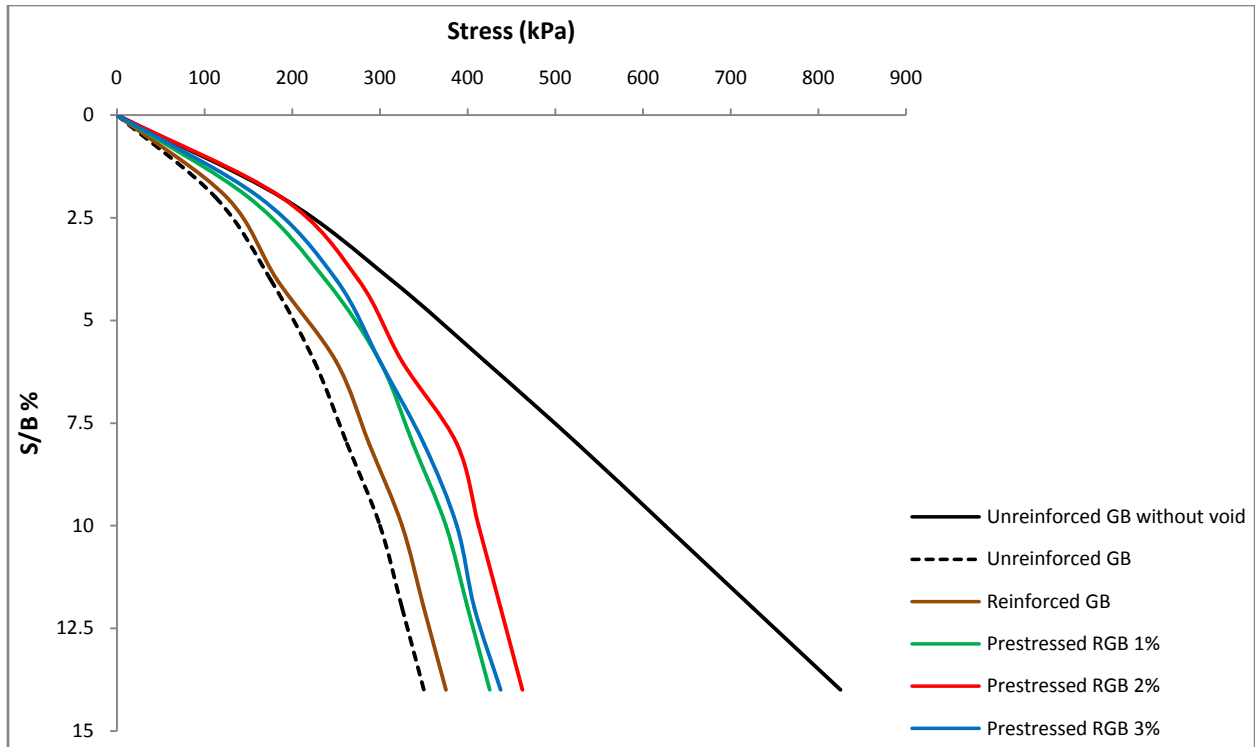


Fig 6.9 Stress vs normalized settlement curves for GB, RGB and PRGB of thickness B with void having $x=0$, $y = B$

Vertical stress vs normalized settlement curves of GB, RGB and PRGB for the above case are presented in Fig 6.9. It can be seen from the figure that the presence of void at a depth of B and zero eccentricity, considerably reduces the bearing capacity. It is observed that maximum improvement is attained when the prestress is equal to 2% of the tensile strength of the reinforcement. It is also observed that the reduction in bearing capacity is comparatively lesser than the previous case ($y=0.7B$).

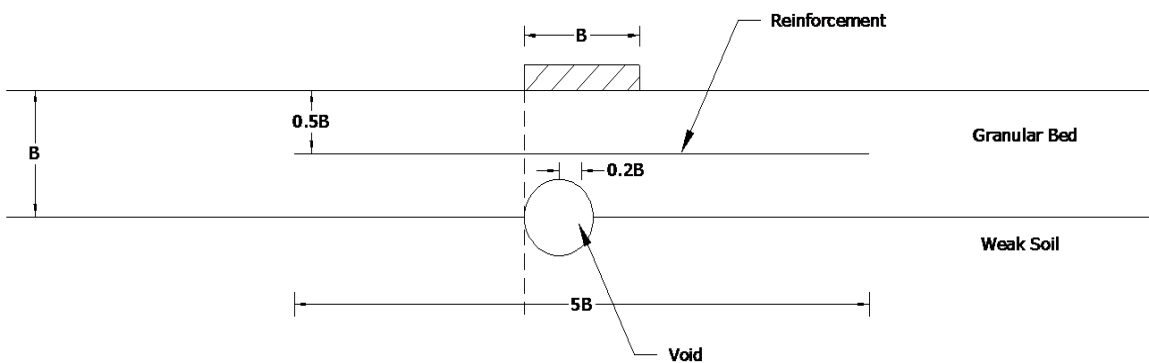


Fig 6.10. Void at the interface between GB and weak soil, $x = 0.2B$, $y = B$

Figure 6.10 shows a PRGB of thickness B with a void placed at the interface between granular bed and weak soil. The upper half of the void is in the GB and lower half in weak soil. The edge of the void is vertically below the edge of the footing and hence has an eccentricity of $0.2B$. Figure 6.11 shows its geometric model for finite element analysis.

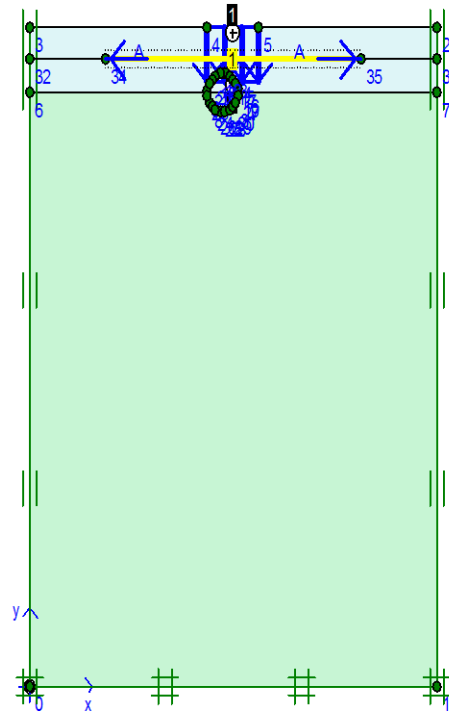


Fig 6.11. Geometric model for PRGB of thickness B having void with $x = 0.2B$, $y = B$

Figure 6.12 presents the vertical stress vs normalized settlement curves of GB, RGB and PRGB for the above case. It can be seen from the figure that the addition of void at a depth of B and eccentricity $0.2B$, considerably reduces the bearing capacity. It is also observed that maximum improvement is attained when the prestress is equal to 2% of the tensile strength of the reinforcement. It is also observed that the reduction in bearing capacity is comparatively lesser than the previous case ($y=0.7B$).

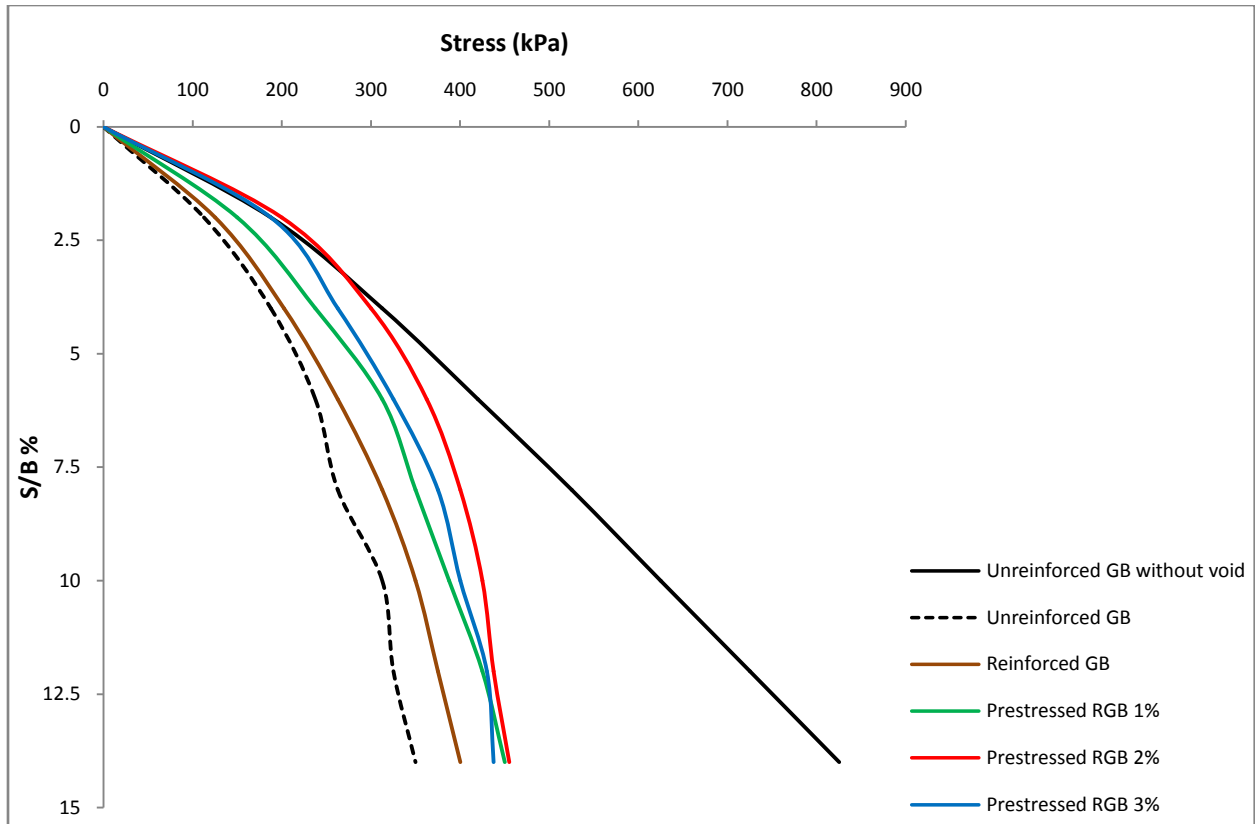


Fig 6.12 Stress vs normalized settlement curves for GB, RGB and PRGB of thickness B with void having $x=0.2B$, $y = B$

6.2.3 Void just below the interface between granular bed and weak soil

Figure 6.13 shows a PRGB with a void placed just below the interface between granular bed and weak soil. The void is placed vertically below the centre line of the footing i.e. eccentricity $x = 0$. Figure 6.14 shows the geometric model for the finite element analysis in PLAXIS.

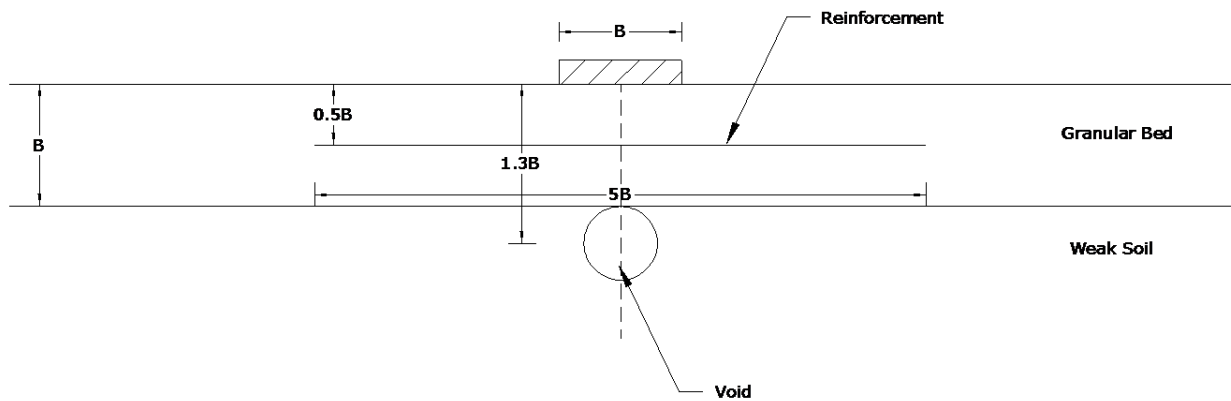


Fig 6.13. Void just below the interface between GB and weak soil, $x = 0$, $y = 1.3B$

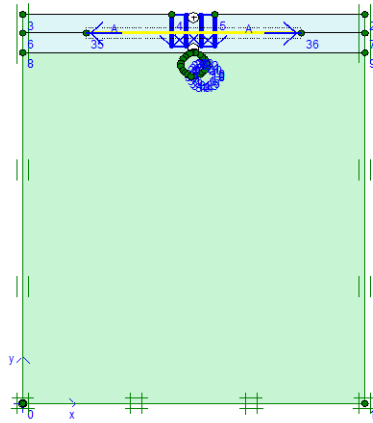


Fig 6.14. Geometric model for PRGB of thickness B having void with $x=0$, $y=1.3B$

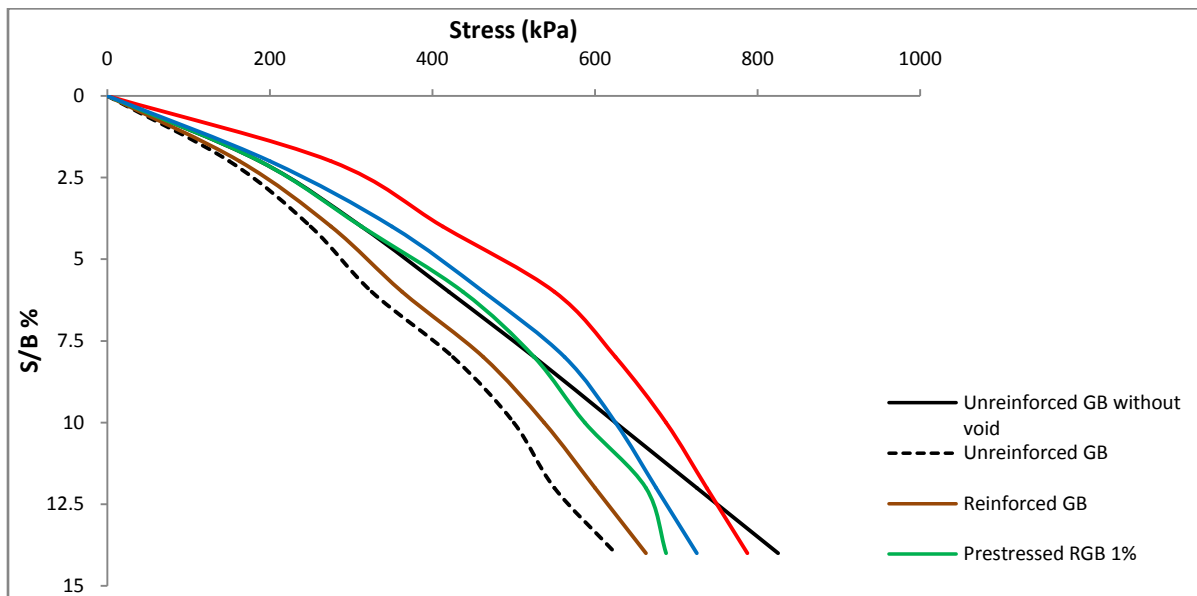


Fig 6.15 Stress vs normalized settlement curves for GB, RGB and PRGB of thickness B with void having $x=0$, $y=1.3B$

Vertical stress vs normalized settlement curves of GB, RGB and PRGB for this case are presented in Fig 6.15. It can be seen from the figure that the presence of void at a depth of $1.3B$ and zero eccentricity, causes a reduction in bearing capacity. It is observed that maximum improvement is attained when the prestress is equal to 2% of the tensile strength of the reinforcement. The reduction in bearing capacity is considerably lesser than the previous case ($y=B$). PRGB with void is giving more bearing capacity than unreinforced GB without void.

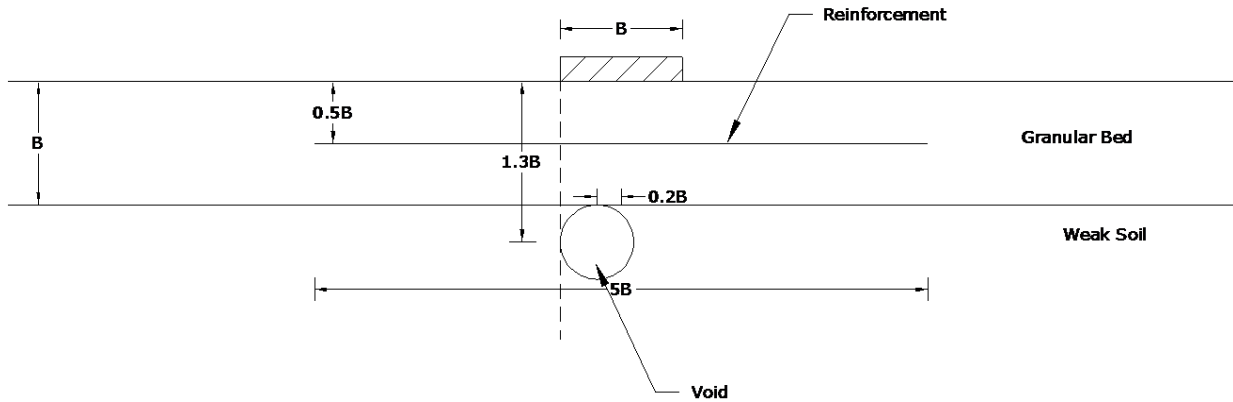


Fig 6.16. Void just below the interface between GB and weak soil, $x = 0.2B$, $y = 1.3B$

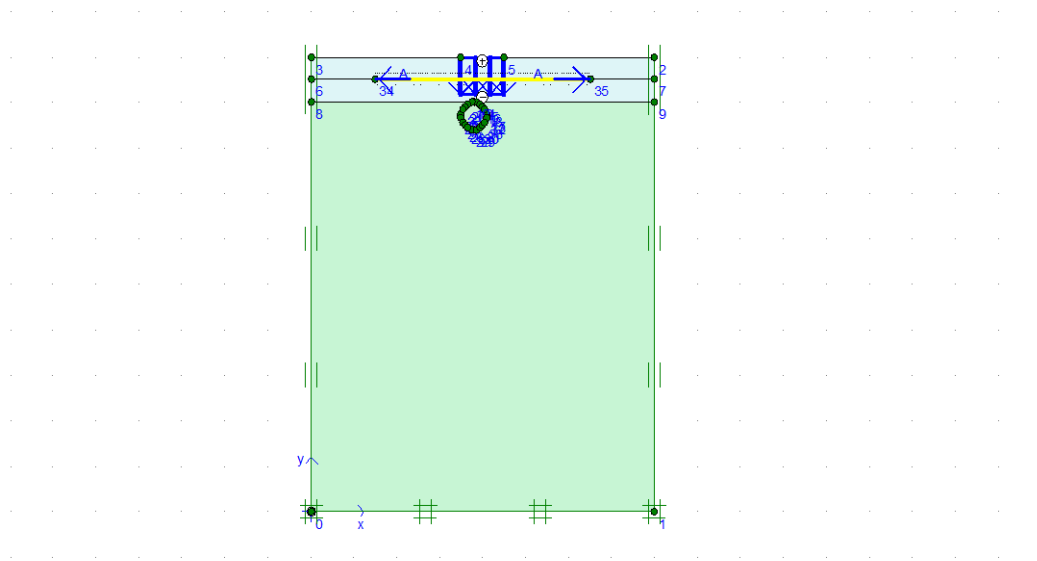


Fig 6.17. Geometric model for PRGB of thickness B having void with $x = 0.2B$, $y = 1.3B$

Figure 6.16 shows a PRGB with a void placed just below the interface between granular bed and weak soil and with an eccentricity of $0.2B$. The edge of the void is vertically below the edge of the footing. Figure 6.17 shows its geometric model for finite element analysis.

Figure 6.18 presents the vertical stress vs normalized settlement curves of GB, RGB and PRGB with void at a depth of $1.3B$ and eccentricity $0.2B$. It can be seen from the figure that the presence of void caused a reduction in bearing capacity. It is also observed that maximum improvement is attained when the prestress is equal to 2% of the tensile strength of the reinforcement. It is also observed here that PRGB with void is performing better than GB without void.

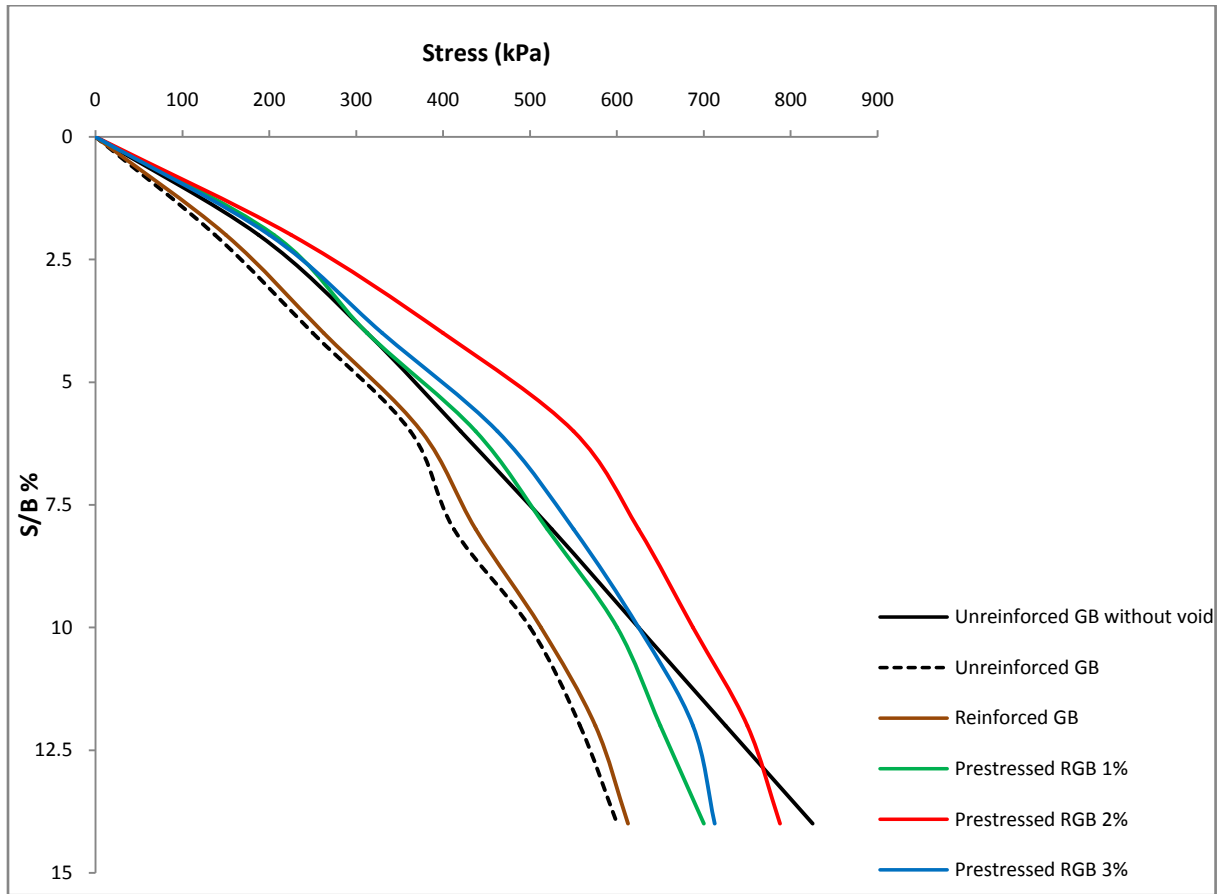


Fig 6.18 Stress vs normalized settlement curves for GB, RGB and PRGB of thickness B with void having $x=0.2B$, $y=1.3 B$

6.2.4 Void at a depth of $0.75B$ below the interface between granular bed and weak soil

Figure 6.19 shows a PRGB with a void placed at a depth of $0.75B$ below the interface between granular bed and weak soil. The void is placed vertically below the centre line of the footing i.e. eccentricity $x = 0$. Figure 6.20 shows the geometric model for the finite element analysis in PLAXIS.

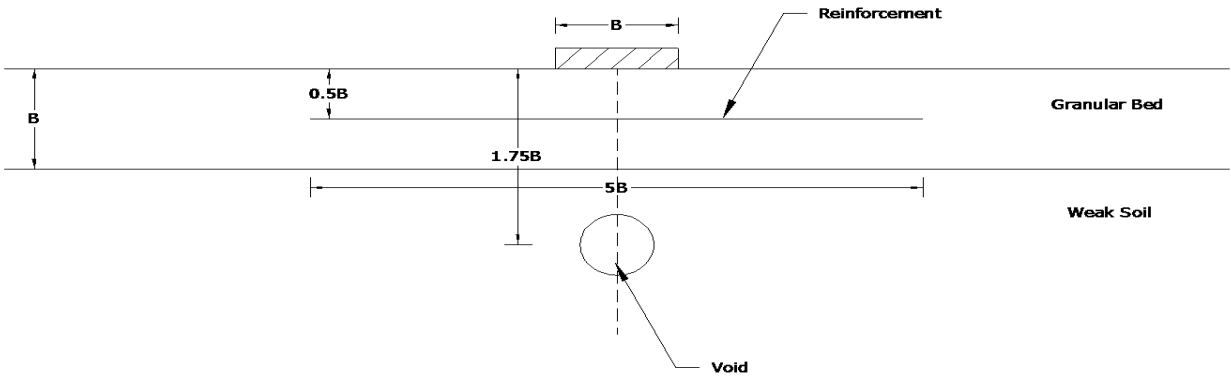


Fig 6.19. Void at a depth of $0.75B$ below the interface between GB and weak soil, $x = 0$, $y = 1.75B$

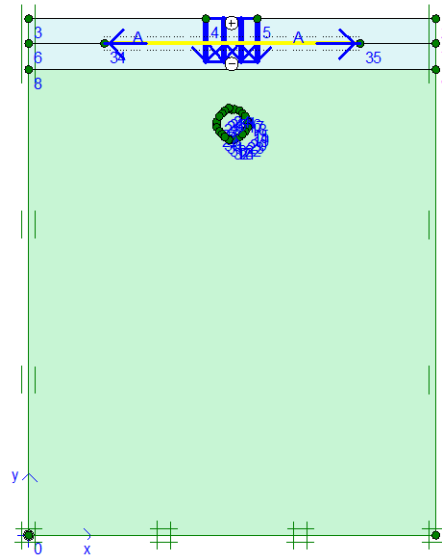


Fig 6.20. Geometric model for PRGB of thickness B having void with $x = 0$, $y = 1.75B$

Vertical stress vs normalized settlement curves of GB, RGB and PRGB for this case are presented in Fig 6.21. It can be seen from the figure that the presence of void at a depth of $1.75B$ and zero eccentricity, causes only a minor reduction in bearing capacity. It is observed that maximum improvement is attained when the prestress is equal to 2% of the tensile strength of the reinforcement. PRGB with void is giving more bearing capacity than unreinforced GB without void.

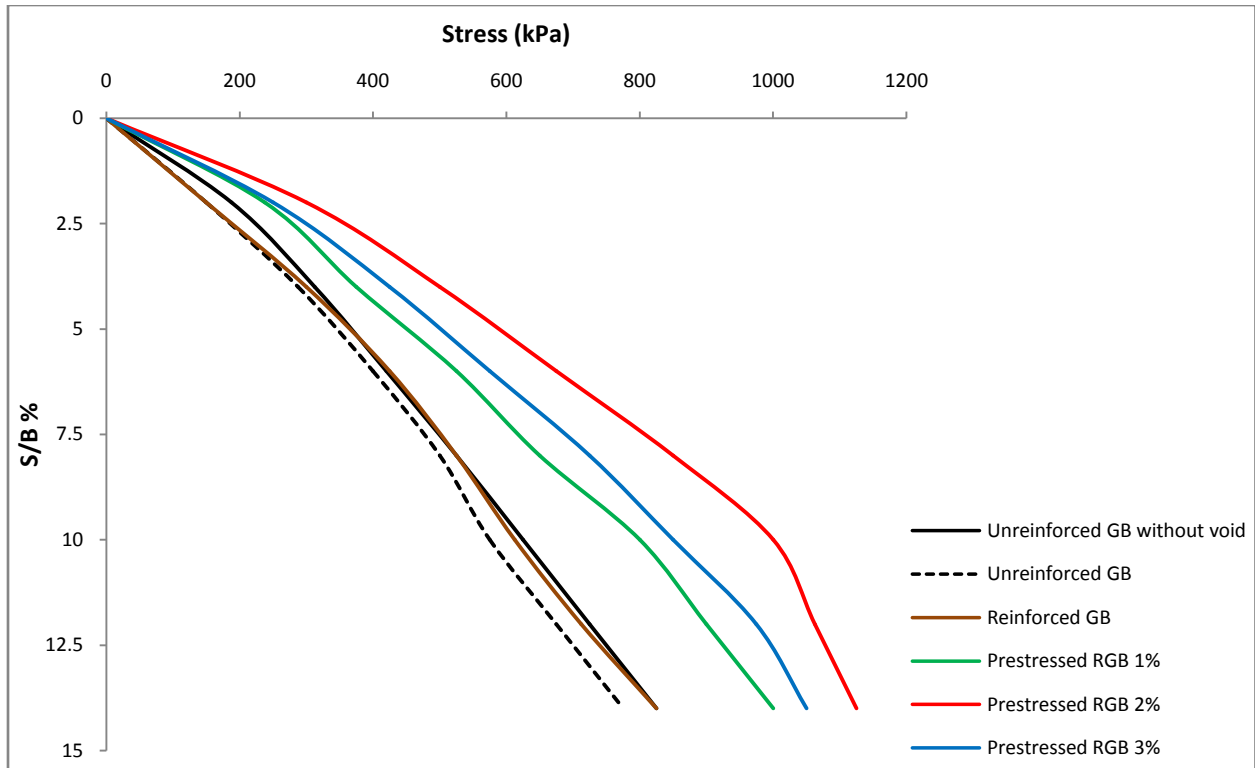


Fig 6.21 Stress vs normalized settlement curves for GB, RGB and PRGB of thickness B with void having $x=0$, $y=1.75 B$

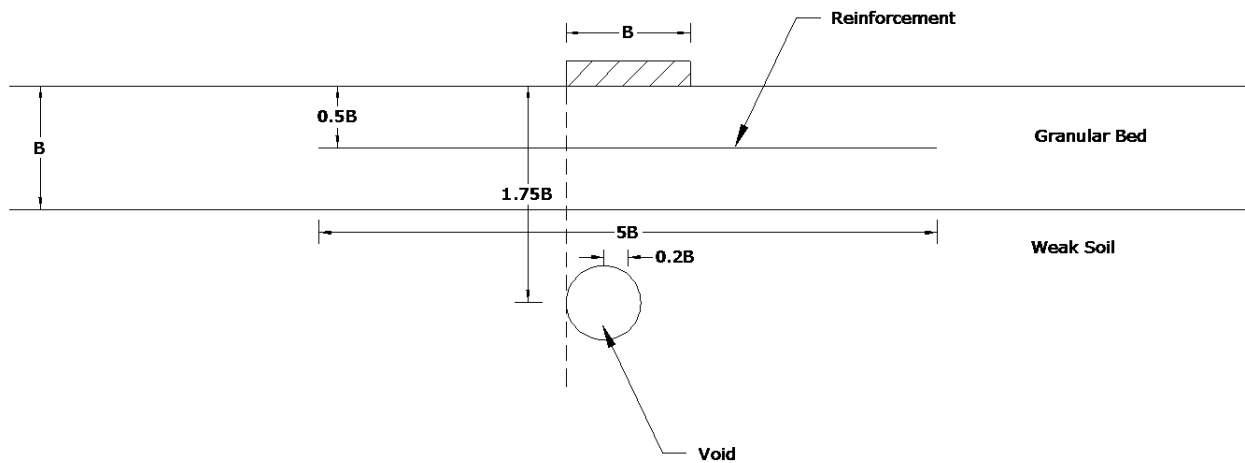


Fig 6.22. Void at a depth of $0.75B$ below the interface between GB and weak soil, $x=0.2B$, $y=1.75B$

Figure 6.22 shows a PRGB with a void placed at a depth of $0.75B$ below the interface between granular bed and weak soil and with an eccentricity of $0.2B$. The edge of the void is vertically below the edge of the footing. Figure 6.23 shows its geometric model for finite element analysis.

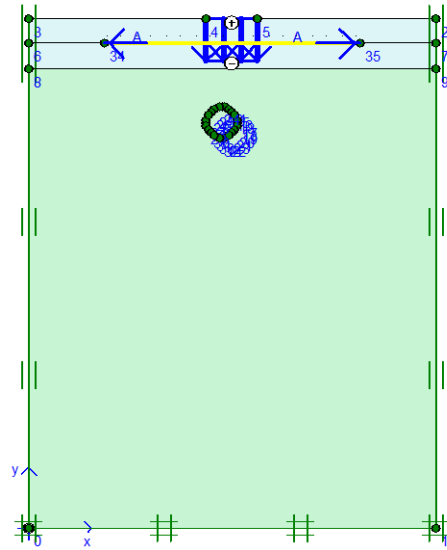


Fig 6.23. Geometric model for PRGB of thickness B having void with $x = 0.2B$, $y = 1.75B$

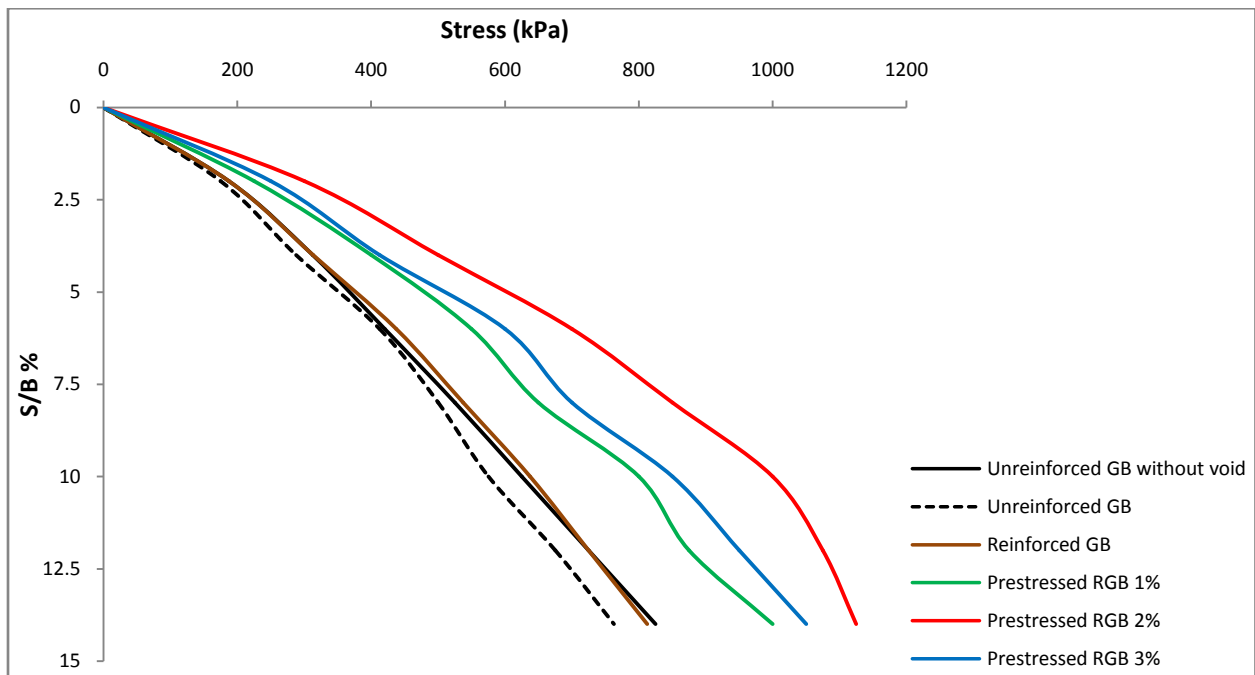


Fig 6.24 Stress vs normalized settlement curves for GB, RGB and PRGB of thickness B with void having $x = 0.2B$, $y = 1.75B$

Figure 6.24 presents the vertical stress vs normalized settlement curves of GB, RGB and PRGB with void at a depth of $1.75B$ and eccentricity $0.2B$. It can be seen from the figure that the presence of void causes only a minor reduction in bearing capacity. It is also observed that

maximum improvement is attained when the prestress is equal to 2% of the tensile strength of the reinforcement.

6.3 GRANULAR BEDS OF THICKNESS $2B$

6.3.1 Void just above the interface between granular bed and weak soil

Figure 6.25 shows a PRGB of thickness $2B$ with a void placed just above the interface between granular bed and weak soil. The void is placed vertically below the centre line of the footing i.e. eccentricity $x = 0$. Figure 6.26 shows the geometric model for the finite element analysis in PLAXIS.

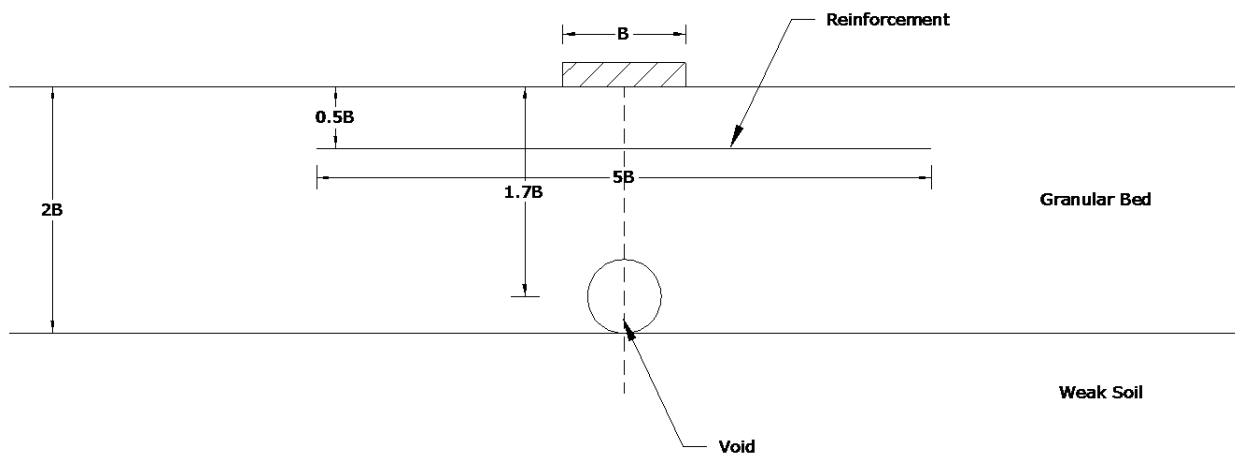


Fig 6.25. Void just above the interface between GB and weak soil, $x = 0$, $y = 1.7B$

Vertical stress vs normalized settlement curves of GB, RGB and PRGB for the above case are presented in Fig 6.27. The curve for unreinforced GB without void also is included so that the reduction in strength due to the presence of void and the improvement due to the addition of reinforcement and prestress could be understood.

From Fig 6.27, it can be seen that the addition of void inside the granular bed at a depth of $1.7B$ and zero eccentricity, drastically reduces the bearing capacity. The reduction in bearing capacity is much less compared to granular bed of thickness B . With the addition of reinforcement and prestress the bearing capacity improved and maximum improvement is seen when the prestress is equal to 3% of the tensile strength of the reinforcement.

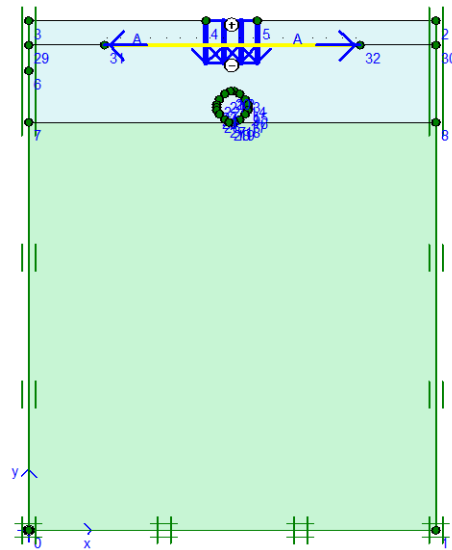


Fig 6.26. Geometric model for PRGB of thickness $2B$ having void with $x = 0, y = 1.7B$

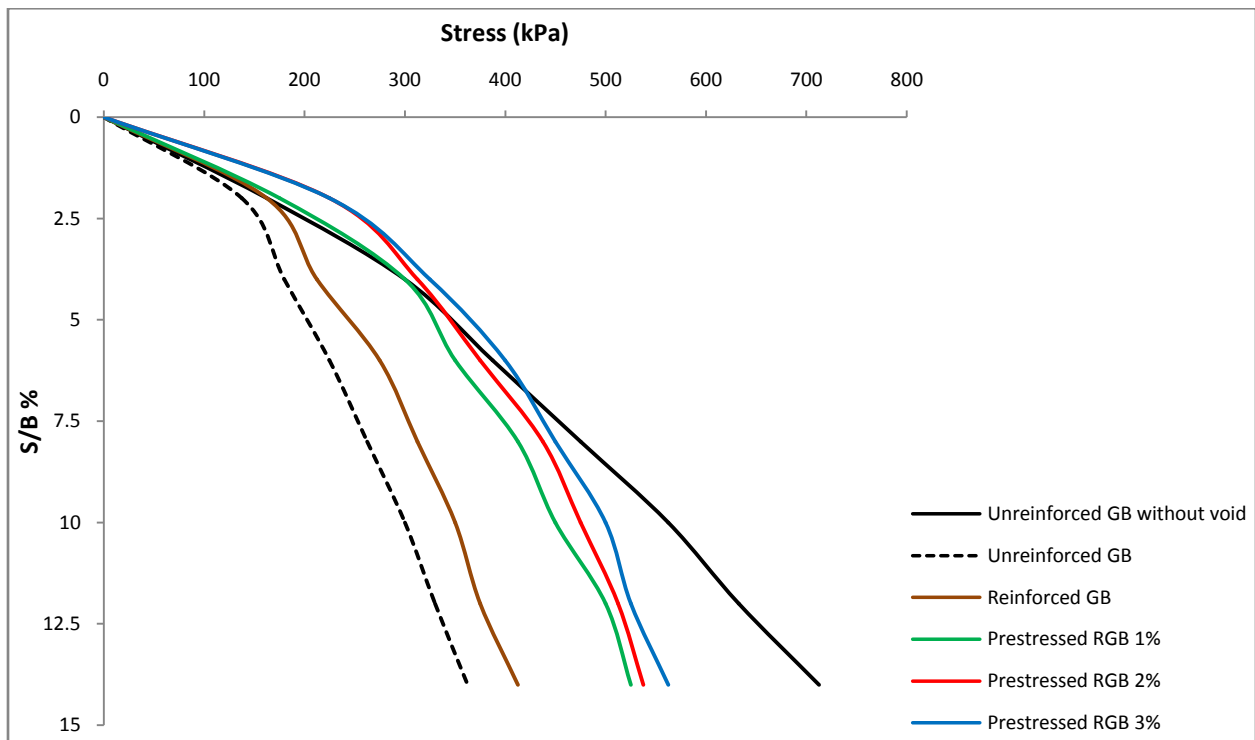


Fig 6.27 Stress vs normalized settlement curves for GB, RGB and PRGB of thickness $2B$ with void having $x=0, y = 1.7 B$

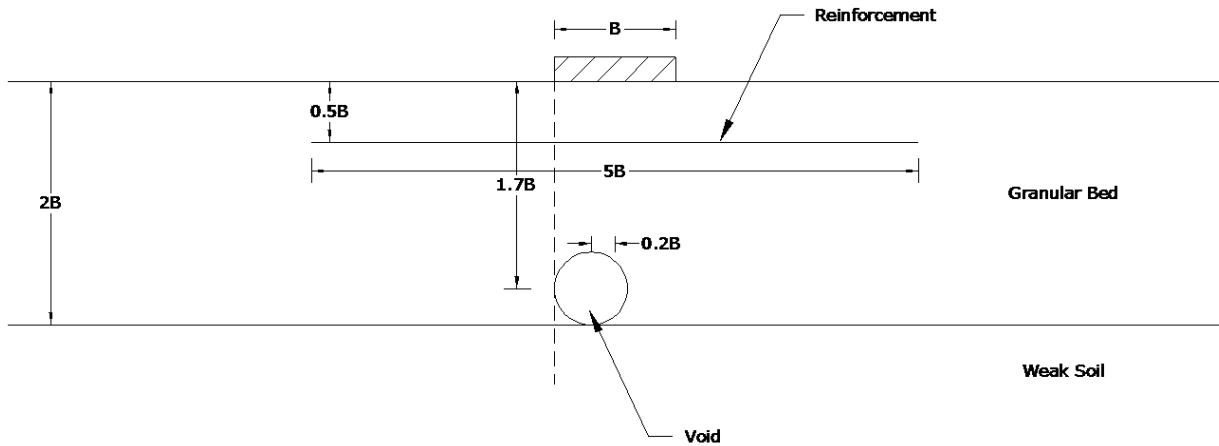


Fig 6.28. Void just above the interface between GB and weak soil, $x = 0.2B$, $y = 1.7B$

Figure 6.28 shows a PRGB of thickness $2B$ with a void placed just above the interface between granular bed and weak soil and at an eccentricity of $0.2B$. The edge of the void is vertically below the edge of the footing. Figure 6.29 shows its geometric model for finite element analysis.

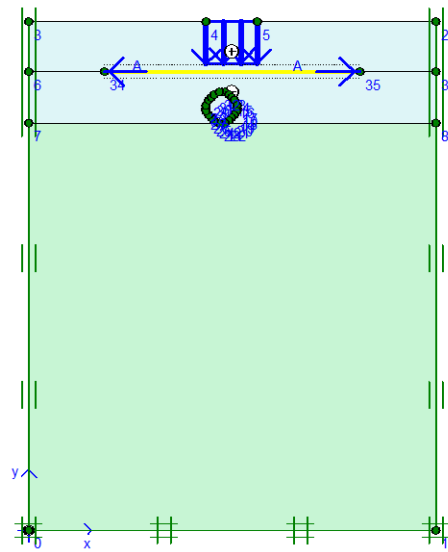


Fig 6.29. Geometric model for PRGB of thickness $2B$ having void with $x = 0.2B$, $y = 1.7B$

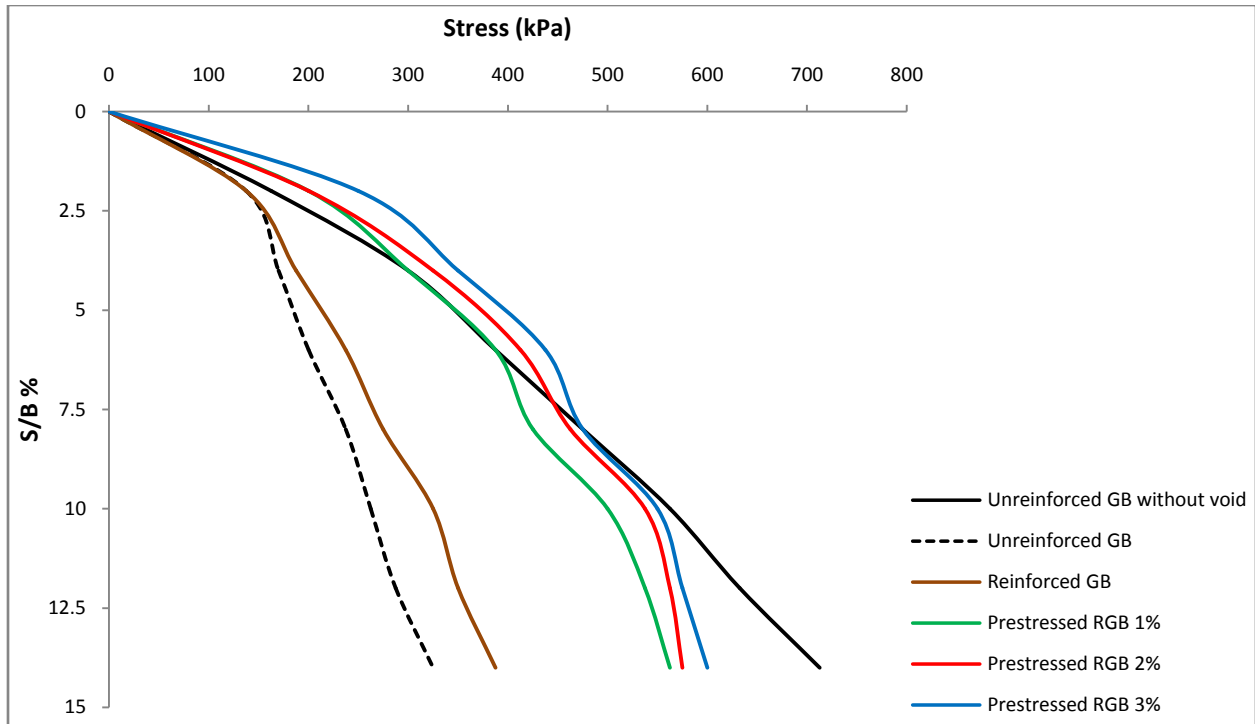


Fig 6.30 Stress vs normalized settlement curves for GB, RGB and PRGB of thickness $2B$ with void having $x=0.2B$, $y=1.7B$

Figure 6.30 presents the vertical stress vs normalized settlement curves of GB, RGB and PRGB of thickness $2B$ with void at a depth of $1.7B$ and eccentricity $0.2B$. It can be seen from the figure that the presence of void causes a reduction in bearing capacity. It is also observed that maximum improvement is attained when the prestress is equal to 3% of the tensile strength of the reinforcement.

6.3.2 Void at the interface between granular bed and weak soil

Figure 6.31 shows a PRGB of thickness $2B$ with a void placed at the interface between granular bed and weak soil. The upper half of the void is in the GB and lower half in weak soil. The void is placed vertically below the centre line of the footing i.e. eccentricity $x=0$. Figure 6.32 shows the geometric model for the finite element analysis in PLAXIS.

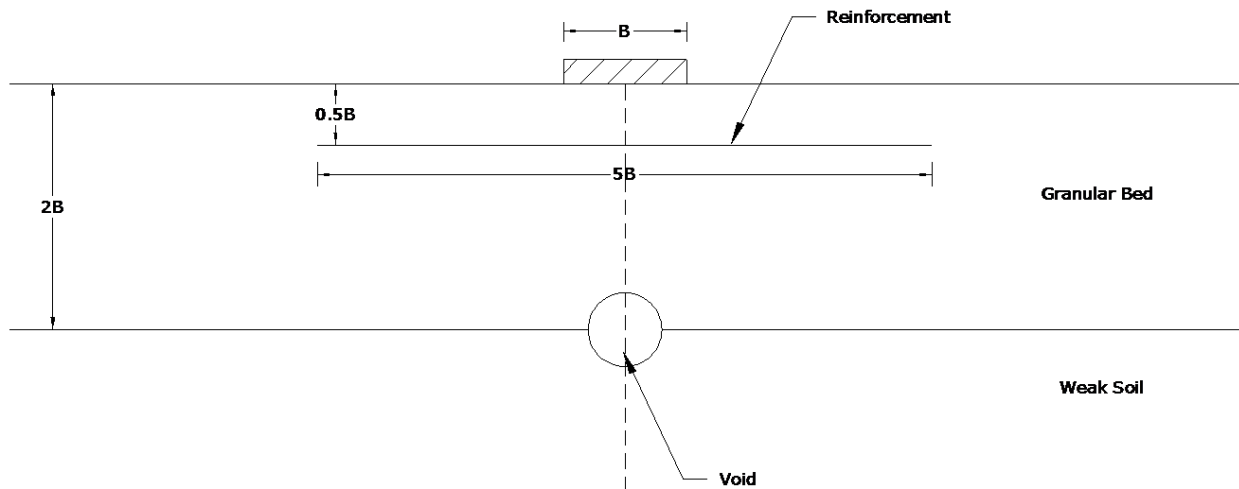


Fig 6.31. Void at the interface between GB and weak soil, $x = 0, y = 2B$

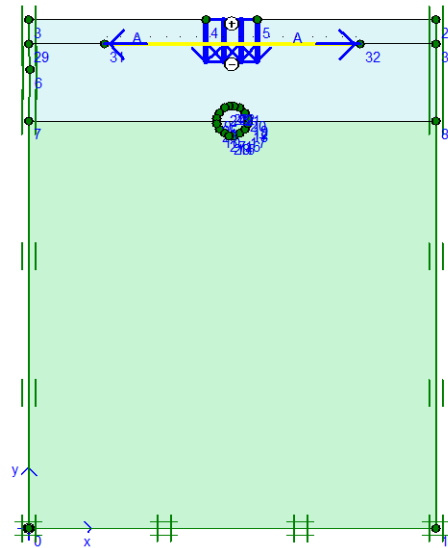


Fig 6.32. Geometric model for PRGB of thickness $2B$ having void with $x = 0, y = 2B$

Vertical stress vs normalized settlement curves of GB, RGB and PRGB of thickness $2B$ with a void placed at the interface between granular bed and weak soil are presented in Fig 6.33. It can be seen that the addition of void inside the granular bed at a depth of $2B$ and zero eccentricity, caused some reduction in bearing capacity. The reduction in bearing capacity is much less compared to granular bed of thickness B . With the addition of reinforcement and prestress the bearing capacity improved and maximum improvement is seen when the prestress is equal to 3% of the tensile strength of the reinforcement.

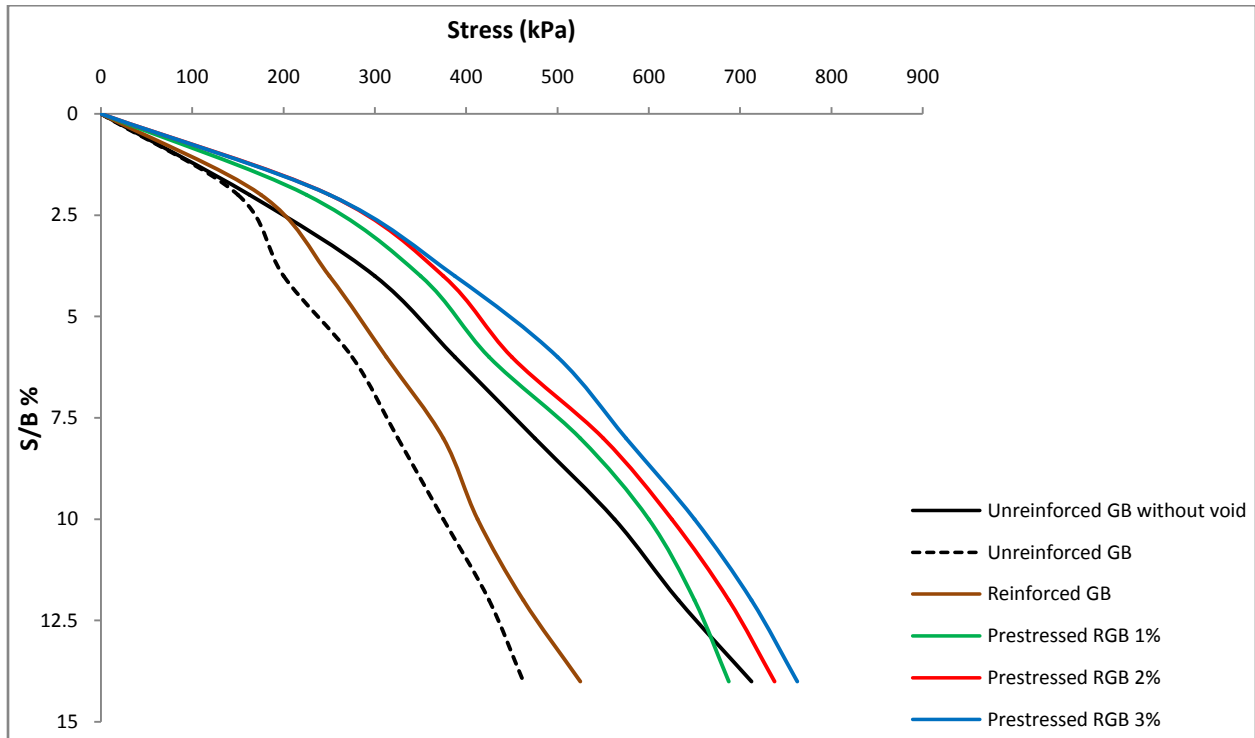


Fig 6.33 Stress vs normalized settlement curves for GB, RGB and PRGB of thickness $2B$ with void having $x=0, y=2B$

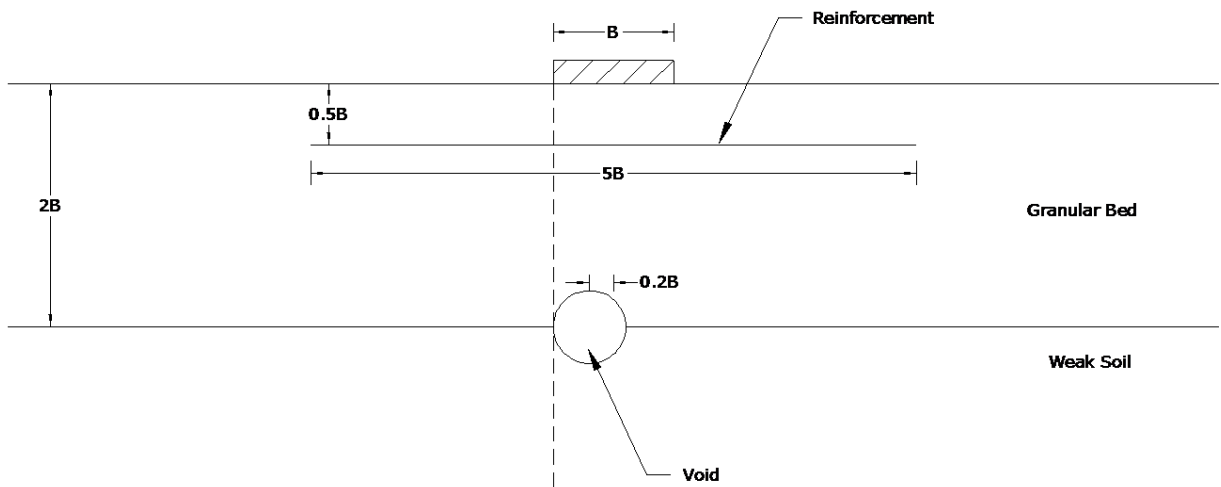


Fig 6.34. Void at the interface between GB and weak soil, $x=0.2B, y=2B$

Figure 6.34 shows a PRGB of thickness $2B$ with a void placed at the interface between granular bed and weak soil and at an eccentricity of $0.2B$. The edge of the void is vertically below the edge of the footing. Figure 6.35 shows its geometric model for finite element analysis.

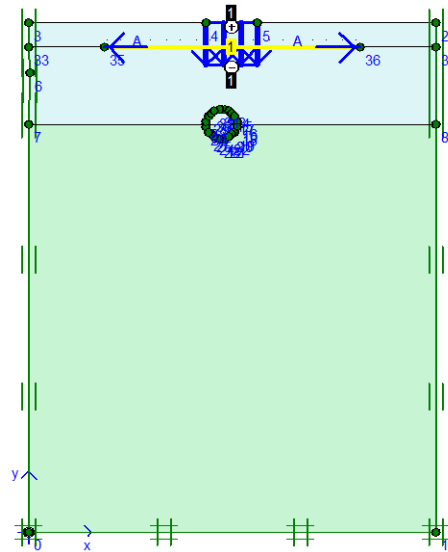


Fig 6.35. Geometric model for PRGB of thickness $2B$ having void with $x = 0.2B$, $y = 2B$

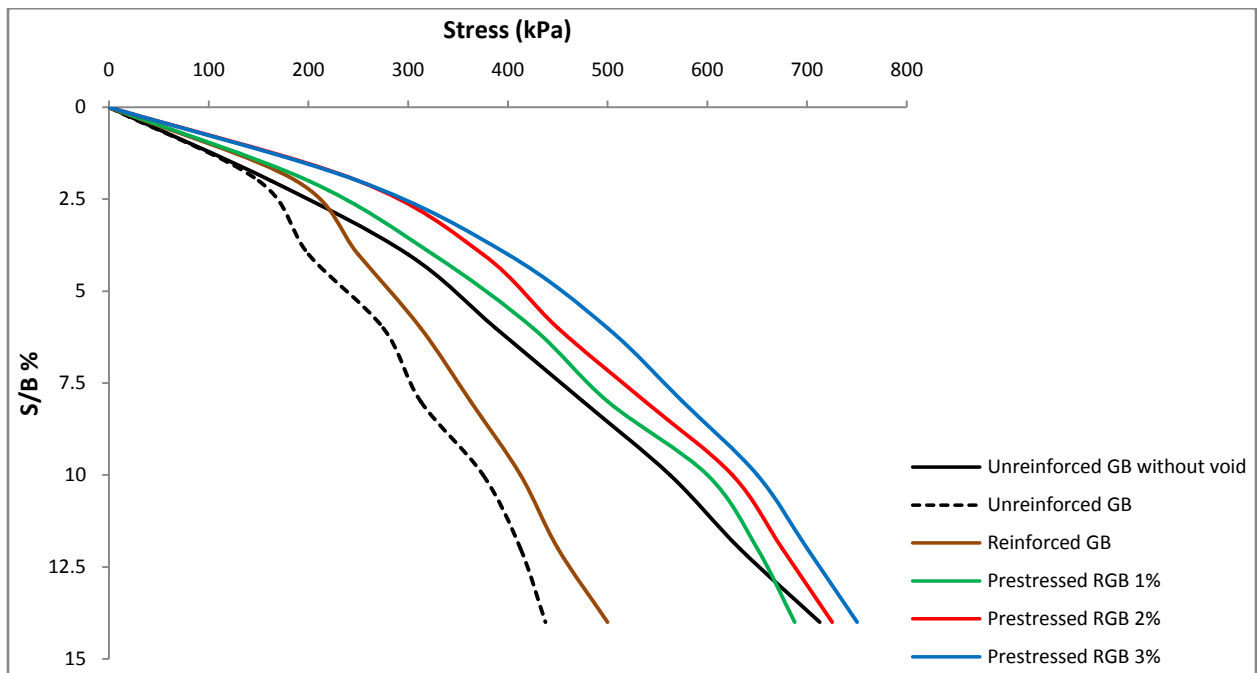


Fig 6.36 Stress vs normalized settlement curves for GB, RGB and PRGB of thickness $2B$ with void having $x=0.2B$, $y=2B$

Figure 6.36 presents the vertical stress vs normalized settlement curves of GB, RGB and PRGB of thickness $2B$ with void at a depth of $2B$ and eccentricity $0.2B$. It can be seen from the figure that the addition of void causes some reduction in bearing capacity. It is also observed that

maximum improvement is attained when the prestress is equal to 3% of the tensile strength of the reinforcement.

6.3.3 Void just below the interface between granular bed and weak soil

Figure 6.37 shows a PRGB of thickness $2B$ with a void placed just below the interface between granular bed and weak soil. The void is placed vertically below the centre line of the footing i.e. eccentricity $x = 0$. Figure 6.38 shows the geometric model for the finite element analysis in PLAXIS.

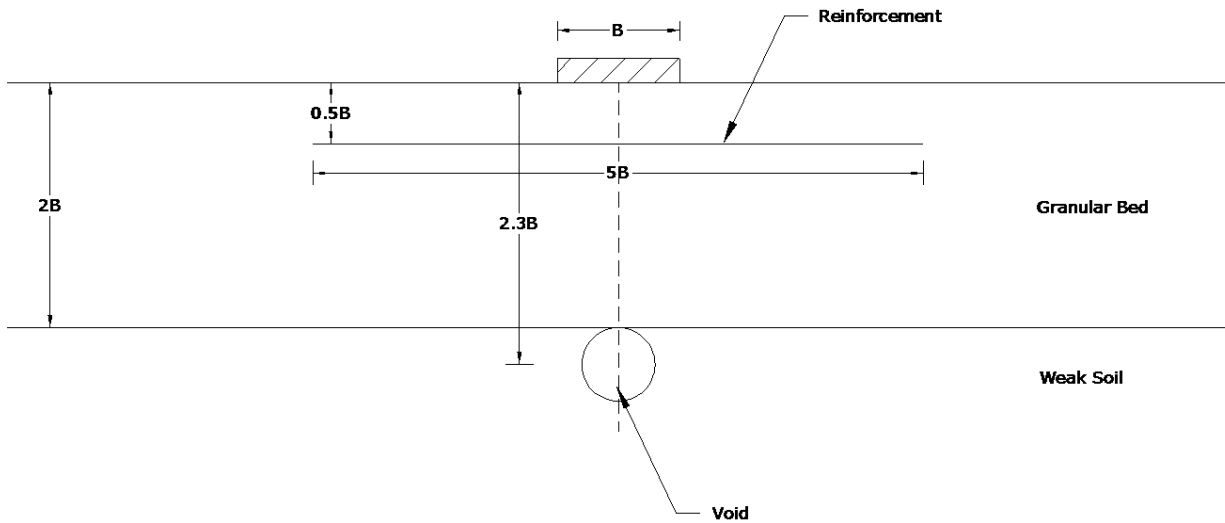


Fig 6.37. Void just below the interface between GB and weak soil, $x = 0$, $y = 2.3B$

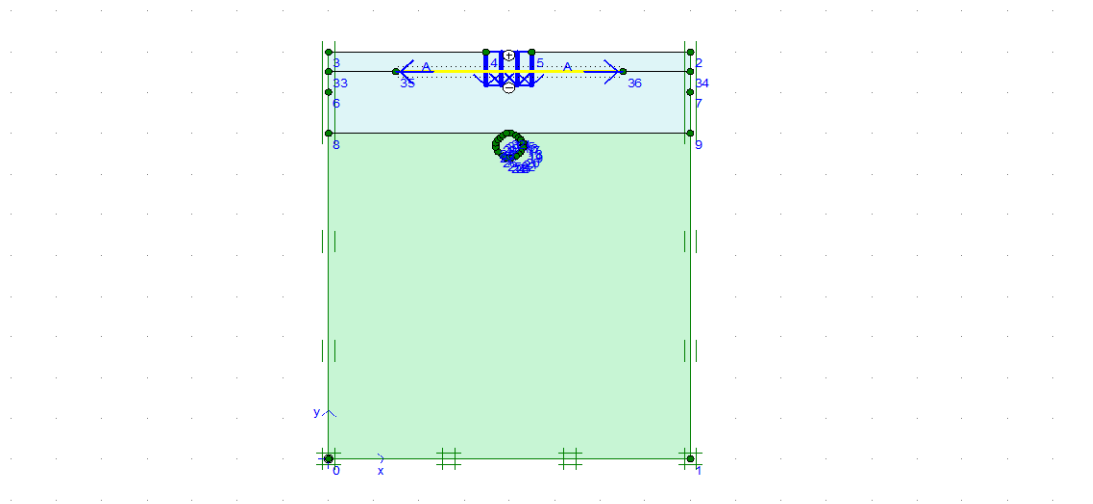


Fig 6.38. Geometric model for PRGB of thickness $2B$ having void with $x = 0$, $y = 2.3B$

Vertical stress vs normalized settlement curves of GB, RGB and PRGB of thickness $2B$ with a void placed just below the interface between granular bed and weak soil are presented in Fig 6.39. It can be seen that the addition of void inside the granular bed at a depth of $2.3B$ and zero eccentricity, caused only a small reduction in bearing capacity. With the addition of reinforcement and prestress the bearing capacity improved and maximum improvement is seen when the prestress is equal to 3% of the tensile strength of the reinforcement.

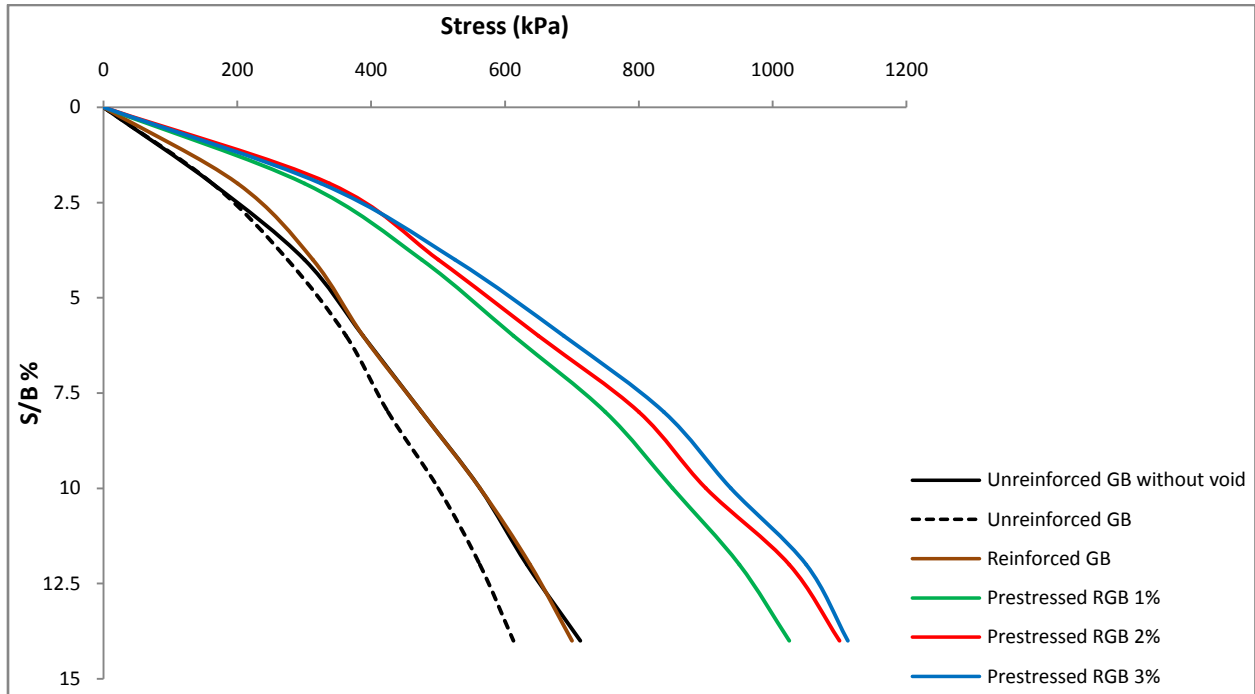


Fig 6.39 Stress vs normalized settlement curves for GB, RGB and PRGB of thickness $2B$ with void having $x=0$, $y=2.3 B$

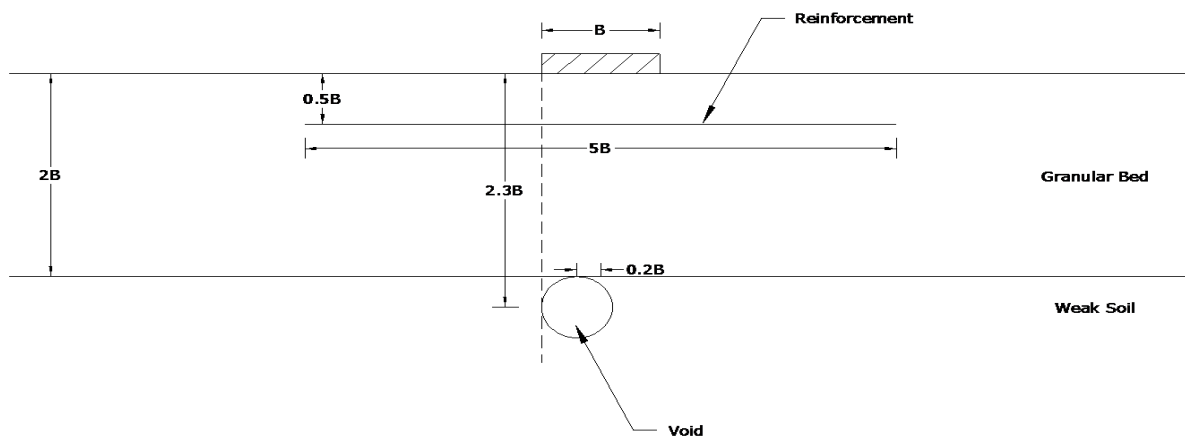


Fig 6.40. Void just below the interface between GB and weak soil, $x = 0.2B$, $y = 2.3B$

Figure 6.40 shows a PRGB of thickness $2B$ with a void placed just below the interface between granular bed and weak soil and at an eccentricity of $0.2B$. The edge of the void is vertically below the edge of the footing. Figure 6.41 shows its geometric model for finite element analysis.

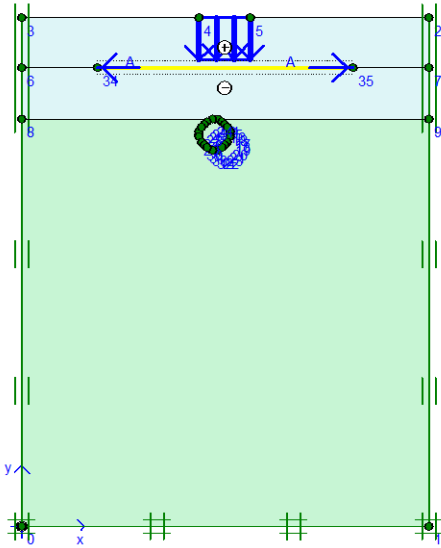


Fig 6.41. Geometric model for PRGB of thickness $2B$ having void with $x = 0.2B$, $y = 2.3B$

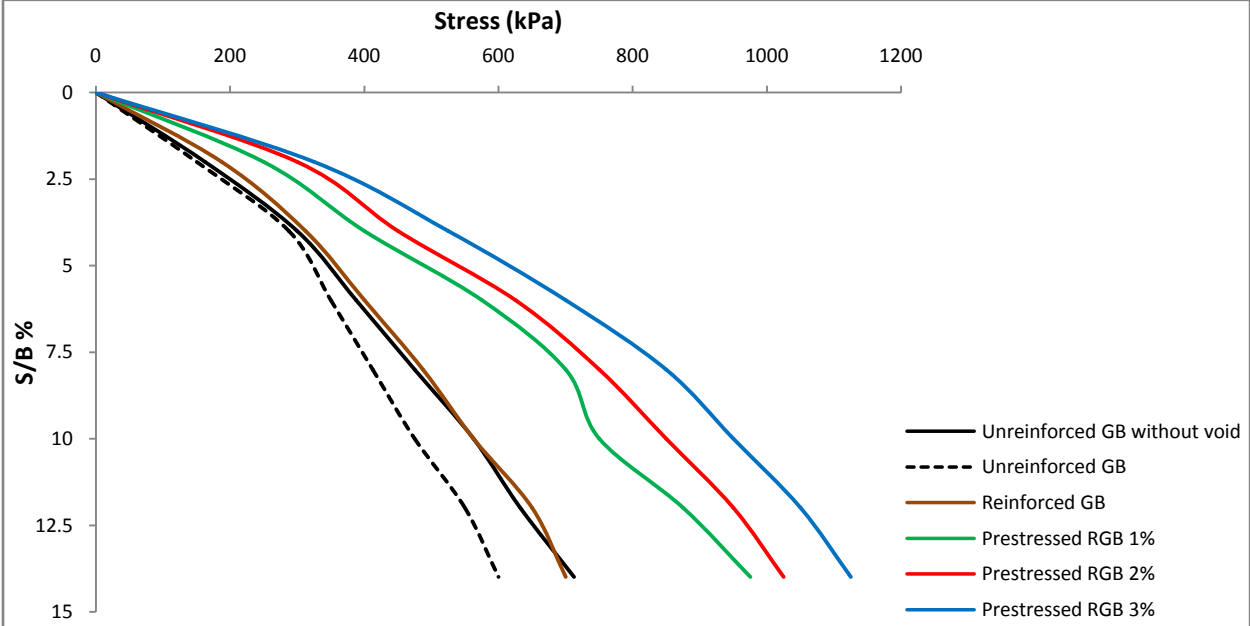


Fig 6.42 Stress vs normalized settlement curves for GB, RGB and PRGB of thickness $2B$ with void having $x = 0.2B$, $y = 2.3 B$

Figure 6.42 presents the vertical stress vs normalized settlement curves of GB, RGB and PRGB of thickness $2B$ with void at a depth of $2.3B$ and eccentricity $0.2B$. It can be seen from the figure that the addition of void causes only a small reduction in bearing capacity. It is also observed that maximum improvement is attained when the prestress is equal to 3% of the tensile strength of the reinforcement.

6.3.4 Void at a depth of $0.75B$ below the interface between granular bed and weak soil

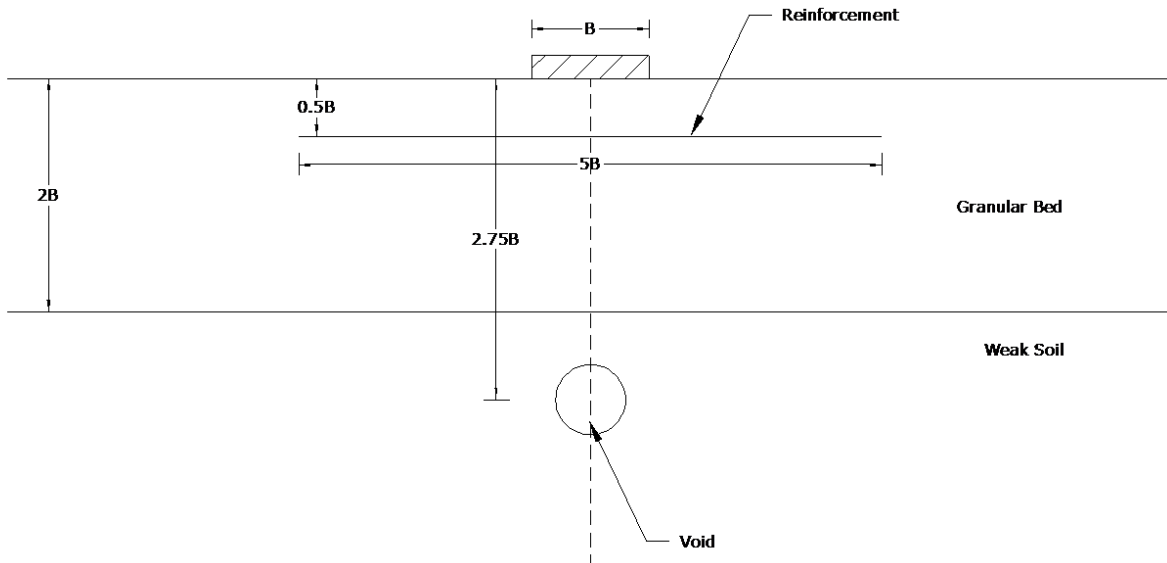


Fig 6.43. Void at a depth of $0.75B$ below the interface between GB and weak soil, $x = 0$, $y = 2.75B$

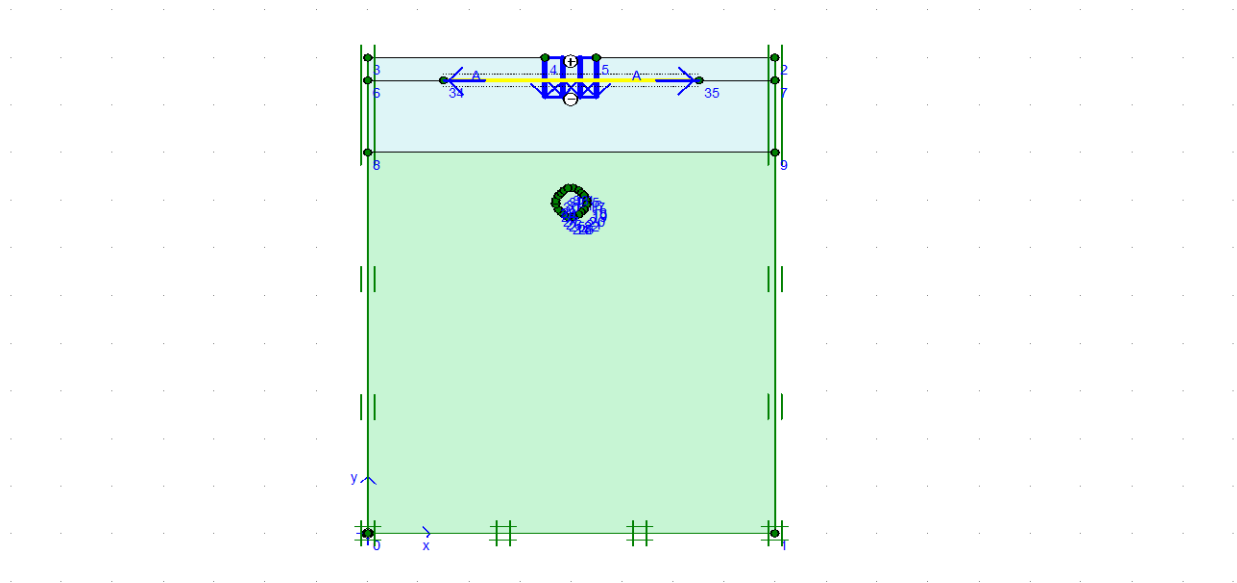


Fig 6.44. Geometric model for PRGB of thickness $2B$ having void with $x = 0$, $y = 2.75B$

Figure 6.43 shows a PRGB of thickness $2B$ with a void placed at a depth of $0.75B$ below the interface between granular bed and weak soil. The void is placed vertically below the centre line of the footing ie eccentricity $x = 0$. Figure 6.44 shows the geometric model for the finite element analysis in PLAXIS.

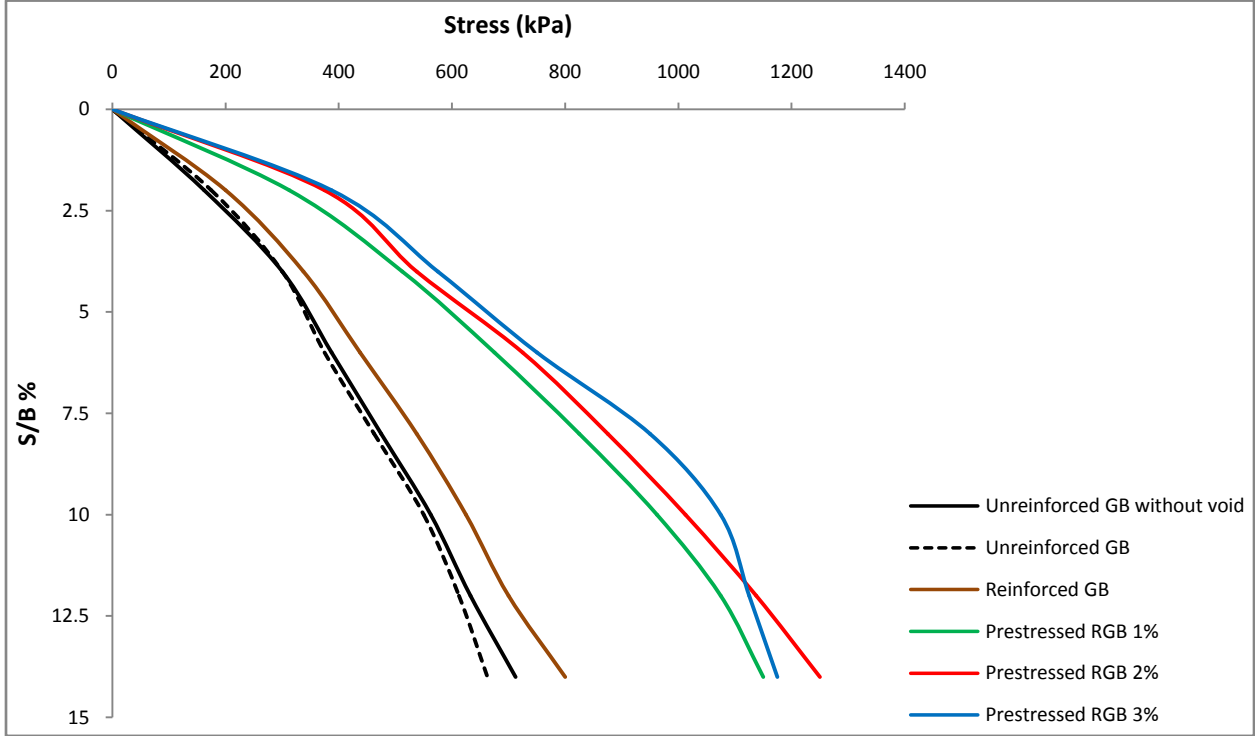


Fig 6.45 Stress vs normalized settlement curves for GB, RGB and PRGB of thickness $2B$ with void having $x=0, y=2.75 B$

Vertical stress vs normalized settlement curves of GB, RGB and PRGB of thickness $2B$ with a void placed at a depth of $0.75B$ below the interface between granular bed and weak soil are presented in Fig 6.45. It can be seen that the addition of void inside the granular bed at a depth of $2.75B$ and zero eccentricity, did not cause any appreciable in bearing capacity. With the addition of reinforcement and prestress the bearing capacity improved and maximum improvement is seen when the prestress is equal to 3% of the tensile strength of the reinforcement.

Figure 6.46 shows a PRGB of thickness $2B$ with a void placed at a depth of $0.75B$ below the interface between granular bed and weak soil and at an eccentricity of $0.2B$. The edge of the void is vertically below the edge of the footing. Figure 6.47 shows the geometric model for the finite element analysis in PLAXIS.

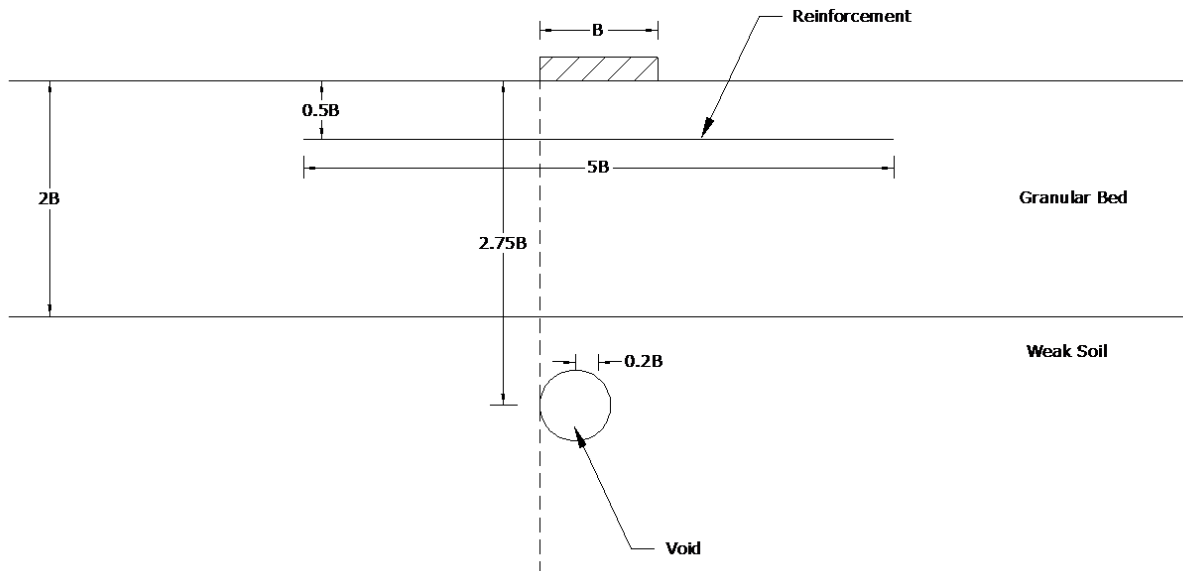


Fig 6.46. Void at a depth of $0.75B$ below the interface between GB and weak soil, $x = 0.2B$, $y = 2.75B$

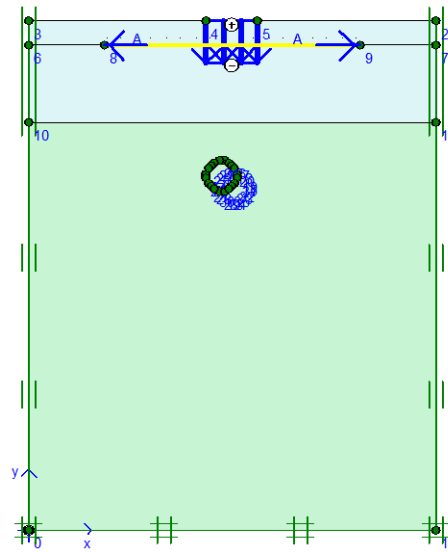


Fig 6.47. Geometric model for PRGB of thickness $2B$ having void with $x = 0.2B$, $y = 2.75B$

Figure 6.48 presents the vertical stress vs normalized settlement curves of GB, RGB and PRGB of thickness $2B$ with void at a depth of $2.75B$ and eccentricity $0.2B$. It can be seen from the figure that the addition of void did not cause any appreciable reduction in bearing capacity. It is also observed that maximum improvement is attained when the prestress is equal to 3% of the tensile strength of the reinforcement.

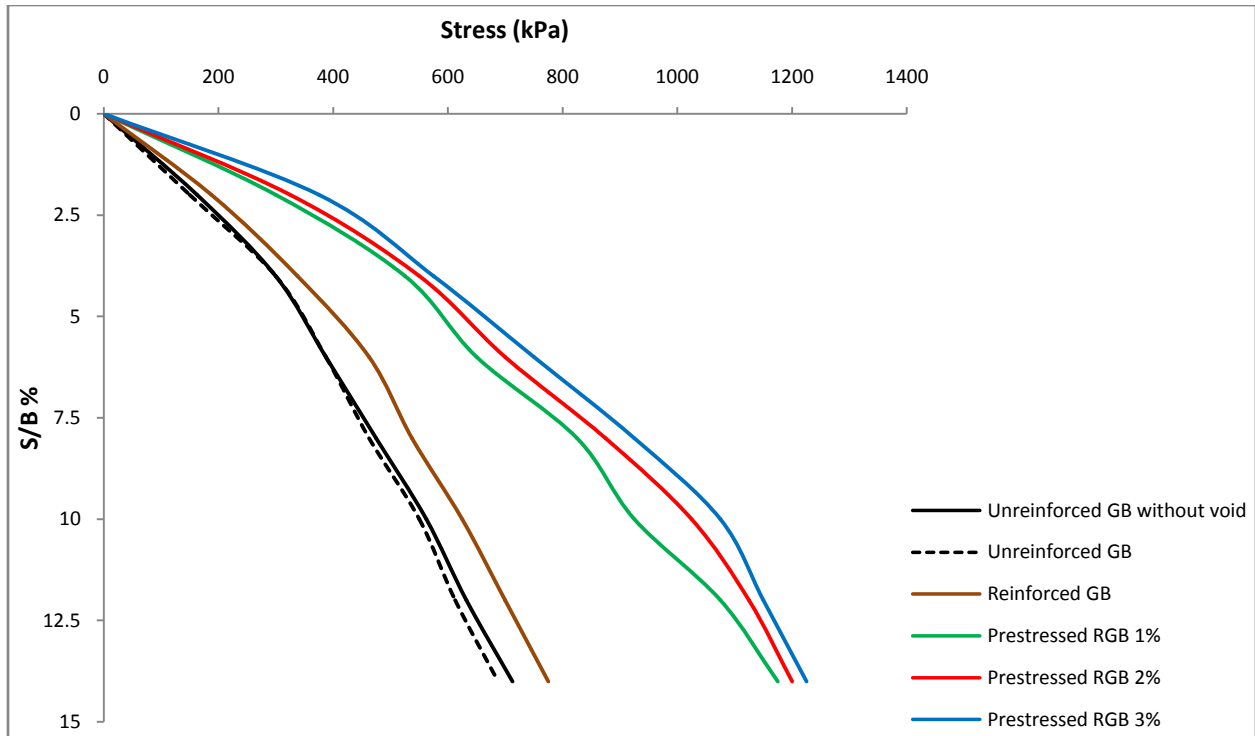


Fig 6.48 Stress vs normalized settlement curves for GB, RGB and PRGB of thickness 2B with void having $x=0.2B$, $y=2.75 B$

6.4 REDUCTION FACTOR

The effect of a single void on bearing capacity is evaluated by the parameter Reduction factor. It is defined as

$$R = (1 - F) \quad \text{----- (6.1)}$$

$$F = q'/q \quad \text{----- (6.2)}$$

Where

R = Reduction factor

F = Reduced Bearing Capacity Factor

q' = Bearing capacity with void at 5 % settlement

q = Bearing capacity without void at 5 % settlement

6.4.1 Variation of Reduction factor with prestress

The variation of reduction factor with prestress for PRGB of thickness B is presented in Fig. 6.49. It can be seen from the figure that in general the reduction factor increases when the

prestress is increased from 1% to 2%. The reduction factor decreases slightly when the prestress is increased from 2% to 3%. As the prestress increases there will be a reduction in the normal stress at the interface between reinforcement and granular soil. This causes a reduction in bearing capacity. When the prestress is further increased, the bearing capacity increases due to higher tensile stresses mobilized in the reinforcement.

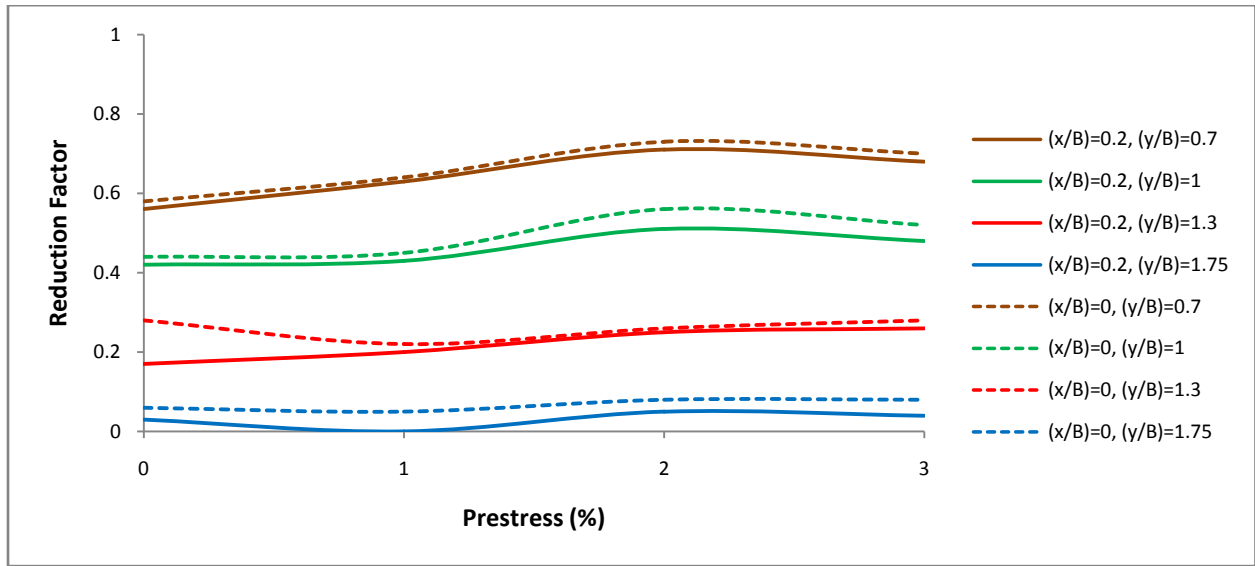


Fig 6.49 Reduction factor vs prestress curves for GB, RGB and PRGB of thickness B with various positions of void

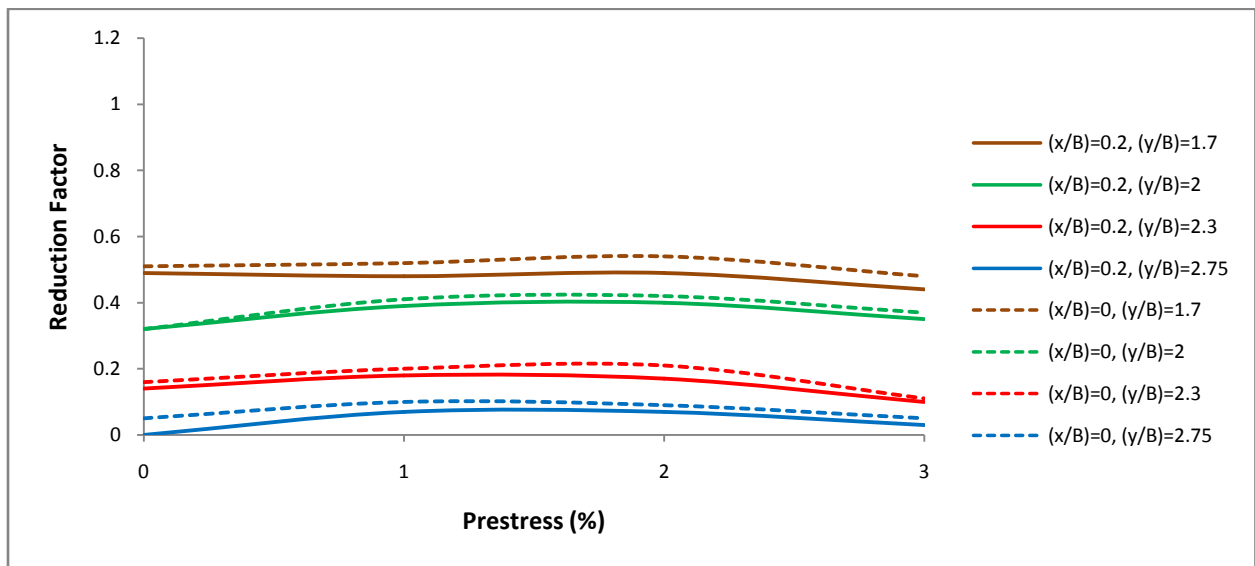


Fig 6.50 Reduction factor vs prestress curves for GB, RGB and PRGB of thickness 2B with various positions of void

The results of studies on PRGB of thickness 2B are presented in Fig. 6.50. The values of reduction factor are comparatively lower when the thickness is 2B. The value of R in general increases when the prestress is increased from 1% to 2%. The reduction factor decreases when the prestress is increased from 2% to 3%.

6.4.2 Variation of Reduction factor with depth of void

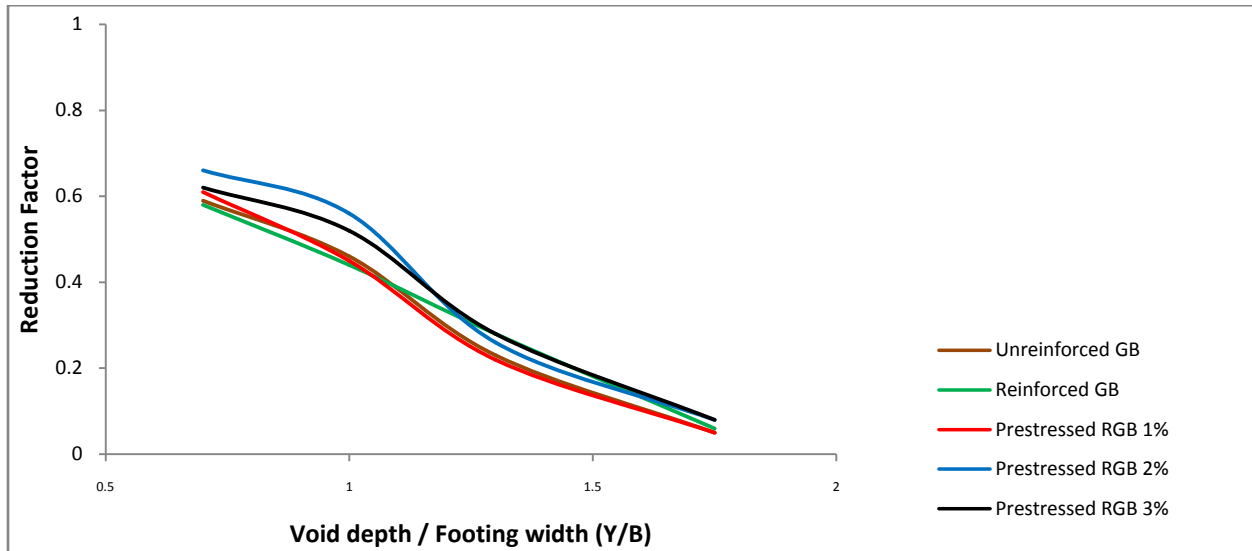


Fig 6.51 Reduction factor vs depth of void curves for GB, RGB and PRGB of thickness B with $x = 0$

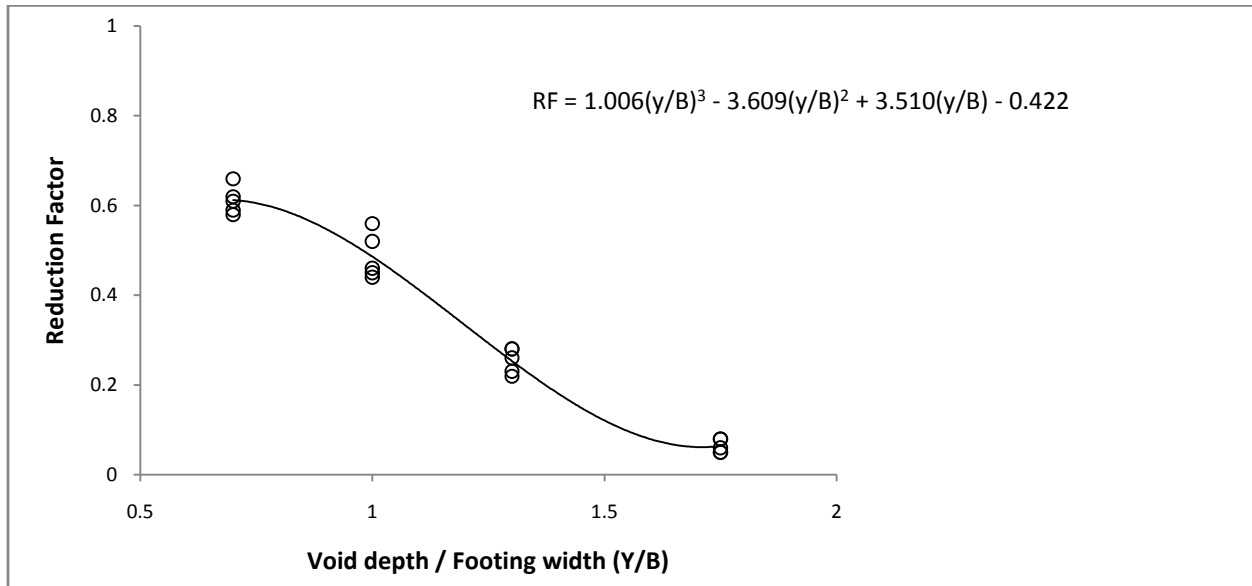


Fig 6.52 Relationship between Reduction factor and depth of void for GB, RGB and PRGB of thickness B with $x = 0$

Figure 6.51 presents the variation of Reduction factor with depth of void for PRGB of thickness B with void having zero eccentricity. It can be seen from the figure that as the depth of void increases, the value of reduction factor decreases. The reduction factor becomes small when (y/B) exceeds 1.75. A best fit curve is developed for the above data and its equation is given in Fig.6.52. It is seen that the reduction factor varies with the cube of (y/B).

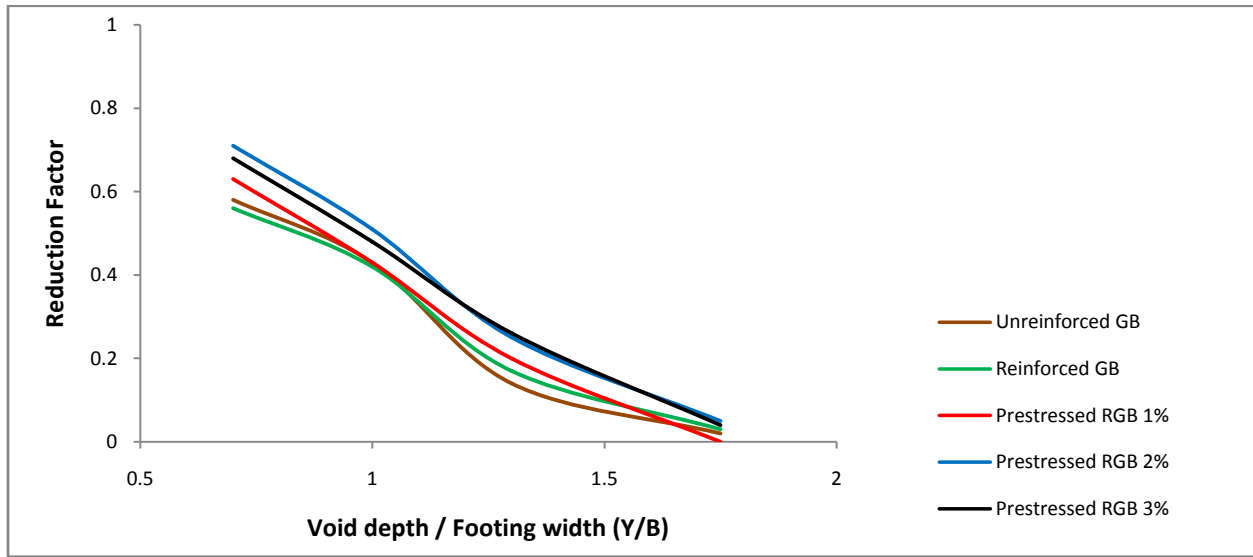


Fig 6.53 Reduction factor vs depth of void curves for GB, RGB and PRGB of thickness B with $x = 0.2B$

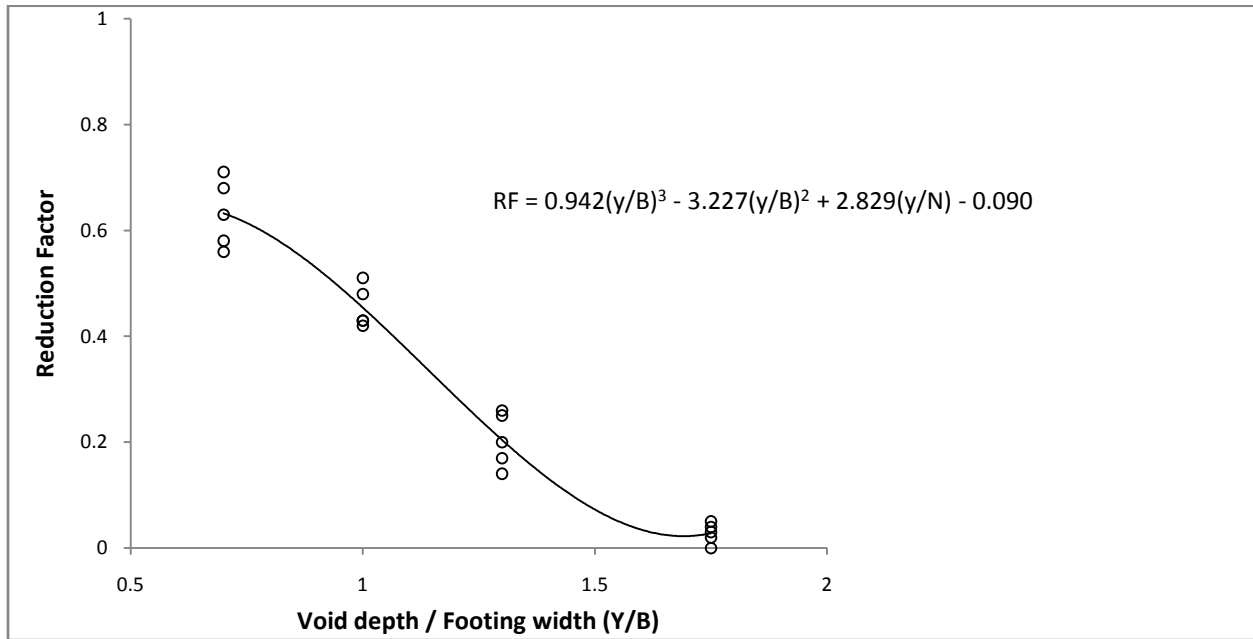


Fig 6.54 Relationship between Reduction factor and depth of void for GB, RGB and PRGB of thickness B with $x = 0.2B$

The variation of Reduction factor with depth of void for PRGB of thickness B with void at an eccentricity of 0.2B is presented in Fig.6.53. Similar to the previous case, the reduction factor becomes small and negligible when (y/B) exceeds 1.75. The best fit curve developed for this case and its equation is given in Fig.6.54. It is seen that, similar to the case without eccentricity, the reduction factor varies with the cube of (y/B).

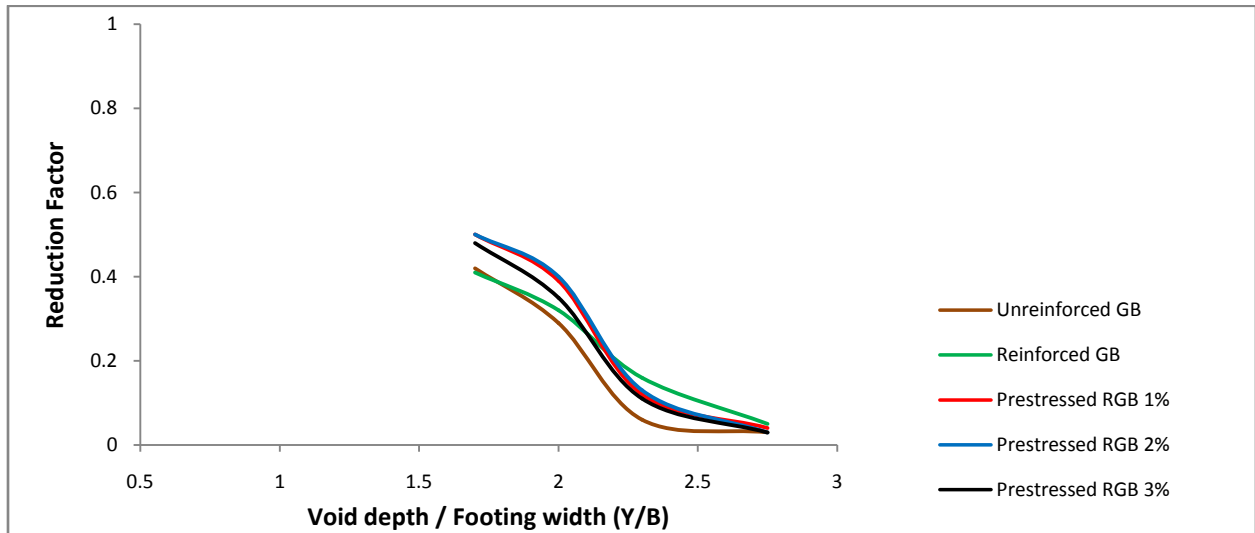


Fig 6.55 Reduction factor vs depth of void curves for GB, RGB and PRGB of thickness 2B with x = 0

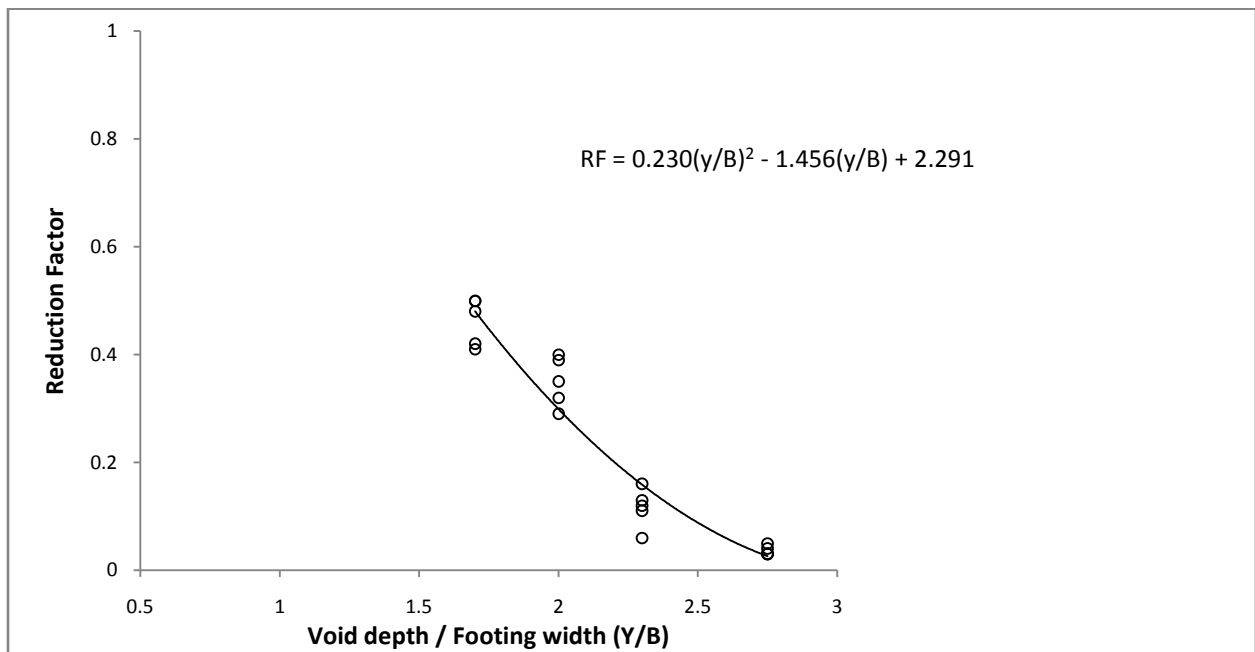


Fig 6.56 Relationship between Reduction factor and depth of void for GB, RGB and PRGB of thickness 2B with x = 0

Figure 6.55 presents the variation of Reduction factor with depth of void for PRGB of thickness 2B with void having zero eccentricity. It can be seen from the figure that as the depth of void increases, the value of reduction factor decreases. The reduction factor becomes small when (y/B) exceeds 2.5. The best fit curve developed for this case and its equation is given in Fig.6.56. It is seen that the reduction factor varies with the square of (y/B) when the thickness of GB is 2B.

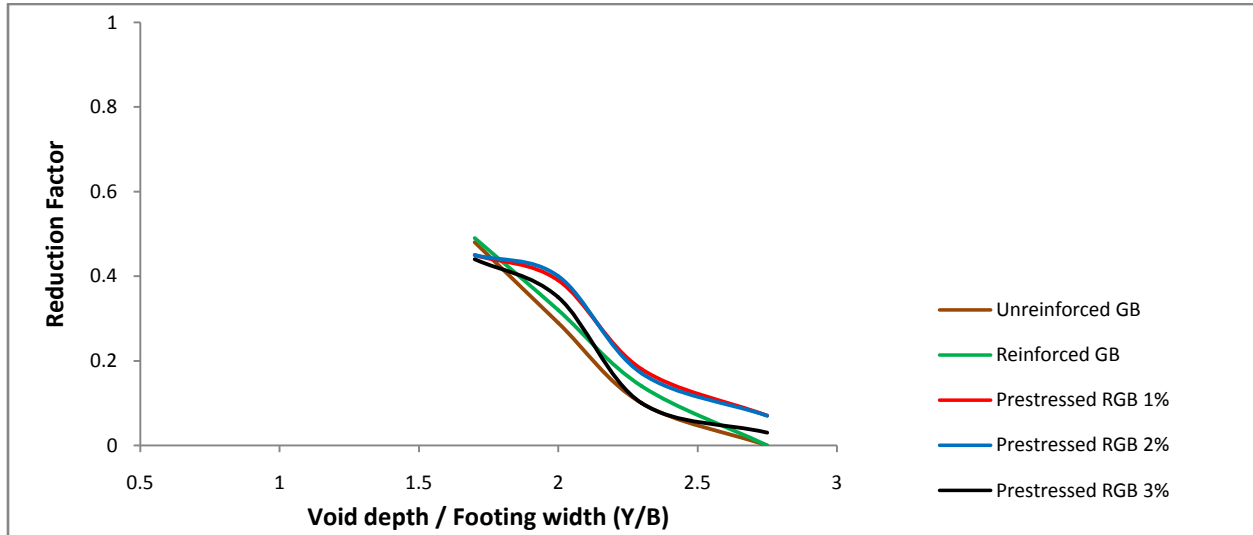


Fig 6.57 Reduction factor vs depth of void curves for GB, RGB and PRGB of thickness 2B with $x = 0.2B$

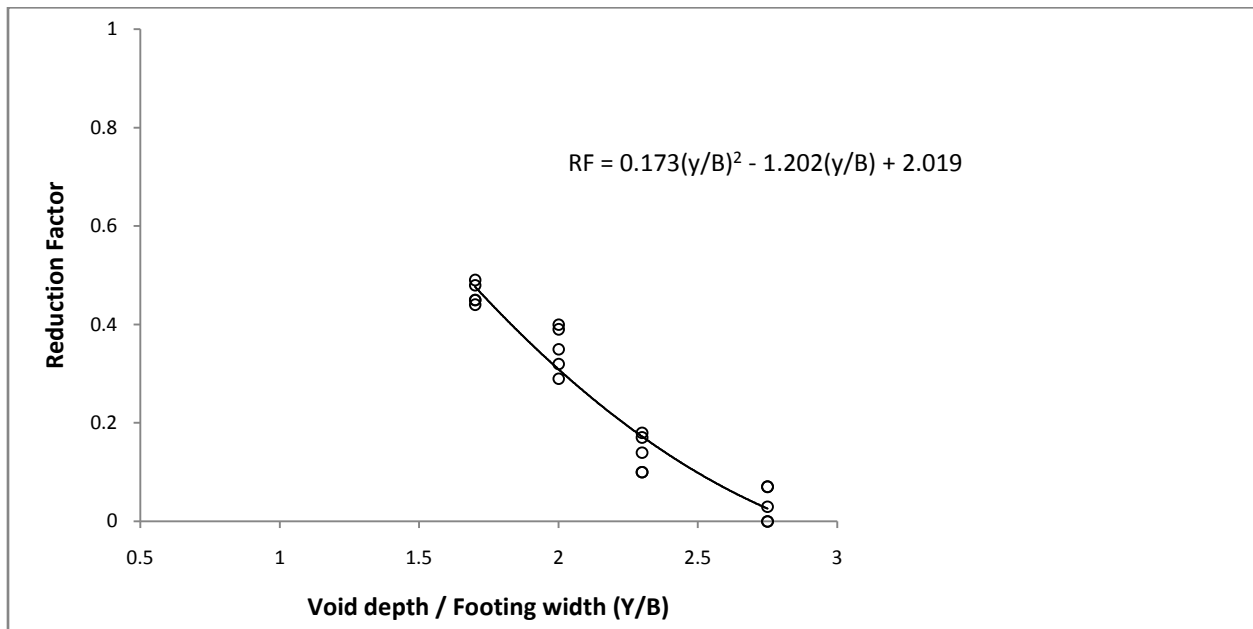


Fig 6.58 Relationship between Reduction factor and depth of void for GB, RGB and PRGB of thickness 2B with $x = 0.2B$

The variation of Reduction factor with depth of void for PRGB of thickness $2B$ with void at an eccentricity of $0.2B$ is presented in Fig.6.57. It is seen from the figure that the reduction factor becomes small / negligible when (y/B) exceeds 2.75 . The best fit curve developed for this case and its equation is given in Fig.6.58. It is seen that, similar to the previous case, the reduction factor varies with the square of (y/B) .

6.4.3 Variation of Reduction factor with eccentricity of void

To study the effect of eccentricity of void, finite element analyses are carried out with two horizontal positions of void. The horizontal distance between the centre of the footing and centre of void is defined by the parameter 'x'. The effects of void at various depths with the following eccentricities are studied.

1. Centre of the void vertically below the central axis of the footing, $(x/B)=0$
2. Edge of the void vertically below the edge of footing, $(x/B) = 0.2$

6.4.3.1 Granular Beds of Thickness B

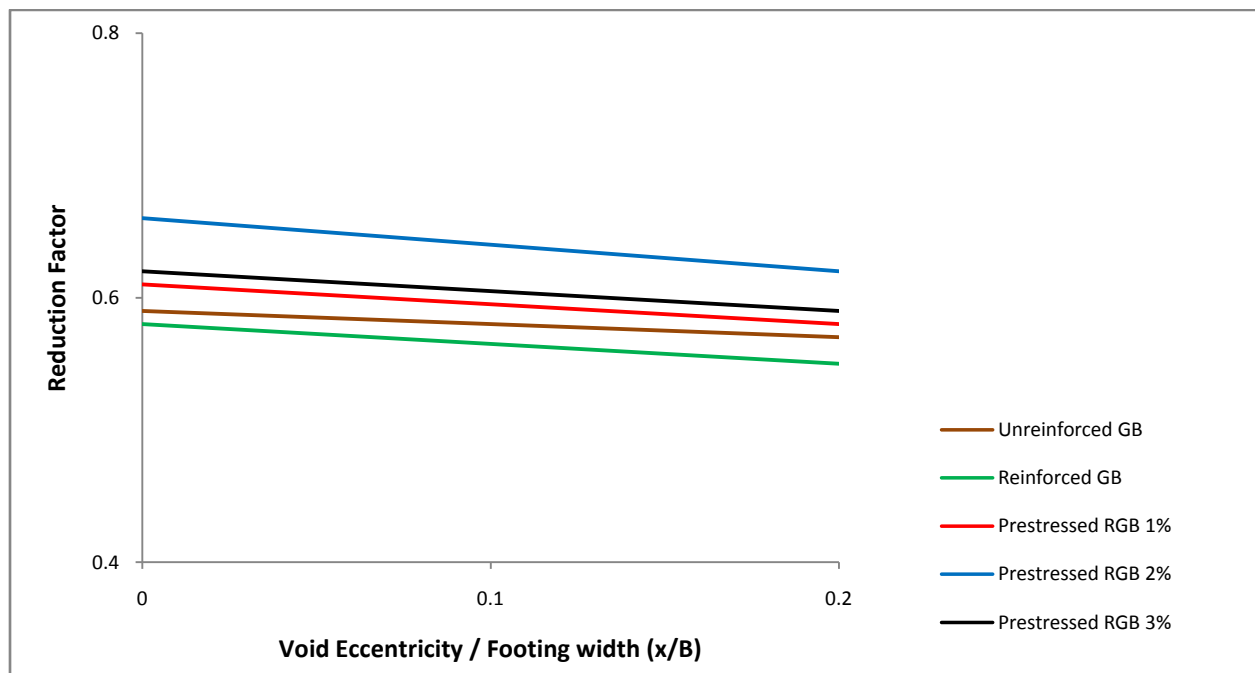


Fig 6.59 Reduction factor vs eccentricity of void curves for GB, RGB and PRGB of thickness B with $y=0.7B$

Figure 6.59 shows the comparison between the reduction factors when the void is placed vertically below the centre of footing ($x=0$) and when placed below the edge of the footing

($x=0.2B$). The thickness of granular bed is B and the void is placed just above the interface between GB and Weak soil ($y/B = 0.7$). It is seen from the figure that the reduction factor is slightly lesser when the void is placed below the edge of the footing.

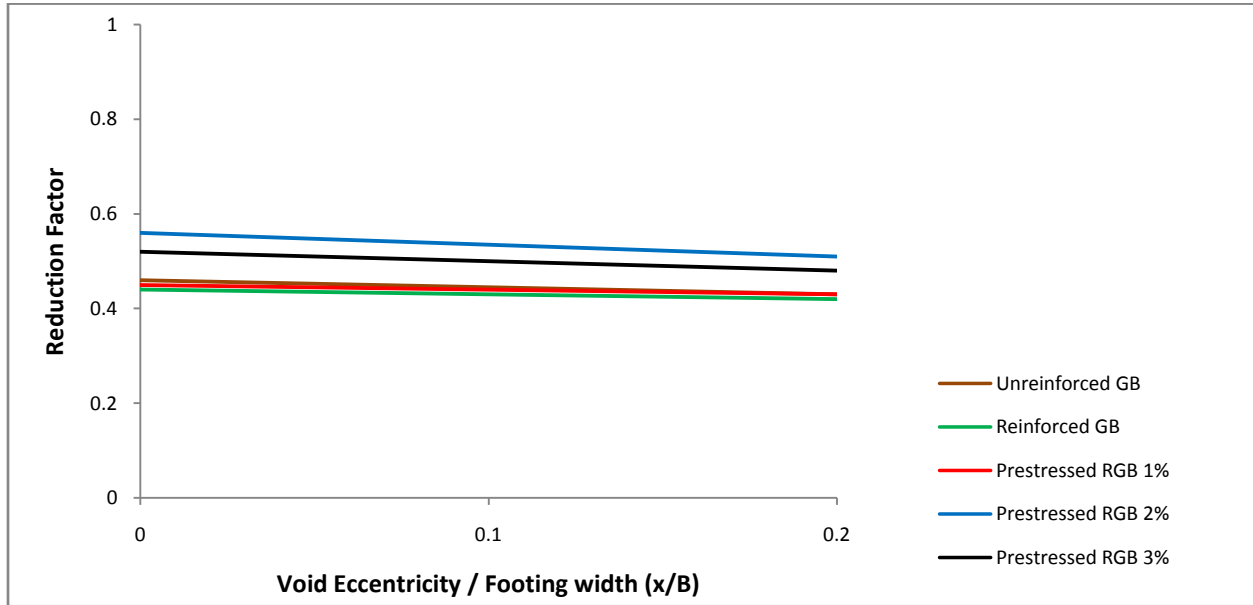


Fig 6.60 Reduction factor vs eccentricity of void curves for GB, RGB and PRGB of thickness B with $y=B$

Figure 6.60 shows the variation of Reduction factor with eccentricity when the void is placed at the interface between GB and weak soil ($y/B = 1$). Upper half of the void is inside the granular bed and the lower half is inside the weak soil. It is seen from the figure that the reduction factor is less when the void is below the edge of the footing.

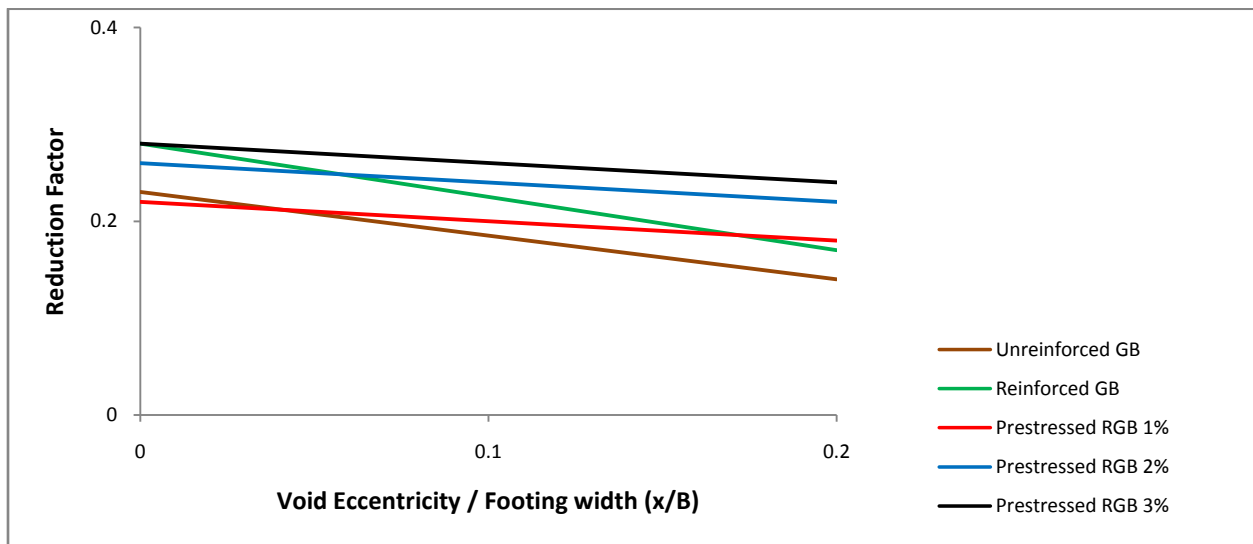


Fig 6.61 Reduction factor vs eccentricity of void curves for GB, RGB and PRGB of thickness B with $y=1.3B$

The variation of reduction factor with eccentricity for void placed just below the interface between GB and weak soil ($y/B = 1.3$) is presented in Fig.6.61. It can be seen from the figure that the value of reduction factor decreases with eccentricity.

Figure 6.62 shows the variation of Reduction factor with eccentricity when the void is placed at a depth of $0.75B$ below the interface between GB and weak soil ($y/B = 1.75$). It is seen from the figure that, similar to the previous cases, the reduction factor decreases with eccentricity of the void.

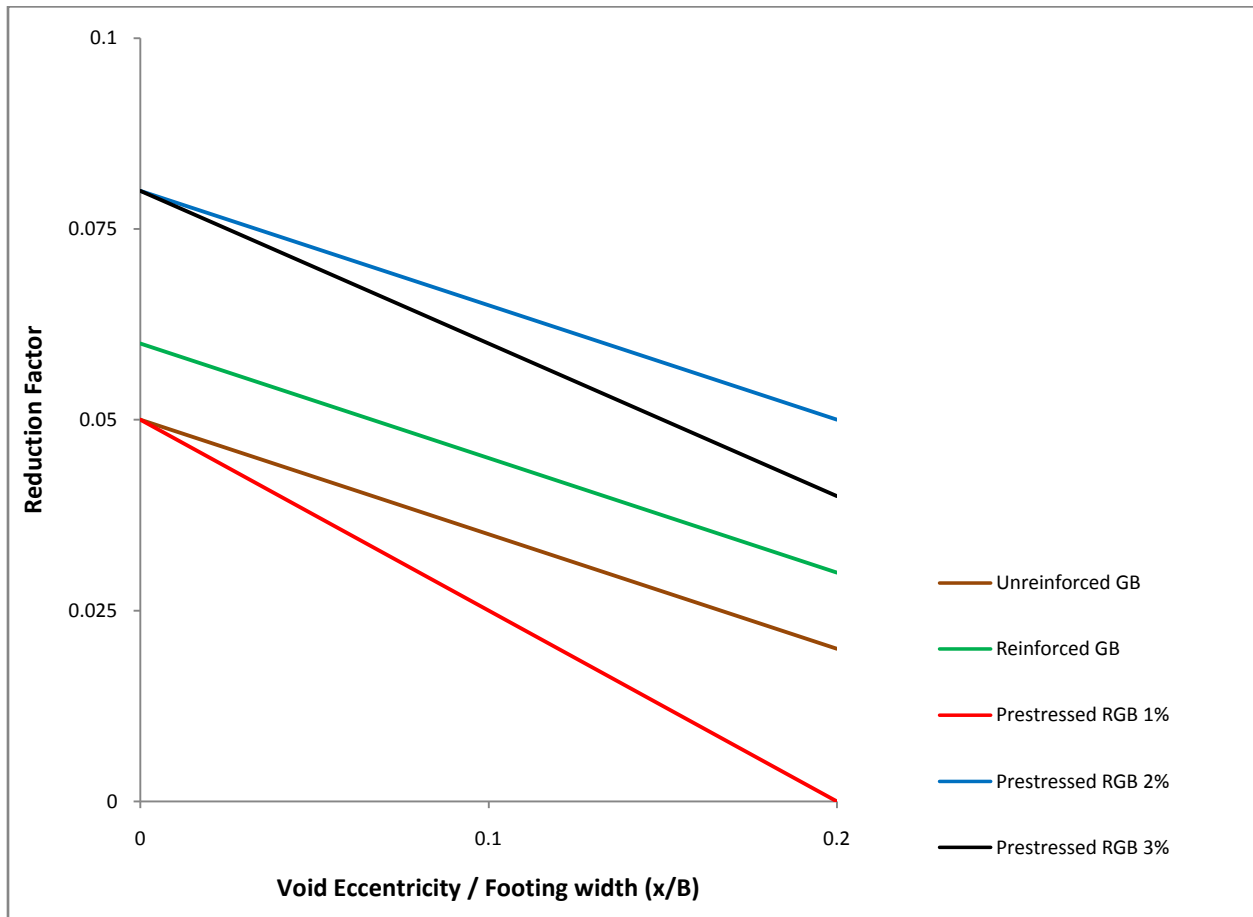


Fig 6.62 Reduction factor vs eccentricity of void curves for GB, RGB and PRGB of thickness B with $y=1.75B$

6.4.3.2 Granular Beds of Thickness $2B$

Figure 6.63 shows the comparison between the reduction factors when the void is placed vertically below the centre of footing ($x=0$) and when placed below the edge of the footing ($x=0.2B$). The thickness of granular bed is $2B$ and the void is placed just above the interface

between GB and Weak soil ($y/B = 1.7$). It is seen from the figure that the reduction factor is slightly lesser when the void is placed below the edge of the footing.

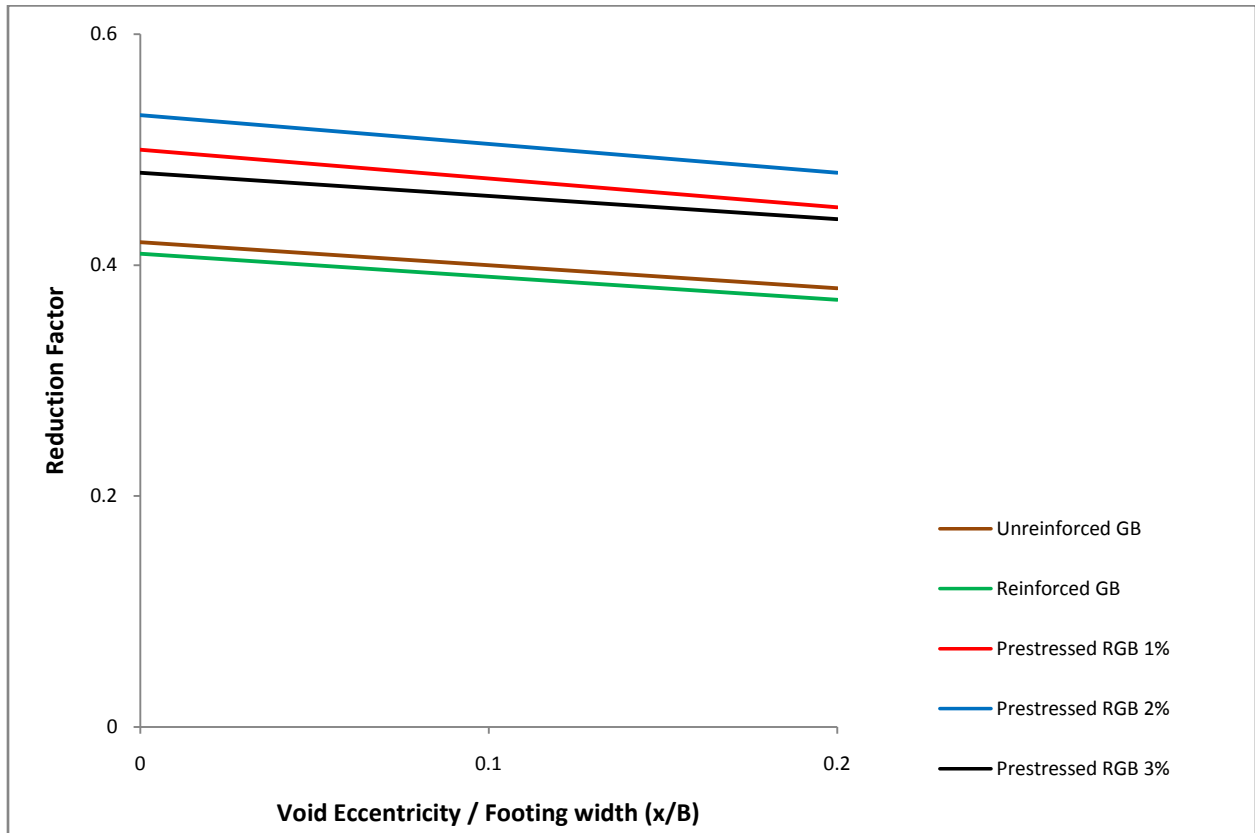


Fig 6.63 Reduction factor vs eccentricity of void curves for GB, RGB and PRGB of thickness $2B$ with $y=1.7B$

Figure 6.64 shows the variation of Reduction factor with eccentricity when the void is placed at the interface between GB and weak soil ($y/B = 2$). Upper half of the void is inside the granular bed and the lower half is inside the weak soil. It is seen from the figure that the reduction factor decreases with the eccentricity of footing.

The variation of reduction factor with eccentricity for void placed just below the interface between GB and weak soil ($y/B = 2.3$) is presented in Fig.6.65. It is seen from the figure that the reduction factor is less when the void is below the edge of the footing.

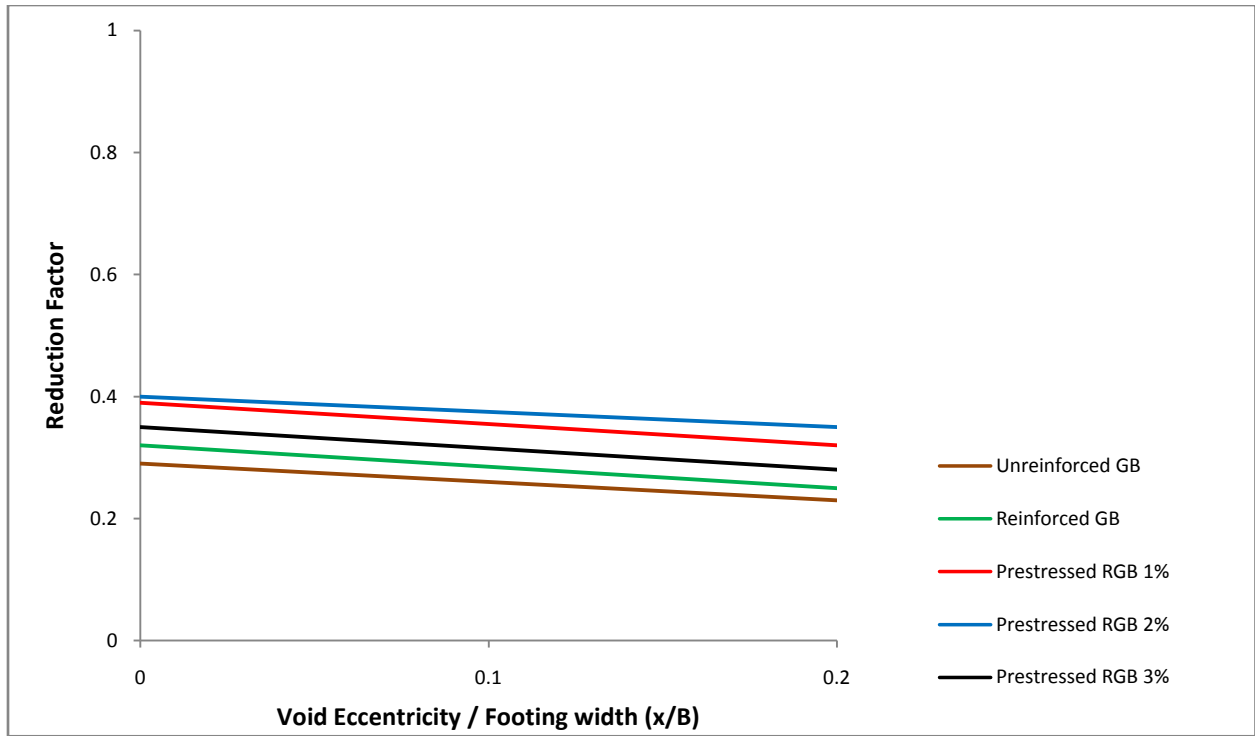


Fig 6.64 Reduction factor vs eccentricity of void curves for GB, RGB and PRGB of thickness 2B with $y=2B$

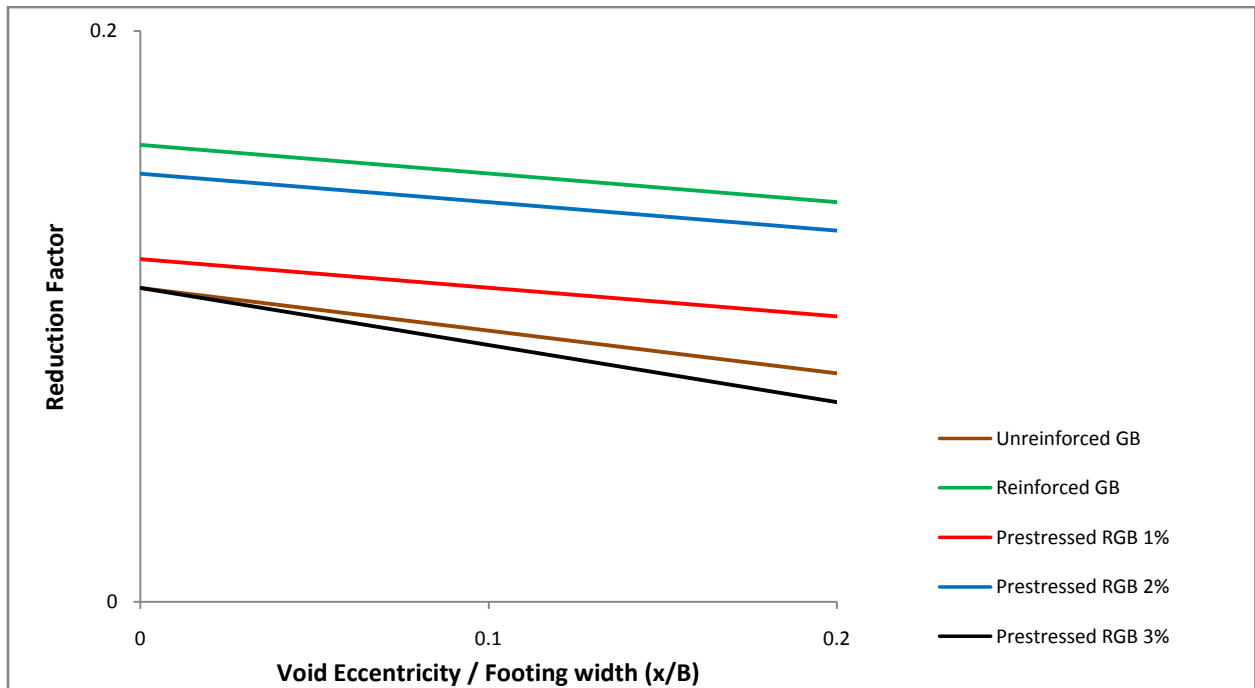


Fig 6.65 Reduction factor vs eccentricity of void curves for GB, RGB and PRGB of thickness 2B with $y=2.3B$

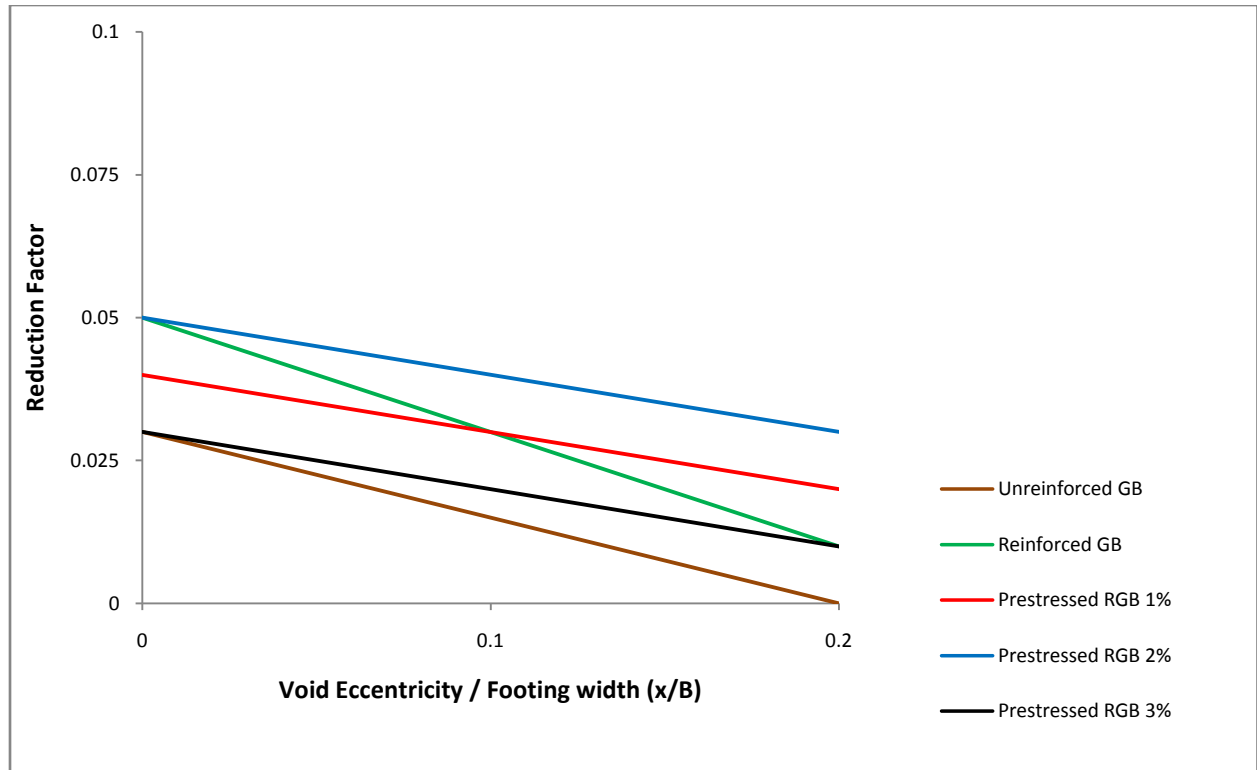


Fig 6.66 Reduction factor vs eccentricity of void curves for GB, RGB and PRGB of thickness $2B$ with $y=2.75B$

Figure 6.66 shows the variation of Reduction factor with eccentricity when the void is placed at a depth of $0.75B$ below the interface between GB and weak soil ($y/B = 2.75$). It is seen from the figure that, similar to the previous cases, the reduction factor decreases with eccentricity of the void.

6.5 CHAPTER SUMMARY

1. The behaviour of PRGB with various positions of a continuous void is presented in this Chapter.
2. It is observed that when the thickness of granular bed is equal to B , the reduction factor varies with the cube of (y/B) and when the thickness of granular bed is equal to $2B$, the reduction factor varies with the square of (y/B) .
3. When the void is located at a depth more than $2B$ from the base of footing, its effect is observed to be negligible.

CHAPTER 7

STRESSES AND SETTLEMENTS AT INTERFACE

7.1 INTRODUCTION

One among the several parameters studied in this investigation is the interaction between granular bed and weak soil. The distribution of settlement and stress at the interface between weak soil and granular bed for various cases, obtained from Finite Element analyses, are studied and presented in this chapter. The reinforcement used is Geogrid of size 2B x 2B.

7.2 STRESS DISTRIBUTION AT INTERFACE

7.2.1 Granular Beds overlying (moist) Weak Soil 1

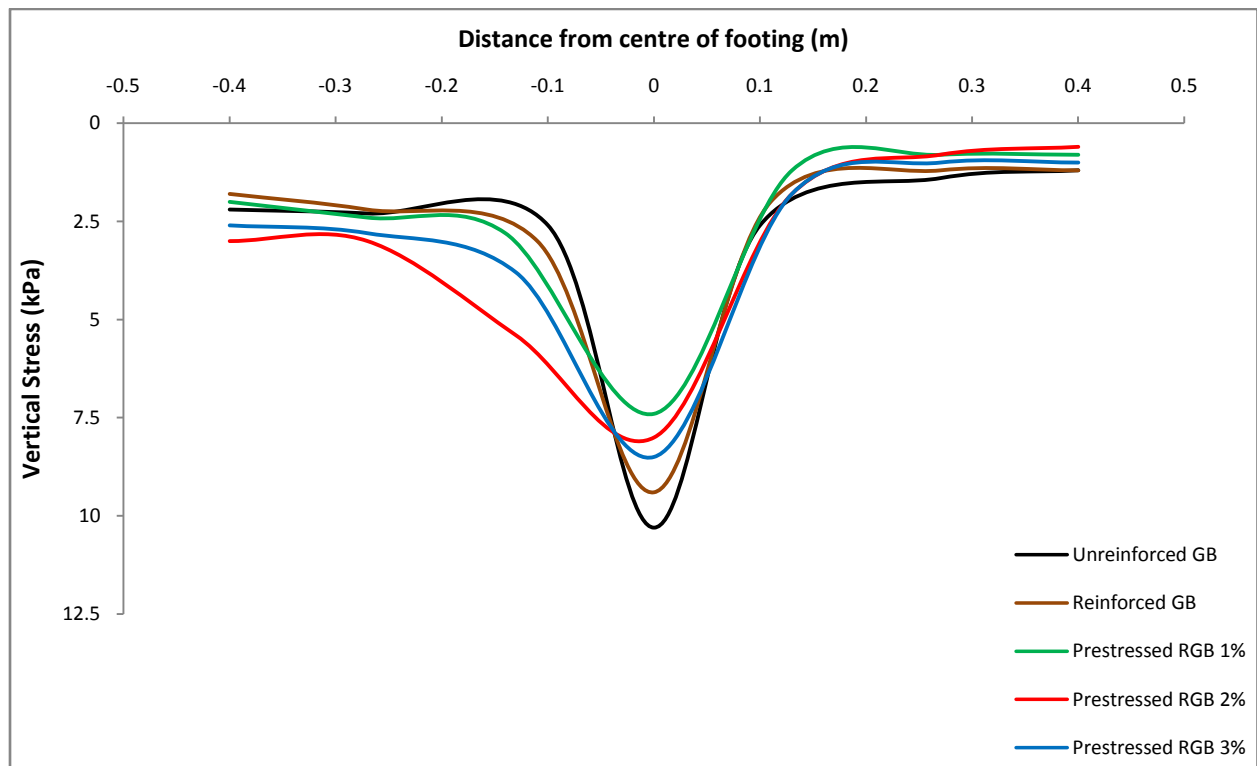


Fig 7.1 Vertical stress at interface vs distance from centre of footing curves for GB, RGB and PRGB of thickness B overlying (moist) weak soil 1

The distribution of vertical stress at the interface between granular bed, of thickness B, and (moist) weak soil 1 is presented in Fig 7.1. The applied vertical stress for this case is reported in

Fig 4.25. It can be seen from the figure that when the reinforcement is prestressed, the interface stress gets distributed to a wider area. This causes a reduction in intensity of interface stress. The intensity of stress at interface is minimum when the prestress is 1% of the tensile strength of reinforcement.

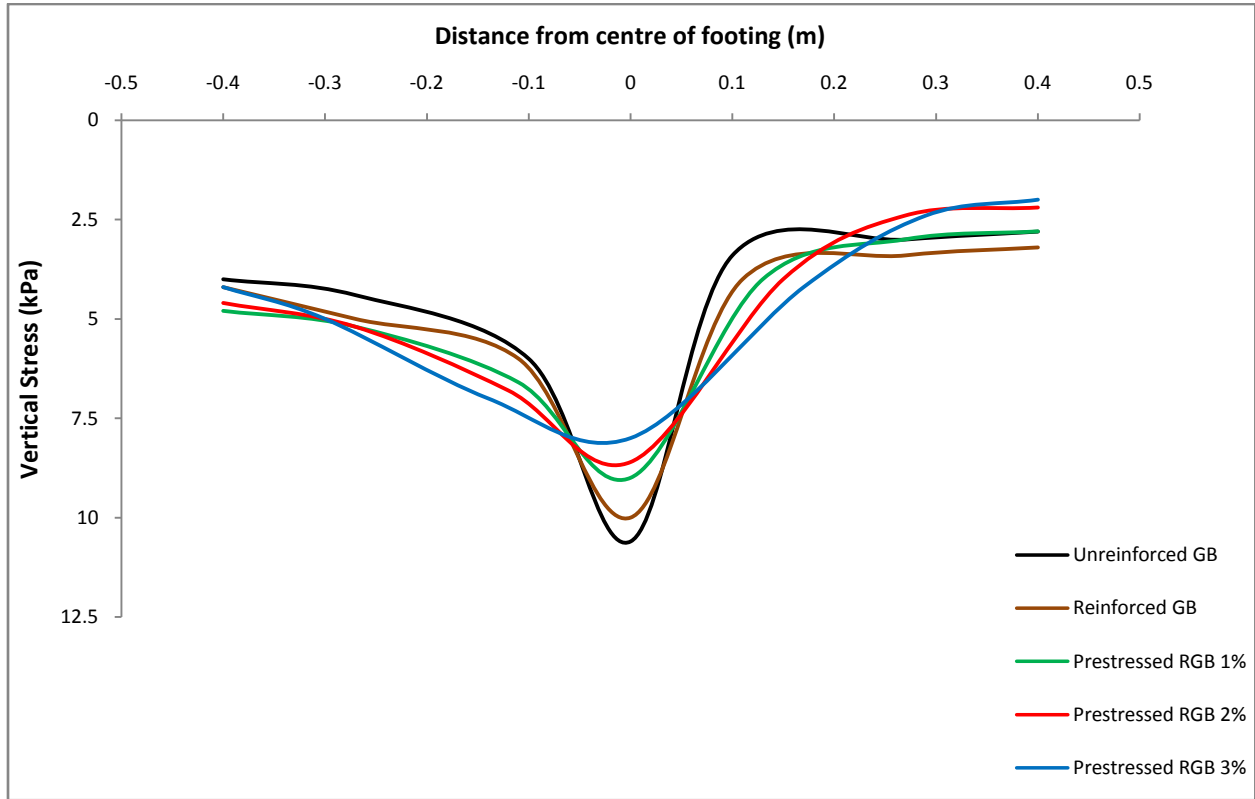


Fig 7.2 Vertical stress at interface vs distance from centre of footing curves for GB, RGB and PRGB of thickness 2B overlying (moist) weak soil 1

Figure 7.2 presents the distribution of vertical stress at the interface between granular bed and (moist) weak soil 1, when the thickness of granular bed is 2B. The applied vertical stress for this case is reported in Fig 4.27. It is seen that prestressing the reinforcement causes a considerable reduction in the intensity of stress at interface between granular bed and weak soil. The intensity of stress at the interface is minimum when the prestress is equal to 3% of the tensile strength of reinforcement.

7.2.2 Granular Beds overlying (submerged) Weak Soil 2

The distribution of vertical stress at the interface between granular bed, of thickness B , and (submerged) weak soil 2 is presented in Fig 7.3. The applied vertical stress for this case is reported in Fig 4.29. It can be seen from the figure that prestressing the reinforcement improves the stress distribution at the interface and causes a reduction in intensity of interface stress. It is seen that the interface stress is most widely distributed when the prestress is 3% and the intensity of stress is minimum when the prestress is 2% of the tensile strength of reinforcement.

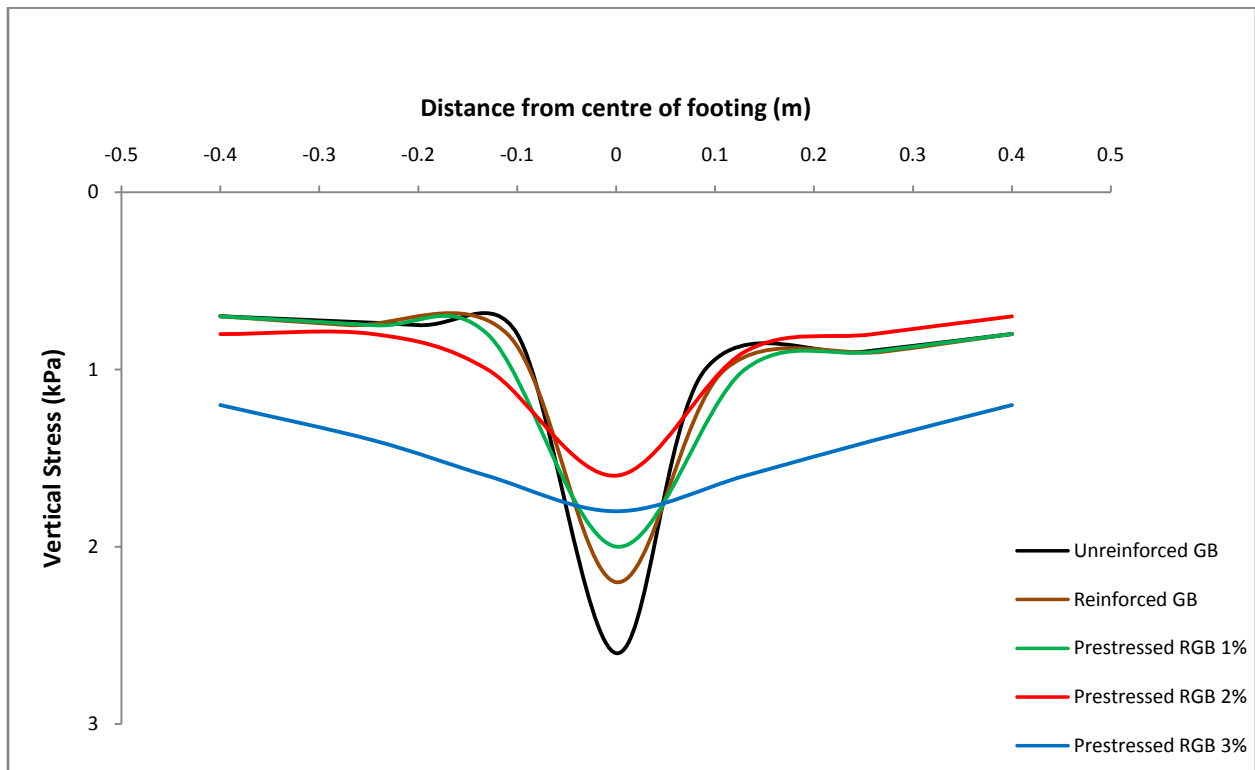


Fig 7.3 Vertical stress at interface vs distance from centre of footing curves for GB, RGB and PRGB of thickness B overlying (submerged) weak soil 2

Figure 7.4 presents the distribution of vertical stress at the interface between granular bed and (submerged) weak soil 2, when the thickness of granular bed is $2B$. The applied vertical stress for this case is reported in Fig 4.31. It is seen that prestressed reinforcement distributes the interface stress to a wider area. The intensity of stress at the interface is minimum when the prestress is equal to 3% of the tensile strength of reinforcement. It is also seen from Figures 7.3 and 7.4 that granular bed of thickness $2B$ distributes the interface stress to a wider area than granular bed of thickness B .

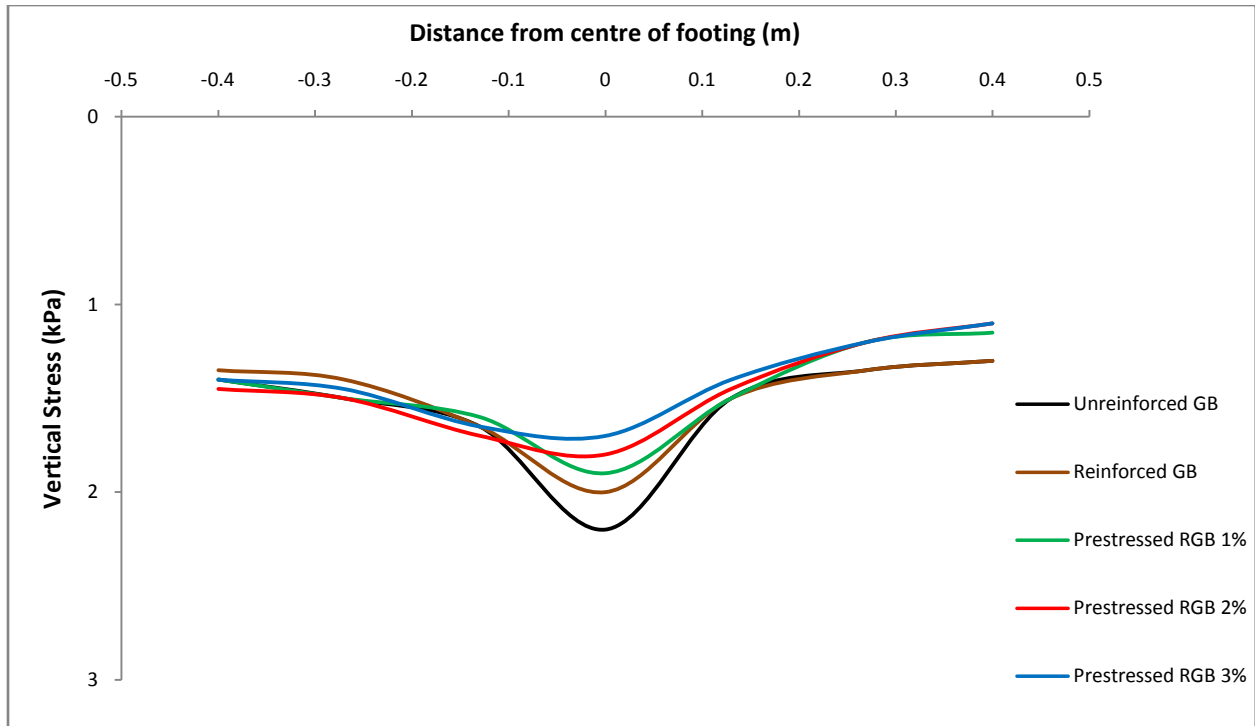


Fig 7.4 Vertical stress at interface vs distance from centre of footing curves for GB, RGB and PRGB of thickness 2B overlying (submerged) weak soil 2

7.3 DISTRIBUTION OF SETTLEMENT AT INTERFACE

7.3.1 Granular Beds overlying (moist) Weak Soil 1

The distribution of settlement at the interface between granular bed, of thickness B, and (moist) weak soil 1 is presented in Fig 7.5. The applied vertical stress for this case is reported in Fig 4.25. It can be seen from the figure that when the reinforcement is prestressed, the interface settlement gets distributed to a wider area. The settlement at interface is minimum when the prestress is 2% of the tensile strength of reinforcement. The area of distribution of interface settlement is maximum when the prestress is equal to 3% of the tensile strength of reinforcement.

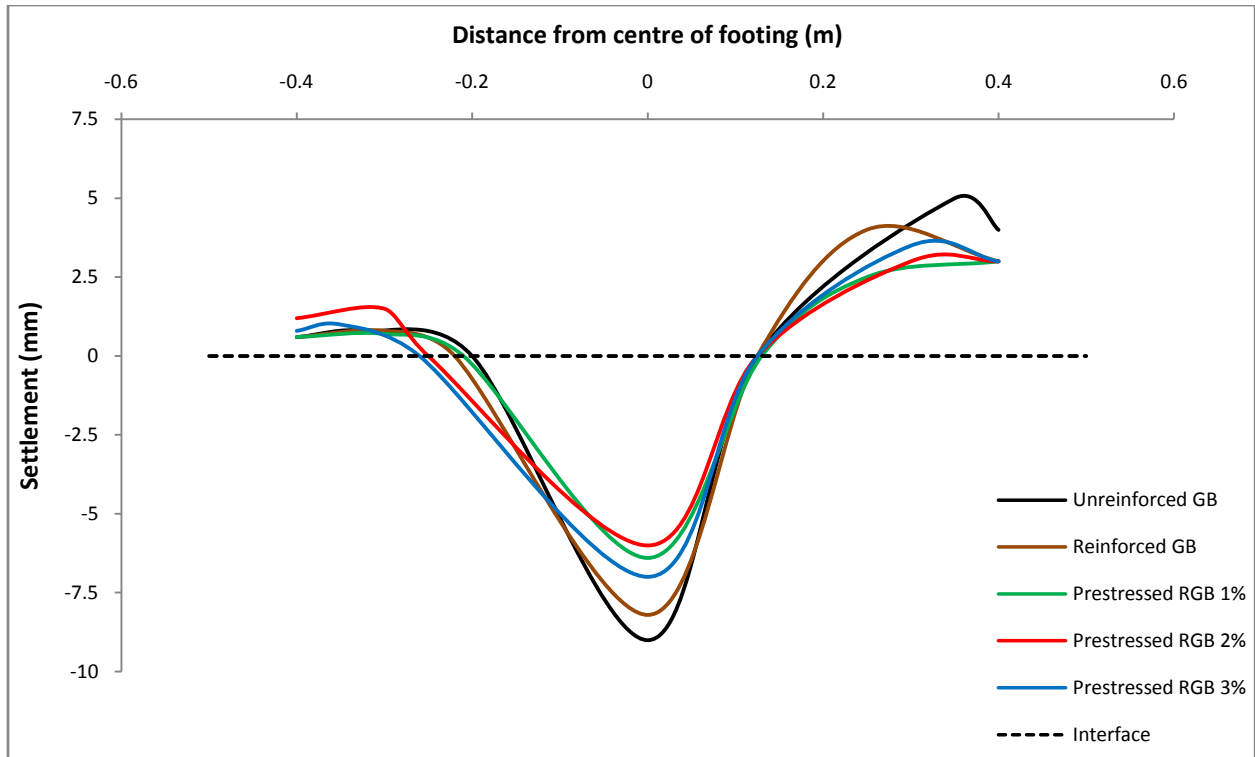


Fig 7.5 Settlement at interface vs distance from centre of footing curves for GB, RGB and PRGB of thickness B overlying (moist) weak soil 1

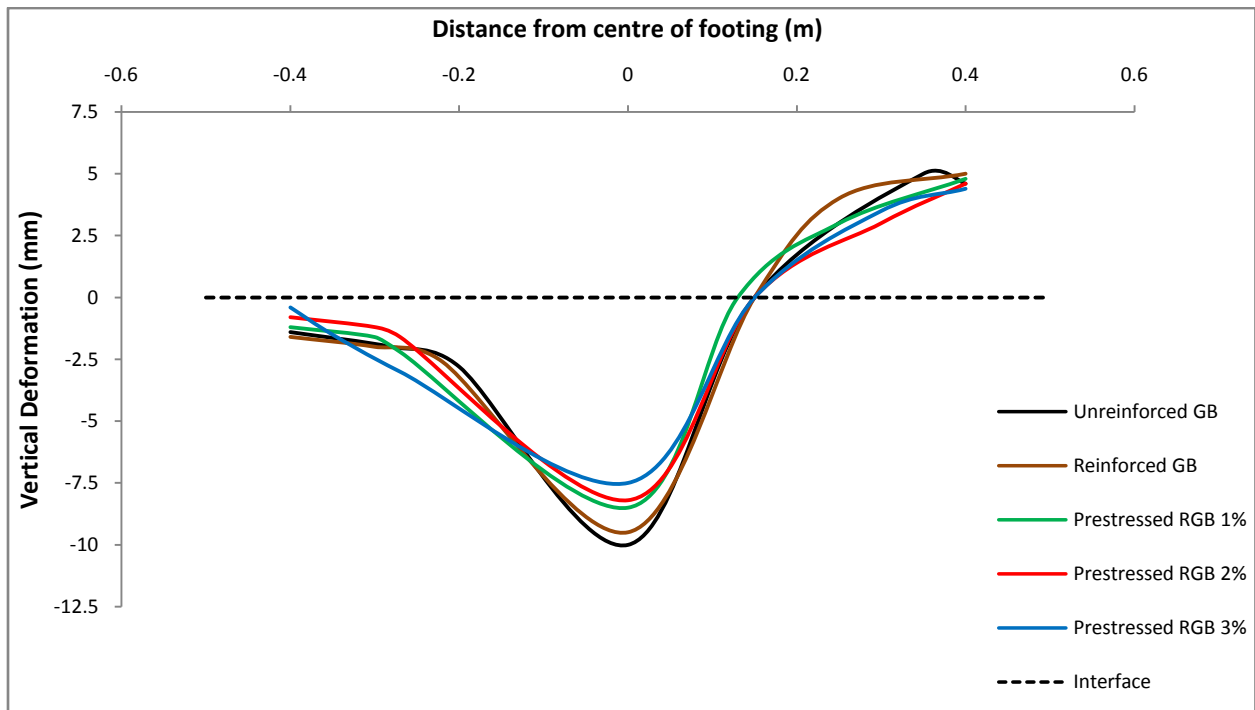


Fig 7.6 Settlement at interface vs distance from centre of footing curves for GB, RGB and PRGB of thickness 2B overlying (moist) weak soil 1

Figure 7.6 presents the distribution of settlement at the interface between granular bed and (moist) weak soil 1, when the thickness of granular bed is 2B. The applied vertical stress for this case is reported in Fig 4.27. It is seen that prestressing the reinforcement causes a considerable reduction in the settlement at interface between granular bed and weak soil. The settlement at the interface is minimum when the prestress is equal to 3% of the tensile strength of reinforcement. It is also seen from Figures 7.5 and 7.6 that granular bed of thickness 2B distributes the interface settlement to a wider area than granular bed of thickness B.

7.3.2 Granular Beds overlying (submerged) Weak Soil 2

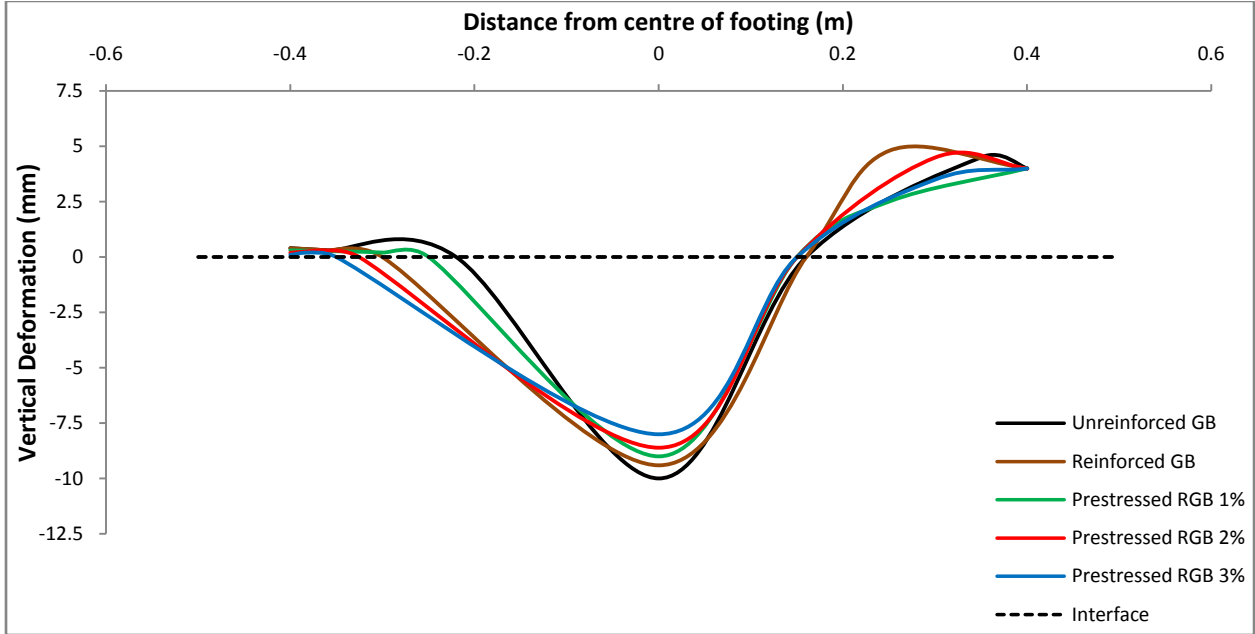


Fig 7.7 Settlement at interface vs distance from centre of footing curves for GB, RGB and PRGB of thickness B overlying (submerged) weak soil 2

The distribution of settlement at the interface between granular bed, of thickness B, and (submerged) weak soil 2 is presented in Fig 7.7. The applied vertical stress for this case is reported in Fig 4.29. It can be seen from the figure that when the reinforcement is prestressed, the interface settlement gets distributed to a wider area. The settlement at interface is minimum when the prestress is 3% of the tensile strength of reinforcement. The area of distribution of interface settlement is also maximum when the prestress is equal to 3% of the tensile strength of reinforcement.

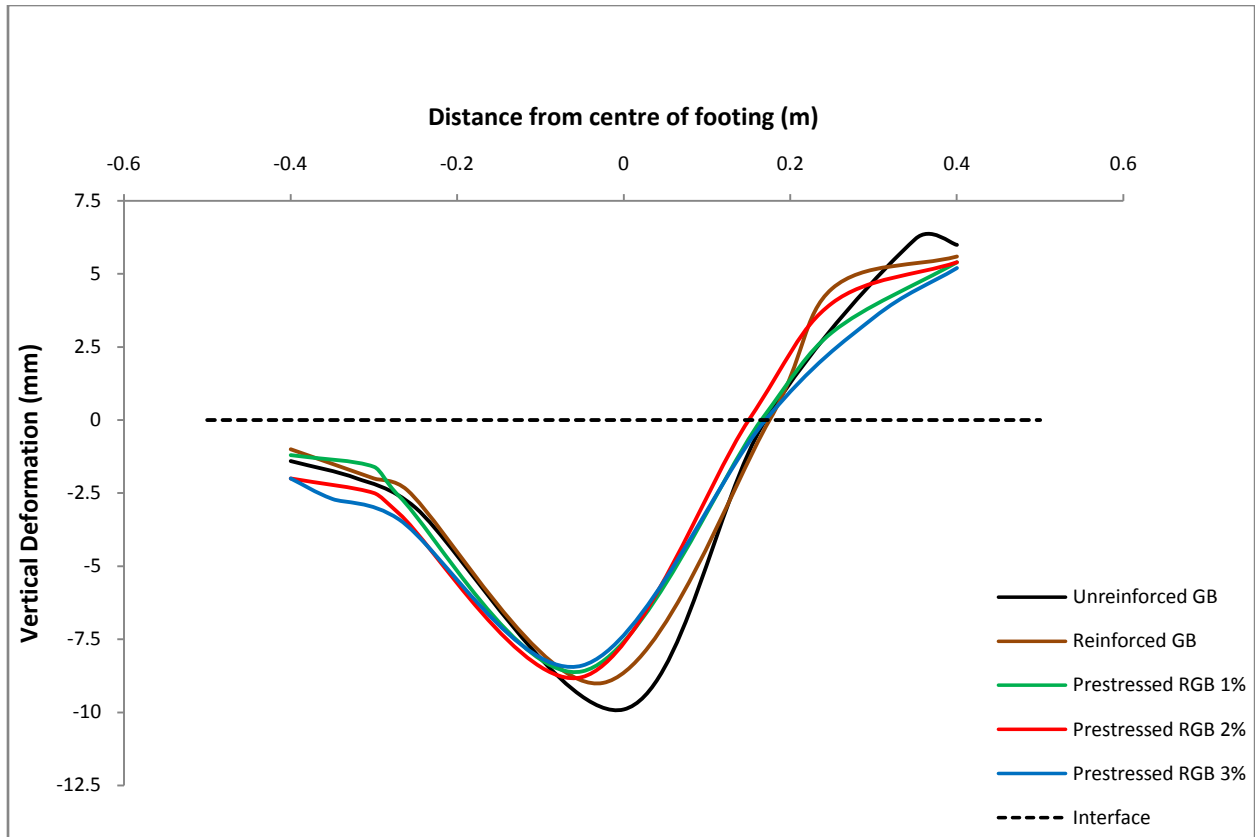


Fig 7.8 Settlement at interface vs distance from centre of footing curves for GB, RGB and PRGB of thickness $2B$ overlying (submerged) weak soil 2

Figure 7.8 presents the distribution of settlement at the interface between granular bed and (submerged) weak soil 2, when the thickness of granular bed is $2B$. The applied vertical stress for this case is reported in Fig 4.31. It is seen that prestressing the reinforcement causes a considerable reduction in the settlement at interface between granular bed and weak soil. The settlement at the interface is minimum when the prestress is equal to 3% of the tensile strength of reinforcement.

7.4 CHAPTER SUMMARY

1. The profiles of settlement and stress for various cases of PRGB overlying weak soil is presented in this Chapter.
2. It is observed that prestressed reinforcement distributes the interface stress and settlement to a more wider area.
3. Prestressing the reinforcement causes a considerable reduction in the stress and settlement at the interface.

CHAPTER 8

SUMMARY, CONCLUSIONS AND FUTURE SCOPE

8.1 SUMMARY

Increased Civil Engineering activity due to rapid urbanization has pushed the need to utilize weak soils and thus necessitating less expensive bearing capacity solutions. The research on bearing capacity of reinforced granular beds has proven to be very encouraging during the past three to four decades with applications in major areas like reclamation of deltaic or tidal lowlands etc. In this research, extensive investigations have been carried out to determine the effects of prestressing the reinforcement on the behaviour of Reinforced Granular Beds overlying soft soil.

The influences of parameters such as magnitude of prestressing force, direction of prestressing force, strength of underlying weak soil, thickness of granular bed, number of layers of reinforcement, size of reinforcement and formation of voids in granular bed and weak soil are investigated through a series of laboratory scale bearing capacity tests, and finite element analyses (using the FE program PLAXIS). Results obtained from finite element analyses are found to be in reasonably good agreement with the experimental results. An analytical model, for the pre-stressed case, based on a punching shear failure mechanism is envisaged. The Bearing Capacity Ratio (BCR) values predicted by the proposed model are found to be in good agreement with those obtained from experimental studies and finite element analyses.

8.2 CONCLUSIONS

The addition of prestress to geosynthetic reinforcement significantly improves the bearing capacity and settlement behaviour of the soil. There is reasonably good agreement between the results of experimental, finite element and analytical studies. Based on the results obtained, the following conclusions are made on the behaviour of prestressed reinforced granular beds overlying weak soils.

8.2.1 Effect of Magnitude of Prestress

From experimental studies as well as finite element analyses, it is observed that BCR increases with the magnitude of prestress up to a certain percentage of prestress. A further increase in prestress causes a reduction in BCR.

The improvement in bearing capacity depends upon the stress at the interface between reinforcement and granular soil. The tensile stress gets mobilized in the reinforcement due to the applied prestress and due to the friction developed between the reinforcement and surrounding granular soil. Results of finite element analysis indicated that in most of the cases, as the prestress increases, the normal stress at the interface between reinforcement and granular soil decreases. Initially as the prestress is applied, the BCR increases due to an increase in the tensile stress in reinforcement and due to an increase in the interface stress. But as the applied prestress is further increased, the stress transfer between reinforcement and surrounding granular soil reduces resulting in a reduction of BCR.

8.2.2 Effect of Direction of Prestress

In general biaxial prestressing is found to give better BCR for RGB with geogrid reinforcement when the underlying weak soil is moist. When the underlying weak soil is submerged, uniaxial prestressing gives better BCR. It is observed that when the underlying weak soil is submerged, capillary water rises into the granular bed and the sand surrounding the reinforcement gets moist. This change in behaviour could be due to the presence of capillary water. For RGB with geotextile reinforcement, uniaxial prestressing gives better BCR.

8.2.3 Effect of Number of layers of reinforcement

To determine the effect of the number of layers of prestressed reinforcement, investigations were carried out with single layer and double layer geogrid reinforcement. In general double layer reinforcement gave better BCR than single layer reinforcement.

It is observed that at 1% and 2% prestress, granular bed of thickness B with biaxially prestressed double layer reinforcement gives more improvement than granular bed of thickness $2B$ with uniaxially prestressed double layer reinforcement. It is also observed that granular bed of thickness $2B$ with biaxially prestressed single layer reinforcement gives more improvement than granular bed of thickness $2B$ with uniaxially prestressed double layer reinforcement.

8.2.4 Effect of Size of reinforcement

Investigations are carried out with reinforcements of two sizes; 5B and 2B, where B is the size of square footing. The improvement in bearing capacity attained with bigger reinforcement is slightly higher than that attained with smaller reinforcement. It is observed that biaxially prestressed RGB of thickness B with reinforcement of size 2B x 2B is giving more improvement than uniaxially prestressed RGB of thickness 2B with reinforcement of size 5B x 5B at 1% and 2% prestress.

8.2.5 Effect of type of geosynthetic reinforcement

In order to determine the effect of type of geosynthetic reinforcement, investigations are carried out with geogrid and geotextile reinforcements. In general PRGB with geotextile reinforcement is giving better improvement than with geogrid reinforcement. The geogrid used for the study is a weak type of geogrid having a tensile strength of only 7.68 KN/m, much lesser than the tensile strength of geotextile. The reason for lesser improvement by geogrid compared to that of geotextile could be attributed to the lower value of tensile strength of the geogrid used.

8.2.6 Effect of thickness of Granular Bed

Investigations are carried out with two thicknesses of granular bed; B and 2B, where B is the size of square footing. It is observed that for all the cases the BCR increases with the thickness of GB.

8.2.7 Effect of strength of underlying weak soil

In order to investigate the effect of the strength of underlying weak soil, the weak soil is used in two conditions namely moist condition (termed as moist soil or weak soil 1) and also used in submerged condition (termed as submerged soil or weak soil 2). It is observed that submergence of weak soil causes a large reduction in the Bearing Capacity. The behaviour of PRGB is also influenced by the presence of capillary moisture in the granular bed. It is observed that improvement is more for weak soil 2 (Submerged soil).

8.2.8 Analytical modeling

An analytical model, for predicting the improvement in bearing capacity due to prestressing, is developed by improvising an earlier model based on punching shear failure mechanism. The improvement in BCR is attributed to three effects, namely Shear Layer Effect, Confinement Effect and additional Surcharge Effect.

In the earlier model, prestressing is not considered and the distribution of additional surcharge stress is assumed to be exponential. In the proposed analytical model, the distribution of additional surcharge stress is taken as uniform in the direction of Prestress.

The analytical model proposed in this study predicts the bearing capacity ratios for all the cases with reasonably good accuracy. Prediction is better for moist soil than for submerged soil, which implies that the punching shear failure mechanism is predominant failure mechanism in case of moist soil.

8.2.9 Effect of development of Voids in Granular Bed and Weak soil

The presence of void in soil causes a considerable reduction in bearing capacity. It is observed that prestressing the reinforcement can decrease the reduction in bearing capacity. The presence of void has only a negligible effect when it is at a depth of more than $2B$ from the base of footing.

It is observed that when the thickness of granular bed is equal to B , the reduction factor varies with the cube of (y/B) and when the thickness of granular bed is equal to $2B$, the reduction factor varies with the square of (y/B) .

8.2.10 Stresses and Settlements at the Interface

It is observed that prestressing the reinforcement spreads the stress at the interface between Granular Bed and weak soil to a wider area. This reduces the intensity of stress and also settlement at the interface.

8.3 SCOPE FOR FUTURE WORK

The possible further research work in this area are detailed below

1. This investigation mainly focused on the short term behaviour of prestressed reinforced granular beds. Before using this technique in field applications, the long term behaviour also must be studied.
2. The effects of possible losses in prestress due to anchorage slip, stress relaxation in reinforcement, shrinkage of soil etc can be studied.
3. The possibility of replacing sand in the granular bed with locally available soil can be studied.
4. Analyse the Reinforced Granular Bed with oblique pull, when the footing settles vertically downwards.

REFERENCES

- Alamshahi,S. and Hataf,N. (2009). Bearing capacity of strip footings on sand slopes reinforced with geogrid and grid-anchor, *Geotextiles and Geomembranes*, 27 (2009) 217 – 226.
- Azam,G., Hseigh,W. and Wang,M,C. (1991). Performance of strip footing on stratified soil deposit with void, *Journal of Geotechnical and Geoenvironmental Engineering*, ASCE, Vol. 117, No. 5, May, pp. 753 – 772.
- Baus,R,L. and Wang,M,C. (1983). Bearing capacity of strip footing above void, *Journal of Geotechnical and Geoenvironmental Engineering*, ASCE, Vol. 109, No. 1, January, pp.1 – 14.
- Bhat,A,K., Shivashankar,R. and Yaji,R.K.(2008), “Case study of land slide in NH 13 at Kethikal near Mangalore, India”, *6th International Conference on Case histories in Geotechnical Engineering*, Arlington, VA, USA, paper no.2.69
- Binquet, J. and Lee, K.L. (1975a). Bearing capacity tests on reinforced earth slabs. *Journal of Geotechnical Engineering Division*, ASCE 101 (12), 1241–1255.
- Binquet, J. and Lee, K.L. (1975b). Bearing capacity analysis of reinforced earth slabs. *Journal of Geotechnical Engineering Division*, ASCE 101 (12), 1257–1270.
- Briancon,L. and Villard,P. (2008). Design of geosynthetic-reinforced platforms spanning localized sink holes. *Geotextiles and Geomembranes*, 26, 416 – 428.
- Chen, Q., Farsakh, M,A. and Sharma, R. (2009). Experimental and Analytical studies of reinforced crushed limestone, *Geotextiles and Geomembranes*, 27, pp 357-367
- Choudhary, A,K, Jha, J,N. and Gill,K,S.(2010). Laboratory investigation of bearing capacity behaviour of strip footing on reinforced flyash slope. *Geotextiles and Geomembranes*, 28, 393 – 402.

Deb,K, Chandra,S. and Basudhar,P,K. 2006, Nonlinear analysis of multilayer extensible geosynthetic reinforced granular bed on soft soil, *Geotechnical and Geological Engineering*, 25, 11 – 23.

Deb,K, et al , 2007, Numerical analysis of multilayer geosynthetic reinforced granular bed on soft fill, *Geotechnical and Geological Engineering*, 25, 639 – 646.

Ghosh,C. and Madhav,M,R.(1994a), Reinforced granular fill soft soil system – membrane effect, *Geotextiles and Geomembranes*, 13(11), pp 743 – 759.

Ghosh,C. and Madhav,M,R.(1994b), Reinforced granular fill soft soil system – confinement effect, *Geotextiles and Geomembranes*, 13(11), pp 727 – 741.

Guido,V.A., Chang,D.K. and Sweeny,M.A. (1986), Comparison of geogrid and geotextile reinforced earth slabs, *Canadian Geotechnical Journal*, 23, 435-440

Huang,C. and Tatsuoka,F. (1990), Bearing capacity of reinforced horizontal sandy ground, *Geotextiles and Geomembranes*, 9, pp 51 – 82.

Kiyosumi,M., Kusakabe,O., Ohuchi, M. and Peng,F,L. (2007), Yielding pressure of spread footing above multiple voids, *Journal of Geotechnical and Geoenvironmental Engineering*, ASCE, Vol. 133, No. 12, December, pp. 1522 – 1531.

Kiyosumi,M., Kusakabe,O. and Ohuchi, M. (2011), Model tests and analyses of bearing capacity of strip footing on stiff ground with voids, *Journal of Geotechnical and Geoenvironmental Engineering*, ASCE, Vol. 137, No. 4, April, pp. 363 – 375.

Lackner,C., Bergado,D,T. and Semprich,S. (2013), Prestressed reinforced soil by geosynthetics – Concepts and experimental investigations, *Geotextiles and Geomembranes*, 37, pp 109 – 123.

Lee,K.M., Manjunath,V.R. and Dewaikar,D.M. (1999). “Numerical and model studies of strip

footing supported by a reinforced granular fill – soft soil system”, *Canadian Geotechnical Journal*, Vol.36, pp. 793-806.

Lovisa,J., Shukla,S,K. and Sivakugan,N. (2010). Behaviour of prestressed geotextile-reinforced sand bed supporting a loaded circular footing, *Geotextiles and Geomembranes*, 28, 23 – 32.

Madhav,M,R. and Datye (1993) Bearing Capacity of clay with variable surcharge of finite extent, *Indian Geotechnical Journal*, Vol. 23(2).

Madhav,M,R. and Sharma,J,S,N. (1991). Bearing capacity of clay overlain by stiff soil, *Journal of Geotechnical Engineering*, Vol. 117, No,12, pp 1941–1948.

Madhav,M,R. and Umashankar,B. (2003). Analysis of inextensible sheet reinforcement subject to transverse displacement / force: linear subgrade response, *Geotextiles and Geomembranes*, 21, pp 69 – 84.

Madhavalatha, G. and Somwanshi, A. (2009a), Bearing capacity of square footings on geosynthetic reinforced sand, *Geotextiles and Geomembranes*, 27, pp 281 – 294.

Madhavalatha, G. and Somwanshi, A. (2009b), Effect of reinforcement form on the bearing capacity of square footings on sand, *Geotextiles and Geomembranes*, 27, pp 409 – 422.

Meyerhof, G,G. (1974). Ultimate bearing capacity of footings on sand layer overlying clay, *Canadian Geotechnical Journal*, Vol. 11, pp 223-229.

Meyerhof, G,G. and Hanna, A,M. (1978). Ultimate bearing capacity of foundations on layered soils under inclined load, *Canadian Geotechnical Journal*, Vol. 15, pp 565-572.

Michalowski, R,L. and Shi, L. (2003). Deformation patterns on reinforced foundation sand at failure, *Journal of Geotechnical and Geoenvironmental Engineering*, ASCE, Vol. 129, No. 6, June, pp. 439-449.

Mohamed, M,H,A. (2010). Two dimensional experimental study for the behaviour of surface footings on unreinforced and reinforced sand beds overlying soft pockets, *Geotextiles and Geomembranes*, 28, pp 589-596.

Roh, H,S. and Tatsuoka, F. (2001). Effects of preloading and prestressing on the strength and stiffness of geosynthetic reinforced clay in plane strain compression, *Geosynthetics International*, Vol.8, No. 5, pp 393 – 444.

Sadoglu, E.,Cure, E., Moroglu, B. and Uzuner, B,A. (2009). Ultimate loads for eccentrically loaded model shallow strip footings on geotextile-reinforced sand, *Geotextiles and Geomembranes*, 27, pp 176-182.

Selvadurai, A.P.S., 1979. Elastic Analysis of Soil-Foundation Interaction, Elsevier Scientific Publishing Company, New York.

Sharma, R., Chen, Q, Farsakh, M, A. and Yoon, S. (2009), Analytical modeling of geogrid reinforced soil foundation, *Geotextiles and Geomembranes*, 27, pp 63-72.

Shivashankar,R., Madhav,M.R. and Miura,N. (1993). Reinforced granular beds overlying softclay, *Proceedings of 11th South East Asian Geotechnical Conference*, Singapore, 409 – 414.

Shivashankar, R. and Reddy, A.C.S. (1998). Reinforced granular bed on poor filled up shedi ground, *Proceedings of the Indian Geotechnical Conference - 1998, Vol.1*, 301-304.

Shivashankar, R. and Setty, K.R.N.S. (2000). “Foundation problems for ground level storage tanks in and around Mangalore”, *Proceedings of Indian Geotechnical Conference 2000*, IIT Bombay, Mumbai.

Shukla, S.K., Yin, J.H., 2006. *Fundamentals of Geosynthetic Engineering*. Taylor and Francis, London

Sireesh, S.,Sitharam, T,G. and Dash, S,K. (2009). Bearing capacity of circular footing on geocell–sand mattress overlying claybed with void, *Geotextiles and Geomembranes*, 27,pp 89-98.

Tafreshi, S,N,M. and Dawson, A,R. (2010a), Comparison of bearing capacity of a strip footing on sand with geocell and with planar forms of geotextile reinforcement, *Geotextiles and Geomembranes*, 28, pp 72-84.

Tafreshi, S,N,M. and Dawson, A,R. (2010b), Behaviour of footings on reinforced sand subjected to repeated loading – Comparing use of 3D and planar geotextile, *Geotextiles and Geomembranes*, 28, pp 434-447.

Terzaghi, K and Peck, R,B.(1948), *Soil Mechanics in Engineering Practice*, Wiley International, New York.

Vinod, P., Bhaskar,A.B. and Sreehari,S. (2009). Behaviour of a square model footing on loose sand reinforced with braided coir rope, *Geotextiles and Geomembranes*, 27, 464 – 474.

Wang, M,C. and Badie, A. (1985). Effect of underground void on foundation stability, *Journal of Geotechnical and Geoenvironmental Engineering*, ASCE, Vol. 111, No. 8, August, pp. 1008 – 1019.

Wang, M,C and Hseigh, C,W. (1987). Collapse load of strip footing above circular void, *Journal of Geotechnical and Geoenvironmental Engineering*, ASCE, Vol. 113, No. 5, May, pp.511 – 515.

Yamamoto, K. and Otani, J. (2002). Bearing Capacity and failure mechanism of reinforced soil based on rigid-plastic finite element formulation, *Geotextiles and Geomembranes*, 20, 367 – 393.

PUBLICATIONS

Journal

- Jayamohan,J and Shivashankar,R. 2012, Some Studies on Prestressed Reinforced Granular Beds Overlying Weak Soil, *ISRN Journal of Civil Engineering*, Volume 2012, Article id 436327
- Ramaiah Shivashankar and Jayamohan Jayaraj. 2013, Behaviour of Prestressed Geosynthetic Reinforced granular beds overlying weak soil, *Indian Geotechnical Journal*. (Published online DOI 10.1007/s40098-013-0070-6)
- R. Shivashankar and J. Jayamohan. 2013, Studies on Effects of prestressing the reinforcement on the behaviour of reinforced granular beds overlying weak soil, *Indian Journal of Geosynthetics and Ground Improvement*, Vol.2, No.2, pp: 3-13
- Ramaiah Shivashankar and Jayamohan Jayaraj. 2013, Effects of prestressing the reinforcement on the behaviour of reinforced granular beds overlying weak soil, *Geotextiles and Geomembranes*. (Published online, DOI information:10.1016 j.geotextmem.2013.08.008)
- R. Shivashankar, J. Jayamohan and K. Srinath Shetty. 2013, Improving bearing capacity of footings on weak and soft soils, *International Journal of Earth Sciences and Engineering*. (Paper accepted, In press)

Conferences

- Shivashankar,R and Jayamohan,J. 2012. Geosynthetic Applications: Some Research Studies and Some Case Studies, *International Symposium on Sustainable Geosynthetics and Green Technology for Climate Change (SGCC) 2012*, Bangkok, Thailand, pp 111 -121. (Accepted and Presented)
- Jayamohan,J and Shivashankar,R. 2012, Studies on Prestressed Reinforced Foundation Beds Overlying weak grounds, *International Conference on Emerging Trends in Engineering (ICETE-12)*, NMAMIT, Nitte, pp 459 – 464. (Accepted and Presented)
- Jayamohan,J., Shivashankar,R., Aswathy,M.S. and Vigey Mary, W.2013, Studies on Behaviour of Footings on Prestressed Geogrid Reinforced Granular Bed Overlying Weak Soil, *Geosynthetics 2013*, California, USA, pp: 100 – 109. (Accepted and Presented)
- R. Shivashankar, J. Jayamohan and K. Srinath Shetty. 2013, Improving bearing capacity of footings on weak and soft soils, *3rd International Engineering Symposium (IES 2013)*,

- Kumamoto University, Japan, pp:C3-3-1 to C3-3-6 (Accepted and Presented)
- R. Shivashankar, J. Jayamohan and Nileena Suresh, Behaviour of Footings on Prestressed Geogrid Reinforced Granular Beds Overlying Weak Soil, *Geo Africa 2013*, Accra, Ghana. Article id 07-02 (Accepted and Presented)
- R. Shivashankar, J. Jayamohan and Venkateswar Reddy, Parametric Study on Reinforced Granular Beds Overlying Weak Soil, *Geosynthetics 2013-India*, New Delhi, pp: 180-190 (Accepted and Presented)
- M.S.Asathy, J.Jayamohan and R. Shivashankar, Behaviour of Prestressed Geosynthetic Reinforced Granular Bed overlying Weak Soil, *Indian Geotechnical Conference*, 2013, Roorkee. (Accepted and Presented)
- R. Shivashankar and J. Jayamohan. 2014, Behaviour of Prestressed Reinforced Foundation Beds Overlying Weak Soil, *Geo Shanghai 2014*, Shanghai, China. (Accepted and Presented)
- R. Shivashankar and J. Jayamohan. 2015, Effects of Formation of Voids on the Behaviour of Prestressed Reinforced Granular Beds overlying Weak soil, *Geosynthetics2015*, Portland, USA. (Abstract accepted, Paper under review)

BIODATA



Name : Jayamohan. J

Occupation : Assistant Professor in Civil Engineering
LBS Institute of Technology for Women, Thiruvananthapuram.

Date of Birth : 22 – 03 – 1970

Permanent Address : TC 11/1085, Watts Lane
Charachira, Nanthencode
Thiruvananthapuram – 695003
Kerala, India

Email : jayamohan7@gmail.com, jayamohan12@yahoo.co.in

Phone : +91-9447017088

Educational Qualification :

Sl.no:	Degree	University	Year of Passing	Class
1	B E in Civil Engineering	Mangalore University	1992	First Class
2	M.Tech in Geotechnical Engineering	Mangalore University (KREC, Surathkal)	1996	First Class with Distinction
3	Ph.D (part time)	NITK, Surathkal	Currently in VIII semester	CGPA 10 in course work

Work Experience :

Sl.no:	Organisation	Post Held	From	To
1	ARTECH Group	Site Engineer	01-01-1993	15-11-1993
2	Kerala State Electricity Board	Graduate Apprentice	17-11-1993	30-07-1994
3	RELCON Foundations Pvt. Ltd	Site Engineer	09-04-1996	17-10-1996
4	L.G Foundations Pvt. Ltd	Site Engineer	21-10-1996	20-02-1998
5	Karunya Institute of Technology, Coimbatore	Lecturer in Civil Engineering	08-06-1998	15-09-2000
6	LBS Engineering Colleges at Kasaragod & Thiruvananthapuram	Assistant Professor in Civil Engineering	20-09-2000	Till date

Total Teaching Experience :15 years

Total Industry Experience :3 years

Short term courses attended:

Sl.no:	Name of course	Organising Institution	From	To
1	Recent Trends in Structural Dynamics	Karunya Institute of Technology, Coimbatore	15-11-1999	28-11-1999
2	Geotechnical Investigations for Infrastructure Projects	College of Engineering, Thiruvananthapuram	13-06-2007	15-06-2007
3	Recent Advances in Flexible Pavement Engineering	Indian Institute of Technology, Madras	16-07-2007	21-07-2007
4	Seismic Soil-Structure Interaction	College of Engineering, Thiruvananthapuram	11-05-2009	15-05-2009
5	Total Station Surveying and Other Advanced Surveying Techniques	National Institute of Technology, Calicut	18-05-2009	29-05-2009
6	Creative Approaches in Teaching	College of Engineering, Thiruvananthapuram	06-12-2006	9-12-2006
7	Recent Advances in the Use of Geosynthetics in Transportation and Geotechnical Engineering	College of Engineering, Thiruvananthapuram	30-11-2011	13-12-2011

Publications

- International Journals - 05
- International Conferences- 08

Subjects Taught at UG Level

- Engineering Mechanics
- Surveying
- Geotechnical Engineering
- Design of Steel Structures
- Design of Reinforced Concrete Structures

Other achievements:

- Scored 86.15 percentile in GATE 94
- Scored a CGPA of 10 in the first semester of Ph.D at NITK, Surathkal
- Proficient in Civil Engineering softwares AUTOCAD and PLAXIS.